

**HEAT CAPACITY AND STRUCTURE IN SMALL MOLECULE  
AND POLYMER SYSTEMS**

by

Marie-Esther Saint Victor

A thesis submitted to the faculty of Graduate Studies and Research in partial fulfillment  
of the requirements for the degree of Doctor of Philosophy.

Department of Chemistry  
McGill University  
Montreal, Quebec, CANADA

December 1988

© Marie-Esther Saint Victor, 1988

*à ma mère*

*et*

*à toutes ces femmes  
du Tiers-Monde qui rêvent  
de concrétiser d'impossibles rêves*

## ABSTRACT

Structural effects in small molecule and polymer systems have been studied through heat capacity measurements (small molecule systems), phase diagrams and heat of mixing measurements (polymer systems). It has been found that structure due to molecular antipathy i.e. large  $H^E$  and  $G^E$  manifests itself through a W-shape  $C_p^E$  which is found to be a summation of two contributions to the thermodynamics: random and non-random. An excellent correlation is made between  $C_p^E$  and the concentration-concentration correlation function ( $S_{CC}$ ). The non-randomness effect increases drastically as T moves towards the UCST. Non-randomness ( $S_{CC}$ ) and the effect of non-randomness ( $C_p^E$ ) are found toward the middle of the concentration range. It has been found that the W-shape is not a wide-spread phenomenon for other second-order quantities such as  $dV^E/dT$  and  $dV^E/dP$ , in spite of a certain similarity of the critical exponent for  $C_p$ ,  $\alpha_p$  and  $\kappa_T$ .  $dV^E/dT$  results have been discussed in terms of Flory theory. The difference between experimental and theoretical values provides a good estimation of the non-random  $dV^E/dT$ .

Structure has also been studied through H-bonding interactions (self-association or complex formation) between methanol, butanol, decanol in  $CCl_4$ , acetonitrile or octanenitrile and dodecanenitrile in n-decane,  $CCl_4$  or xylene.  $C_p^E$  are predicted using the Treszczanowicz-Kehiaian theory.

Structure in polymer solutions has been associated with specific interactions which lead to a low temperature LCST. An extended Flory-Huggins-Prigogine theory has been used to interpret the phase diagram of specifically interacting polymer systems. Compatibility between polymer pairs is also linked to the presence of these specific interactions which are associated with an exothermic heat of mixing.  $\Delta H_M$  has been measured for ternary systems i.e. two polymers and a mutual solvent. Exothermic  $\Delta H_M$  is observed if the pair strongly interacts while  $\Delta H_M$  is positive if the polymers are

incompatible or if they do not interact similarly with the solvent, in which case non-randomness plays a major role.

## RÉSUMÉ

Les effets structuraux de liquides et de polymères en solution ont été étudiés par des mesures de chaleur spécifique (petites molécules), de diagramme de phase et des mesures de chaleur de mélange (polymères). Nous avons trouvé que la structure résultant "d'une antipathie moléculaire", c'est-à-dire  $H^E$  et  $G^E$  élevée, se traduit par une courbe de  $C_p^E$  ayant la forme d'un W. Nous avons trouvé que l'allure de cette courbe est due à deux contributions à la thermodynamique: Distribution aléatoire (random) et non-aléatoire (non-random). Une excellente relation a été établie entre  $C_p^E$  et  $S_{CC}$  (fonction de corrélation concentration-concentration). L'effet de distribution non-aléatoire des molécules augmente considérablement quand la température tend vers la température critique de démixtion supérieure (TCDS) (UCST). La distribution non-aléatoire et son effet ont été observés dans les régions médianes de l'échelle de concentration. Considérant d'autres quantités de second-ordre telles que  $dV^E/dT$  et  $dV^E/dP$ , nous avons trouvé que la forme W n'était pas un phénomène aussi général que dans le cas de  $C_p^E$ , quoi qu'on ait observé une certaine "singularité" (singularity) de l'exposant critique de  $C_p$ ,  $\alpha_p$  et  $\kappa_T$ . Les résultats de  $dV^E/dT$  ont été discutés à la lumière de la théorie de Flory. La différence entre les valeurs expérimentales et théoriques nous a permis d'estimer la contribution due à la distribution non-aléatoire à  $dV^E/dT$ .

Nous avons également étudié la structure de liquides pouvant former des ponts-hydrogène (auto-association ou formation de complexe) dans des solutions contenant du méthanol, du butanol, du décanol dans le  $CCl_4$ , l'acétonitrile, ou l'octanenitrile et le dodécanenitrile dans le n-décane, le  $CCl_4$  ou le xylène. Les valeurs de  $C_p^E$  ont été prédites à l'aide de la théorie de Treszczanowicz-Kehiaian.

La structure créée par des molécules de polymères en solution a été associée à des interactions spécifiques que forment ces polymères avec le milieu ambiant (solvant ou

un autre polymère). Nous avons prouvé que ces interactions spécifiques sont à l'origine de la température critique de démixtion inférieure (TCDI) (LCST). Les diagrammes de phase de ces solutions ont été interprétés selon une nouvelle théorie combinant la théorie de Flory–Huggins à celle de Prigogine–Flory. La compatibilité entre deux molécules de polymères dépend aussi de ces interactions spécifiques qui sont, dans ce cas, associées à une chaleur de mélange exothermique. Nous avons mesuré  $\Delta H_M$  pour des systèmes ternaires constitués de deux polymères et d'un solvant commun.  $\Delta H_M$  s'est révélée négative si les deux polymères font des interactions spécifiques. Par contre,  $\Delta H_M$  est positive si les polymères sont incompatibles ou s'ils interagissent différemment avec le solvant, dans un tel cas, la distribution des molécules dans le mélange se fait de façon non--aléatoire.

## FOREWORD

In accordance with current regulations from the Faculty of Graduate Studies and Research, McGill University, the following text is cited:

The Candidate has the option, subject to the approval of the Department, of including as part of the thesis the text of an original paper, or papers, suitable for submission to learned journals for publication. In this case the thesis must still conform to all other requirements explained in Guideline Concerning Thesis Preparation (available at the Thesis Office). Additional material (experimental and design data as well as descriptions of equipment) must be provided in sufficient detail to allow a clear and precise judgement to be made of the importance and originality of the research reported. Abstract, full introduction and conclusion must be included, and where more than one manuscript appears, connecting texts and common abstracts, introduction and conclusions are required. A mere collection of manuscripts is not acceptable; nor can reprints of published papers be accepted.

While the inclusion of manuscripts co-authored by the Candidate and others is not prohibited by McGill, the Candidate is warned to make an explicit statement, on who contributed to such work and to what extent, and Supervisors and others will have to bear witness to the accuracy of such claims before the Oral Committee. It should be also noted that the task of the External Examiner is made much more difficult in such cases, and it is in the Candidate's interest to make authorship responsibilities perfectly clear.

The thesis is divided into three different parts, part one is composed of three chapters while part two and three contain each two chapters. Chapter one has been published in *Fluid Phase Equilibria*, 35, 237, 1987, while the other chapters will subsequently be submitted to suitable journals either in the present form or in slightly modified form.

## ACKNOWLEDGEMENTS

I wish to express my deepest gratitude to Professor Donald Patterson for his guidance and constant interest throughout the course of this work, for his patience and precious assistance in the preparation of this thesis, for the innumerable enriched discussions and for everything I have learned from him.

I would like to thank Mr. Fred Kluck for his competent work in the design and construction of the apparatus used in Chapter 6 of the thesis and for his various help all these years and Mr. Georges Kopp for his collaboration in the design and blowing of glass vessels and his helpful assistance for computer devices.

Thanks are also due to Ms. Chantal Marotte for her competent work and constant collaboration in typing the thesis, her mother, Mrs. Marotte for her precious help, Ms. Renée Charron and Aline Charade for their various help and kindness all these years.

I am indebted to my sister Denise for her encouragement and for having been always present and to all friends and colleagues who have helped me in many ways throughout these years.

## TABLE OF CONTENTS

	Page
Abstract	i
Résumé	iii
Foreword	v
Acknowledgements	vi
Table of contents	vii
List of figures	xiv
List of tables	xxi
General Introduction	1
I. Structure due to association	4
1. Weak association	4
A. Destruction of order in n-alkanes	4
B. Creation of order in mixtures containing alkane molecules	7
2. Strongly associated mixtures	7
II. Structure due to molecular antipathy	14
III. Structure in polymer systems	18
– Structure and LCST	18
References	31

## TABLE OF CONTENTS (continued)

	Page
<b>PART I</b>	<b>33</b>
<b>Chapter 1</b>	
The W-shape concentration dependence of $C_p^E$ and solution non-randomness: Ketones + normal and branched alkanes	34
Abstract	35
Introduction	36
Effect of solution non-randomness	37
Experimental	45
Results and discussion	46
1. Excess heat capacities	46
2. Excess volumes	63
Acknowledgements	65
List of symbols	66
References	67
<b>Chapter 2</b>	
W-shape concentration dependence of $C_p^E$ and solution non-randomness: Systems approaching the UCST	71
Introduction	72
Experimental	75
Results and discussion	76
1. Nitroethane and nitropropane + cyclohexane	76
2. Propionitrile + CyC <sub>6</sub>	81
3. Perfluoro n-heptane + 2,2,4-trimethylpentane	84
4. Ethylacetate + n-C <sub>16</sub> and brC <sub>16</sub>	84

## TABLE OF CONTENTS (continued)

	Page
References	96
Appendix 1: Tables of results	97
Appendix 2: Program listing for $S_{CC}$ calculation	110
 Chapter 3	
Local non-randomness and excess second-order thermodynamic quantities	114
Introduction	115
$C_p^E$ at the LCST	117
$(\kappa_T V^E = -dV^E/dP)$	117
$dV^E/dT$	120
Experimental	122
Results and discussion	124
References	130
Appendix 3: Tables of results	131
 PART II	
	147
 Chapter 4	
Thermodynamic studies of alcohol self-association in proton acceptor solvents	148
Introduction	149
Experimental	162
Results and discussion	163
1. Butanol + acetonitrile	163
2. Butanol + $CCl_4$	169

## TABLE OF CONTENTS (continued)

	Page
3. Butanol + different PA	179
a. Apparent molar heat capacity	179
b. Excess heat capacity ( $C_p^E$ )	184
4. Decanol + $CCl_4$	189
5. Methanol + acetonitrile	195
References	203
Appendix 4: Tables of results	204
Chapter 5	
Thermodynamic studies of the self-association of alkylnitriles in inert and proton acceptor solvents	211
Introduction	212
Experimental	214
Results and discussion	217
1. Alkylnitrile + inert solvent	217
A. Heat capacity	217
B. Excess volumes	225
2. Alkylnitrile + active solvent	229
A. Dodecanenitrile + active solvent	229
B. Acetonitrile + $CCl_4$	235
References	241
Appendix 5: Tables of results	242
PART III	250
Chapter 6	
LCST and specific interactions in polymer-solvent and polymer-polymer mixtures	251

## TABLE OF CONTENTS (continued)

	Page
Introduction	252
Theoretical model for the prediction of the LCST	262
1. Goldstein model	262
2. New model for LCST in hydrogen bonding polymer solutions	264
A. The interactional term	264
B. The free volume term	269
Experimental	279
1. Methods	279
2. Apparatus	279
3. Materials	280
Results and discussion	281
LCST and specific interaction in polymer-solvent mixtures	281
1. Polyethylene oxide + water	281
2. Polyethylene oxide + chlorinated solvents	281
a. heat precipitation of PEO solutions	284
3. Poly(p-phenylene-ether sulfone) + dichloromethane	284
4. Poly(acyclic acid) + p-dioxane	289
5. Stabilization of a partially miscible solution by the presence of a small amount of electrolytes	292
LCST in polymer-polymer mixture: PS + PVME	292
Application of the new model described in this work	292
References	297
Appendix 6: Program listing for the ( $\chi$ -T) phase diagram	298

## TABLE OF CONTENTS (continued)

	Page
<b>Chapter 7</b>	
<b>Polymer–polymer compatibility in ternary systems:</b>	
<b>A calorimetric approach</b>	305
<b>Introduction</b>	306
<b>Experimental</b>	310
1. Materials	310
2. Methods	310
A. Heat of mixing	310
B. Heat of dilution	315
<b>Results and discussion</b>	316
1. Mixtures of poly(vinylchloride) + component 2 + THF	316
A. PVC + PCL + THF mixtures	316
B. PVC + terpolymer and copolymer of ethylene vinyl acetate (Elvaloy, Elvax) + THF	320
C. PVC + PMMA + THF	320
D. PVC + plasticizers	320
2. Mixtures containing components both having carbonyl group	321
A. Phenoxy + PCL + THF	321
B. Phenoxy + polyethylene glycol + THF	323
3. Polystyrene + PVME	325
A. Heat of mixing	325
– in Toluene	325
– in Ethylacetate	330
B. Heat of dilution	330
4. Polyisobutylene + PDMS	330
<b>References</b>	332
<b>Appendix 7: Derivation of <math>\Delta H_M</math> for ternary system</b>	333

**TABLE OF CONTENTS** (continued)

	<b>Page</b>
Contribution to original knowledge	337
Suggestions for further work	340

## LIST OF FIGURES

<u>Figures</u>		<u>Pages</u>
	<u>General Introduction</u>	
1	Molar excess heat capacity as a function of mole fraction of cyclohexane for cyclohexane + normal hexadecane at 25 and 55°C.	5
2	Schematic representation of the energy diagram for an alcohol molecule in the pure alcohol and in solution at different concentrations.	9
3	Schematic representation of the Schottky peak heat capacity for an alcohol molecule as a function of T, at different concentrations.	11
4	Molar excess heat capacity as a function of 1,4-dioxane mole fraction for dioxane + CyC <sub>6</sub> .	15
5	Schematic representation of the thermodynamic effects of the free volume contribution.	19
6	Schematic representation of the thermodynamic effects of the interactional contribution.	21
7	Schematic representation of the phase diagram for a polymer-solvent mixture.	23
8	"Closed immiscibility loop" phase diagram of iso-butylether in water.	26

**Figures****Pages****Chapter 1**

- 1 Schematic  $C_p^E$  against mole fraction curves (a) non-random contribution; (b) random contribution; (c) total W-shape; (d) curve having two regions of positive curvature separated by one of negative curvature. 41
- 2 Excess molar heat capacities of acetone + 2,2,4,4,6,8,8-heptamethylnonane at 10 and 25°C. 47
- 3 Excess molar heat capacities for acetone + dodecane at 15 and 25°C; acetone + n-hexane at 25°C. 50
- 4 Excess molar heat capacities for alkanones + 2,2,4,4,6,8,8-heptamethylnonane at 25°C. 55

**Chapter 2**

- 1 Concentration dependence of  $S_{CC}$  as a function of mole fraction of nitroethane in cyclohexane at 25, 27, 30, 35°C and nitropropane in cyclohexane at 25°C. 77
- 2 Excess molar heat capacities of nitroethane + cyclohexane at 25, 27, 30, 35, 45°C and nitropropane + cyclohexane at 25°C. 79
- 3 Excess molar heat capacity of propionitrile + cyclohexane at 15, 25, 40°C. 82

<u>Figures</u>	<u>Pages</u>
4 Excess molar heat capacity of perfluoro n-heptane + 2,2,4-trimethylpentane at 30°C.	85
5 Concentration dependence of $S_{CC}$ for perfluoro n-heptane + 2,2,4-trimethylpentane at 25, 27, 30, 67, 92, 177°C.	87
6 Excess molar heat capacity of ethylacetate + n-hexadecane at 25°C and 2,2,4,4,6,8,8-heptamethylnonane at 25°C.	89
7 Concentration dependence of $S_{CC}$ for ethylacetate + n-heptane at 25°C.	91
8 Comparison between $S_{CC}^{-1}$ vs $\log(T-T_c)$ for nitroethane + CyC <sub>6</sub> ; acetone + n-C <sub>6</sub> ; nitrobenzene + n-C <sub>7</sub> .	93

#### Chapter 4

1a Energy diagram for an alcohol in inert solvent.	150
1b Schottky peaks for an alcohol in inert solvent.	152
2 Schematic representation of the formation of an H-bond.	156
3a Energy diagram for butanol + acetonitrile for the pure butanol and for the solutions at different concentrations and butanol + n-C <sub>7</sub> at different concentrations.	164

<u>Figures</u>	<u>Pages</u>
3b Schottky peaks for butanol + acetonitrile at different concentrations.	166
4 Comparison between experimental and theoretical $\phi_{C(\text{assoc})}$ for butanol + acetonitrile, at 25°C.	170
5a Energy diagram for butanol + CCl <sub>4</sub> , for the pure butanol and for solutions at different concentrations.	172
5b Schottky peaks for butanol + CCl <sub>4</sub> , at different concentrations.	174
6 Comparison between experimental and theoretical $\phi_{C(\text{assoc})}$ for butanol + CCl <sub>4</sub> at 25°C.	177
7a Schottky peaks for butanol in n-C <sub>7</sub> and in CCl <sub>4</sub> , acetonitrile, and octanenitrile.	180
7b Experimental $\phi_{C(\text{assoc})}$ as a function of hydroxyl concentration for butanol in inert and proton acceptor solvents, at 25°C.	182
8a Experimental excess heat capacity $C_p^E$ as a function of mole fraction of butanol for butanol + acetonitrile, CCl <sub>4</sub> , octanenitrile at 25°C.	185
8b Experimental $C_p^E$ as a function of mole fraction of butanol at high dilution of butanol + CCl <sub>4</sub> at 25°C.	187

<u>Figures</u>	<u>Pages</u>
9 Experimental $\phi_{C(\text{assoc})}$ for decanol + $\text{CCl}_4$ , and + n-C <sub>7</sub> at 25°C.	190
10 Experimental $C_p^E$ results for decanol + $\text{CCl}_4$ , at 25°C.	193
11 Experimental $C_p^E$ results for methanol + acetonitrile, at 25°C.	195
12 Theoretical and experimental $V^E$ results for butanol + acetonitrile, at 25°C.	199
13 Theoretical and experimental $V^E$ results for methanol + acetonitrile, at 25°C.	201

#### Chapter 5

1 Theoretical and experimental $\phi_c$ for C <sub>11</sub> CN + n-C <sub>10</sub> at 25 and 40°C.	218
2 Theoretical and experimental $\phi_{C(\text{assoc})}$ for C <sub>11</sub> CN + n-C <sub>10</sub> at 25 and 40°C.	220
3 Experimental $C_p^E$ for C <sub>11</sub> CN + n-C <sub>10</sub> at 25 and 40°C as a function of mole fraction of C <sub>11</sub> CN.	222
4 Experimental $V^E$ for C <sub>11</sub> CN + n-C <sub>10</sub> at 25 and 40°C and octanenitrile + n-C <sub>10</sub> at 25°C.	225

<b>Figures</b>	<b>Pages</b>
5 Theoretical and experimental $\phi_{C(\text{assoc})}$ for $C_{11}\text{CN}$ + xylene and $+ \text{CCl}_4$ at $25^\circ\text{C}$ .	230
5a Experimental $C_p^E$ for $C_{11}\text{CN} + \text{CCl}_4$ at $25^\circ\text{C}$ .	232
6 Experimental $C_p^E$ for acetonitrile + $\text{CCl}_4$ at 25 and $40^\circ\text{C}$ .	237
7 Experimental $V^E$ for acetonitrile + $\text{CCl}_4$ at 25 and $40^\circ\text{C}$ .	239

### Chapter 6

1 Closed-loop temperature-composition ( $T-\chi$ ) phase diagram.	254
2 Schematic phase diagram for a polymer-solvent system.	256
3 Schematic representation of a typical phase diagram of a polymer-polymer system.	258
4 Schematic representation of the energy diagram of the pure components and their mixtures.	265
5 Theoretical interactional $\chi$ parameter: total $\chi_{G(\text{int})}$ , $\chi_{H(\text{int})}$ , $\chi_{S(\text{int})}$ , as a function of $T$ .	270

<u>Figures</u>	<u>Pages</u>
6 Theoretical free volume X parameter, $\chi_{G(FV)}$ , $\chi_{H(FV)}$ , $\chi_{S(FV)}$ as a function of T.	275
7 Theoretical $\chi_{total}$ , $\chi_{int(total)}$ , $\chi_{FV(total)}$ as a function of T.	277
8 (T-x) phase diagram for mixture of low M.W. poly(p-phenylene ether sulfone) + dichloromethane.	285
9 (T-x) phase diagram for mixture of high M.W. poly(p-phenylene ether sulfone) + dichloromethane.	287
10 (T-x) phase diagram for mixture of poly(acrylic acid) + p-dioxane for different M.W. samples 32,000, 180,000, 250,000.	290
11 Variation of $\chi_{total}$ with T for mixture of polystyrene + polyvinyl-methylether).	294

#### Chapter 7

1 Concentration dependence of the $\chi_{12}$ parameter as a function of weight fraction of PVC for PVC + PCL at 25°C.	318
2 Experimental $\Delta H_M$ as a function of volume fraction of PS for PS + PVME at 25°C.	326
3 Variation of $\chi_{12}$ as a function of volume fraction of PS for PS + PVME at 25°C.	328

## LIST OF TABLES

<u>Tables</u>		<u>Pages</u>
	<u>Chapter 1</u>	
1	Excess molar heat capacity at constant pressure of acetone + 2,2,4,4,6,8,8–heptamethylnonane at 10 and 25°C.	49
2	Excess molar heat capacity at constant pressure of acetone + n–hexane at 25°C.	52
3	Excess molar heat capacity at constant pressure of acetone + n–dodecane at 15, 25°C.	53
4	Excess molar heat capacity at constant pressure of 2–butanone + 2,2,4,4,6,8,8–heptamethylnonane at 25°C.	57
5	Excess molar heat capacity at constant pressure of 3–hexanone + 2,2,4,4,6,8,8–heptamethylnonane at 25°C.	58
6	Excess molar heat capacity at constant pressure of 4–heptanone + 2,2,4,4,6,8,8–heptamethylnonane at 25°C.	59
7	Excess molar heat capacity at constant pressure of 5–nonanone + 2,2,4,4,6,8,8–heptamethylnonane at 25°C.	60
8	Excess molar heat capacity at constant pressure of 4–decanone + 2,2,4,4,6,8,8–heptamethylnonane at 25°C.	61
9	Redlich–Kister coefficients ( $a_1$ ) and standard deviation for $V^E$ .	64

**Tables****Pages****Chapter 2**

1	Excess molar heat capacity as a function of mole fraction of nitroethane + cyclohexane at 25°C.	98
2	Excess molar heat capacity as a function of mole fraction of nitroethane + cyclohexane at 27°C.	99
3	Excess molar heat capacity as a function of mole fraction of nitroethane + cyclohexane at 30°C.	100
4	Excess molar heat capacity as a function of mole fraction of nitroethane + cyclohexane at 35°C.	101
5	Excess molar heat capacity as a function of mole fraction of nitropropane + cyclohexane at 10°C.	102
6	Excess molar heat capacity as a function of mole fraction of nitropropane + cyclohexane at 25°C.	103
7	Excess molar heat capacity as a function of mole fraction of propionitrile + cyclohexane at 15°C.	104
8	Excess molar heat capacity as a function of mole fraction of propionitrile + cyclohexane at 25°C.	105
9	Excess molar heat capacity as a function of mole fraction of propionitrile + cyclohexane at 40°C.	106

<u>Tables</u>	<u>Pages</u>
10 Excess molar heat capacity as a function of mole fraction of perfluoro n-heptane + 2,2,4-trimethylpentane at 30°C.	107
11 Excess molar heat capacity as a function of mole fraction of ethylacetate + normal hexadecane at 25°C.	108
12 Excess molar heat capacity as a function of mole fraction of ethylacetate + 2,2,4,4,6,8,8-heptamethylnonane at 25°C.	109

### Chapter 3

1 Parameters for pure components at 25°C.	123
2 Thermodynamic quantities for ketones in normal and branched alkanes.	125
3 Thermodynamic quantities for benzonitrile and nitrobenzene in several alkanes.	127
4 Thermodynamic quantities for propionitrile, nitroethane, nitropropane + cyclohexane.	128
5 Excess volumes as a function of mole fraction of nitroethane for nitroethane + cyclohexane at 25, 30, 35°C.	132
6 Excess volumes as a function of mole fraction of nitropropane for nitropropane + CyC <sub>6</sub> at 10, 25°C.	134

<u>Tables</u>	<u>Pages</u>
7 Excess volumes as a function of mole fraction of propionitrile for propionitrile + CyC <sub>6</sub> at 15, 25, 40°C.	135
8 Excess volumes as a function of mole fraction of nitrobenzene for nitrobenzene + brC <sub>16</sub> at 40 and 50°C.	137
9 Excess volumes as a function of mole fraction of benzonitrile for benzonitrile + n-C <sub>6</sub> at 25 and 30°C.	138
10 Excess volumes as a function of mole fraction of benzonitrile for benzonitrile + n-C <sub>8</sub> at 25 and 30°C.	139
11 Excess volumes as a function of mole fraction of benzonitrile for benzonitrile + n-C <sub>16</sub> at 30 and 40°C.	140
12 Excess volumes as a function of mole fraction of benzonitrile for benzonitrile + brC <sub>16</sub> at 40 and 50°C.	141
13 Excess volumes as a function of mole fraction of acetone for acetone + n-C <sub>6</sub> at 10, 15, 25°C.	142
14 Excess volumes as a function of mole fraction of 2-butanone for 2-butanone + br-C <sub>16</sub> at 25, 30, 40°C.	144
15 Excess volumes as a function of mole fraction of 2-butanone for 2-butanone + br-C <sub>16</sub> at 25 and 40°C.	145
16 Excess volumes as a function of mole fraction of hexanone for hexanone + n-C <sub>16</sub> at 25, 30, 40°C.	146

**Tables****Pages****Chapter 4**

1	Association parameters for butanol in $\text{CCl}_4$ , acetonitrile, octanenitrile at $25^\circ\text{C}$ .	168
2	Excess heat capacities and excess volumes as a function of mole fraction of butanol in acetonitrile at $25^\circ\text{C}$ .	205
3	Excess heat capacities and excess volumes as a function of mole fraction of butanol in $\text{CCl}_4$ at $25^\circ\text{C}$ .	206
4	Excess heat capacities and excess volumes as a function of mole fraction of decanol in $\text{CCl}_4$ at $25^\circ\text{C}$ .	207
5	Excess heat capacities and excess volumes as a function of mole fraction of methanol in acetonitrile at $25^\circ\text{C}$ .	208
6	Excess heat capacities and excess volumes as a function of mole fraction of butanol in acetonitrile at $15^\circ\text{C}$ .	209
7	Excess heat capacities and excess volumes as a function of mole fraction of butanol for butanol + octanenitrile at $25^\circ\text{C}$ .	210

**Chapter 5**

1	Density and heat capacity of the pure components at 25 and $40^\circ\text{C}$ .	215
2	TX model parameters for solutions of $\text{C}_{11}\text{CN}$ at $25^\circ\text{C}$ .	224

<u>Tables</u>	<u>Pages</u>
3    Equation of state parameters for the pure components at 25°C.	228
4    Excess heat capacities and excess volumes of dodecanenitrile + n-decane at 25°C.	243
5    Excess heat capacities and excess volumes of dodecanenitrile + n-decane at 40°C.	244
6    Excess heat capacities and excess volumes of dodecanenitrile + CCl <sub>4</sub> at 25°C.	245
7    Excess heat capacities and excess volumes of dodecanenitrile + xylene at 25°C.	246
8    Excess heat capacities and excess volumes of octanenitrile + n-decane at 25°C.	247
9    Excess heat capacities and excess volumes of acetonitrile + CCl <sub>4</sub> at 25°C.	248
10   Excess heat capacities and excess volumes for acetonitrile + CCl <sub>4</sub> at 40°C.	249

<u>Tables</u>	<u>Pages</u>
<u>Chapter 6</u>	
1 Table of several systems exhibiting low temperature LCST.	261
2 Critical temperatures of polyethylene oxide + water as a function of M.W. of PEO.	282
3 Critical temperatures for polyethylene oxide + chlorinated solvent as a function of M.W.	283
4 Temperature – Composition – Phase diagram including free volume for PS–PVME mixture.	293
<u>Chapter 7</u>	
1 Chemical structure of the polymers and their analogs.	311
2 List of polymers and solvents used and their sources.	313
3 Heat of mixing and interaction parameter $\chi_{12}$ for mixtures of PVC + polymer 2 in THF at 25°C as a function of weight fraction of PVC.	317
4 Heat of mixing for mixtures composed of phenoxy + polymer 2 or their analogs in THF as a function of weight fraction of phenoxy at 25°C.	322
5 Heat of mixing as a function of phenol for mixtures of phenol + component 2 in THF at 25°C.	324

GENERAL INTRODUCTION

The amount of heat supplied per unit rise of temperature to heat a unit of a material is called heat capacity. As shown by eqns. 1 and 2 respectively, the heat capacity at constant pressure,  $C_p$ , corresponds to the temperature dependence of the enthalpy (H), the entropy (S) times T and to the curvature of the free energy at constant pressure times T.

$$C_p = T \left[ \frac{\partial S}{\partial T} \right]_p = \left[ \frac{\partial H}{\partial T} \right]_p = -T \left[ \frac{\partial^2 G}{\partial T^2} \right]_p \quad (1)$$

$$C_v = T \left[ \frac{\partial S}{\partial T} \right]_v = \left[ \frac{\partial U}{\partial T} \right]_v = -T \left[ \frac{\partial^2 A}{\partial T^2} \right]_v \quad (2)$$

Thermodynamic order or "structure" in a liquid should lower H and S of the liquid but must decrease with increase of T. For instance, molecular alignment must decrease with increase of T. Any such break-up of structure requires energy and hence  $C_p$  is enhanced. Therefore, heat capacity reveals itself to be a good indicator of structure. Structural effects are, however, rather difficult to detect in the pure components, since they are usually small compared with the internal heat capacities of the molecules themselves. However, structure is usually affected if the liquid is mixed with another. For instance, the molecular alignment found in chain-molecule liquids is destroyed by mixing with a spherical molecule liquid. We are therefore led to consider the change of  $C_p$  brought about by mixing two liquids.

While  $\Delta C_p$  (or  $\Delta C_v$ ) of the solution is the actual change observed during the mixing of the components, expressed per mole, the excess heat capacity ( $C_p^E$ ) is defined as the difference between the molar  $C_p$  for the experimental solution and its value for an "ideal" solution formed through an ideal mixing process. Since  $\Delta C_p$  is zero for an ideal solution,  $\Delta C_p = C_p^E$ , and one can think of  $C_p^E$  as just the change of  $C_p$  due to mixing.

A large body of excess heat capacity data at constant pressure ( $C_p^E$ ) have been reported in the last decade. The reason for this recent emergence of  $C_p^E$  results is the extreme difficulty faced in the past for the direct measurement of the heat capacity. Apart from very few exceptions, for instance, the pioneering work of Ziegler on alcohol mixtures<sup>1</sup>, data reported suffered from lack of precision and few direct measurements of  $C_p$  were mentioned. This function was usually obtained from  $H^E$  measurements made at different temperatures. However, the Picker flow microcalorimeter, now, enables direct measurements for  $C_p$  of both the solution and the pure components and  $C_p^E$  can be calculated from these results. The principle and the procedure are simple and described in references 2 and 3. Very recently, Patrick Picker won the Manning Award in recognition of his brilliant invention<sup>4</sup>.

Excess heat capacity at constant volume ( $C_v$ ) could also be used as an indicator of structure. However, direct measurement of  $C_v$  is difficult since it is impossible to make a vessel strong enough to confine the liquid to constant volume as the temperature is raised.

We will study, in the next section, two kinds of structure: structure due to molecular association or due to molecular antipathy.

Many  $C_p^E$  data reported in the last decade show these structural effects in different types of mixtures. In the next section, we will make a review of several  $C_p^E$  results in terms of structure.

## I. STRUCTURE DUE TO ASSOCIATION

Mixtures of non-electrolytes are often classified into two broad groups depending on whether the constituent molecules form or do not form hydrogen bonds. Alkane mixtures belong to the weakly associated, or unassociated group, while H-bond molecules (alcohols for instance), constitute strongly associated groups.

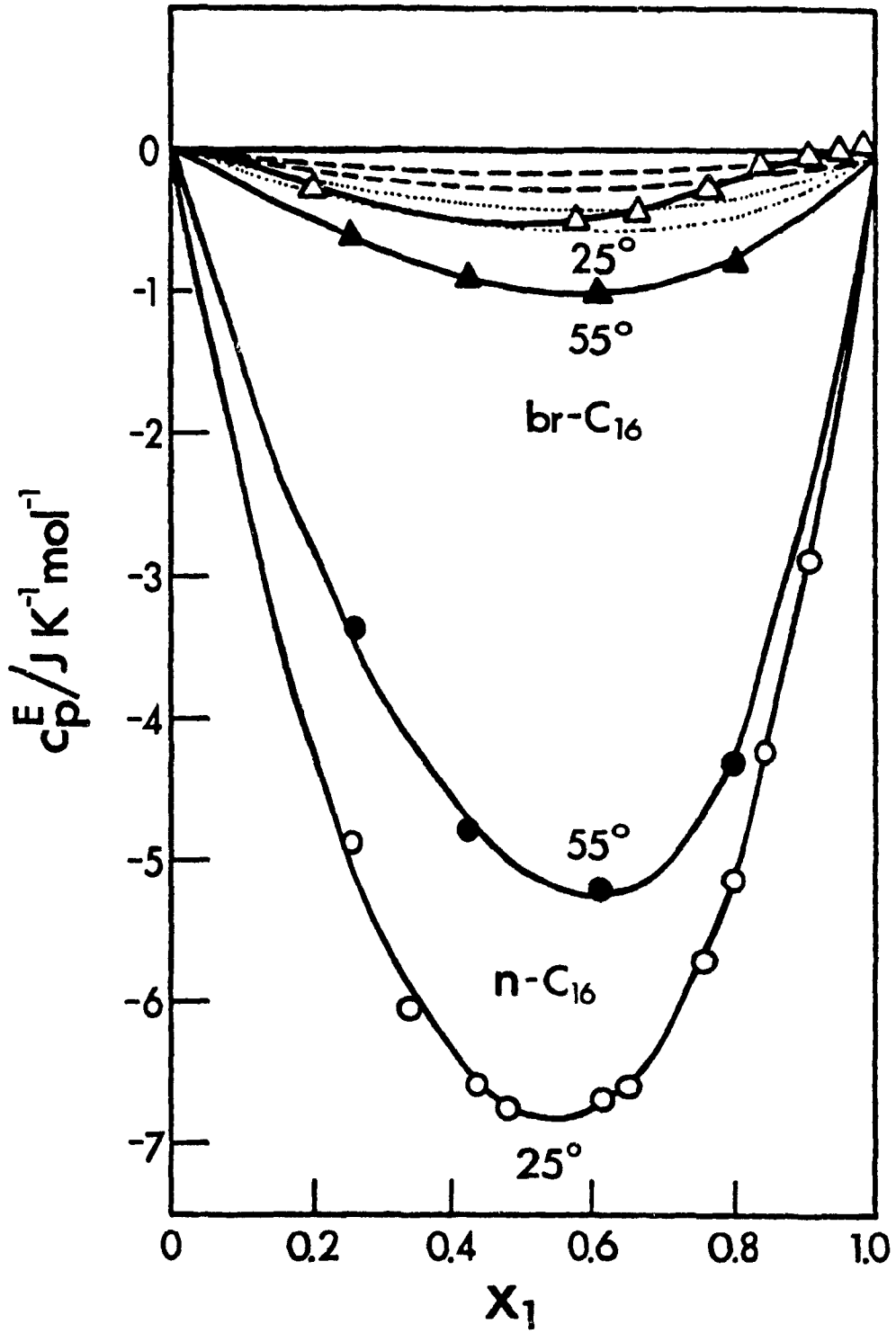
### 1. Weak association

Mixtures containing exclusively alkane molecules are governed mainly by dispersion forces or van der Waals forces. However, both thermodynamic and depolarized scattering measurements indicate that when components 1 and 2 are both n-alkanes the contact energy for the 1-1, 2-2 and 1-2 pairs are all affected by correlations of molecular orientation (CMO), i.e. intermolecular alignment.

#### A. Destruction of order in n-alkanes

If a long chain n-alkane is mixed with a quasi-spherical molecule, a "structure-breaker" such as cyclohexane or 2,2-dimethylbutane, the 1-2 pairs are uncorrelated, i.e. there is a destruction of CMO during the mixing process. It has been shown by calorimetric and depolarized Rayleigh scattering measurements<sup>5-8</sup> that the n-alkane order decreases with temperature. Therefore,  $C_p^E$  is not only a structure indicator but also provides information on its temperature dependence. Mixtures composed of a long chain n-alkane such as n-C<sub>16</sub> + CyC<sub>6</sub>, as shown in Fig. 1, exhibit strongly negative  $C_p^E$  indicating a destruction of CMO in the pure n-C<sub>16</sub> when mixed with CyC<sub>6</sub><sup>9</sup>. However, as T increases,  $C_p^E$  becomes less negative indicating a rapid

Fig. 1 Molar excess heat capacity as a function of mole fraction of cyclohexane for cyclohexane + normal hexadecane at 25 and 55°C.  
Data from ref. 9.



decrease in CMO in the pure n-alkane as T is increased.

## B. Creation of order in mixtures containing alkane molecules

Mixtures containing a highly branched and sterically hindered alkane + a "plate-like" molecule such as cyclopentane or + a short chain normal alkane ( $n \leq 10$ ) show surprising results. For instance, 3,3-dimethylpentane + cyclopentane mixture shows negative  $H^E$  and positive  $C_p^E$  indicating the creation of order in this mixture<sup>10</sup>. 1-chloronaphthalene + n-C<sub>n</sub> systems show again positive  $C_p^E$ <sup>11</sup>. However, the same trend is not observed when 3,3-dimethylpentane is mixed with CyC<sub>6</sub> or CyC<sub>8</sub>,  $H^E$  is conversely positive and  $C_p^E$  negative<sup>10</sup>. Patterson et al<sup>12</sup> suggested that a rotational order was created associated with a hindrance of the rotation of the flat cyclopentane molecule by the flat or sterically-hindered molecule.

### 2. Strongly associated mixtures

The associating forces are now mainly H-bonds, much stronger than the dispersion forces seen previously. In these systems structure is imposed through the H-bonds: H-bonds resulting from self-association of alcohol molecules or from complex formation when the alcohol molecules are mixed with a proton-acceptor solvent. Both types of association lead to the same  $C_p^E$  pattern.

Both the concentration and the temperature dependences of  $C_p^E$  can be predicted and explained by a simple association theory such as the Treszczanowicz and Kehiaian (TK) model<sup>13</sup>. The apparent molar heat capacity ( $\phi_c$ ) is the heat capacity of the alcohol molecule itself in the solution ( $\phi_c = C_p^E/x_1 + C_p^0$ ), while  $C_p^E$  is the comparison between the  $\phi_c$  in solution with the heat capacity of the molecules in the pure alcohol

$(C_p^0)$ . The limit of  $\phi_C$  as  $x \rightarrow 0$  gives the heat capacity of the isolated alcohol molecule, i.e. without any association effects. Then,

$$\phi_{C(\text{assoc})} = \phi_C - \lim_{x \rightarrow 0} \phi_C$$

$\phi_C$  is a more useful quantity than  $C_p$ , since the associational part of  $\phi_C$  can be deduced and hence the nature of the association process involved in both the pure state and the solution.

In the TK model, two energy levels are assigned to each molecule: the dissociated and the associated states. Fig. 2 gives a schematic representation of the energy diagram for an alcohol molecule in the pure alcohol liquid and in solution at different concentrations. At very low temperature, the energy level is low corresponding to strong H-bonds between the alcohol molecules. As T is increased, the energy of the alcohol molecule increases for both the pure alcohol and the solutions, indicating a breaking up of the H-bonds as T is raised.

A similar analysis can be made for  $\phi_{C(\text{assoc})}$  as a function of T and concentration. The slopes of the energy curves  $\frac{dU}{dT}(\text{assoc})$  correspond to  $\phi_{C(\text{assoc})}$  of the solution. The schematic representations of  $\phi_{C(\text{assoc})}$  vs T (Fig. 3) showing "Schottky peaks", are good indicators of structure, which is strongly concentration dependent. At a given temperature, three different patterns can be deduced depending upon the concentration considered. At the ambient temperature, at extremely low concentration, the alcohol molecules are all almost completely dissociated; there is no structure since no H-bond exists.

As the concentration is increased, more H-bonds are formed and the maximum of the Schottky peak at ambient T is bigger indicating that more structure has been formed. However, as the concentration of alcohol molecules increases further, fig. 3

Fig. 2 Schematic representation of the energy diagram for an alcohol molecule in the pure alcohol (O) and in solution, at different concentrations III (low concentration,  $x < 0.01$ ), II (intermediate,  $0.01 < x < 0.1$ ), I (high concentration,  $x > 0.1$ ).

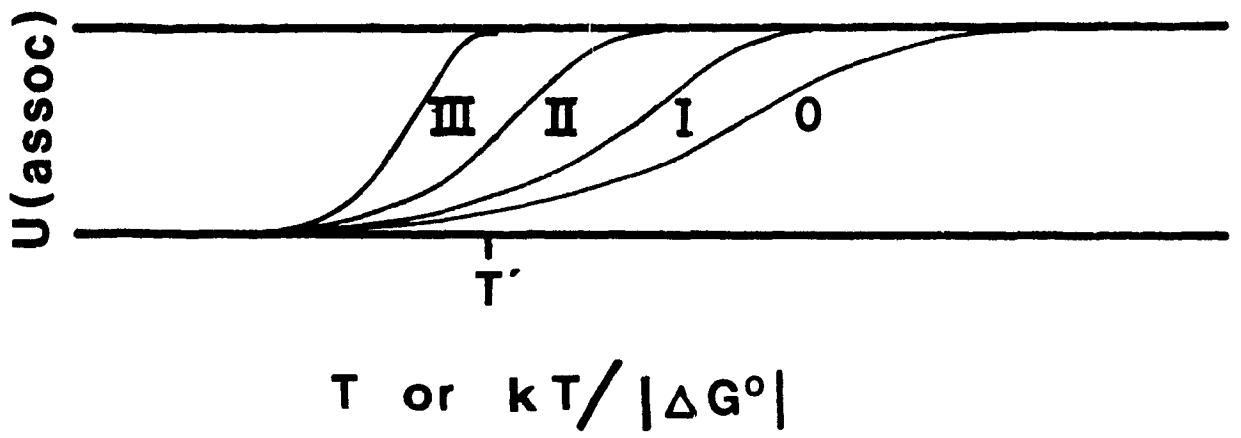
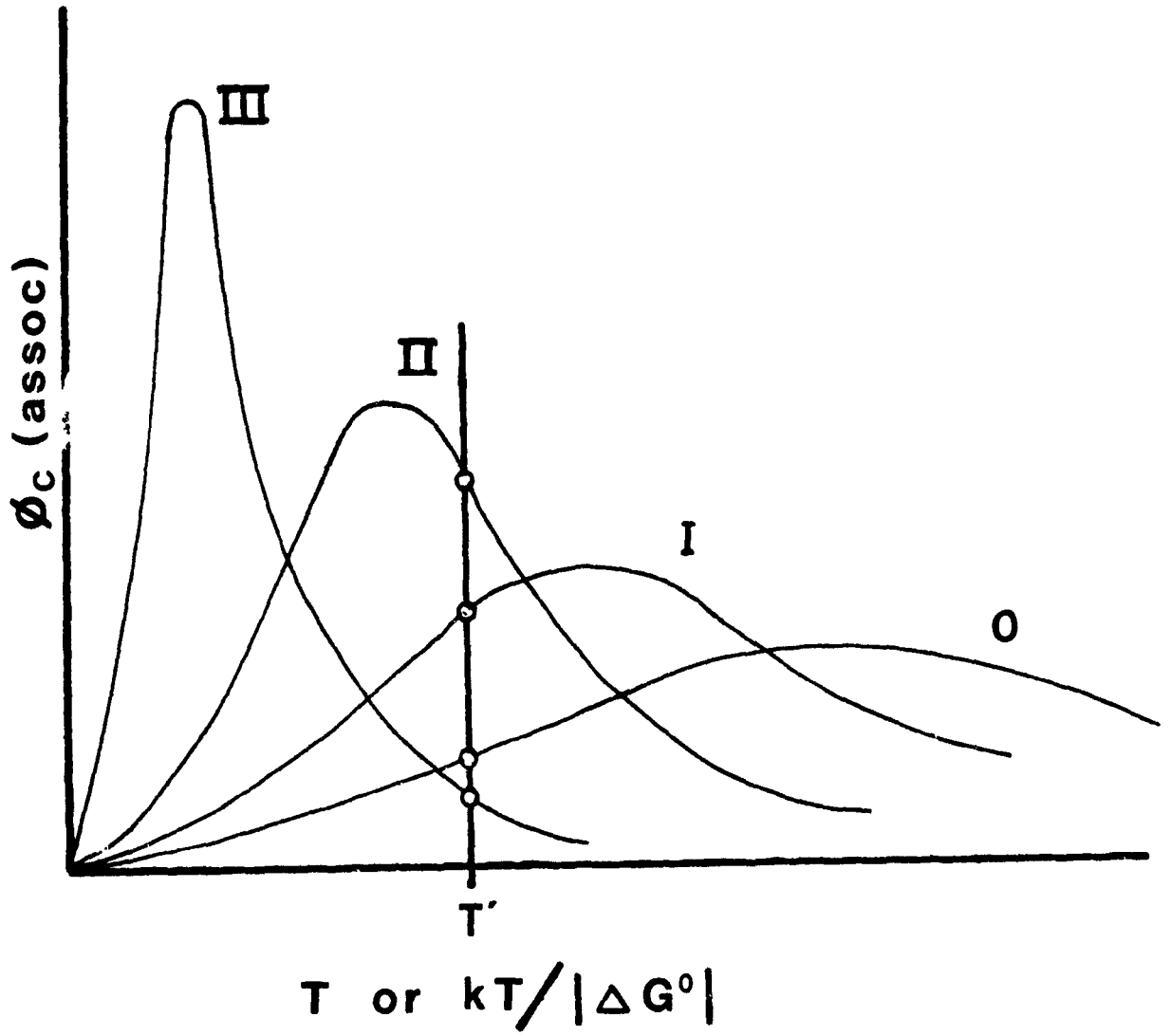


Fig. 3 Schematic representation of the Schottky peak heat capacity for an alcohol molecule as a function of T, at different concentrations: (0, pure), (III, low), (II, intermediate), I (high).



shows that  $\phi_{C(\text{assoc})}$  decreases in spite of increasing H-bonding. This may be interpreted as corresponding to a decrease of "structure" or non-randomness since association of alcohol molecules now takes place over shorter distances in the solution. At a given T,  $C_p^E$  is obtained as the difference between the Schottky peak at a given concentration and the Schottky peak for the pure alcohol. According to the model,  $C_p^E$  has to be negative at low concentration indicating a breaking down of structure existing in the pure alcohol. As the concentration is increased,  $C_p^E$  becomes positive indicating that more structure is involved in the solution.

## II. STRUCTURE DUE TO MOLECULAR ANTIPATHY

Grolier et al<sup>14</sup> have found an unusual concentration dependence of  $C_p^E$  called W-shape. Fig. (4) shows an example of a W-shape  $C_p^E$  for dioxane + n-alkanes. The W-shape  $C_p^E$  is usually composed of a positive maximum between two minima of opposite signs. Even without the maximum and the minima, two regions of positive curvature may occur separated by a region of negative curvature

Very recently, a large body of W-shape  $C_p^E$  data have been reported. Grolier et al studied several systems going from alkanones + n-alkanes<sup>15</sup>, alkanoates + n-alkane<sup>16</sup> and very recently, alkanoates + cyclohexane or + branched alkanes<sup>17</sup>. Other branched ethers or esters + normal or branched alkanes have also been reported by Benson et al<sup>18</sup> and Kohler and collaborators<sup>19</sup>.

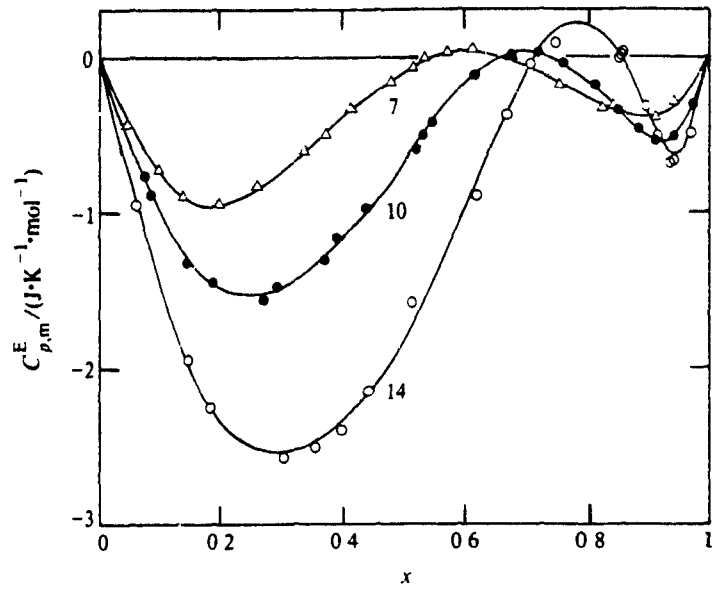
Grolier attributed the origin of the W-shape  $C_p^E$  to conformational changes in either of the two component molecules. Component 1 is usually polar, while component 2 may be a normal, branched or cyclic alkane. Indeed, the normal alkanes have the capability of undergoing transitions between the trans and gauche conformers. However, no such conformers exist for the branched isomers; and cyclohexane merely interconverts between two equivalent chair conformations.

Therefore the W-shape observed for systems composed of a short molecule like acetone or methylacetate + a sterically hindered branched alkane or + cyclohexane can be hardly attributed to conformational change, since neither of the two component molecules can undergo such transitions.

Nevertheless, a common feature observed for all these W-shapes is that they all exhibit large heat of mixing and large excess free energy. The present thesis will suggest that there are two main contributions to the thermodynamics:

One is the usual or normal random contribution which is positive on  $H^E$ . It is found negative on  $C_p^E$  for weakly association. However for strong association, the

Fig. 4 Molar excess heat capacity as a function of 1,4-dioxane mole fraction for dioxane + n-alkanes.  $\Delta$ , n = 7;  $\bullet$ , n = 10;  $\circ$ , n = 14. From ref. 14.



random contribution has been observed to be negative at low concentration and positive at higher concentration.

The second contribution is attributed to non-randomness. Such non-randomness would be associated with large heat of mixing and large excess free energy. As the temperature increases, non-randomness should decrease rapidly, leading to more positive values of  $H^E$  and  $S^E$ . Therefore, the non-randomness contribution to  $C_p^E$  would be positive, and decreases as  $T$  increases, hence  $d C_p^E/dT < 0$ . According to the Quasi-Chemical approximation of Guggenheim<sup>20</sup>, the non-randomness contribution to  $C_p^E$  is positive and vanishes at both ends of the concentration range, where only one component is at high dilution in the other one. Then the two components are completely randomly distributed. Non-randomness may then play a role in the concentration dependence of  $C_p^E$ .

We would like therefore to propose as an alternative to the conformational change explanation, the possibility that W-shape  $C_p^E$  is due to local composition non-randomness in solution associated with large  $H^E$  and large  $G^E$ . This local composition non-randomness is viewed as a manifestation of the critical state occurring far ( $\sim 100^\circ\text{C}$ ) from  $T_c$ . However the non-randomness contribution should go to infinity as the solution approaches the UCST or the LCST.

### III. STRUCTURE IN POLYMER SYSTEMS

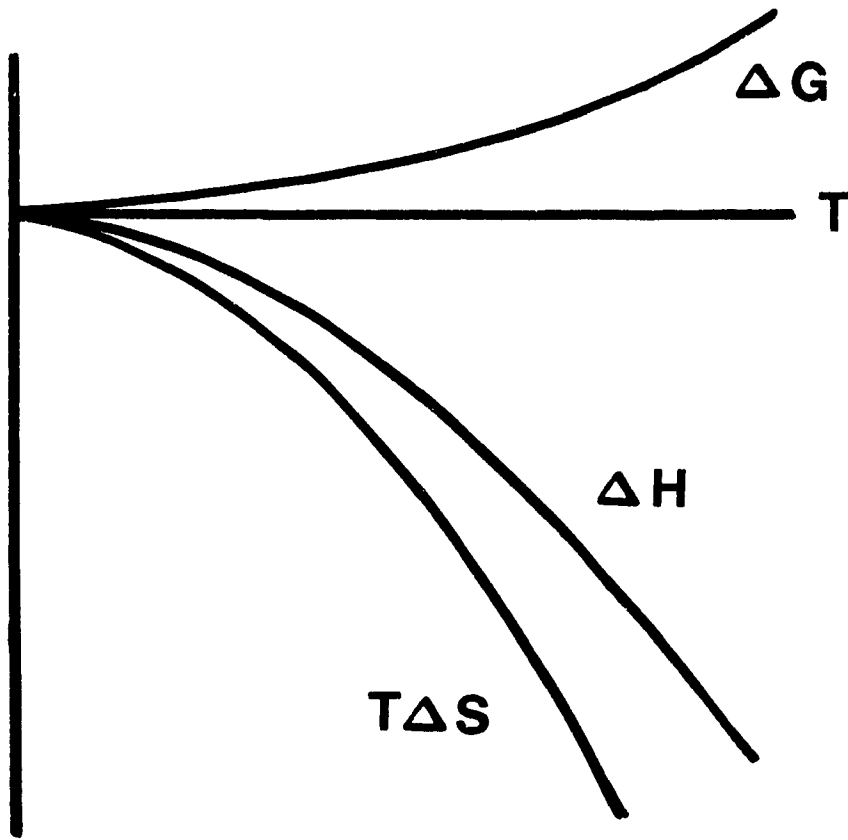
As for small molecule systems, structural effects can be viewed for polymer molecules in both pure state and solution. Structure in polymer solution or polymer blends is imposed by two factors: (1) the free volume contribution arising when a dense liquid (polymer) is mixed with an expansible liquid (solvent). The solvent collapses around the polymer. This contraction of the solvent gives rise to thermodynamic effects represented schematically on Fig. 5. The contributions to either volume, heat or entropy of mixing are negative, but the contribution to the free energy is positive<sup>21</sup>. The free volume contribution, increases with increase of T and goes to infinity as T approaches the liquid–vapour critical temperature of the solvent, (2) the second factor is interactional and it is due to the antipathy or dissimilarity between "unlike" contacts. The interactional term has almost always a positive contribution on  $H^E$  except for strongly interacting systems. Its effect on entropy is small. Therefore, the contribution to the free energy is positive. The thermodynamic effects of the interactional term are shown on Fig. 6.

The contact dissimilarity and the free volume difference lead to phase separation on either lowering the temperature to a UCST or on raising the temperature to a LCST. Fig. (7) shows the usual phase diagram for a polymer–solvent system. The stability of polymer solutions can be predicted by the basic Flory–Huggins theory<sup>22</sup>, and studied through the interaction parameter ( $\chi$ ). The  $\chi$  parameter is taken as the summation of enthalpy and entropy contributions. In other words,  $\chi$  should reflect the contributions coming from both the interactions and the free volume terms.

#### Structure and LCST

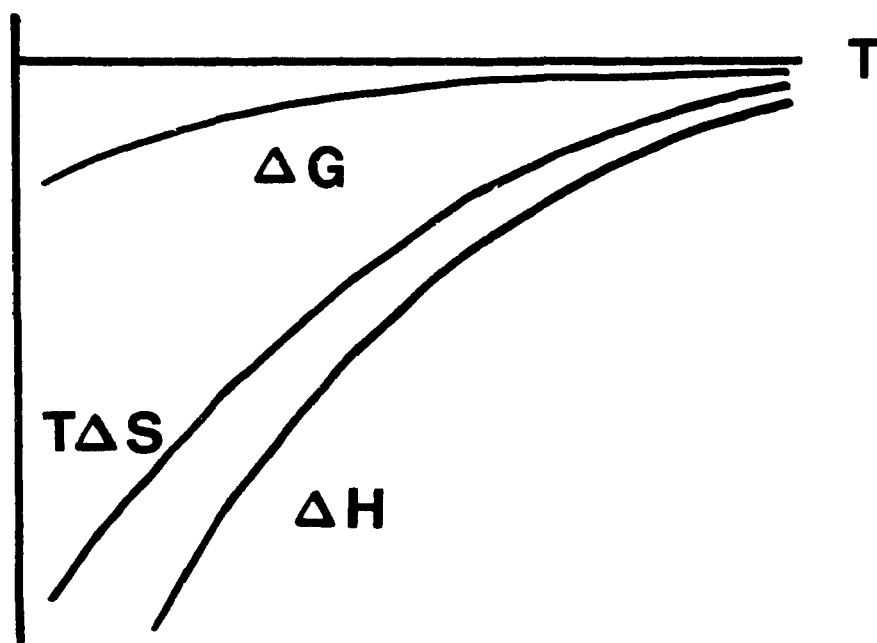
Structure is strongly temperature dependent. At high T, the free volume

Fig. 5 Schematic representation of the thermodynamic effects of the free volume contribution.



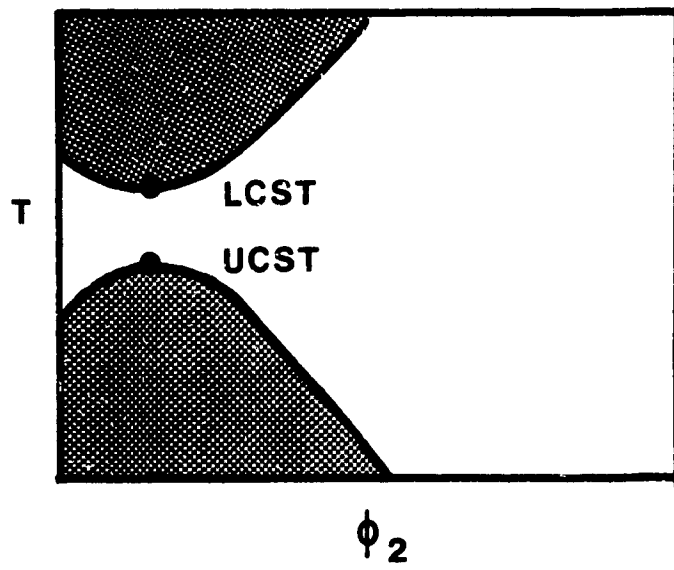
$$\Delta G = \int_0^T -S dT \quad (>0)$$

Fig. 6 Schematic representation of the thermodynamic effects of the interactional contribution.



$$\Delta G = \int_{\infty}^T -S \, dT \quad (< 0)$$

Fig. 7 Schematic representation of the phase diagram for a polymer-solvent mixture.



contribution increases and becomes more positive. According to eqn. 1,

$$\Delta G = \int_0^T -SdT > 0 \quad (1)$$

With  $\Delta G$  due to free volume being zero at low  $T$ , hence the 0 being the lower limit for temperature. As  $T$  increases,  $\Delta G$  becomes more positive leading to an unstable solution, this instability yields an LCST at higher temperature which is a consequence of the free volume dissimilarity increasing with  $T$  and opposing mixing. This increasing free volume structure at high  $T$  opposes the mixing process.

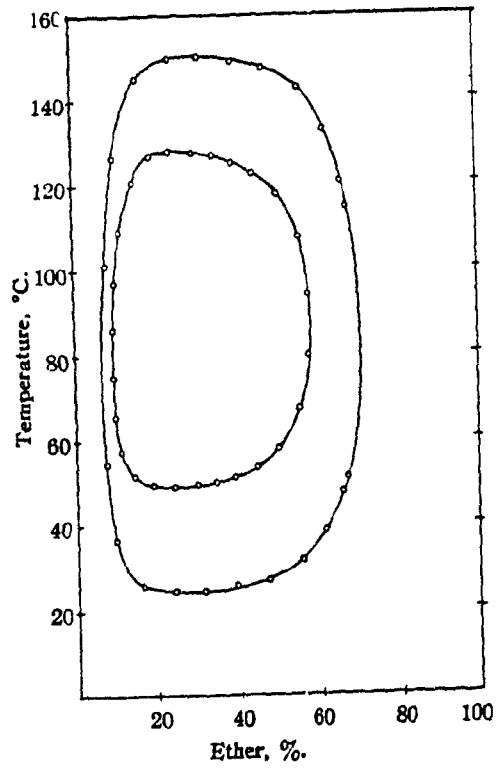
However, polar molecules or molecules containing acceptor or donor groups yield, on mixing, to relatively strong interactions. This is true for either small molecule mixtures or mixtures containing at least one polymer molecule. Thermodynamic properties of these mixtures reflect these specific interactions. For instance, mixtures of polyethylene oxide or ethylene oxide with chlorinated hydrocarbon ( $\text{CCl}_4$ ,  $\text{CHCl}_3$ ) show negative heat of mixing and strongly negative free energy of mixing and therefore negative  $\Delta S_M$ . Hence, specific interactions between the chlorinated group and the free electron pair on oxygen lead to specific interactions between the components.

Thermodynamic effects of these specific interactions are negative in both  $H$  and  $S$ . They are positive in  $C_p$ , but reach a maximum at low  $T$  and decrease as  $T$  increases. Hence specific interactions involve structure to the mixtures at low temperature. And structure decreases as  $T$  increases. Further, it can be seen from eqn. 2

$$\Delta G = \int_{\infty}^T -SdT < 0 \quad (2)$$

where here the structure is zero at high temperature, hence the lower limit of  $\infty$  for the

Fig. 8 "Closed immiscibility loop" phase diagram of iso-butyl ether in water.  
The inner curve is that of n-butylether; the outer is that of iso-butylether.



temperature that going from infinity to a given T,  $\Delta G$  becomes more and more negative. Lowering T confers stability to the systems. Indeed, structure at low T favors mixing. This low temperature structure is then directly related to the specific interactions taking place in the mixtures. As T increases a LCST is reached but which has a different origin from the usual free volume LCST.

However, numerous aqueous systems (small molecules) have been reported, which show a so-called "closed immiscibility loop"<sup>23</sup> (Fig 8). The solution shows a one-phase-region at low temperature up to a LCST, while a two-phase-region is observed until a UCST is reached as T increases. The solution is then miscible again. This type of LCST is observed for strongly interacting systems. Apart from very few exceptions, the small molecule systems exhibiting this low temperature LCST are all aqueous systems, suggesting that "iceberg" formation might be responsible for the LCST when water is the solvent.

It has been observed that almost all the compatible pair of polymers exhibit a LCST as T is raised. The origin of LCST constitutes a controversial matter. It was suggested that the LCST in polymer-polymer system was a free volume effect. But the free volume difference in these systems is almost negligible. Therefore, we would rather believe that this LCST is related to specific interactions between the polymers.

The purpose of this part of the thesis is to study thermodynamic effects of structure in different types of mixtures. The thesis is divided into three different parts.

Part One is concerned with systems in which structure is due to molecular antipathy, these systems almost all show a UCST. Effect of non-randomness in solution is studied, its contribution on second-order quantities is widely investigated, in Chapters 1 to 3.

Chapter 1 deals with W-shape  $C_p^E$  for a homologous series of ketones ( $C_1$  to  $C_{10}$ ) in normal and branched alkanes. These mixtures, where no conformational

changes can be observed, were chosen to discuss the validity of this explanation of W–shape. Furthermore, the role of a local composition non–randomness on  $C_p^E$  shape is discussed.

In Chapter 2, the role of non–randomness is further discussed. Non–randomness is taken as a manifestation of the critical state at temperature far removed from the critical point ( $\sim 100^\circ\text{C}$ ). Mixtures containing different moderately associated components were investigated at different temperatures and specially in the vicinity of the UCST. Correspondence is made between  $C_p^E$  and  $S_{CC}$  (concentration–concentration structuring factor) for several systems near their UCST.  $S_{CC}$  is shown to be also an indicator of structure and a direct measurement of local composition non–randomness.

In Chapter 3, the non–randomness effect is studied towards other second order quantities such as excess thermal expansivity and excess compressibility. It is discussed the eventual occurrence of W–shape for these quantities.

Part Two deals with mixtures in which structure comes from association: self–association (inert solvents) or complex formation in active solvent.

Chapter 4 treats the self–association of butanol and decanol in acetonitrile and carbon tetrachloride.  $\text{CCl}_4$  is taken as active solvent, conversely to spectroscopists who have always considered  $\text{CCl}_4$  as an inert solvent. The results are discussed in terms of the TK model.

Chapter 5 discusses the self–association of dodecanenitrile in inert and active solvent. The results are discussed in terms of the TK model.

Part Three of the thesis is concerned with structural effects involved in polymer systems.

Chapter 6 deals with the controversial origin of the LCST observed in polymer

mixtures. The Goldstein's approach based on the Flory-Huggins theory is adapted to polymer solvent and polymer-polymer mixtures. The model takes into account not only the interactional term as in its previous form, but also the free volume term which is important for polymer-solvent system. The new model which is well described in Chapter 6 gives excellent predictions for well-known polymer pairs. It is able to predict the specific interaction LCST (low T), the UCST and the free volume LCST (high T) for systems exhibiting a closed-loop of immiscibility. Furthermore, the model predicts the specific interaction LCST in polymer-polymer mixtures. It is clearly shown that the LCST observed in polymer-polymer mixtures or polymer blends is due rather to specific interactions than to free volume.

In Chapter 7, the effect of solvent on polymer compatibility is investigated through calorimetric studies in a ternary system where several pairs of compatible polymers are used. Heat of mixing and heat of dilution data are presented.

REFERENCES

1. S.C.P. Hwa and W.T. Ziegler, *J. Phys. Chem.*, 70, 8, 2572, 1966.
2. J.L. Fortier and G.C. Benson, *J. Chem. Thermodyn.*, 8, 411, 1976.
3. P. Picker, J.-P. Leduc, P.R. Philip, and J.E. Desnoyers, *J. Chem. Thermodyn.*, 3, 631, 1971.
4. *Commerce*, p. 94, Mai 1988.
5. V.T. Lam, P. Picker, D. Patterson, and P. Tancrede, *J. Chem. Soc. Faraday Trans. 2*, 70, 1465, 1974.
6. M.D. Croucher and D. Patterson, *J. Chem. Soc. Faraday Trans. 2*, 71, 985, 1975.
7. P. Tancrede, P. Bothorel, P. de St. Romain, and D. Patterson, *J. Chem. Soc. Faraday Trans. 2*, 73, 15, 1977.
8. P. Tancrede, D. Patterson, and P. Bothorel, *J. Chem. Soc. Faraday Trans. 2*, 73, 29, 1977.
9. S.N. Bhattacharyya and D. Patterson, *J. Solution Chem.*, 9, 247, 1980.
10. P. de St. Romain, H. Van Tra, and D. Patterson, *J.C.S. Faraday Trans. I*, 75, 1700, 1979.
11. G. Tardajos, E. Aicart, M. Costas, and D. Patterson, *J. Chem. Soc. Faraday Trans. 1*, 82, 2977, 1986.
12. S.N. Bhattacharyya, M. Costas, D. Patterson, and H.-V. Tra, *Fluid Phase Equilibria*, 20, 27, 1985.
13. H. Kehiaian and A.J. Treszczanowicz, *Bull. Acad. Chim. Fr.*, 1561, 1969.
14. A. Inglese, J.-P. E. Grolier, E. Wilhelm, *J. Chem. Thermodyn.*, 16, 67, 1984.
15. J.-P. E. Grolier and G.C. Benson, *Can. J. Chem.*, 62, 949, 1984.
16. M.C. Baluja, R. Bravo, M. Pintos, M.I. Paz-Andrade, G. Roux-Desgranges, and J.-P. E. Grolier, *Calorim. Anal. Therm.*, 16, 138, 1985.
17. M. Pintos, R. Bravo Baluja, M.I. Paz-Andrade, G. Roux-Desgranges, and J.-P.

- E. Grolier, *Can. J. Chem.*, 66, 1179, 1988.
18. F. Kimura, P.J. D'Arcy, M.E. Sugamori, and G.C. Benson, *Thermochim. Acta*, 64, 149, 1983.
  19. H. Kalali, F. Kohler, P. Svejda, *Fluid Phase Equilibria*, 20, 75, 1985.
  20. E. Guggenheim, *Mixtures*, Clarendon Press, Oxford p. 83, 1952.
  21. D. Patterson, *Polymer Eng. Sci.*, 22, #2, 64, 1982.
  22. P.J. Flory, *Disc. Faraday Soc.*, 49, 7, 1970.
  23. H.L. Cox and L.H. Cretcher, *J.A.C.S.*, 48, 451, 1926.

C

C

PART I

C

CHAPTER 1

THE W-SHAPE CONCENTRATION DEPENDENCE OF  $C_p^E$   
AND SOLUTION NON-RANDOMNESS:  
KETONES + NORMAL AND BRANCHED ALKANES

**ABSTRACT**

The excess heat capacity ( $C_p^E$ ) has been measured for acetone + 2,2,4,4,6,8,8–heptamethylnonane (br- $C_{16}$ ) (10 and 25°C), + n- $C_{12}$  (15 and 25°C) + n- $C_6$  (25°C).  $C_p^E$  is large and positive but becomes negative at both extremes of the concentration range, i.e. it is W-shaped. It becomes rapidly more positive on lowering T, approaching phase separation at the UCST. br- $C_{16}$  mixed with 2–butanone, 3–hexanone, 4–heptanone and 5–nonanone also give W-shaped  $C_p^E(x)$  curves although the negative  $C_p^E$  appearing at very high ketone mole fraction (0.95) are extremely small, less than  $0.05 \text{ J K}^{-1} \text{ mol}^{-1}$ . As the length of the ketone molecule is increased, the W-shape becomes less pronounced and has disappeared for br- $C_{16}$  + 4–decanone where  $C_p^E$  is negative throughout the composition range. The present systems, which show W-shape  $C_p^E$ , and those in the literature, have large equimolar  $H^E$  values,  $\approx 1000 \text{ J mol}^{-1}$  or larger, and often are close to phase separation. It is suggested that the W-shape arises from two  $C_p^E$  contributions. One is negative and of parabolic concentration dependence. The other, due to non-randomness and associated with extremely large  $H^E$  and  $G^E$  values, is shown by the Guggenheim quasi-chemical theory to be positive, concave downwards in the middle of the composition range, but concave upwards at the extremes, i.e. it has the correct concentration dependence to give W-shape. The excess volume has been measured for acetone + br- $C_{16}$ , + n- $C_{12}$  and + n- $C_6$ . It is large and positive while  $dV^E/dT$ , for systems near the UCST, is more positive than predicted by the Flory Theory, i.e. its behavior is analogous to  $C_p^E$ . It is suggested that: (1) polar (but not H-bonded) systems where  $H^E$  is very large,  $\approx 1000 \text{ J mol}^{-1}$  or larger should exhibit the W-shape  $C_p^E$ , becoming more pronounced with decrease of temperature, and (2) the curvature of  $H^E/x_1x_2$  against x should be positive and large, increasing with decreasing T.

## INTRODUCTION

Grolier, Wilhelm and their collaborators have recently found many systems for which the concentration dependence of the excess heat capacity ( $C_p^E$ ) has a "W-shape", i.e. two minima occur, separated by a maximum. Even without the minima and maximum, two regions of positive  $C_p^E(x)$  curvature may occur, separated by a region of negative curvature. Both types of concentration dependence are shown schematically in Fig.1. The systems have usually comprised normal or cycloalkanes mixed with a chemically dissimilar liquid: 1,4-dioxane (Inglese and Grolier, 1984; Inglese et al., 1984) and trioxanonane (Kimura et al., 1983), but not oxane (Inglese and Grolier, 1984); 2-butanone and 3-pentanone (Grolier and Benson, 1984); 1,2-dichloroethane (Lainez et al., 1985c); 1,1,2,1-tetrachloroethane (Lainez et al., 1984); 1,4-dichlorobutane (Lainez et al., 1985d); 1,6-dichlorohexane (Lainez et al., 1985a), but not 1-chlorobutane (Lainez et al., 1985d). Other systems have been 2,2,4-trimethylpentane + bisdichloroethylether (Kalali et al., 1985), and methyl acetate + 1-decanol (Deshpande, unpublished results). Clearly this surprising concentration dependence of  $C_p^E$  is of wide occurrence. It has been suggested (Grolier et al., 1982; Lainez et al., 1985c,d; Wilhelm, 1985) that the phenomenon is associated with a component existing as conformers of different polarity, the relative proportions of which are changed through mixing with the other component, e.g. the alkane, which itself is capable of conformational change.

## EFFECT OF SOLUTION NON-RANDOMNESS

While agreeing that conformational change may play an important role in the thermodynamics of mixtures, we would like nevertheless to propose another possibility for consideration, namely that the W-shape may be due to a deviation of local from bulk composition, i.e. non-randomness in the solution. Such non-randomness would be associated with extremely large positive  $H^E$  and  $G^E$  values, occurring when a polar or associated liquid is mixed with an inert solvent. Values of  $H^E$  are available for almost all the systems which show the W-shape  $C_p^E$  and at equimolar concentration are in the 1000–2000 J mol<sup>-1</sup> range. Where equimolar  $G^E$  are available they lie in the 800–1200 J mol<sup>-1</sup> range, and  $S^E$  is typically positive in these mixtures. Thus, for 1,4-dioxane + cyclohexane (Andrews and Morcom, 1971) at 25°C the equimolar  $H^E$  and  $G^E$  are, respectively, 1600 and 1000 J mol<sup>-1</sup> while oxane + cyclohexane (Cabani and Ceccanti, 1973), which does not show the W-shape, has an equimolar  $H^E$  of 463 J mol<sup>-1</sup>. Similarly, for 1,4-dichlorobutane + n-C<sub>7</sub> (Grolier and Kehiaian, 1973), the equimolar  $H^E$  is  $\approx$  1500 J mol<sup>-1</sup> at 25°C while 1-chlorobutane + n-C<sub>7</sub> (Grolier et al., 1973) where the  $C_p^E$  curve is normal has  $H^E \approx$  530 J mol<sup>-1</sup>. In a similar vein, Kalali et al. (1985) call attention to the proximity of the UCST in discussing the bisdichloroethylether + 2,2,4-trimethylpentane system. Grolier and collaborators (Lainez et al., 1985b; Wilhelm et al., 1985) have also found large positive  $C_p^E$  for systems near a UCST, discussing the results in terms of conformational change. Nicolaides and Eckert (1978) have measured  $H^E$  for nitrobenzene + hexane, nitroethane + hexane and aniline + cyclohexane at two or three temperatures lying from 5 to 30°C above the UCST.  $C_p^E$  values from  $dH^E/dT$  are large and positive but for the first two systems, and perhaps for the third,  $C_p^E$  becomes negative at both extremes of concentration, i.e.  $C_p^E$  is W-shaped. The above results support the conjecture that non-randomness may play a role in the concentration dependence of  $C_p^E$ .

It is clear that relaxation toward non-randomness in the solution must lower  $H^E$  and  $S^E$  below their values for a completely random mixture. As the temperature is raised, non-randomness should decrease, falling asymptotically to zero so that  $H^E$  and  $S^E$  will be more positive, giving a positive contribution to  $C_p^E$  with negative  $dC_p^E/dT$ . The following semi-quantitative argument indicates that this positive non-randomness contribution should have the right concentration dependence to give the W-shape when combined with a negative  $C_p^E$  contribution of parabolic concentration dependence. The simple Guggenheim (1952) quasi-chemical theory gives (his eqn.4.27.8) an expression for  $H^E$  taking account of non-randomness. We split  $H^E$  into random and non-random contributions

$$H^E/N_0 = \underset{\text{RANDOM}}{x_1x_2 (w - T dw/dT)} + \underset{\text{NON-RANDOM}}{x_1x_2 (w - T dw/dT) (\Gamma_{12}-1)} \quad (1)$$

Here  $w$  is the usual temperature-dependent cooperative free energy (Guggenheim, 1952) and  $\Gamma_{12}$ , termed  $2/(\beta + 1)$  by Guggenheim is a non-randomness parameter (Panayiotou and Vera, 1980) equal to unity in a random solution. A consideration of Panayiotou and Vera (1980) shows quite generally that  $\Gamma_{12}$  must tend to unity at both ends of the concentration range where the non-randomness contribution must fall to zero compared with the random. This accords with the intuitive requirement that when either component is dispersed at high dilution in the other, it must tend to be randomly distributed. To illustrate this we take the quasi-chemical approximation where

$$\Gamma_{12} = 1 - x_1x_2 (e^{2w/zkT} - 1) + 2 (x_1x_2)^2 (e^{2w/zkT} - 1)^2 - 5(x_1x_2)^3 (e^{2w/zkT} - 1)^3 \dots \quad (2)$$

whence  $\Gamma_{12} \leq 1$  for  $w \geq 0$  expressing the fact that, for a net repulsion between components, the neighbourhood of any component molecule is poorer in the other component than if the solution were random. Equation (1) becomes

$$\frac{H^E}{N_0} = \underbrace{x_1 x_2 (w - T dw/dT)}_{\text{RANDOM}} - \underbrace{(x_1 x_2)^2 (w - T dw/dT) (e^{2w/zkT} - 1)}_{\text{NON-RANDOM}} + \dots \quad (3)$$

given by Guggenheim (1952). Thus the non-random term in  $H^E$  should become apparent as a negative contribution manifested toward the middle of the concentration range. An indication of such a negative contribution would be a positive curvature of  $H^E/x_1 x_2$  against  $x$ , i.e. a positive value of  $a_2$  in the Redlich-Kister equation

$$\frac{H^E}{x_1 x_2} = \sum_{i=0} a_i (1 - 2x_2)^i \quad (4)$$

According to eqn. (3), keeping higher terms from eqn. (2), both the second and fourth derivatives of  $H^E/x_1 x_2$  with  $x$  should be positive with the same sign for the corresponding coefficients,  $a_2$  and  $a_4$  in the Redlich-Kister representation of  $H^E$ . These conjectures are borne out by experimental data when  $H^E$  is very large, and in particular for the W-shape systems. Furthermore the coefficients usually increase with decreasing  $T$ , i.e. increasing non-randomness. Indeed, it is known (Widom and Khosla, 1980) that  $H^E$  itself and  $V^E$  have zero curvature against  $x$  at the UCST. From eqn. (4) this would lead to  $a_2 = a_0$  at the UCST, i.e.  $a_2$  should be large and positive. (In fact, a non-analytic composition dependence of  $H^E$  and  $V^E$  at the UCST (Widom and Khosla, 1980) indicates that results from eqn. (4) can only be approximate.) Other effects may contribute to the coefficients. For instance if, as suggested by Scatchard (1931), the random molar  $H^E$  divided by volume is symmetrical in volume fraction

rather than mole fraction, then it is easily shown that

$$\frac{H^E}{x_1 x_2} = A \frac{V_1 V_2}{x_1 V_1 + x_2 V_2} \quad (5)$$

A being a constant with dimensions of  $J \text{ cm}^{-3}$ , with the Redlich-Kister coefficients  $a_i$  given by

$$a_0 = 2AV_1V_2/(V_1 + V_2), \quad a_i = a_0 \left[ \frac{V_2 - V_1}{V_2 + V_1} \right]^i \quad (6)$$

Here  $V_1$  and  $V_2$  are the molar volumes. For moderate size-differences between the components this contribution to  $a_2$  and  $a_4$  will be small compared with that arising from the non-random contribution.

Turning now to the temperature-derivative of eqn. (3)

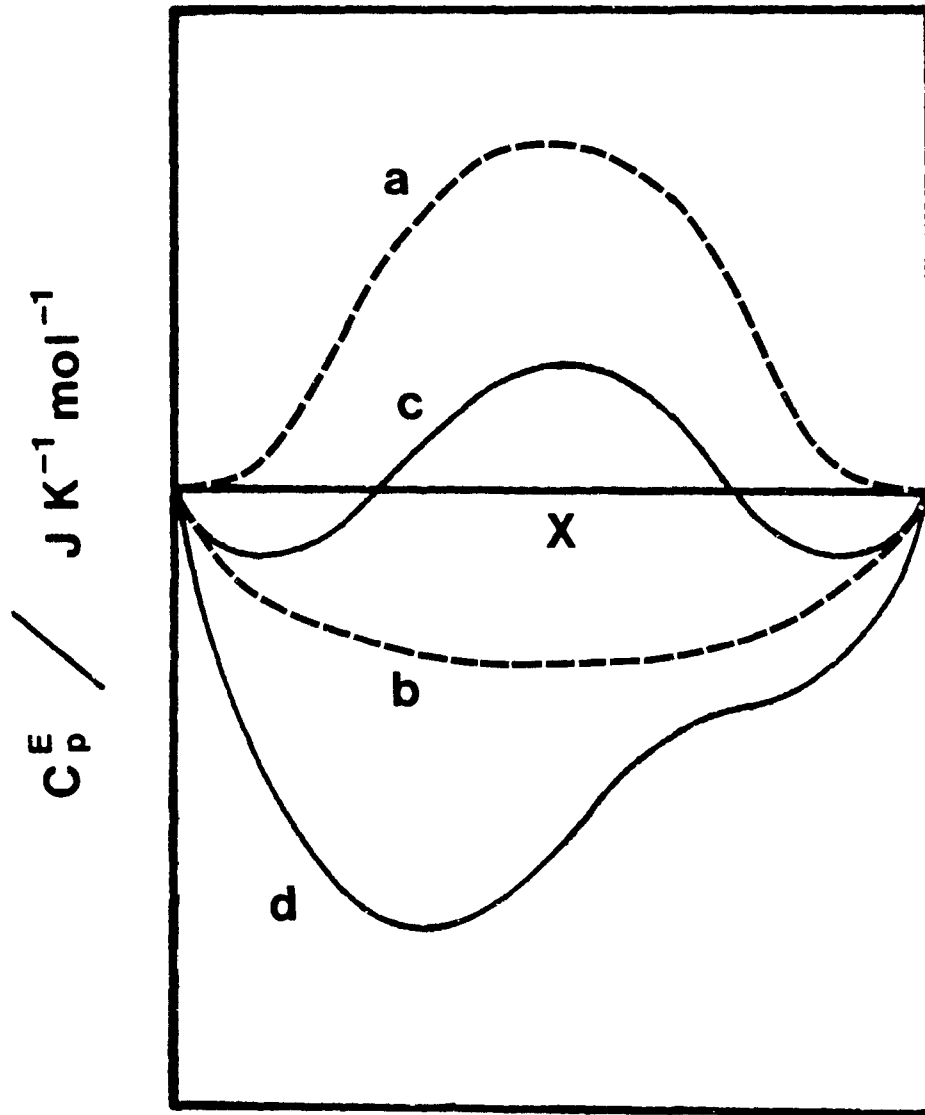
$$\begin{aligned} \frac{C_p^E}{N_0} = & \underbrace{-x_1 x_2 T \frac{d^2 W}{dT^2}}_{\text{RANDOM}} + \underbrace{(x_1 x_2)^2 \left[ W - T \frac{dW}{dT} \right]^2 \left[ \frac{2}{zkT^2} \right]}_{\text{NON-RANDOM}} \\ & + \underbrace{(x_1 x_2)^2 T \frac{d^2 W}{dT^2} (e^{2W/zkT} - 1)}_{\text{RANDOM}} \end{aligned} \quad (7)$$

For the present systems where one component is polar or weakly associated  $W$  should decrease with increasing temperature but with a positive curvature  $d^2W/dT^2$  against  $T$ .

A form

$$W = \alpha + \beta/T \quad (8)$$

Fig. 1 Schematic  $C_p^E$  against mole fraction curves. (a) non-random contribution; (b) random contribution; (c) total W-shape; (d) curve having two regions of positive curvature separated by one of negative curvature.



has been suggested (Kalali et al., 1985) for polar + inert systems whence the random term in  $C_p^E$  is negative as expected for a system where dipolar or weak association order not involving hydrogen bonds is being broken during mixing. On the other hand, the non-random contribution to  $C_p^E$  is positive, consistent with an increase of randomness on raising T. Furthermore, according to eqn. (7) this term has a zero slope against x at both ends of the concentration range. The random and non-random contributions are shown schematically in Fig. 1 together with the W-shape total  $C_p^E$ . According to eqn. (7) the non-randomness contribution and  $C_p^E$  itself in the middle of the concentration range should increase in magnitude with decrease of T, and particularly so as phase separation at a UCST is approached. Equation (8) suggests that the random contribution should also be enhanced as T is lowered making  $C_p^E$  more negative at the extremes of concentration.

A rough approximation may be obtained for eqn. (7) by neglecting the second term of the non-random contribution. The quantity  $(w - T dw/dT)$  is then given by eqn. (3) neglecting the non-random contributions in  $H^E$ . Then

$$\frac{C_p^E}{N_0} \simeq -x_1x_2 T \frac{d^2w}{dT^2} + \frac{2k}{z} \left[ \frac{H^E}{RT} \right]^2 \quad (9)$$

It must now be stressed that with reasonable values of  $H^E$  and z in eqn. (9) the non-randomness contribution of  $C_p^E$  is small,  $\simeq 1 \text{ J K}^{-1} \text{ mol}^{-1}$  or less. It is known, however, that the non-random contribution to  $C_p^E$  is severely underestimated by the quasi-chemical approximation and indeed  $C_p^E \rightarrow \infty$  at the UCST. However the quasi-chemical approximation may be used as a qualitative indicator of the shape of the  $C_p^E$  curve, and it does reproduce the essential features of the situation, namely  $C_p^E(\text{non-random}) \geq 0$ ,  $C_p^E(\text{random}) \leq 0$  and  $C_p^E(\text{non-random})/C_p^E(\text{random}) \rightarrow 0$  as  $x_1, x_2 \rightarrow 0$ .

The purpose of our experimental work is to search for W-shape  $C_p^E$  amongst systems where conformational change should not be a factor and where  $H^E$  is large. These conditions are met for acetone + the highly-branched 2,2,4,4,6,8,8-heptamethylnonane (br- $C_{16}$ ) where steric hindrance must impart conformational rigidity. The W-shaped  $C_p^E$  was found here, and similar results were found for acetone mixed with the flexible n- $C_{12}$  and n- $C_6$  so that flexibility does not seem critical. Finally, br- $C_{16}$  was mixed with the series of alkanones: 2-butanone, 3-hexanone, 4-heptanone, 5-nonanone and 4-decanone where  $H^E$  becomes progressively smaller than with acetone.

## EXPERIMENTAL

The alkanones and the normal and branched alkanes were "Gold Label" products from Aldrich Chemical Co. of at least 99% purity except for 3-hexanone, 4-heptanone and 5-nonanone which were 98%. They were used without treatment, the lower ketones being kept over molecular sieves. The heat capacities were measured using a Picker flow microcalorimeter (Sodev, Sherbrooke, Quebec, Canada) with procedures described in the literature (Picker et al., 1971; Fortier and Benson, 1976; Fortier et al., 1976). Considerable difficulty was encountered using the volatile acetone. However, the accuracy on  $C_p^E$  as determined from repetition of runs and results with other systems should be  $\pm 0.1 \text{ J K}^{-1} \text{ mol}^{-1}$ . Density measurements to transform volumetric  $C_p$  values into molar, and also to obtain  $V^E$  itself were made using a flow densitometer from Sodev. The accuracy of the  $V^E$  measurement is estimated as  $\pm 0.01 \text{ cm}^3 \text{ mol}^{-1}$  and for  $dV^E/dT$ ,  $\pm 1 \times 10^{-3} \text{ cm}^3 \text{ K}^{-1} \text{ mol}^{-1}$ . A Tian-Calvet microcalorimeter (Setaram, Lyon, France) was used to measure some enthalpies of mixing at  $25^\circ\text{C}$ . A few visual determinations of the temperature of phase separation around the UCST were made using a water + ethylene glycol constant temperature bath.

## RESULTS AND DISCUSSION

### 1. Excess heat capacities

Figure 2 and Table 1 show  $C_p^E$  for acetone + br- $C_{16}$  at 25 and 10°C. It is positive and extremely large through most of the concentration range but becomes negative at the extremes of concentration, i.e. it is W-shaped and similar to  $C_p^E$  of bisdichloroethylether + 2,2,4-trimethylpentane, nitrobenzene and nitroethane + hexane and nitrobenzene and benzonitrile + n-alkanes, all systems close to their UCSTs. Conformational changes should not be important in either of the present components. On the other hand,  $H^E$  is large being  $\approx 1100 \text{ J mol}^{-1}$  at 25°C and equimolar composition, the maximum occurring at higher acetone concentrations. The system is in fact close to phase separation which was observed to occur at 5°C for  $x_1 = 0.7$ .  $C_p^E$  increases as T decreases approaching the UCST. However, at the ends of the concentration range, where the random contribution to  $C_p^E$  should dominate,  $C_p^E$  becomes more positive rather than more negative as suggested by eqns. (7) and (8) for the random contribution. Using the theory of Flory (1965), together with a value of the  $X_{12}$  parameter obtained by fitting the theory to the equimolar  $H^E$ , we calculated the equimolar  $C_p^E$  as  $-0.29 \text{ J mol}^{-1}$ . This incorrect result is consistent with the large positive value of  $C_p^E$  found experimentally being due to a special effect not considered by the theory.

The UCST for acetone + n- $C_{16}$  lies (Messow et al., 1977) at 27°C and Fig. 3 and Table 2 show instead  $C_p^E$  for the acetone + n- $C_{12}$  system at 25 and 15°C close to the UCST at 13°C. The  $C_p^E$  curves are again W-shaped becoming negative at both ends of the concentration range. At high acetone concentration, however, the negative  $C_p^E$  is extremely small and appears only at mole fraction 0.99. For acetone + n- $C_{12}$ ,  $C_p^E$  increases to  $9 \text{ J K}^{-1} \text{ mol}^{-1}$  at 15°C, higher than the maximum of  $6.3 \text{ J K}^{-1} \text{ mol}^{-1}$

Fig. 2 Excess molar heat capacities of acetone + 2,2,4,4,6,8,8-heptamethylnonane  
at 10 (■) and 25°C (●).

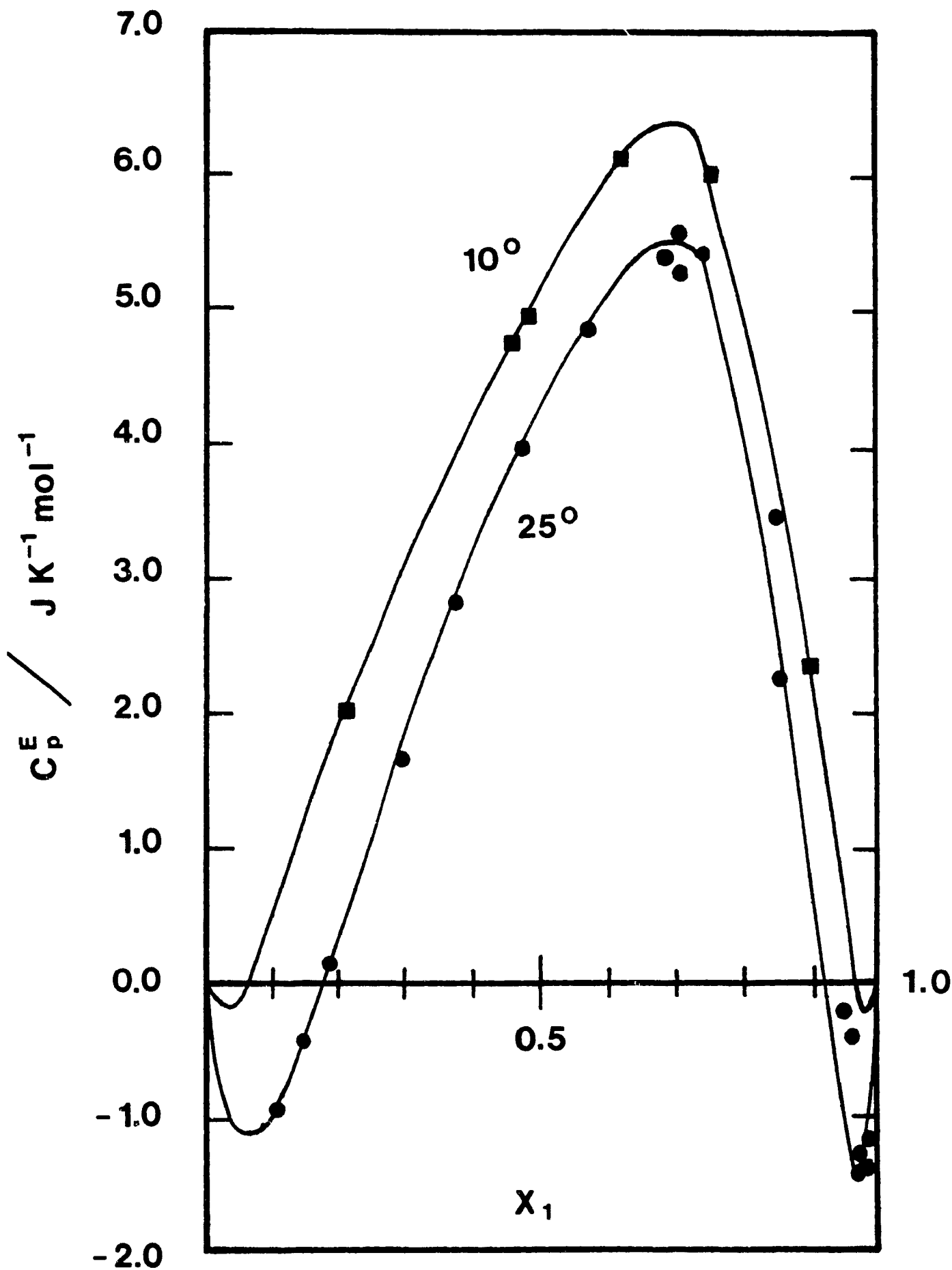


TABLE 1  
 Excess molar heat capacity at constant pressure of acetone + 2,2,4,4,6,8,8--  
 heptamethylnonane at 10°C and 25°C (UCST: 5°C)

$x_1$	$C_p^E$ (J K <sup>-1</sup> mol <sup>-1</sup> )	$x_1$	$C_p^E$ (J K <sup>-1</sup> mol <sup>-1</sup> )	$x_1$	$C_p^E$ (J K <sup>-1</sup> mol <sup>-1</sup> )
T = 10°C					
0.0039	-0.03	0.4574	4.70	0.9182	2.98
0.0594	0.17	0.4785	4.87	0.9563	2.15
0.0858	0.83	0.6154	6.09	0.9735	1.90
0.2119	2.02	0.7569	5.95	0.9923	-0.09
T = 25°C					
0.1053	-0.90	0.4782	4.20	0.8504	3.61
0.1534	-0.35	0.5704	5.09	0.9471	-0.23
0.1889	0.13	0.6880	5.59	0.9621	-0.41
0.2955	1.84	0.6997	5.50	0.9657	-1.45
0.3867	3.03	0.7400	5.62	0.9791	-1.37

Fig. 3 Excess molar heat capacities for acetone + dodecane at 15°C (●) and at 25°C (▲); acetone + n-hexane at 25°C (■).

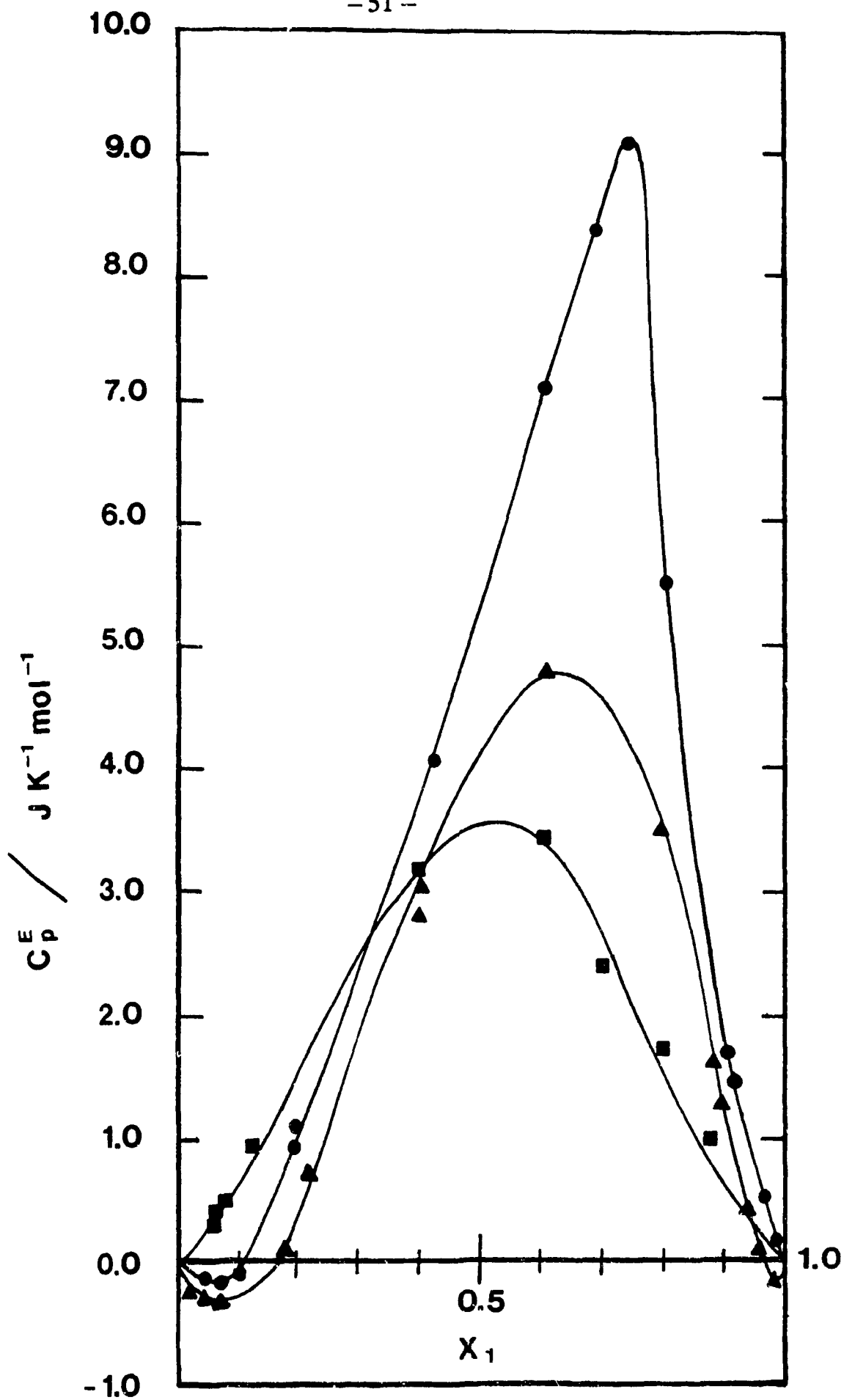


TABLE 2  
 Excess molar heat capacity at constant pressure of acetone + n-hexane  
 at 25°C (UCST: -39°C)

$x_1$	$C_p^E$ (J K <sup>-1</sup> mol <sup>-1</sup> )	$x_1$	$C_p^E$ (J K <sup>-1</sup> mol <sup>-1</sup> )	$x_1$	$C_p^E$ (J K <sup>-1</sup> mol <sup>-1</sup> )
0.0611	0.31	0.1952	1.08	0.7949	1.76
0.0667	0.41	0.4012	3.21	0.8033	2.43
0.0747	0.51	0.4036	3.07	0.8925	1.01
0.0749	0.57	0.6123	3.49	0.9371	0.87
0.1240	1.04	0.6888	2.42		

TABLE 3  
Excess molar heat capacity at constant pressure of acetone + n-dodecane at  
15 and 25°C (UCST: 13°C)

$x_1$	$C_p^E$ (J K <sup>-1</sup> mol <sup>-1</sup> )	$x_1$	$C_p^E$ (J K <sup>-1</sup> mol <sup>-1</sup> )	$x_1$	$C_p^E$ (J K <sup>-1</sup> mol <sup>-1</sup> )
T = 15°C					
0.0410	-0.25	0.4165	4.04	0.8997	1.70
0.0741	-0.23	0.6124	7.09	0.9096	1.48
0.1040	-0.13	0.6626	8.54	0.9581	0.28
0.10540	0.07	0.7569	9.18	0.9804	0.02
0.1925	0.95	0.8007	5.50	0.9950	-0.09
T = 25°C					
0.0358	-0.17	0.3958	2.79	0.9357	0.43
0.0699	-0.03	0.6096	4.72	0.9586	0.11
0.1044	0.02	0.7975	3.53	0.9803	-0.02
0.1820	0.07	0.8948	1.28		

found with br-C<sub>16</sub> at 10°C, and presumably associated with a closer approach to the UCST for the system. The similarity of C<sub>p</sub><sup>E</sup> when acetone is mixed with a normal or a branched alkane suggests that flexibility and conformation are not important here. Very recently, however, Costas has found the W-shaped C<sub>p</sub><sup>E</sup> for chloronaphthalene – br-C<sub>16</sub> (unpublished) whereas chloronaphthalene + n-C<sub>16</sub> gives (Grolier et al., 1981) a positive C<sub>p</sub><sup>E</sup> of normal concentration dependence.

Figure 3 and Table 2 also give C<sub>p</sub><sup>E</sup> for the acetone + n-C<sub>6</sub> system at 25°C. The UCST of this system lies at – 39°C (Ralston et al., 1944), considerably lower than for acetone + br-C<sub>16</sub> and + n-C<sub>12</sub> systems. Consistent with lower non-randomness in the solution at 25°C, C<sub>p</sub><sup>E</sup> is considerably smaller and the W-shape was not found although a change of sign of the curvature does occur towards the ends of the concentration range. Shafer and Rohr (1960) give C<sub>p</sub><sup>E</sup> values for the system obtained from the temperature dependence of H<sup>E</sup>. Maxima of 4.45, 5.25 and 6.0 J K<sup>-1</sup> mol<sup>-1</sup> occur at +20, 0 and –20°C, respectively, exhibiting an increase as the UCST is approached. Furthermore, there is a strong indication from C<sub>p</sub><sup>E</sup>(x) that at the lowest temperatures C<sub>p</sub><sup>E</sup> becomes negative at the extremes of the concentration range.

Figure 4 and Tables 4–8 give C<sub>p</sub><sup>E</sup> for a single hydrocarbon, br-C<sub>16</sub>, mixed at 25°C with a series of alkanones of increasing chain length. With increasing alkane character of the alkanone, the equimolar H<sup>E</sup> rapidly falls. Group theoretical calculations following Nguyen and Ratchiffe (1971) give equimolar H<sup>E</sup> values for the series of alkanones mixed with n-C<sub>16</sub>. They range from 2500 for acetone and 1850 for 2-butanone to 1100 for decanone. In fact, H<sup>E</sup> with br-C<sub>16</sub> will be less by several hundred J mol<sup>-1</sup> as shown by the experimental results of Pouchly et al. (1978) for 2-butanone + n-C<sub>16</sub> (1915 J mol<sup>-1</sup>) compared with 2-butanone + br-C<sub>16</sub> (1504 J mol<sup>-1</sup>). However, the decrease of H<sup>E</sup> with alkanone chain-length will be similar for both n-C<sub>16</sub> and br-C<sub>16</sub>. The UCSTs for all the systems save that containing acetone are below the freezing point of the solutions, i.e. ≤ – 70°C. Consistent with this, and

Fig. 4 Excess molar heat capacities for alkanones + 2,2,4,4,6,8,8-heptamethyl-nonane at 25°C; acetone (•); 2-butanone (○); 3-hexanone (▲); 4-heptanone (△); 5-nonanone (■); and 4-decanone (□). At high ketone concentration points have been omitted for clarity. The data are found in Tables 4 – 8.

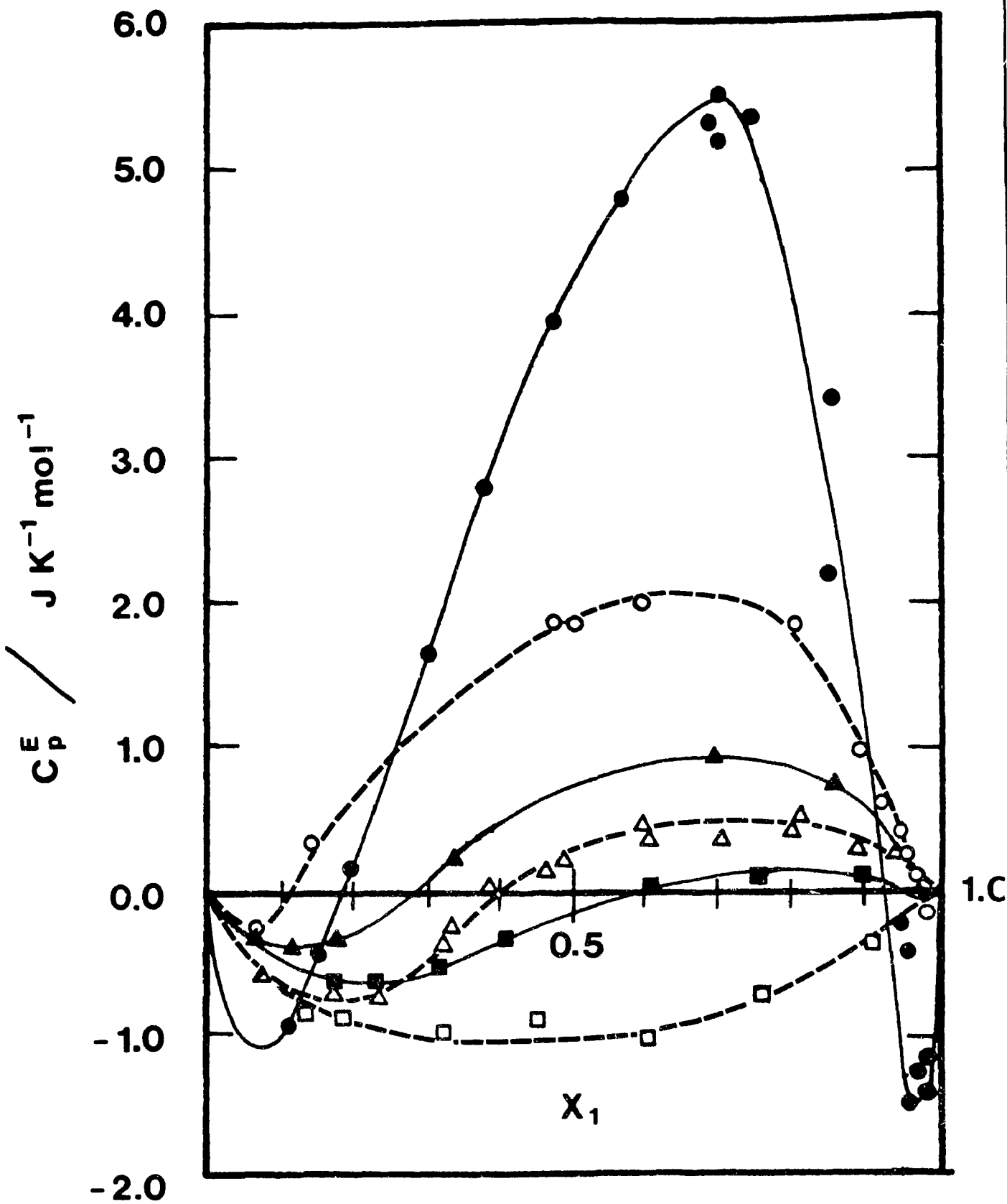


TABLE 4  
 Excess molar heat capacity at constant pressure of 2-butanone + 2,2,4,4,6,8,8-  
 heptamethylnonane at 25°C (UCST: < -57°C)

$x_1$	$C_p^E$ (J K <sup>-1</sup> mol <sup>-1</sup> )	$x_1$	$C_p^E$ (J K <sup>-1</sup> mol <sup>-1</sup> )	$x_1$	$C_p^E$ (J K <sup>-1</sup> mol <sup>-1</sup> )
0.0417	-0.03	0.5887	2.22	0.9494	0.31
0.1030	0.08	0.6495	2.34	0.9559	0.30
0.1398	0.40	0.7980	1.59	0.9861	0.13
0.2272	0.89	0.8000	1.59	0.9929	-0.06
0.2483	0.87	0.8937	1.07	0.9978	-0.07
0.4492	2.05	0.8998	1.02		
0.4679	2.05	0.9198	0.62		

TABLE 5

Excess molar heat capacity at constant pressure of 3-hexanone + 2,2,4,4,6,8,8-heptamethylnonane at 25°C (UCST: < -70°C)

$x_1$	$C_p^E$ (J K <sup>-1</sup> mol <sup>-1</sup> )	$x_1$	$C_p^E$ (J K <sup>-1</sup> mol <sup>-1</sup> )	$x_1$	$C_p^E$ (J K <sup>-1</sup> mol <sup>-1</sup> )
0.1152	-0.28	0.6911	1.17	0.9702	0.25
0.1714	-0.18	0.8502	0.86	0.9950	0.01
0.3259	0.38	0.9302	0.62		

TABLE 6

Excess molar heat capacity at constant pressure of 4-heptanone + 2,2,4,4,6,8,8-heptamethylnonane at 25°C (UCST: < -70°C)

$x_1$	$C_p^E$ (J K <sup>-1</sup> mol <sup>-1</sup> )	$x_1$	$C_p^E$ (J K <sup>-1</sup> mol <sup>-1</sup> )	$x_1$	$C_p^E$ (J K <sup>-1</sup> mol <sup>-1</sup> )
0.0684	-0.58	0.3805	0.00	0.8060	0.53
0.1411	-0.90	0.4587	0.12	0.8947	0.29
0.1698	-0.69	0.4918	0.21	0.8973	0.51
0.2334	-0.79	0.5963	0.46	0.9423	0.21
0.3077	-0.38	0.6070	0.36		
0.3287	-0.27	0.7033	0.32		

TABLE 7

Excess molar heat capacity at constant pressure of 5-nonanone + 2,2,4,4,6,8,8-heptamethylnonane at 25°C (UCST: < -70°C)

$x_1$	$C_p^E$ (J K <sup>-1</sup> mol <sup>-1</sup> )	$x_1$	$C_p^E$ (J K <sup>-1</sup> mol <sup>-1</sup> )	$x_1$	$C_p^E$ (J K <sup>-1</sup> mol <sup>-1</sup> )
0.1737	-0.65	0.7512	0.11	0.9595	-0.03
0.3194	-0.52	0.8602	0.13	0.9793	-0.06
0.4046	-0.34	0.8920	0.08	0.9941	-0.02
0.6085	-0.02	0.9201	0.05		

TABLE 8  
 Excess molar heat capacity at constant pressure of 4-decanone + 2,2,4,4,6,8,8-  
 heptamethylnonane at 25°C (UCST: < -70°C)

$x_1$	$C_p^E$ (J K <sup>-1</sup> mol <sup>-1</sup> )	$x_1$	$C_p^E$ (J K <sup>-1</sup> mol <sup>-1</sup> )	$x_1$	$C_p^E$ (J K <sup>-1</sup> mol <sup>-1</sup> )
0.1014	-0.80	0.4519	-1.22	0.7424	-0.75
0.1861	-1.08	0.4534	-1.22	0.7560	-0.95
0.2605	-1.22	0.5065	-1.12	0.9079	-0.45
0.3115	-1.28	0.5573	-1.24	0.9305	-0.16
0.4074	-1.26	0.6056	-1.33		

with the decrease of  $H^E$ , the maximum  $C_p^E$  values decreases and the W-shape is less pronounced. The negative  $C_p^E$  appearing at very high ketone mole fraction ( $> 0.95$ ) are extremely small, less than  $0.05 \text{ J K}^{-1} \text{ mol}^{-1}$ . Somewhat similarly, Grolier and Benson (1984) found a W-shape for 2-butanone + n-heptane while a less positive  $C_p^E$  of S-shape was found for 3-pentanone + n-heptane.

## 2. Excess volumes

Table 9 gives Redlich-Kister coefficients (eqn. (4) with  $V^E$  replacing  $H^E$ ) for acetone + br- $C_{16}$ , +n- $C_{12}$  and +n- $C_6$  at the temperatures indicated. The  $V^E$  are positive and extremely large as expected for mixtures with such large  $H^E$  values. Another interesting feature is the rapid increase of  $V^E$  with T. The Flory theory has been used to predict  $V^E$  at 25°C with equation of state data for the pure components taken from the literature and with the  $X_{12}$  parameter fitted to  $H^E$  values for the systems. The theoretical  $V^E$  values are then much too large, by 0.5–1.0 cm<sup>3</sup> mol<sup>-1</sup>. This failure of the theory was encountered before (Costas and Patterson, 1982) with other systems containing a polar and a non-polar component. In the present work, the  $X_{12}$  parameter was fitted to  $V^E$  at equimolar concentration and using the Flory theory,  $dV^E/dT$  was predicted at 25°C. Values of  $dV^E/dT$  have previously been found (Bhattacharyya and Patterson, 1985) to be reliable in the absence of special effects such as order in the solution or components. For acetone + br- $C_{16}$ ,  $dV^E/dT$  is predicted to be  $5 \times 10^{-3}$  cm<sup>3</sup> K<sup>-1</sup> mol<sup>-1</sup> at 25°C and would change only slightly with T. Experimental  $V^E$  data at 15, 25 and 40°C give  $dV^E/dT = 17 \times 10^{-3}$  and  $5 \times 10^{-3}$  cm<sup>3</sup> K<sup>-1</sup> mol<sup>-1</sup> at 17.5 and 32.5°C. The strikingly large value at 17.5°C would seem to be due to the proximity of the UCST at 5°C. The acetone + n- $C_{12}$  system is similar. The predicted value is  $7 \times 10^{-3}$  cm<sup>3</sup> K<sup>-1</sup> mol<sup>-1</sup> while the data at 15 and 25 give a value of  $12.5 \times 10^{-3}$  cm<sup>3</sup> K<sup>-1</sup> mol<sup>-1</sup> at 20°C. Again, the large discrepancy may reasonably be associated with the proximity of the UCST, i.e.  $dV^E/dT$  is similar to  $C_p^E$  in containing a positive non-randomness contribution. It is known that as the UCST is approached both  $dV/dT$  and  $C_p$  of the solution diverge with the same critical exponent (Klein and Woermann, 1978). However, acetone + n- $C_6$  has a predicted value of  $9.5 \times 10^{-3}$  which compares with an experimental value of  $10 \times 10^{-3}$  cm<sup>3</sup> K<sup>-1</sup> mol<sup>-1</sup> at 20°C using  $V^E$  data at 15 and 25°C. Here the UCST lies further below the

TABLE 9

Redlich-Kister coefficients ( $a_i$ ) and standard deviation for  $V^E$   
 $(V^E = x_1x_2[a_0 + a_1(x_1 - x_2) + a_2(x_1 - x_2)^2 + a_3(x_1 - x_2)^3 + a_4(x_1 - x_2)^4])$

	T (°C)	$a_0$	$a_1$	$a_2$	$a_3$	$a_4$	s.d.
Acetone	15	3.741	-0.548	1.270	-0.446	-1.170	0.006
+n-hexane (n-C <sub>6</sub> )	25	4.204	-0.373	0.351	-0.980	0.558	0.016
Acetone	15	4.479	0.202	0.620	1.509	1.713	0.006
+dodecane (n-C <sub>12</sub> )	25	4.984	0.479	1.079	0.803	1.287	0.001
Acetone	10	3.541	0.761	0.186	0.139	2.469	0.003
+2,2,4,4,6,8,8- heptamethylnonane	25	4.556	0.996	0.942	0.341	-0.303	0.001
(br-C <sub>16</sub> )	35	4.571	1.052	0.339	0.783	2.186	0.004
	40	4.703	1.053	0.826	1.164	1.081	0.002

experimental  $T$ , at  $-39^{\circ}\text{C}$  which may be the reason for good agreement between theory and experiment

In conclusion we suggest that all polar or weakly associated systems without hydrogen bonds with large  $H^E$ , i.e.  $1000\text{--}2000\text{ J mol}^{-1}$ , and hence large  $G^E$  should, due to non-randomness, show the W-shape  $C_p^E$  curve becoming more pronounced on lowering the temperature. A further consequence of non-randomness should be a large positive value of the curvature of  $H^E/x_1x_2$  against composition, i.e. of the Redlich-Kister constant  $a_2$ , and this should increase with decrease of  $T$ .

#### ACKNOWLEDGEMENTS

We thank the Natural Sciences and Engineering Research Council of Canada for support to which the Ministère de l'Éducation du Québec also contributed, and we are grateful to Professor F. Kohler for considerable constructive criticism.

## LIST OF SYMBOLS

$a_i$	Redlich–Kister coefficients
$C_p$	heat capacity at constant pressure
$G$	Gibbs free enthalpy
$H$	enthalpy
$N_0$	Avogadro's Number
$R$	gas constant
$S$	entropy
s.d.	standard deviation
$w$	cooperative free energy interchange parameter
$x$	mole fraction
$X_{12}$	enthalpic interchange parameter of Flory theory
$z$	lattice coordination number

## GREEK LETTERS

$\alpha, \beta$	constants in eqn. (7)
$\beta$	Guggenheim non–randomness parameter
$\Gamma_{12}$	non–randomness parameter (Panayiotou and Vera, 1980)

## SUBSCRIPTS

1,2	components
-----	------------

## SUPERSCRIPTS

E	excess
---	--------

## REFERENCES

- Andrews, A.W. and Morcom, K.W., 1971. Thermodynamic properties of some hydrocarbon + cyclic ether mixtures. Enthalpies of mixing. *J. Chem. Thermodyn.*, 3: 519–525.
- Battacharyya, S.N. and Patterson, D., 1985. Liquid structure and the excess volumes of cyclohexane+normal and branched alkane mixtures. *J. Chem. Soc., Faraday Trans. 1*, 81: 375–385.
- Cabani, S. and Ceccanti, N., 1973. Thermodynamic properties of binary mixtures of cyclohexane with cyclic amines or cyclic ethers at 298.15 K. *J. Chem. Thermodyn.*, 5: 9–20.
- Costas, M. and Patterson, D., 1982. Volumes of mixing and the  $P^*$  effect: part II. Mixtures of alkanes with liquids of different internal pressures. *J. Solution Chem.*, 11: 807–821.
- Flory, P.J., 1965. Statistical thermodynamics of liquid mixtures. *J. Am. Chem. Soc.*, 87: 1833–1838.
- Fortier, J.L. and Benson, G.C., 1976. Excess heat capacities of binary liquid mixtures determined with a Picker flow calorimeter. *J. Chem. Thermodyn.*, 8: 411–423.
- Fortier, J.L., Benson, G.C. and Picker, P., 1976. Heat capacities of some organic liquids determined with the Picker flow calorimeter. *J. Chem. Thermodyn.*, 8: 289–299.
- Grolier, J.-P.E. and Kehiaian, H.V., 1973. Enthalpies de mélange des  $\alpha,\omega$ -dichloroalkanes avec des hydrocarbures. *J. Chim. Phys.*, 70: 807–810.
- Grolier, J.-P.E. and Benson, G.C., 1984. Thermodynamic properties of binary mixtures containing ketones. Heat capacities and volumes of some n-alkane mixtures at 298.15 K. *Can. J. Chem.*, 62: 949–953.
- Grolier, J.-P.E., Inglese, A., Roux, A.H. and Wilhelm, E., 1981. Thermodynamics of

(1-chloronaphthalene+n-alkanes): excess enthalpies, excess volumes and excess heat capacities. *Ber. Bunsenges Phys. Chem.*, 85: 768–772.

Grolier, J.-P.E., Sosnkowska-Kehiaian, K. and Kehiaian, H.V., 1973. Enthalpies de mélange des chlorures organiques avec des hydrocarbures. *J. Chim. Phys.*, 70: 367–373.

Grolier, J.-P.E., Inglese, A., Roux, A.H. and Wilhelm, E., 1982. Induced conformational changes in mixtures containing n-alkanes. In: S.A. Newman (Editor), *Chemical Engineering Thermodynamic*. Ann Arbor Science Publishers, Ann Arbor, Chapter 40, pp. 483–486.

Guggenheim, E., 1952. *Mixtures*. Clarendon Press, Oxford, p. 83.

Inglese, A. and Grolier, J.-P.E., 1984. Excess volumes and excess heat capacities of oxane+cyclohexane and 1,4-dioxane+cyclohexane. *Fluid Phase Equilibria*, 15: 287–294.

Inglese, A., Grolier, J.-P.E., and Wilhelm, E., 1984. Excess molar heat capacities of (1,4-dioxane+n-alkane): an unusual composition dependence. *J. Chem. Thermodyn.*, 16: 67–71.

Kalali, H., Kohler, F. and Svejda, P., 1985. Excess properties of binary mixtures of 2,2,4-trimethylpentane with one polar component. *Fluid Phase Equilibria*, 20: 75–80.

Kimura, F., D'Arcy, P.J., Sugamori, M.E. and Benson, G.C., 1983. Excess enthalpies and heat capacities for 2,5,8-trioxanonane+n-heptane mixtures. *Thermochim. Acta*, 64: 149–154.

Klein, H. and Woermann, D., 1978. Analysis of light-scattering and specific heat data of binary liquid mixtures in terms of the two-scale-factor universality. *Ber. Bunsenges Phys. Chem.*, 82: 1084–1086.

Lainez, A., Wilhelm, E. and Grolier, J.-P.E., 1984. Thermodynamics of halogenated ethane or ethane+n-alkanes. IUPAC Conference on Chemical Thermodynamics, Hamilton, Ontario, Canada. Paper 139.

Lainez, A., Grolier, J.-P.W. and Wilhelm, E., 1985a. Excess molar heat capacity and excess molar volume of 1,6-dichlorohexane + n-octane. *Thermochim. Acta*, 91: 243.

Lainez, A., Rodrigo, M., Roux, A.H., Grolier, J.-P.E. and Wilhelm, E. 1985b. Relation structure–propriétés thermodynamiques. Capacités calorifiques de substances polaires (nitrobenzene et benzonitrile) en solution dans les alcanes. *Cal. Anal. Therm.* vol. XVI, 153.

Lainez, A., Roux-Desgranges, G., Grolier, J.-P.E. and Wilhelm, E., 1985c. Mixtures of alkanes with polar molecules showing internal rotation: an unusual composition dependence of  $C_p^E$  of 1,2-dichloroethane + an n-alkane. *Fluid Phase Equilibria*, 20: 47–56.

Lainez, A., Wilhelm, E., Roux-Desgranges, G. and Grolier, J.-P.E., 1985d. Excess molar quantities of (a halogenated n-alkane + an n + alkane), a comparative study of mixtures containing either 1-chlorobutane or 1,4-dichlorobutane. *J. Chem. Thermodyn.*, 1154–1161.

Messow, U., Doyé, Y., Kuntzsch, S. and Kuchenbecker, D., 1977. Thermodynamische Untersuchungen und Lösungsmittel / n-Parafin-Systemen. *Z. Phys. Chem. Leipzig*, 258: 90–96.

Nguyen, T.H. and Ratchiff, G.A., 1971. Prediction of heats of mixing of liquid mixtures containing aliphatic hydrocarbons and ketones by a group solution model. *Can. J. Chem. Eng.*, 49: 889–891.

Nicholaidis, G.L. and Eckert, C.A., 1978. Experimental heats of mixing of some miscible and partially miscible nonelectrolyte systems. *J. Chem. Eng. Data*, 23, No.2: 152–156.

Panayiotou, C. and Vera, J.H., 1980. The quasi-chemical approach for non-randomness in liquid mixtures. Expressions for local surfaces and local compositions with an application to polymer solutions. *Fluid Phase Equilibria*, 5: 55–80.

- Picker, P., Leduc, J.-P., Philip, P.R. and Desnoyers, J.E., 1971. Heat capacity of solutions by flow microcalorimetry. *J. Chem. Thermodyn.*, 3: 631-642.
- Pouchly, J., Zivny, A. and Biros, J., 1978. Heats of mixing of butanone and chloroform with alkanes: ternary systems. *Collect. Czech. Chem. Commun.*, 43: 837-847.
- Ralston, A.W., Hoerr, C.W. and Crews, L.T., 1944. Solubilities of some normal saturated aliphatic hydrocarbons. *J. Org. Chem.*, 9: 319-328.
- Schäfer, K. and Rohr, F.J., 1960. Kalorische Untersuchungen Mischungen von Aceton mit Normal Kohlenwasserstoffen. *Z. Phys. Chem. N.F.*, 24: 130-151.
- Scatchard, G., 1931. Equilibria in nonelectrolyte solutions in relation to the vapor pressures and densities of the components. *Chem. Rev.*, 8: 321-333.
- Widom, B. and Khosla, M.P. 1980. Densities of binary liquid mixtures near their consolute points. *J. Chem. Soc., Faraday Trans. 1*, 1980, 76: 2043-2051.
- Wilhelm, E., 1985. Molecular thermodynamics of flexible-molecule fluids. *Thermochim. Acta*, 94: 47-66.
- Wilhelm, E., Lainez, A., Rodrigo, M., Roux, A.H. and Grolier, J.-P.E., 1985. A calorimetric study of conformational changes in binary mixtures containing an n-alkane. Heat capacities of (a substituted aromatic hydrocarbon + an n-alkane) at 298.15 K. 40th Annual Calorimetry Conference, Asilomar, CA, 25-29 August 1985: Paper no. 14.

CHAPTER 2

W-SHAPE CONCENTRATION DEPENDENCE OF  $C_p^E$  AND  
SOLUTION NON-RANDOMNESS:  
SYSTEMS APPROACHING THE UCST

## INTRODUCTION

The excess heat capacity,  $C_p^E$ , has been found to have a surprising W-shape concentration dependence in a wide variety of systems. Either two minima appear in  $C_p^E(x)$  separated by a maximum, as in Fig. 2 of this paper, or two regions of positive  $C_p^E(x)$  curvature separated by a region of negative curvature.

The W-shape has been interpreted as due to the superposition of two contributions in  $C_p^E$ , (1), a "normal", parabolic term of negative sign arising when polar and non-polar components are mixed, the corresponding contributions in  $G^E$  and  $H^E$  being positive. Any other mixing process in which order is destroyed will give similar signs. (2) an "anomalous" positive contribution associated with local non-randomness in the solution caused by values of  $G^E$  and  $H^E$  larger than  $\approx 800$  and  $\approx 1000$  J/mol respectively. Since non-randomness must disappear at the ends of the concentration range, contribution 2 with 1 can give the W-shape. It has been suggested by Rubio et al<sup>2</sup> that concentration fluctuations in solution or local composition non-randomness can be studied through the radial distribution functions  $G_{ij}(r)$  or more specifically through the concentration-concentration correlation function  $S_{CC}$ , as suggested by Bathia and Thornton<sup>3</sup>.  $S_{CC}$  is obtainable through light scattering<sup>2</sup> or vapour pressure measurements and is given by:

$$S_{CC} = \left[ \left[ \frac{\partial^2 (G/RT)}{\partial x^2} \right]_{P,T} \right]^{-1} \quad (1)$$

$$= x_2 \left[ \left[ \frac{\partial (\mu_1/RT)}{\partial x_1} \right]_{P,T} \right]^{-1} \quad (2)$$

Theoretical values of  $S_{CC}$  may be obtained through the use of the Flory-Huggins theory, in which  $G^E$  is given by:

$$\frac{G^E}{RT} = x_1 \ln \frac{\phi_1}{x_1} + x_2 \ln \frac{\phi_2}{x_2} + \chi_1 (x_1 + x_2 r) \phi_1 \phi_2 \quad (3)$$

where  $\phi_1$  and  $\phi_2$  are the volume fractions of components 1 and 2,  $r$  the ratio of molar volumes of the components and  $\chi_1$ , the interaction parameter given as:

$$\chi_1 = \frac{z\Delta W}{RT} \quad (4)$$

Where  $z$  is the coordination number,  $\Delta W$  the interchange free energy. Combining eqns. (1) and (3) leads to this expression of  $S_{CC}$

$$\frac{x_1 x_2}{S_{CC}} = 1 + \frac{x_1 x_2 (r-1)^2}{(x_1 + x_2 r)^2} - \frac{2 \chi_1 x_1 x_2 r^2}{(x_1 + x_2 r)^3} \quad (5)$$

As suggested in ref. 2, if the interaction parameter  $\chi$ , is small, then  $S_{CC}$  is mainly given by the first two terms of eqn. 5. Therefore the maximum of  $S_{CC}$  decrease as  $r$  increases and shifts to lower values of  $x_1$ . This will be tested in the discussion section below.

However, if  $\chi$  is large, the third term dominates in eqn. 5 and the maximum of  $S_{CC}$  increases with  $r$  and shifts towards higher values of  $x_1$ , until for sufficiently large  $\chi_1$ ,  $S_{CC}$  tend to infinity at the critical point.

It is known that  $\frac{\partial^2(G/RT)}{\partial x^2} = 0$  at the critical point. Therefore, according to eqn. 1,  $S_{CC}$  should go to infinity as  $T$  goes to  $T_c$ . Since non-randomness is expressed as a manifestation of the critical state, even at  $T$  well removed from  $T_c$ ,  $S_{CC}$  can then be taken as an indicator of non-randomness. As  $T$  decreases toward  $T_c$ , non-randomness increases and therefore  $S_{CC}$  becomes more positive. However, the ideal value of  $S_{CC}$  ( $S_{CC}^{id}$ ) where  $r = 1$ ,  $\chi = 0$  corresponding to a random solution is given as

$$S_{CC}^{id} = x_1 x_2.$$

We have suggested in a previous paper<sup>5</sup> that the sharp increase observed in W-shape  $C_p^E$  when T approaches the UCST was due to non-randomness increasing as T goes to  $T_C$ . It seems evident as suggested by Rubio et al<sup>2</sup> that a correlation exists between  $S_{CC}$  and  $C_p^E$  although no singular critical exponent could be found for these two quantities.

Experiment suggests that  $C_p^E$  becomes W-shaped when  $S_{CC} \geq 0.7$ <sup>2</sup>. Lowering the temperature enhances  $S_{CC}$  and W-shape. Approaching the UCST:

$$(\partial^2 G / \partial x^2)_{P,T} \longrightarrow 0 \text{ as } (T - T_C)^{1.24}$$

i.e.  $S_{CC} \longrightarrow \infty$  as  $(T - T_C)^{-1.24}$ <sup>4</sup> and  $C_p \longrightarrow \infty$  as  $(T - T_C)^{-0.125}$  indicating that the critical positive peak of  $C_p^E$  increases dramatically as the UCST is approached.

This was found for acetone + hydrocarbons<sup>5</sup> and in the present work W-shape is investigated for several systems within 50°C of their UCSTs and comparison is made with the behaviour of  $S_{CC}$ .

## EXPERIMENTAL

The chemicals are from Aldrich Chemical Co. and are at least of 99% of purity. They were used without further treatment.

Heat capacity was measured using a Picker flow micro calorimeter from Sodev Inc. A densitometer (Sodev, Sherbrooke) was used to transform volumetric heat capacity and to calculate excess volumes. Procedures and instrumentation are described elsewhere<sup>6</sup>.

Heat capacity measurements were made for mixtures of nitroethane + cyclohexane at 25, 27, 30, 35°C; nitropropane + cyclohexane at 25°C; propionitrile + cyclohexane at 15, 25, 40°C; perfluoro n-heptane + isooctane at 30°C; ethylacetate + n-C<sub>16</sub> and brC<sub>16</sub> at 25°C.

$S_{CC}$  was calculated for the different systems using literature data of  $G^E$  obtained either from light scattering or vapour pressure measurements. The computer program used to calculate  $S_{CC}$  is provided in appendix 2.

## RESULTS AND DISCUSSION

### 1. Nitroethane and nitropropane + cyclohexane

Marsh has made a thorough study of the composition dependence of  $G^E$  at  $318.15^\circ\text{K}$  and of  $H^E$  at both  $318.15^\circ\text{K}$  and  $298.15^\circ\text{K}$  for both nitroethane + cyclohexane<sup>7</sup> and nitropropane + cyclohexane<sup>8</sup>. These data were used to give approximate  $G^E(x)$  at various temperatures i.e taking  $C_p^E$  to be an average obtained from the two temperatures  $H^E$  measurements. Eqn. (1) then gives  $S_{CC}(x,T)$  as seen in Fig. (1), where  $S_{CC}(x)$  is given at different temperatures for both nitroethane and nitropropane + cyclohexane mixtures.

In all cases,  $S_{CC}$  of the solution is much greater than  $S_{CC}$  ideal indicating a non-randomness contribution to these mixtures. As  $T$  approaches the UCST which lies at  $23.3^\circ\text{C}$ <sup>9</sup>,  $S_{CC}$  diverges strongly from the ideal value indicating an increase of the non-randomness associated with large values of  $G^E$  and  $H^E$  respectively 1413 and 1687 J/mole for this system.

Similar behaviour can be seen in Fig. 2 showing the W-shape.  $C_p^E$  shows a positive maximum and two negative minima at the extremities of the concentration range. The W-shape increases as  $T$  decreases towards the UCST. At  $25^\circ\text{C}$  (within  $1.7^\circ\text{C}$  from the UCST) both  $C_p^E$  and  $S_{CC}$  show sharp maxima indicating a rapid increase in the non-random contribution.

The maximum of the  $C_p^E$  curve occurs at a concentration lower than 0.5 for  $T$  relatively far from UCST. But it moves toward the middle of the concentration range as  $T$  decreases and approaches the UCST. Nevertheless even at  $T$  close to the UCST, the maximum is still not in agreement with the Flory Theory which would predict a critical concentration near 0.50. This small discrepancy is probably due to the polar forces which are not taken into account by the theory.

Fig. 1 Concentration dependence of  $S_{CC}$  as a function of mole fraction of nitroethane in cyclohexane at • 25°C; ○ 27°C; Δ 30°C; △ 35°C; □ 45°C and nitropropane in cyclohexane □ at 25°C.

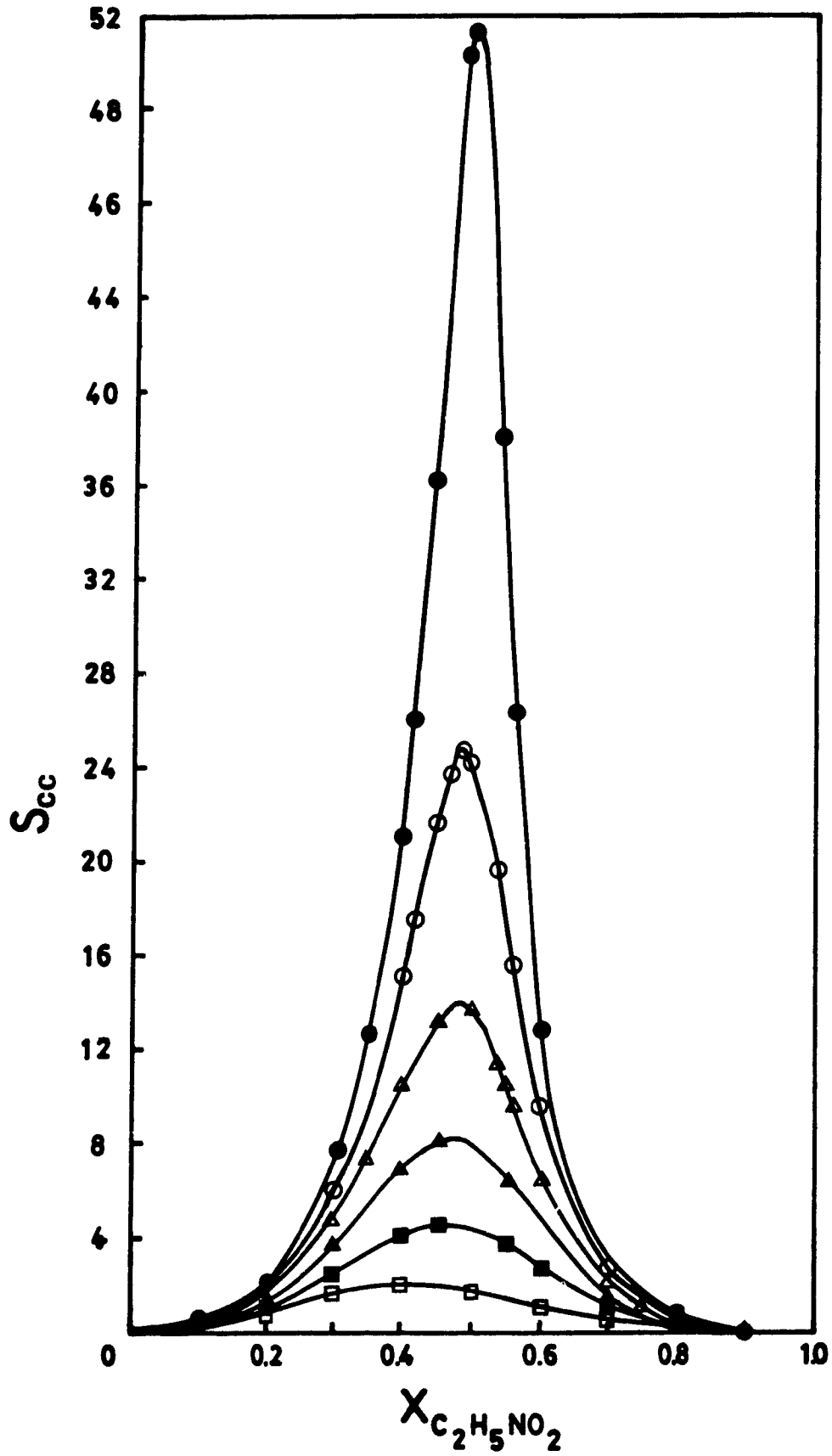
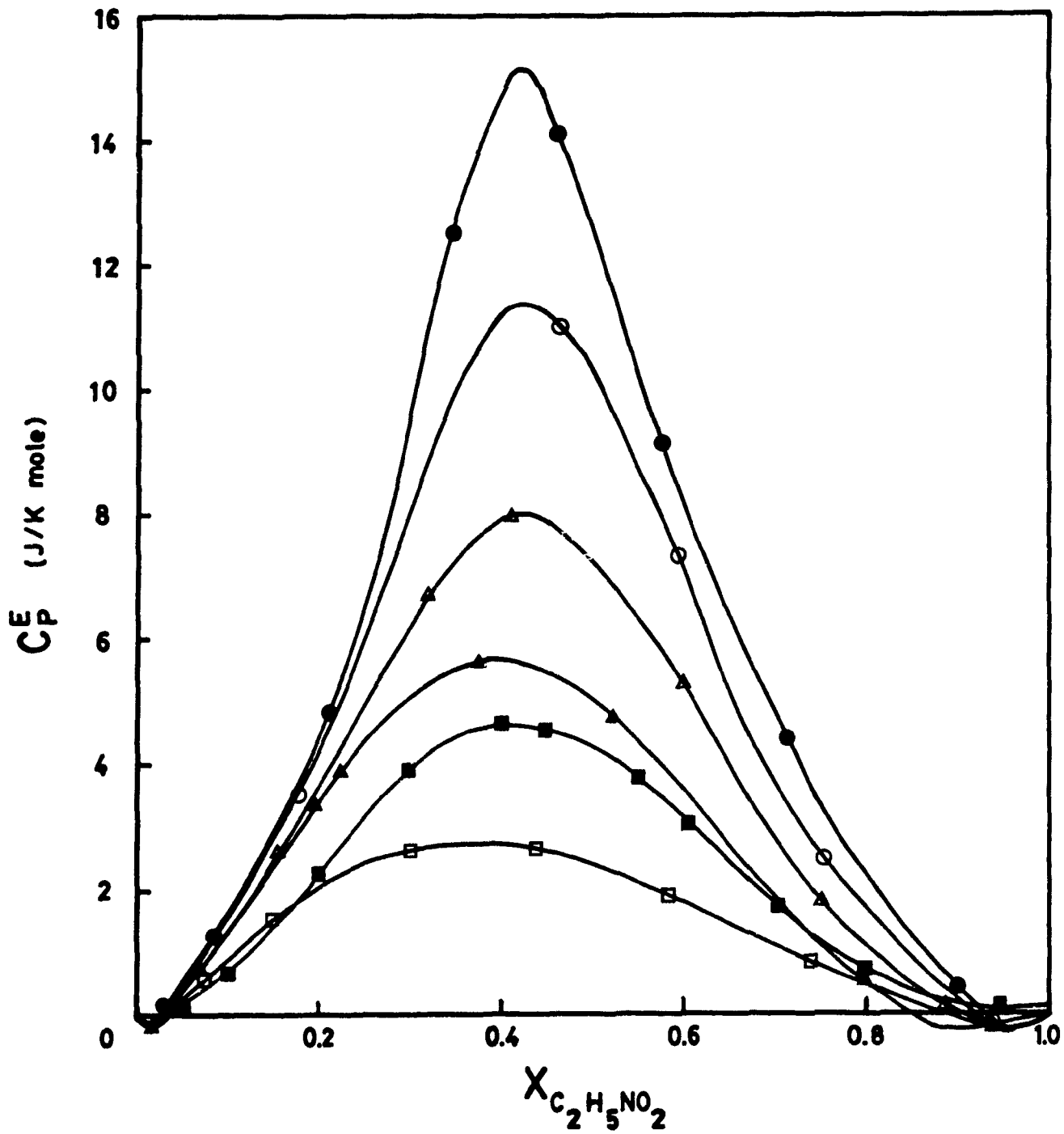


Fig. 2 Excess molar heat capacities of nitroethane + cyclohexane at • 25°C; ○ 27°C; Δ 30°C; Δ 35°C; □ 45°C; and nitropropane + cyclohexane □ at 25°C.



The critical concentration of  $S_{CC}$  is 0.50 i.e. in agreement with the Flory–Huggins Theory at 25°C while it is lower as T is removed from  $T_C$ .

Fig 1 and 2 show also  $S_{CC}$  and  $C_p^E$  results for nitropropane +  $CyC_6$  at 25°C. The UCST for this system is well below the experimental temperature ( $< -70^\circ C$ ).

$$S_{CC} \text{ max} = 2 \quad \text{while} \quad C_p^E \text{ max} = 2.7 \text{ J/K mol.}$$

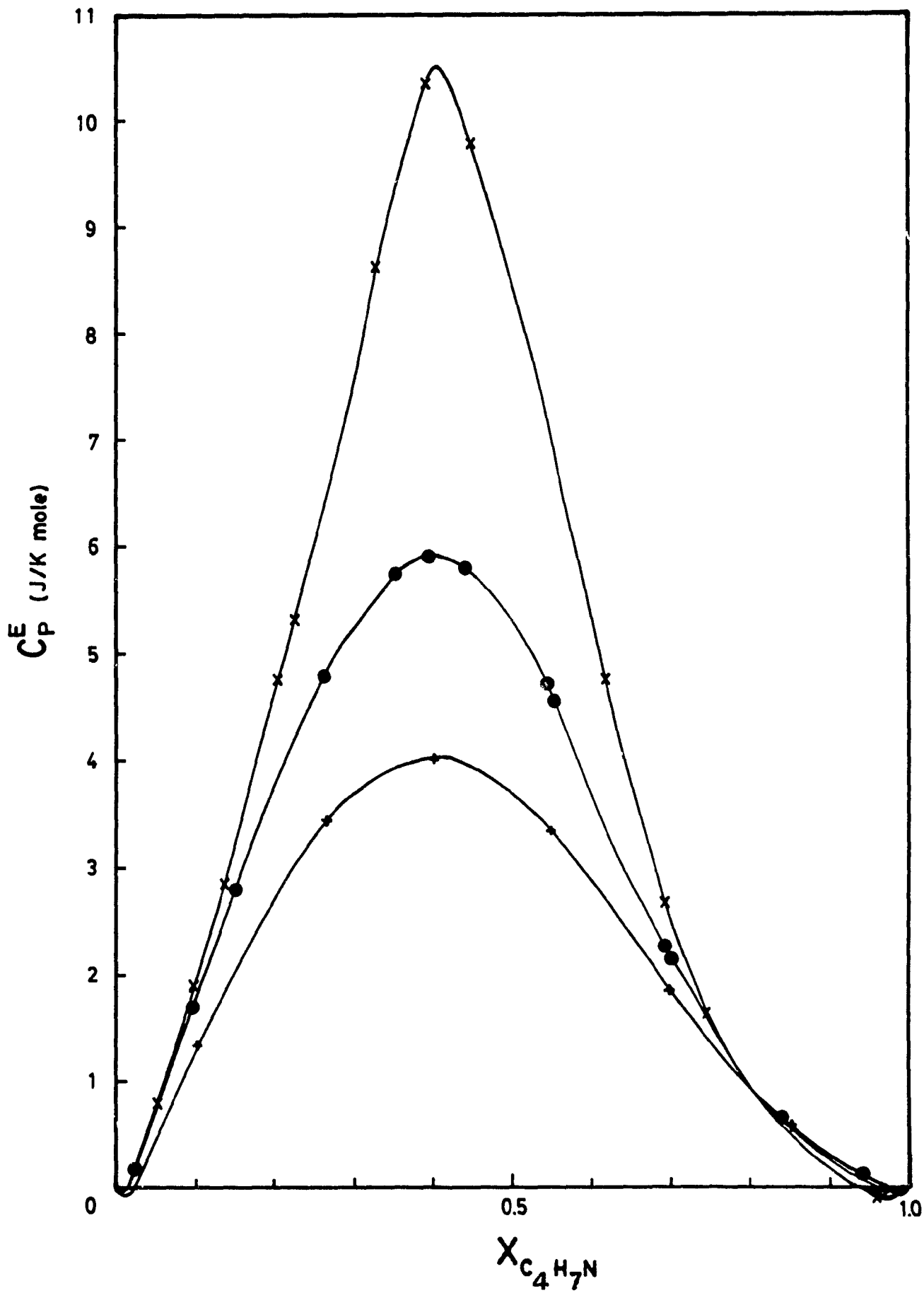
The equimolar values of  $G^E$  and  $H^E$  for this system are large (respectively 1160 and 1507 J/mol at 25°C)<sup>10</sup>, but not as large as for nitroethane (1413 and 1687 J/mol at 25°C). The difference in excess quantities reflects the smaller fraction of the nitropropane molecule which is of  $NO_2$  character. Correspondingly,  $S_{CC}$  for nitropropane is smaller at 25°C than for nitroethane and  $C_p^E$ , although W-shaped, is nevertheless not so pronounced.

Here again a correlation can be made between the lower non-randomness indicated by a lower value of  $S_{CC}$  and the smaller maximum observed for  $C_p^E$ .  $S_{CC}$  is just above the limit of 0.7 suggested by Rubio et al for the observation of a W-shape.

## 2. Propionitrile + $CyC_6$

Fig. 3 shows  $C_p^E$  results for propionitrile +  $CyC_6$  mixtures at 15, 25, 40°C. The UCST is observed at 12.2°C<sup>8</sup> and the mixture is largely endothermic ( $H^E \approx 1500$  J/mol). Propionitrile +  $CyC_6$  behaves similarly to nitropropane +  $CyC_6$ . Both systems are close to their UCST and both exhibit a large and positive W-shape which is very sharp as T approaches the UCST. No reliable values of  $G^E(x)$  could be found in the literature, but  $S_{CC}$  should show the same picture as nitroethane +  $CyC_6$ .

Fig. 3 Excess molar heat capacity of propionitrile + cyclohexane at  $\times 15^{\circ}\text{C}$ ,  $\bullet 25^{\circ}\text{C}$ ,  
 $+ 40^{\circ}\text{C}$  (UCST =  $12.2^{\circ}\text{C}$ ).



3. Perfluoro n-heptane + 2,2,4-trimethylpentane (brC<sub>8</sub>)

Fig. 4 shows  $C_p^E$  for perfluoro n-heptane + 2,2,4-trimethylpentane at 30°C. The proximity of the UCST (23°C) and the large and positive values observed<sup>14</sup> for both  $H^E$  (~ 2100 J/mol) and  $G^E$  (~ 1362 J/mol) predict large W-shape. Indeed, experiment reveals a large and sharp W-shape whose maximum occurs at ~ 0.4 mole fraction.

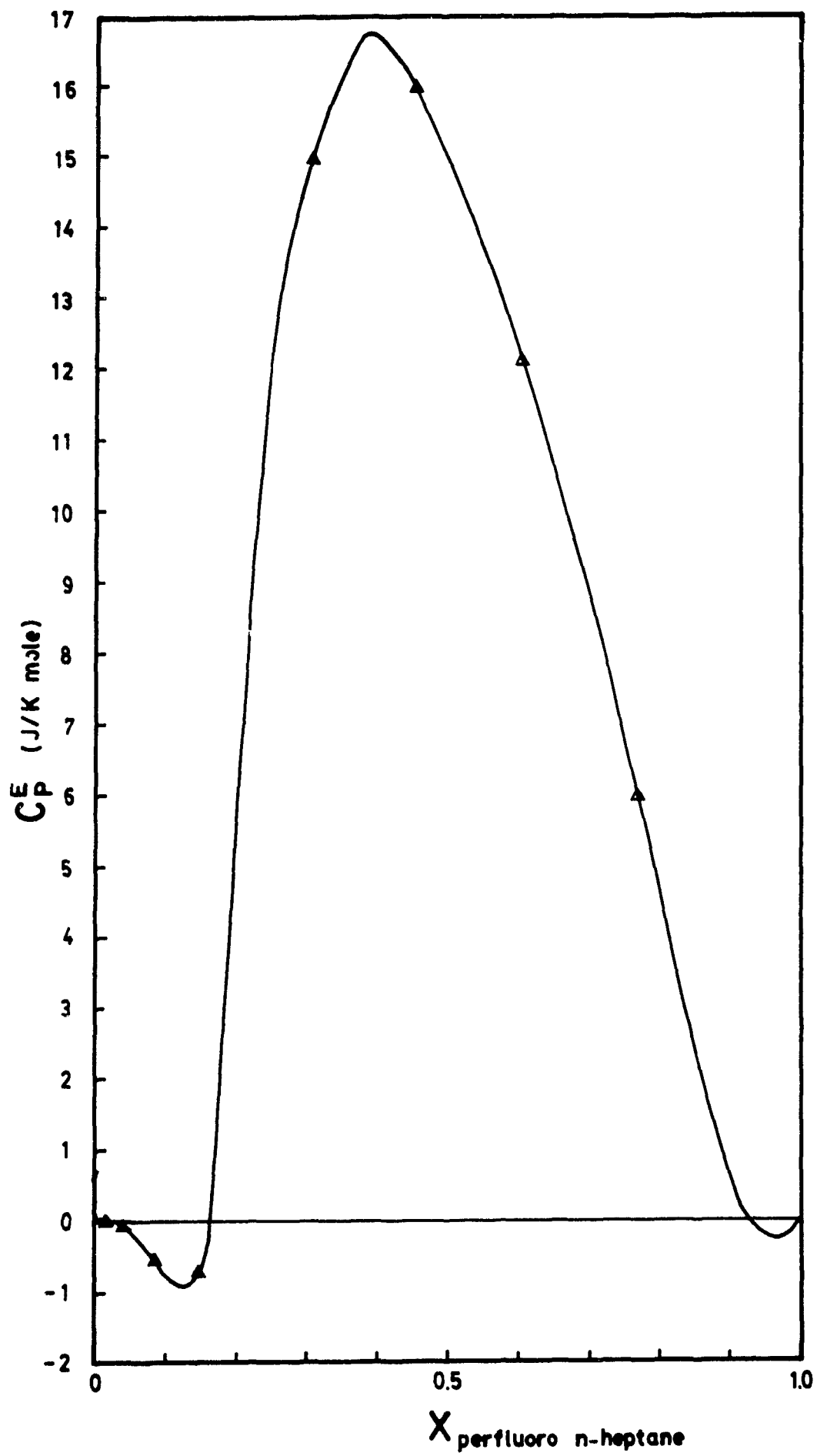
Conversely to the previous components, perfluoro n-heptane is not a strictly polar compound. Hence W-shape is observed, due to a large non-randomness contribution to  $C_p^E$ . This non-randomness contribution can be more or less quantified through the  $S_{CC}$  curve which also reveal a sharp peak as T approaches the UCST. The critical concentration of  $S_{CC} \rightarrow 0.5$  as  $T \rightarrow T_c$ . Values of  $G^E(x)$  used to calculate  $S_{CC}$  were obtained from Scott<sup>14</sup>,  $S_{CC}$  calculations are shown in fig. 5.

4. Ethylacetate + n-C<sub>16</sub> and brC<sub>16</sub>

Fig. 6, however, shows W-shape  $C_p^E$  for ethylacetate mixed with n-C<sub>16</sub> and brC<sub>16</sub>. Although the large values of  $H^E$  (~ 1750 J/mol)<sup>12</sup> for these mixtures no UCST has been observed, meaning that T may be ~ 100°C away from the UCST. Then, the non-randomness effect would be small compared to  $C_p^E$ . Indeed,  $C_p^E$  shows a negative W-shape in both n-C<sub>16</sub> and brC<sub>16</sub> cases. n-C<sub>16</sub> solutions show a much larger negative  $C_p^E$  than brC<sub>16</sub>, due to the negative contribution implemented in  $C_p^E$  and coming from the destruction of correlation of molecular orientation going from the pure n-C<sub>16</sub> to the solution.

Fig. 7 shows an extremely small value of  $S_{CC}$  for ethylacetate + n-C<sub>7</sub> which is the only system in this series for which ( $G^E(x)$ ) was available<sup>13</sup>. The curve is just above the limit value of  $S_{CC}$  for the observation of a W-shape  $C_p^E$ .  $S_{CC}$  should be a

Fig. 4 Excess molar heat capacity of perfluoro n-heptane + 2,2,4-trimethylpentane at 30°C.



$X_{\text{perfluoro n-heptane}}$

Fig. 5 Concentration dependence of  $S_{CC}$  for perfluoro n-heptane + 2,2,4-trimethylpentane at  $\circ$  25°C; \* 27°C; + 30°C; x 67°C; • 92°C;  $\nabla$  177°C.

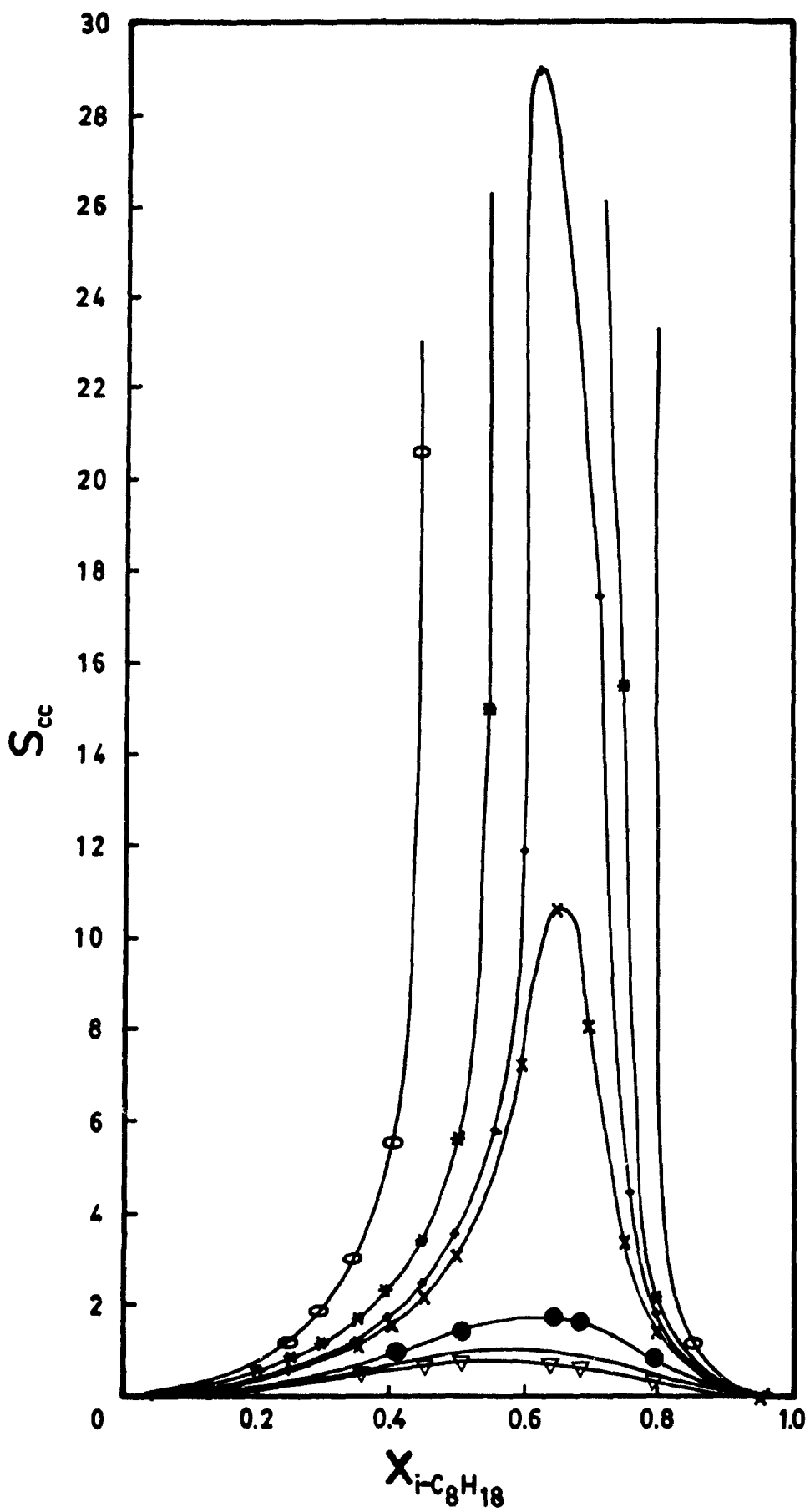


Fig. 6 Excess molar heat capacity of ethylacetate + n-hexadecane at • 25°C; and  
2,2,4,4,6,8,8-heptamethylnonane × at 25°C.

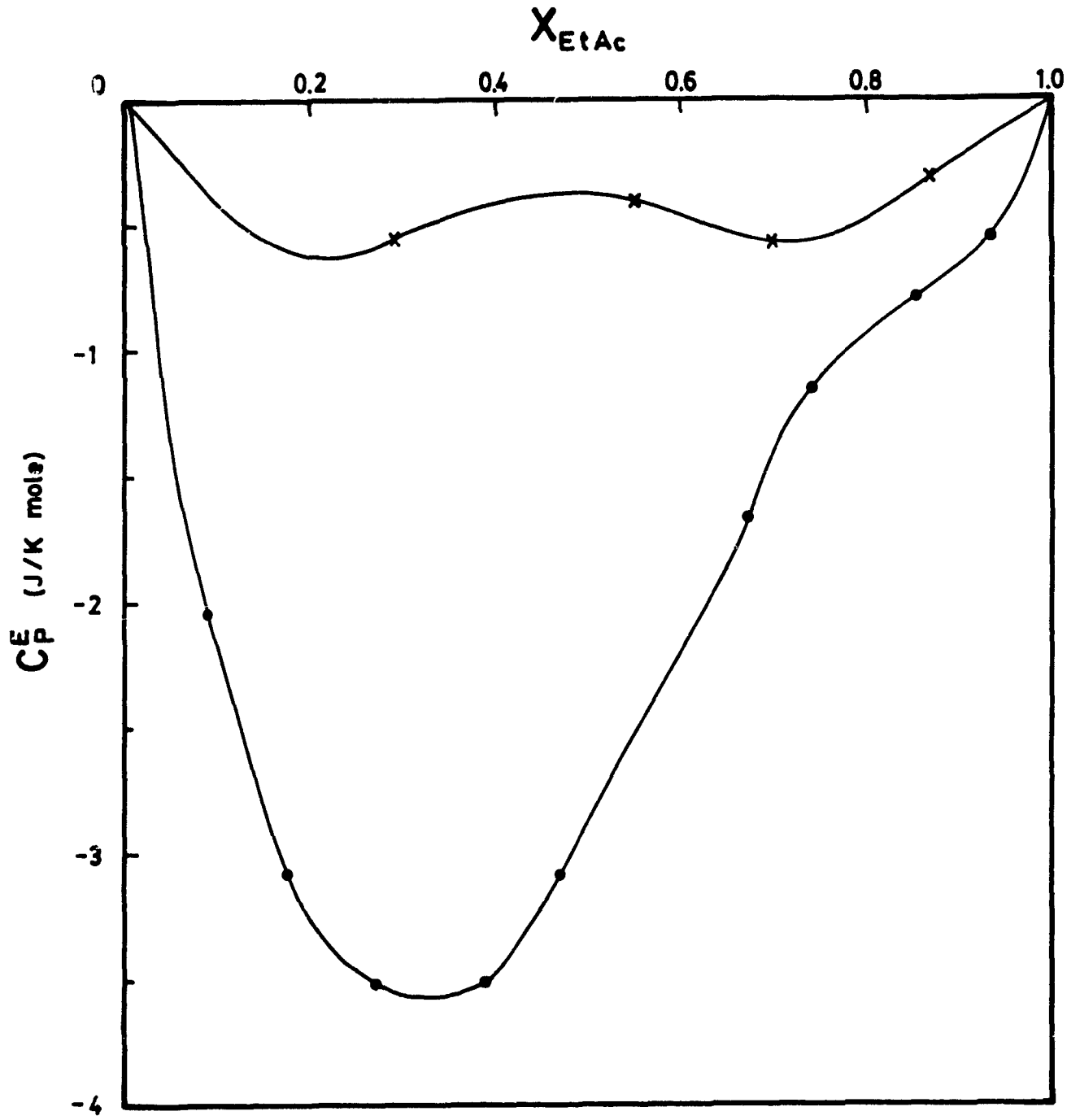


Fig. 7 Concentration dependence of  $S_{CC}$  for ethylacetate + n-heptane at 25°C.

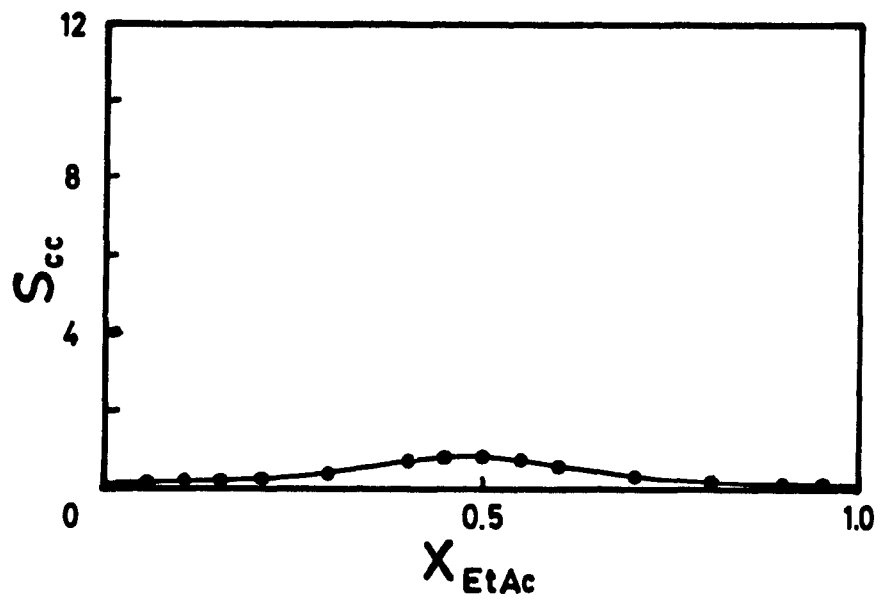
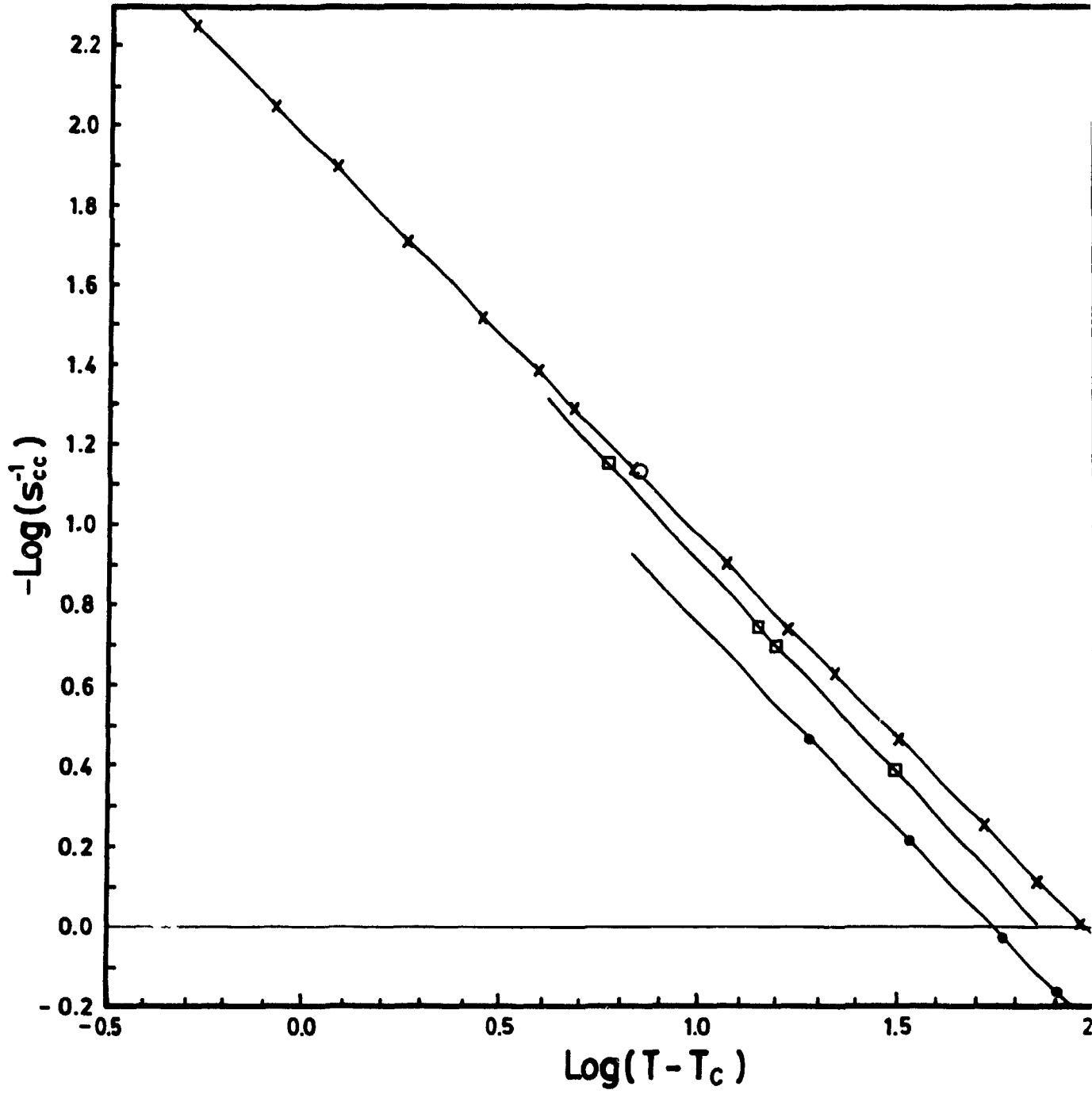


Fig. 8 Comparison between  $S_{CC}^{-1}$  vs  $\log (T - T_c)$  for  $\times$  nitroethane +  $CyC_6$ ;  $\bullet$  acetone +  $n-C_6$ ;  $\square$  acetone +  $n-C_{10}$ ;  $O$  nitrobenzene +  $n-C_7$ .



little bit larger for a longer chain alkane such as hexadecane. But, still non-randomness will be small compared to any system close to its UCST, and that explains the negative W-shape  $C_p^E$  observed.

Fig. 8 shows the variation of  $S_{CC}^{-1}$  against  $\log(T - T_C)$  for several systems showing W-shape  $C_p^E$ . As  $S_{CC}$  goes to infinity, a certain singularity is observed for the critical exponent of  $(T - T_C)$  ( $-1.2$ ) which converges to the expected ( $-1.24$ ) value, although it is evident that in order to observe this value one has to be extremely close to the critical point. The different systems lie on different curves which are, however, parallel. This deviation must be explained by the dependence of  $S_{CC}$  on the ratio of the molar volume of the components ( $r$ ). As  $r$  decreases, the curves move to the left, indicating a lower value of  $S_{CC}$  for the same value of  $(T - T_C)$ .

In all the systems studied, the similarity of  $C_p^E$  and  $S_{CC}$  is striking and confirms that:

- (1) non-randomness increasing with decreasing  $T$  toward the UCST
- (2) In both  $C_p^E$  and  $S_{CC}$  cases, concentration dependence gives curves concave downward, i.e. non-randomness ( $S_{CC}$ ) and the effect of non-randomness (central peak of  $C_p^E$ ) is found mainly toward the middle of the concentration range.

REFERENCES

1. A. Inglese, J.-P. E. Grolier and E. Wilhelm, *J. Chem. Thermodyn.* 16, 67, 1984.
2. R.G. Rubio, M. Caceres, R.M. Masegosa, L. Andreoli-Ball, M. Costas, and D. Patterson, submitted to *Ber. Bunsenges. Phys. Chem.* 1988.
3. A.B. Bathia and D.E. Thornton, *Phys. Rev.* 2B, 3004, 1970.
4. J.S. Rowlinson and F.L. Swinton, *Liquids and Liquids Mixtures*, Third Edition, Butterworths, 1982.
5. M.-E. Saint Victor and D. Patterson, *Fluid Phase Equilibrium* 35, 237, 1987.
6. P. Picker, J.-P. Leduc, P.R. Phillips, J.E. Desnoyers, *J. Chem. Thermodyn.*, 3, 631, 1971.
7. K.N. Marsh, H.T. French, and H.P. Rogers, *J. Chem. Thermodyn.* 11, 897, 1979.
8. a) K.N. Marsh, *J. Chem. Thermodyn.* 17, 600, 1985.  
b) K.N. Marsh, W.A. Allan, and A.E. Richards, *J. Chem. Thermodyn.* 16, 1107, 1984.
9. A.W. Francis, *Critical Solution Temperatures*, #31, *Advances in Chemistry Series*, American Chemical Society, 1961.
10. A. McLure and A.T. Rodriguez, *J. Chem. Thermodyn.* 14, 439, 1982.
11. A. Alessandrini, P. Alessi, and I. Kikic, *Ann. Chim. (Rome)* 70, 293, 1980.
12. J.P.E. Grolier, D. Ballet, and A. Viillard, *J. Chem. Thermodyn.* 6, 895, 1974.
13. G.G. Hua, L. Yuen, L. Qinlong, Z. Rui, and S. Xianda, *J. Tsinghua Univ.* 24, #2, 1984.
14. A.G. Williamson and R.L. Scott, *J. Phys. Chem.* 65, 275, 1961.

APPENDIX 1

Tables of Results

TABLE 1

Excess molar heat capacities as a function of mole fraction of  
nitroethane + cyclohexane at 25°C

$x_1$	$C_p^E$ J/K mol
0.0310	0.04
0.0902	1.17
0.2212	4.72
0.2220	5.10
0.3491	12.54
0.4598	13.88
0.4664	14.09
0.5658	9.07
0.6436	7.04
0.7197	5.17
0.8968	-0.23

TABLE 2

Excess molar heat capacities as a function of mole fraction of  
nitroethane + cyclohexane at 27°C

$x_1$	$C_p^E$ J/K mol
0.0012	0.03
0.1272	2.46
0.1794	3.50
0.3087	15.28
0.5043	10.55
0.5939	6.91
0.5980	7.31
0.7435	1.64
0.7533	2.45
0.8688	0.84
0.8906	-0.09
0.9492	-0.16

TABLE 3

Excess molar heat capacities as a function of mole fraction of  
nitroethane + cyclohexane at 30°C

$x_1$	$C_p^E$ J/K mol
0.0658	0.58
0.3196	2.61
0.4116	7.91
0.6009	5.38
0.7443	1.65
0.8893	0.05
0.9438	-0.07

TABLE 4

Excess molar heat capacities as a function of mole fraction of  
nitroethane + cyclohexane at 35°C

$x_1$	$C_p^E$ J/K mol
0.2234	4.08
0.3638	5.65
0.5208	4.76
0.6026	3.48
0.7536	0.94
0.8955	-0.12

TABLE 5

Excess molar heat capacities as a function of mole fraction of  
nitropropane + cyclohexane at 10°C

$x_1$	$C_p^E$ J/K mol
0.0181	-0.06
0.0370	0.09
0.3594	3.96
0.4638	3.51
0.6049	2.18
0.7540	0.83
0.9034	-0.02
0.9483	-0.001

TABLE 6

Excess molar heat capacities as a function of mole fraction of  
nitropropane + cyclohexane at 25°C

$x_1$	$C_p^E$ J/K mol
0.0678	0.42
0.1534	1.60
0.3039	2.62
0.4438	2.58
0.5795	1.84
0.7422	0.93
0.8912	0.05
0.9368	-0.05
0.9654	-0.08

TABLE 7

Excess molar heat capacities as a function of mole fraction of  
propionitrile + cyclohexane at 15°C

$x_1$	$C_p^E$ J/K mol
0.0525	0.81
0.0972	1.87
0.1352	2.85
0.2013	4.84
0.2244	5.37
0.3260	8.63
0.3940	10.38
0.4471	9.76
0.6196	4.75
0.6961	2.69
0.7541	1.62
0.8423	0.59
0.9576	-0.01

TABLE 8

Excess molar heat capacities as a function of mole fraction of propionitrile + cyclohexane at 25°C

$x_1$	$C_r^E$ J/K <sup>2</sup> mol
0.0249	0.18
0.0993	1.71
0.0998	1.67
0.1519	2.76
0.2639	4.82
0.2663	4.81
0.3501	5.75
0.3952	5.89
0.4430	5.78
0.5448	4.72
0.5530	4.53
0.6936	2.29
0.6949	2.13
0.8408	0.66
0.8417	0.49
0.9321	0.22
0.9413	0.15

TABLE 9

Excess molar heat capacities as a function of mole fraction of  
propionitrile + cyclohexane at 40°C

$x_1$	$C_p^E$ J/K mol
0.1013	1.36
0.2634	3.45
0.4002	4.04
0.5462	3.32
0.6990	1.81
0.8461	0.60
0.9443	0.14

TABLE 10

Excess molar heat capacities as a function of mole fraction of  
perfluoro n-heptane + 2,2,4-trimethylpentane at 30°C

$x_1$	$C_p^E$ J/K mol
0.0236	-0.01
0.0434	-0.05
0.0895	-0.51
0.1545	-0.76
0.3133	14.94
0.4492	16.02
0.6053	12.21
0.7838	5.99

TABLE 11

Excess molar heat capacities as a function of mole fraction of ethylacetate + normal hexadecane at 25°C

$x_1$	$C_p^E$ J/K mol
0.0881	-2.08
0.1768	-3.14
0.2693	-3.53
0.3919	-3.50
0.4700	-3.16
0.6562	-1.80
0.7427	-1.28
0.8565	-0.80
0.9459	-0.59

TABLE 12

Excess molar heat capacities as a function of mole fraction of ethylacetate + 2,2,4,4,6,8,8-heptamethylnonane at 25°C

$x_1$	$C_p^E$ J/K mol
0.2861	-0.51
0.4277	-0.30
0.5550	-0.39
0.7029	-0.63
0.8726	-0.51

APPENDIX 2

Program listing for  $S_{CC}$  calculation

```

'REM *****
          SCC  PROGRAM  *****
'
'THIS PROGRAM CALCULATES SCC FROM THE SECOND DERIVATIVE OF
GE.THE PROGRAM
'WILL BE USING PARAMETERS FOR REDLISH-KISTER EQUATION FOR
GE.
'
DEFSNG A-Z
DEFSTR C
DIM  A(100)
'****
INPUT "COMPONENT 1"; COMPONENT1
INPUT "COMPONENT2"; COMPONENT2
INPUT "PRINT ?"; ANSWER$
INPUT "ALFA"; ALFA
INPUT "BETA"; BETA
INPUT "T(K)"; T
IF ANSWER$ = "Y" THEN
  LPRINT
  "-----"
  LPRINT TAB(5); COMPONENT1, "+", COMPONENT2
  LPRINT
  "-----"
  LPRINT
  LPRINT "T: "; T
END IF
FOR I = 1 TO 5
  INPUT "A"; A(I - 1)
  IF ANSWER$ = "Y" THEN
    LPRINT "A("; I - 1; ");"; A(I - 1)
  ELSE PRINT "A("; I - 1; ");"; A(I - 1)
  END IF
NEXT I
IF ANSWER$ = "Y" THEN
  LPRINT "ALFA"; ALFA
  LPRINT "BETA"; BETA
  LPRINT
  LPRINT
  "-----"
  LPRINT TAB(5); "x1"; TAB(15); " GE"; TAB(28); "
  d2GE / d2x1"; TAB(42); "SCC"
  LPRINT
  "-----"
  LPRINT
ELSE
  PRINT "ALFA: "; ALFA
  PRINT "BETA: "; BETA
END IF
'COMPUTE PARAMETER VALUE FOR X=0 AND NOT GREATER THAN 1 IF
X > 1 THEN STOPS
'****
x1 = 495
WHILE x1 <= .52
  'IF x1 >= .4 AND x1 <= .6 THEN x1 = x1 + .02

```

```
NUM! = x1 * (1 - x1)
DENO! = ALFA + BETA * x1
P! = NUM / DENO
'PRINT "NUM="; NUM; "DENO="; DENO, "P="; P
'****
'INITIALIZATION OF Q,DQ,D2Q THAT WILL BE USING FOR THE
SUMMATION '****
Q! = 0!
dQ! = 0!
d2Q! = 0!
'*** COMPUTE THE VALUES OF Q, dQ, d2Q THROUGH A
SUMMATION OF POWER 4 ***
PROD! = 1 - 2 * x1
FOR II = 1 TO 5
  I = II - 1
  PRODU! = PROD ^ I
  'PRINT "PROD="; PROD, "PRODU="; PRODU
  QUU! = A(I) * PRODU
  'PRINT "I="; I, "A(I)="; A(I)
  Q! = Q + QUU
  'PRINT "QUU="; QUU, "Q="
  PRODI! = PROD ^ (II - 1)
  SUM! = II * A(II) * PRODI
  'PRINT "PRODI="; PRODI, "SUM="; SUM
  dQ! = dQ + SUM
  MI! = II + 1
  BB! = PROD ^ (MI - 2)
  SOMM! = BB * A(MI) * MI * (MI - 1)
  d2Q! = d2Q + SOMM
  'PRINT "dQa="; dQ; "BB="; BB, "SOMM="; SOMM;
    "d2Qa="; d2Q
NEXT II
dQ = -(2 * dQ)
d2Q = 4 * d2Q
'PRINT "dQ="; dQ, "d2Q="; d2Q
'*** COMPUTE THE VALUES OF dP AND d2P ***
'****
NUME! = DENO * PROD - NUM * BETA
DENOM! = DENO ^ 2
dP! = NUME / DENOM
'PRINT "NUME="; NUME; "DENOM="; DENOM, "dP="; dP
'*****COMPUTE THE DIFFERENT TERMS IN THE EXPRESSION OF
d2Q '*****
TERM1! = BETA * PROD / DENO
M2! = BETA ^ 2 * NUM
TERM2! = M2 / DENOM
TERM3! = 2 / DENO
TERM4! = TERM2 - TERM1 - 1
d2P! = TERM3 * TERM4
'PRINT "TERM1="; TERM1; "M2="; M2; "TERM3="; TERM3;
  "TERM4="; TERM4
'RINT "d2P="; d2P
'****
'***** COMPUTE d2PQ/dx2
```

```
'****
PA! = P * Q
GE! = PA * 8.3143 * T
d2PQ! = P * d2Q + 2 * dP * dQ + Q * d2P
x2! = 1 - x1
d2G! = 1 + x1 * x2 * d2PQ
'RINT "d2PQ="; d2PQ; "d2G="; d2G
'****
'*****COMPUTE VALUE OF SCC*****
'****
SCC! = x1 * x2 * (1 / d2G)
'RINT "d2G="; d2G; "SCC="; SCC
'****
'*****PRINT THE RESULTS FOR EACH VALUE OF X *****
'*****
  x1 = INT((x1 * 1000) + .5) / 1000
  SCC = INT((SCC * 10000) + .5) / 10000
  GE = INT((GE * 10000) + .5) / 10000
  d2PQ = INT((d2PQ * 100000) + .5) / 100000
IF ANSWER$ = "Y" THEN
  LPRINT TAB(4); x1; TAB(15); GE; TAB(30); d2PQ;
  TAB(40); SCC
  LPRINT
ELSE
  PRINT x1, GE, d2PQ, SCC
END IF
'****INCREMENT x1 BY 0.05 ****
'****
'F x1 >= .4 AND x1 <= .6 THEN x1 = x1 + .02
x1 = x1 + .001
WEND
END
```

CHAPTER 3

LOCAL NON-RANDOMNESS AND EXCESS SECOND - ORDER  
THERMODYNAMIC QUANTITIES

## INTRODUCTION

In recent publications<sup>1</sup> a W-shape concentration dependence of  $C_p^E$  has been ascribed to the presence in  $C_p^E$  of two contributions: (1) a "normal", parabolic curve of negative sign arising when polar and non-polar components are mixed, or more generally when order is destroyed during the mixing process and (2) an anomalous positive contribution associated with local non-randomness in the solution which appears towards the middle of the concentration range. A measure of non-randomness, the concentration-concentration correlation function,  $S_{CC}$ , is defined by<sup>2</sup>:

$$S_{CC} = \left[ \left( \frac{\delta^2(G/RT)}{\delta x^2} \right)_{P,T} \right]^{-1}$$

and a minimum value of  $S_{CC} \approx 0.7$  corresponding to  $G^E \approx 800 \text{ J mol}^{-1}$  has been suggested<sup>2</sup> for the appearance of the W-shape.

Both  $S_{CC}$  and  $C_p$  tend to infinity<sup>3</sup> at the critical point, the former as  $(T-T_c)^{-1.24}$  and the latter as  $(T-T_c)^{-1.25}$ . Lowering the temperature toward the UCST thus increases  $S_{CC}$  and the central maximum of the W-shape. For example, at 40, 25 and 15°C approaching the UCST at 13°C, in the propionitrile-cyclohexane system, the central maximum of  $C_p^E$  at  $x \approx 0.5$  is 3, 6 and 10  $\text{J K}^{-1} \text{mol}^{-1}$  i.e. already large at 40°C and becoming rapidly larger as T is lowered. It is argued<sup>4</sup> that the W-shape is a manifestation of the critical state which continues  $\approx 100^\circ\text{C}$  above  $T_c$  there being no essential difference between critical and non-randomness contributions to  $C_p^E$ . The excess quantity  $C_p^E$  is much more sensitive to the critical contribution than  $C_p$  of the solution itself because in  $C_p^E$  the various background contributions to  $C_p$  of the solution have been mainly eliminated through subtraction of the pure component  $C_p$ 's. Although the critical contribution to  $C_p$  of the solution may be small 50 – 100°C

from  $T_C$  perhaps  $1 - 3 \text{ J K mol}^{-1}$ , it is nevertheless discernible in  $C_p^E$  because the "normal" contribution to  $C_p^E$  is of the same order, and is of opposite sign with a different concentration dependence<sup>1</sup>.

Other second order thermodynamic quantities, i.e. the thermal expansion coefficient,  $\alpha_p$  and the isothermal compressibility,  $\kappa_T$ , also tend to infinity at  $T_C$  with the same critical exponent  $0.125^5$  as  $C_p$ . In the present work we consider the possibility of discerning the non-random or critical contribution in  $dV^E/dP$  and  $dV^E/dT$  after first considering  $C_p^E$  approaching the LCST rather than the UCST.

C<sub>p</sub><sup>E</sup> AT THE LCST :

As the UCST or LCST is approached and non-randomness is increased, H<sup>E</sup> is reduced in magnitude causing the non-random or critical contribution to C<sub>p</sub><sup>E</sup>. Approaching the LCST, where H<sup>E</sup> is negative, the non-random contribution to dH<sup>E</sup>/dT = C<sub>p</sub><sup>E</sup> is therefore positive. Two types of LCST are known: (1) in aqueous systems at low temperatures where the "normal" C<sub>p</sub><sup>E</sup> is also positive. Here the critical contribution will not appear as a W-shape, but as an enhancement and change of concentration dependence of an already positive C<sub>p</sub><sup>E</sup>. This may well be discernible but only relatively close to the LCST. (2) In systems where a large difference in free volume exists between the two components, as in a polymer-solvent system or one composed of two hydrocarbons of widely different carbon number, e.g. methane + 2-methylpentane<sup>6</sup>. The normal C<sub>p</sub><sup>E</sup> must be strongly negative and hence these systems are candidates for observation of the W-shape.

$$\underline{(\kappa_T V)^E = -(dV^E/dP)}$$

The critical contributions to C<sub>p</sub>, κ<sub>T</sub> and α<sub>p</sub> of the solutions are closely related. Thus Griffith and Wheeler<sup>7</sup> give for the solution in the critical region

$$(\kappa_T V)_{\text{crit}} = - \left[ \frac{dV}{dP} \right]_{\text{crit}} = \frac{(C_p)_{\text{crit}}}{T_c} \left[ \frac{dT_c}{dP} \right]^2 \quad (1)$$

We take the same relation to hold at temperatures more removed from T<sub>c</sub> and correspondingly the same equation is followed by the excess quantities. Since<sup>5</sup>,

$$\frac{dT_c}{dP} = T_c \frac{(d^2V/dx^2)_c}{(d^2H/dx^2)_c} \approx T_c \frac{V^E}{H^E} \quad (2)$$

We have

$$(\kappa_T V)^E_{\text{crit}} = - \left[ \frac{dV^E}{dP} \right]_{\text{crit}} = (C_p^E)_{\text{crit}} T_c \left[ \frac{V^E}{H^E} \right]^2 \quad (3)$$

The negative sign of  $(dV^E/dP)_{\text{crit}}$  is consistent with Lechatelier's Principle or with the following argument based on the displacement of  $T_c$  by pressure. The effect of non-randomness is to reduce the magnitude of  $V^E$ , e.g. if  $V^E$  is  $+(-)$ ,  $V^E$  due to non-randomness or  $(V^E)_{\text{crit}}$  is  $-(+)$ . From eq. (2), the effect of pressure for  $V^E$   $+(-)$  is to increase (decrease)  $T_c$  so that at  $T > \text{UCST}$ , the magnitude of the critical contribution to  $V^E$  will be increased (decreased) by pressure. Thus  $dV^E_{\text{crit}}/dP$  is negative for both signs of  $V^E$ . The sign of  $-(dV^E/dP)_{\text{crit}}$  is positive and could be expected to give the W-shape if the normal contribution to  $-dV^E/dP$  were negative. The Flory theory<sup>8</sup> shows this sign is attained when  $V^E$  is negative and although this sign is rarer than positive, it is found for systems which combine a component of high thermal pressure coefficient  $\gamma$  and low  $\alpha_p$  with one of low  $\gamma$  and high  $\alpha_p$ . Other model calculations using the Flory theory suggest that when  $V^E < 0$

$$(\kappa_T V)^E = - \frac{dV^E}{dP} \approx 20 * 10^{-3} V^E \text{ cm}^6 \text{ J}^{-1} \text{ mol}^{-1} \quad (4)$$

Putting  $V^E \approx -1 \text{ cm}^3 \text{ mol}^{-1}$ ,  $H^E \approx 1500 \text{ J mol}^{-1}$  and comparing eqns. (3) and (4) the value  $(C_p^E)_{\text{crit}}$  which would give critical and random contributions of equal magnitude in  $(dV^E/dP)$ , is  $100 \text{ J K}^{-1} \text{ mol}^{-1}$ . Such a large value of  $(C_p^E)_{\text{crit}}$  would only be achieved at an experimental temperature a fraction of degree from  $T_c$ . We conclude

that the W-shape in  $-(dV^E/dP)$  cannot be a wide-spread phenomenon as for  $C_p^E$ . This conclusion is consistent with previous work<sup>9</sup> where the Flory theory gave good predictions for  $-dV^E/dP$  in systems where  $C_p^E$  and  $dV^E/dT$  were sensitive to effects of structure in solution i.e. in  $dV^E/dP$  the "normal" contribution is too large to allow any effects of structure to be discerned.

$dV^E/dT$

According to the Prigogine–Flory theory<sup>10</sup>,  $V^E$  is composed of three terms: interactional,  $P^*$  and  $\bar{V}$  curvature.  $dV^E/dT$  may be considered as the sum of three corresponding terms which may be shown to be almost directly proportional to the  $V^E$  terms. Thus, the total  $dV^E/dT$  and  $V^E$  must be almost proportional, i.e.

$$dV^E/dT \approx 10 * 10^{-3} V^E \quad (5)$$

Furthermore, the critical contribution to  $dV^E/dT$  is given by<sup>6</sup>

$$\frac{dV^E}{dT_{crit}} = (C_p^E)_{crit} \frac{1}{T_c} \frac{dT}{dP} \approx (C_p^E)_{crit} \frac{V^E}{H^E} \quad (6)$$

$$\approx 5 * 10^{-4} (C_p^E)_{crit} V^E \quad (7)$$

Thus, approaching the UCST both normal and critical contributions to  $dV^E/dT$  will be of the same sign, i.e. that of  $V^E$ , and the conditions for the occurrence of the W-shape are not met in the case of  $dV^E/dT$ . Furthermore, the critical contribution to  $dV^E/dT$  is small. From eq. (5) and (6) this contribution becomes equal to the normal when  $C_p^E \approx 20 \text{ J K}^{-1} \text{ mol}^{-1}$  which corresponds to the experimental temperature being only a few degrees from  $T_c$ . Thus although  $dV^E/dT$  near the UCST is a more sensitive indicator of non-randomness than  $dV^E/dP$ , its observation will still require special conditions of temperature close to  $T_c$ . Nevertheless, it seems worthwhile to compare Flory theory predictions with experimental values of  $dV^E/dT$  near the UCST to determine if a discrepancy between the two can be associated with a critical contribution to  $dV^E/dT$ .

Before doing this we consider  $dV^E/dT$  approaching the two types of LCST mentioned above. Aqueous systems<sup>11</sup> exhibit negative  $V^E$  and positive  $dV^E/dT$  approaching the LCST. Since  $H^E$  is negative (or if S-shaped,  $\frac{\delta^2 H}{\delta x^2}$  is positive) while  $(C_p^E)_{crit}$  is positive. Eqn. (6) shows that  $(dV^E/dT)_{crit}$  is also positive. Thus both normal and critical contributions to  $dV^E/dT$  are again of the same sign as they are when approaching the UCST and the W-shape will not arise.

However, as with  $C_p^E$ , the second type of LCST caused by a large free volume difference between the components has  $V^E$  and  $dV^E/dT$  negative while  $(dV^E/dT)_{crit}$  is positive. Systems approaching sufficiently close to this type of LCST should show a W-shape concentration dependence of  $dV^E/dT$ . A possible such system is methane + 2-methylpentane where volume changes have been determined<sup>6</sup> approaching the LCST of 194.7°K, without however any obvious W-shape being discernible.

## EXPERIMENTAL

The chemicals were from standard sources and were of high purity label, at least 99%. They were used without any further treatment.

Excess volumes data were obtained through density measurements using a flow densitometer from Sodev. Measurements were carried out as described in the literature<sup>12</sup>.  $V^E$  data were fitted to Redlich-Kister equations for each temperature. Equimolar values of  $V^E$  were then used to calculate  $dV^E/dT$  at different temperatures. Reduction parameters,  $P^*$ ,  $V^*$ ,  $T^*$  required by the Prigogine-Flory theory were taken from the literature<sup>13,14</sup>. State equation parameters are given in Table 1.

$V^E$  measurements were carried out for mixtures of: nitroethane + cyclohexane at 25, 27, 30, 35, 50°C; nitropropane + cyclohexane at 10, 25°C; propionitrile + CyC<sub>6</sub> at 15, 25, 40°C; butanone + hexadecane (n-C<sub>16</sub>) at 25, 30, 40°C, + 2,2,4-heptamethyl nonane (brC<sub>16</sub>) at 25, 40°C; hexanone + n-C<sub>16</sub> at 25, 30, 40°C; benzonitrile + n-C<sub>6</sub>, n-C<sub>8</sub> at 25, 30°C + n-C<sub>16</sub> at 30, 40°C and brC<sub>16</sub> at 40, 50°C; nitrobenzene + brC<sub>16</sub> at 40, 50°C.  $V^E$  results are given as a function of concentration of component 1 in Appendix 3.

The accuracy of the  $V^E$  measurement depends on the system studied i.e. it is greater for the nitriles or nitro compounds than for the ketones for instance, but in any case it is estimated as being not less than  $\pm 0.01 \text{ cm}^3 \text{ mol}^{-1}$  for  $V^E$  and not less than  $\pm 1 * 10^{-3} \text{ cm}^3 \text{ K}^{-1} \text{ mol}^{-1}$  for  $dV^E/dT$ .

TABLE 1

Parameters for pure components at 25°C

	$P^*$ J cm <sup>-3</sup>	$\alpha$ $\times 10^{-3}$ (K <sup>-1</sup> )	$\rho$ g cm <sup>-3</sup>	$s$ (A°) <sup>-1</sup>
acetone	589.6	1.42	0.78502	0.85
2-butanone	582	1.29	0.7999	0.89
propionitrile	675	1.119	0.9953	1.0
nitroethane	682	1.117	1.0446	1.07
nitropropane	675	1.119	0.9953	1.0
benzonitrile	728	0.884	1.00053	1.0
nitrobenzene	710.67	0.825	1.1977	1.04
n-hexane (n-C <sub>6</sub> )	423	1.384	0.6554	1.04
n-octane (n-C <sub>8</sub> )	439	1.165	0.6983	0.99
n-hexadecane (n-C <sub>16</sub> )	463	0.884	0.7699	0.90
2,2,4,4,6,8,8-heptamethyl- nonane (br-C <sub>16</sub> )	399	0.872	0.7856	0.77
cyclohexane (CyC <sub>6</sub> )	530	1.217	0.7739	0.93

## RESULTS AND DISCUSSION

Tables (2–4) give for the different systems studied the experimental temperature for  $dV^E/dT$ , equimolar values of experimental and theoretical  $dV^E/dT$ , values of  $V^E$  measured at 25°C and values of the interaction parameter ( $X_{12}$ ) fitted to  $V^E$ .

For most of the systems investigated  $V^E$  is positive (except for mixtures of benzonitrile and nitrobenzene with low alkanes ( $n$  smaller or equal to 8));  $dV^E/dT$  is always proportional to  $V^E$  and of the same sign. Equation (5) is satisfied for any system taken in the vicinity of the UCST, i.e.  $\frac{dV^E}{dT} \frac{1}{V^E} \geq 10.0$ .

An attempt has been made to evaluate the critical part of  $dV^E/dT$ . Since the Flory theory has successfully predicted  $dV^E/dT$  for mixtures of alkanes where the components are believed to be randomly mixed, taking then the predicted value to be approximately the random contribution, the discrepancy between experimental and predicted values for each system will give the sign of the critical or non-random  $dV^E/dT$  and a crude approximation of its magnitude.

It is observed in the tables that this difference is temperature dependent and increases faster as  $T$  is closer to the critical point. At any temperature farther than a few degrees from  $T_c$ , this difference vanishes, and the theory correctly predicts the results. Contrary to  $C_p^E$  where the effect of the critical state is still discernible at  $\approx 100^\circ\text{C}$  from  $T_c$ , the effect of the critical state on  $dV^E/dT$  is perceptible only within a few degrees from  $T_c$ .

Mixtures of acetone + normal or branched alkanes, nitroethane and propionitrile +  $\text{CyC}_6$  all satisfy Eqn. (5) and the critical  $dV^E/dT$  shows the same sign as  $V^E$ . It decreases rapidly with increase of  $T$  and vanishes, leading to good agreement with Flory theory's prediction. Mixtures of butanone, hexanone with normal and  $\text{brC}_{16}$ , nitropropane +  $\text{CyC}_6$  are all far from their UCST and the results all agree with the

TABLE 2

Thermodynamic quantities for ketones in normal and branched alkanes

(1)	(2)	UCST (°C)	T (°C)	$V^E$ cm <sup>3</sup> mol <sup>-1</sup>	$dV^E/dT$ cm <sup>3</sup> mol <sup>-1</sup> Exp.	$dV^E/dT^*$ cm <sup>3</sup> mol <sup>-1</sup> Theor.	$X_{12}$
acetone +	n-C <sub>6</sub>	-39	20	1.025	10.5	9.7	45.2
	n-C <sub>16</sub>	13	20	1.255	12.6	8.2	55.9
	brC <sub>16</sub>	5	17.5	1.155	17.0	6.98	32.5
2-butanone +	n-C <sub>16</sub>	<m.p.	32.5	1.08	5.0	4.9	35.00
	brC <sub>16</sub>	<m.p.	32.5	0.85	5.54	4.1	12.85
3-hexanone +	n-C <sub>16</sub>	<m.p.	32.5	0.79	2.7		

\* with  $X_{12}$  fitted to  $V^E$

theoretical predictions.

Benzonitrile was mixed with different alkanes ( $n = 6, 8, 10, 16$ , brC16).  $V^E$  has been observed to be positive, negative or S-shaped<sup>15</sup>.  $dV^E/dT$  takes the sign of  $V^E$  in each case. The calculated non-random  $dV^E/dT$  also shows the same sign as  $V^E$ . Thereby, it can be concluded that the non-random contribution may be either positive or negative. The critical  $dV^E/dT$  calculated for the  $n-C_6$  mixture is negative and large, it is  $\approx 0$  for  $n-C_8$  and positive for  $n-C_{16}$  and brC<sub>16</sub>. brC<sub>16</sub> mixtures exhibit a large discrepancy between experimental and theoretical values, as expected because of the proximity of the UCST, while surprisingly  $n-C_{16}$  mixtures show good agreement with Flory's theory predictions, even though the system is near the UCST. The existence of correlation of molecular orientations (CMO) in alkane liquids such as  $n-C_{16}$  has been suggested by Tancrede et al<sup>16</sup>. (CMO) during mixing is manifested by a negative contribution to  $dV^E/dT$ <sup>17</sup>. It can then be suggested that  $dV^E/dT$  for benzonitrile +  $n-C_{16}$  contains a negative contribution caused by the destruction of CMO in  $n-C_{16}$  and that could probably counterbalance the positive contribution coming from non-randomness in solution. Hence the observed value of  $dV^E/dT$  should only reflect the random or "normal" contribution which is well predicted by Flory's theory. However, it has been shown<sup>17</sup> that orientational order decreases with the degree of branching of alkane molecules, leading to an absence of any CMO in the highly branched hexadecane (brC<sub>16</sub>). The large critical or non-random part should then be responsible for this large discrepancy between experimental and theoretical values of  $dV^E/dT$ .

$C_p^E$  and  $V^E$  of Nitrobenzene mixtures<sup>15</sup> reveal similar results with benzonitrile and a similar conclusion can be reached for  $dV^E/dT$  results. However, Table 4 shows mixtures containing cyclohexane. One should note that despite of the proximity of the UCST, no discrepancy has been observed between experimental and theoretical values of  $dV^E/dT$  for propionitrile + CyC<sub>6</sub> systems. Flory's theory agrees well at all

TABLE 3

Thermodynamic quantities for benzonitrile and nitrobenzene in several alkanes

(1)	(2)	UCST (°C)	T (°C)	$V^E$ cm <sup>3</sup> mol <sup>-1</sup>	$dV^E/dT$ cm <sup>3</sup> mol <sup>-1</sup> Exp.	$dV^E/dT^*$ cm <sup>3</sup> mol <sup>-1</sup> Theor.	$X_{12}$
benzonitrile +							
	n-C <sub>6</sub>		27.5	-.775	-15.0	-8.44	44.5
	n-C <sub>8</sub>		27.5	-.310	-1.1	-3.16	32.4
	n-C <sub>16</sub>		35	.265	5.0	2.9	23.4
	br-C <sub>16</sub>		45	.435	10.15	1.76	11.2
nitrobenzene +							
	n-C <sub>6</sub>	20.3	23	-.99	-17.0	-10.5	45.5
	br-C <sub>16</sub>		45	.07	-6.2	0.65	16.7

\* with  $X_{12}$  fitted to  $V^E$

TABLE 4

Thermodynamic quantities for propionitrile, nitroethane, nitropropane + cyclohexane

(1)	(2)	UCST (°C)	T (°C)	$V^E$ $\text{cm}^3\text{mol}^{-1}$	$dV^E/dT$ $\text{cm}^3\text{mol}^{-1}$ Exp.	$dV^E/dT^*$ $\text{cm}^3\text{mol}^{-1}$ Theor.	$X_{12}$
propionitrile +							
	CyC <sub>6</sub>	12.2	20	0.70	5.0	6.13	50
nitroethane +							
	CyC <sub>6</sub>	23	26	0.8	10	6.53	73.0
			37.5		4.0		
nitropropane +							
	CyC <sub>6</sub>	<m.p.	20	0.72	3.67	5.63	57.0

\* with  $X_{12}$  fitted to  $V^E$

temperatures studied, regardless of the flatness observed as  $T$  approaches the UCST, indicating a large non-random contribution. Furthermore,  $C_p^E$  for these systems shows a large and positive W-shape<sup>4</sup> even at  $T \approx 40^\circ\text{C}$  away from UCST.

The W-shape concentration dependence is definitely a more general phenomenon for  $C_p^E$  than it is for  $dV^E/dT$ . However, if approaching the UCST the W-shape  $dV^E/dT$  seems to be an extremely rare phenomenon, its observation should be possible for certain systems (large free volume difference) as  $T$  approaches the LCST, since in those particular cases, the "normal" and the critical contributions to  $dV^E/dT$  are expected to be of opposite signs.

REFERENCES

1. M.–E. Saint Victor and D. Patterson, *Fluid Phase Equilibria*, 35, 237, 1987.
2. R.G. Rubio, M. Caceres, R.M. Masegosa, L. Andreoli–Ball, M. Costas, and D. Patterson, to be published.
3. J. S. Rowlinson and F.L. Swinton, *Liquids and Liquid mixtures*, Third Edition, Butterworths, 1981.
4. M.–E. Saint Victor and D. Patterson, Chapter 2.
5. H. Klein and D. Woermann, *Ber. Bunsenges Phys. Chem.*, 82, 1084, 1978.
6. A. J. Davenport and J. S. Rowlinson, *J. Chem. Soc. Faraday Trans.*, 59, 78, 1963
7. R.B. Griffith and J.C. Wheeler, *Phys. Rev., A*, 2, No. 3, 1047, 1970.
8. P.J. Flory, *J. Am. Chem. Soc.*, 87, 1833, 1965.
9. M. Costas, S. N. Battacharyya and D. Patterson, *J. Chem. Soc., Faraday Trans. 1*, 81, 387, 1985.
10. H. T. Van and D. Patterson, *J. Sol. Chem.*, 11, 11, 1982.
11. J. Lara and J.E. Desnoyers, *J. Sol. Chem.*, 10, 7 1981.
12. P. Picker, E. Tremblay, and C. Jolicoeur, *J. Sol. Chem.*, 3, 577, 1974.
13. M. Costas and D. Patterson, *J. Chem. Soc., Faraday Trans. I*, 81, 635, 1985.
14. R. Gonzalez, F. M.Guevara, A. Trejo, *J. Sol. Chem.*, 15, No 10, 1986.
15. A. Lainez, M. Rodrigo, A.H. Roux, J.–P.E. Grolier, *Wilhelm, Cal. et Anyl. Therm.*, Vol. XVI, 153, 1985
16. P. Tancrede, P. Bothorel, P. de St. Romain, and D. Patterson, *J. Chem. Soc., Faraday Trans. 2*, 73, 29, 1977. P. Tancrede, D. Patterson, and P. Bothorel, 73, 29, 1977.
17. S. N. Battacharyya and D. Patterson, *J. Chem. Soc., Faraday Trans.*, 1, 81, 375, 1985.
18. O. Kiyohara, P. J. D'Arcy and G.C. Benson, *Can. J. Chem.*, 56, 2803, 1978.

APPENDIX 3

Tables of Results

TABLE 5  
 Excess volumes as a function of mole fraction of nitroethane for  
 nitroethane + cyclohexane at 25, 27, 30, 35°C

1	2
$x_1$	$V^E$ (cm <sup>3</sup> /mol)
$T = 25^\circ\text{C}$	
0.0309	0.1647
0.0902	0.4198
0.2220	0.6500
0.4664	0.7910
0.6990	0.6701
$T = 27^\circ\text{C}$	
0.1271	0.5211
0.3087	0.8283
0.4634	1.0466
0.5043	0.9370
0.5980	0.9384
0.7533	0.8211
0.8688	0.6185
$T = 30^\circ\text{C}$	
0.0657	0.3083
0.1682	0.4356
0.3196	0.7646
0.4115	0.8561
0.6008	0.7758
0.7443	0.6198
0.8893	0.3253
0.9438	0.1763

TABLE 5 (continued)

$x_1$	$v^E$ (cm <sup>3</sup> /mol)
T = 35°C	
0.0384	0.2111
0.0571	0.2867
0.0776	0.3617
0.0901	0.4096
0.1108	0.4625
0.1972	0.6485
0.4008	0.8344
0.6044	0.8078
0.7901	0.5574
0.9427	0.1814

TABLE 6  
 Excess volumes as a function of mole fraction of nitropropane for  
 nitropropane + CyC<sub>6</sub> at 10 and 25°C

$x_1$	$v^E$ (cm <sup>3</sup> /mol)
T = 10°C	
0.0181	0.0778
0.0370	0.1322
0.3594	0.6206
0.4638	0.6425
0.6049	0.5997
0.7540	0.4598
0.9034	0.2122
0.9483	0.1122
T = 25°C	
0.0176	0.0833
0.0678	0.2721
0.1534	0.4515
0.3039	0.6537
0.4438	0.7017
0.5795	0.6596
0.7422	0.7553
0.8912	0.2471
0.9368	0.1513
0.9654	0.0856

TABLE 7  
 Excess volumes as a function of mole fraction of propionitrile for  
 propionitrile + CyC<sub>6</sub> at 15, 25, 40°C

$x_1$	$v^E$ (cm <sup>3</sup> /mol)
T = 15°C	
0.0525	0.2028
0.0972	0.3193
0.1352	0.4018
0.2013	0.5131
0.3260	0.6167
0.3940	0.6504
0.4471	0.6616
0.6196	0.6431
0.6961	0.5875
0.7541	0.5207
0.8423	0.3781
0.9576	0.1212
T = 25°C	
0.0993	0.3498
0.2663	0.6186
0.3952	0.7030
0.5448	0.7117
0.6936	0.6142
0.8408	0.3864
0.9413	0.1568

TABLE 7 (continued)

$x_1$	$v^E$ (cm <sup>3</sup> /mol)
T = 40°C	
0.1013	0.3890
0.2634	0.6844
0.4002	0.7846
0.5462	0.7832
0.6990	0.6570
0.8461	0.4014
0.9443	0.1582

TABLE 8  
 Excess volumes as a function of mole fraction of nitrobenzene for  
 nitrobenzene + brC<sub>16</sub> at 40 and 50°C

$x_1$	$V^E$ (cm <sup>3</sup> /mol)	
	40°C	50°C
0.0549	0.0992	0.1088
0.2874	0.1468	0.1321
0.4028	0.1072	0.0540
0.5453	0.1166	0.0524
0.5749	—	0.1823
0.6731	0.0157	0.0053
0.8040	—	-0.0516
0.9480	-0.0307	-0.0626

TABLE 9  
 Excess volumes as a function of mole fraction of benzonitrile for  
 benzonitrile + n-C<sub>6</sub> at 25 and 30°C

x <sub>1</sub>	v <sup>E</sup> (cm <sup>3</sup> /mol)	
	25°C	30°C
0.0565	-0.0773	-0.0842
0.1072	-0.1907	-0.2064
0.2053	-0.3811	-0.4185
0.2969	-0.5563	-0.6062
0.3933	-0.6874	-0.7557
0.4975	-0.7562	-0.8283
0.5828	-0.7985	-0.8895
0.7149	-0.7393	-0.8130
0.8788	-0.4223	-0.4730

TABLE 10  
 Excess volumes as a function of mole fraction of benzonitrile for  
 benzonitrile + n-C<sub>8</sub> at 25 and 30°C

x <sub>1</sub>	V <sup>E</sup> (cm <sup>3</sup> /mol)	
	25°C	30°C
0.0535	0.0264	0.0272
0.1017	0.0138	0.0158
0.2420	-0.1024	-0.1013
0.3248	-0.1674	-0.1672
0.4057	-0.2320	-0.2335
0.5025	-0.3115	-0.3166
0.6012	-0.3535	-0.3594
0.7342	-0.3744	-0.3794
0.9287	-0.1663	-0.1704

TABLE 11  
 Excess volumes as a function of mole fraction of benzonitrile for  
 benzonitrile + n-C<sub>16</sub> at 30 and 40°C

x <sub>1</sub>	V <sup>E</sup> (cm <sup>3</sup> /mol)	
	30°C	40°C
0.0567	0.1348	0.1618
0.1051	0.2166	-0.2327
0.2064	0.3057	0.3418
0.3093	0.3902	0.4303
0.4355	0.2234	0.2791
0.5126	0.3807	0.4150
0.6229	—	0.2176
0.7633	—	0.2129
0.8867	0.0525	0.0832

TABLE 12  
 Excess volumes as a function of mole fraction of benzonitrile for  
 benzonitrile + brC<sub>16</sub> at 40 and 50°C  
 1                      2

$x_1$	$V^E$ (cm <sup>3</sup> /mol)	
	40°C	50°C
0.0566	0.1396	0.1390
0.1081	0.2397	0.2442
0.3576	0.3087	0.3761
0.4554	0.2865	0.3373
0.5452	0.2408	0.3431
0.6983	0.1404	0.2511
0.8890	0.0549	0.0575



TABLE 13 (continued)

$x_1$	$v^E$ (cm <sup>3</sup> /mol)
T = 25°C	
0.0405	0.3073
0.0611	0.4144
0.0667	0.3580
0.0747	0.3921
0.1240	0.5776
0.1820	0.7391
0.1823	0.7188
0.3950	1.18405
0.4036	1.0631
0.6055	0.9639
0.6888	0.8616
0.7823	0.6860
0.7949	0.6358
0.8925	0.3634
	0.3694
0.9371	0.2511

TABLE 14  
 Excess volumes as a function of mole fraction of 2-butanone for  
 2-butanone + n-C<sub>16</sub> at 25, 30, 40°C  
 1                      2

x <sub>1</sub>	v <sup>E</sup> (cm <sup>3</sup> /mol)		
	25°C	30°C	40°C
0.0031	0.0230	—	0.0158
0.0071	0.0468	—	0.0482
0.0118	0.0697	—	0.0701
0.0566	0.2436	—	0.2487
0.0586	0.2288	0.2308	0.2300
0.1107	0.4017	0.4087	0.4226
0.2086	0.6674	0.6822	0.7134
0.4698	1.0488	1.0751	1.1202
0.6090	1.0614	1.0888	1.1391
0.7957	0.8434	0.8656	0.9039
0.9374	0.3801	—	0.3993
0.9488	0.3278	0.3343	0.3460
0.9755	0.1717	—	0.1795
0.9945	0.0395	—	0.0416
0.9972	0.02307	—	0.0244
0.9990	0.0069	—	0.0079

TABLE 15  
 Excess volumes as a function of mole fraction of 2-butanone for  
 2-butanone + brC<sub>16</sub> at 25 and 40°C  
 1                      2

$x_1$	$V^E$ (cm <sup>3</sup> /mol)
T = 25°C	
0.0417	0.1286
0.1031	0.2972
0.2483	0.5957
0.4492	0.8141
0.6495	0.8140
0.8000	0.6414
0.9494	0.2344
T = 40°C	
0.1360	0.4034
0.2259	0.6082
0.2830	0.7122
0.3895	0.8467
0.5125	0.9202
0.5898	0.9217
0.6951	0.8554
0.8016	0.6993
0.9000	0.4425

TABLE 16  
 Excess volumes as a function of mole fraction of hexanone for  
 hexanone + n-C<sub>16</sub> at 25, 30, 40°C  
 1            2

$x_1$	$V^E$ (cm <sup>3</sup> mol <sup>-1</sup> )		
	25°C	30°C	40°C
0.00932	0.0366	0.0304	0.0310
0.0576	0.1747	0.1733	0.1784
0.1672	0.4337	0.4370	0.4472
0.2284	0.5470	0.5517	0.5672
0.4247	0.7614	0.7591	0.7945
0.5912	0.7849	0.7957	0.8208
0.7079	0.7057	0.7080	0.7387
0.8880	0.3846	—	0.4032
0.9378	0.2366	0.2389	0.2448
0.9400	0.2322	—	0.2412
0.9809	0.0801	—	0.0827

PART II

CHAPTER 4

THERMODYNAMIC STUDIES OF ALCOHOL SELF-ASSOCIATION  
IN PROTON ACCEPTOR SOLVENTS

## INTRODUCTION

H-bonding in alcohols has been the subject of numerous investigations carried out with classical physico-chemical methods, such as vapor pressure<sup>1</sup>, spectroscopic techniques, principally infrared and NMR<sup>2</sup>, and calorimetry<sup>3</sup> including, very recently, heat capacity measurements. Much of the literature on hydrogen bonding of alcohols is concerned with self-association of alcohols in inert solvents. We will focus our attention on heat capacity. As a good structure indicator  $C_p$  turns out to be one of the most useful quantities for the study of H-bonding<sup>4</sup>.

Fig. 1a shows a schematic representation of the energy diagram for an alcohol in the pure state and in an inert solvent. Two levels of energy are represented. The lower corresponds to the state of association of the alcohol molecules through H-bonds and the higher is assigned to the state where all the alcohol molecules are completely dissociated. Curve 0 refers to the pure alcohol. At low T, the alcohol molecules are all associated and as the temperature is increased, the energy will rise to the level of complete dissociation. Curves I to III correspond to solutions at different concentrations, going towards higher dilution of alcohol in an inert solvent. At high dilution,  $x \leq 0.01$ , the H-bonds break up at a lower T and the molecules reach the dissociation state the faster, the more dilute the solution. The slopes of the energy curves give  $C_p(T)$  or the apparent heat capacity ( $\phi_c$ ) of the alcohol at different concentrations as shown in fig. 1b. They are called "Schottky peaks".

The excess heat capacity of the solution,  $C_p^E$ , is given as the difference between the apparent molar heat capacity,  $\phi_c$ , which is the heat capacity of the alcohol in the solution, and the heat capacity of the pure component. Therefore  $C_p^E$  compares two curves:

$$C_p^E = x_1 (\phi_{c_1} - C_{p_1}^0)$$

Fig. 1a Energy diagram of an alcohol in inert solvent.

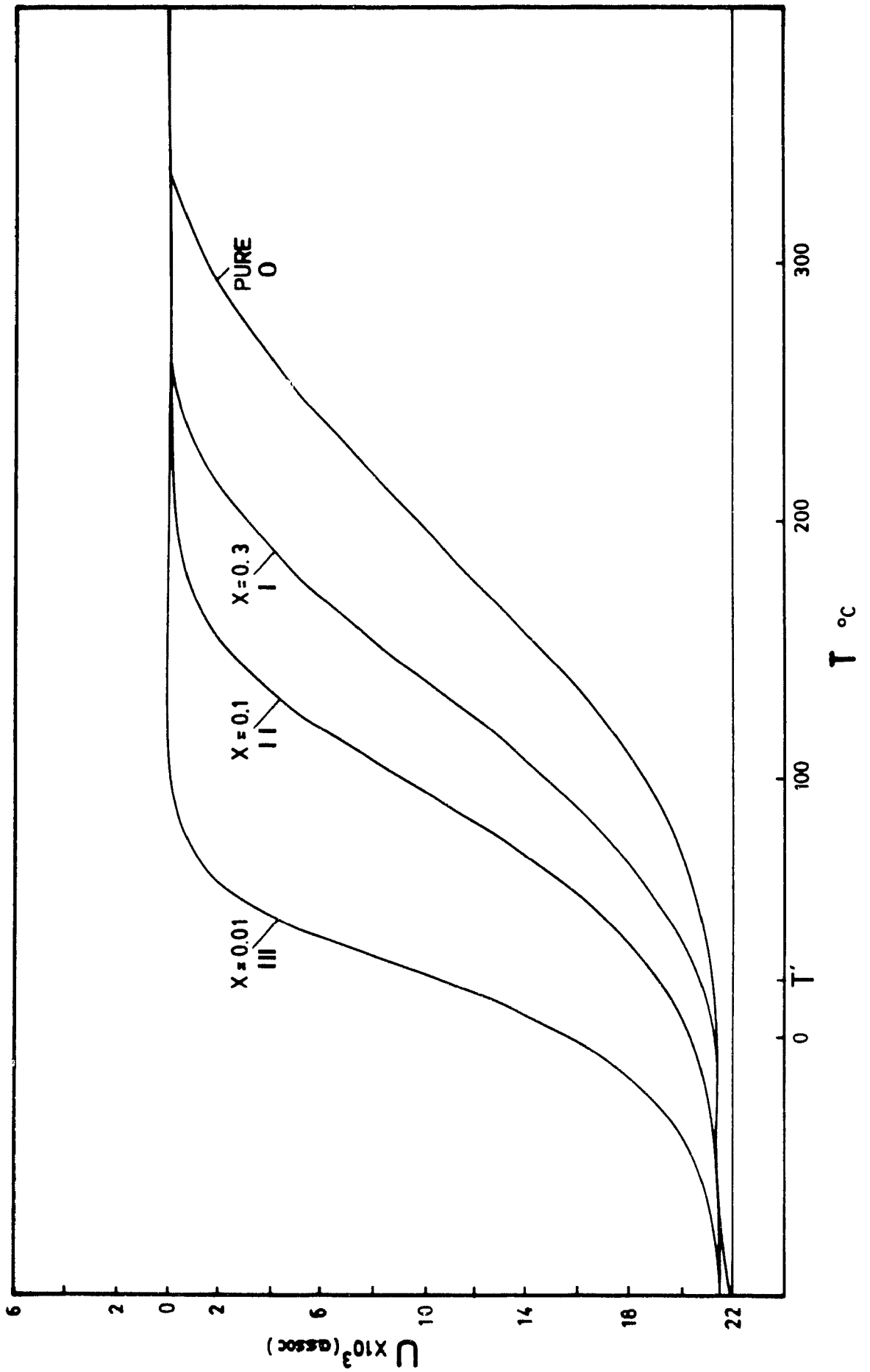
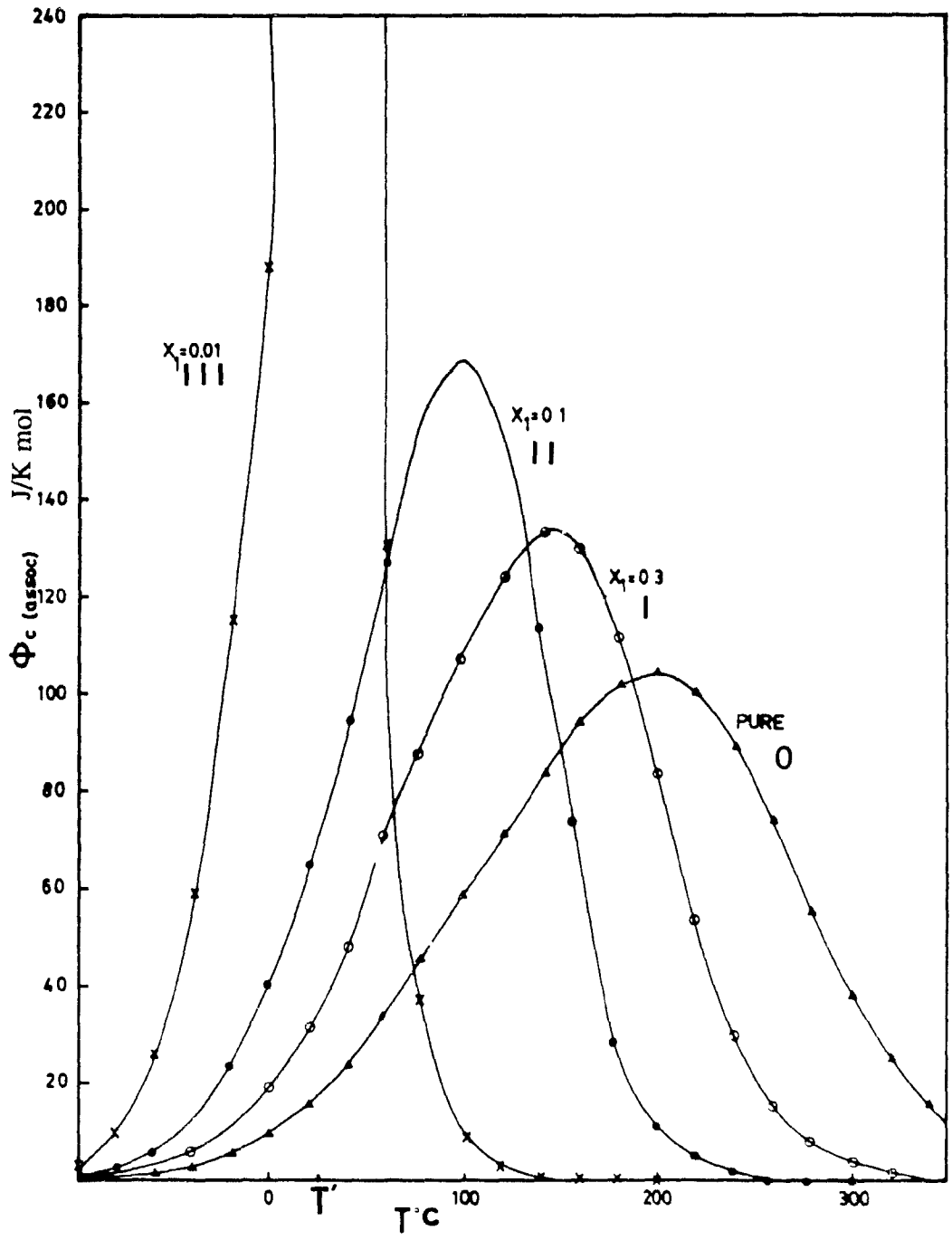


Fig. 1b Schottky peaks for an alcohol in inert solvent.



Thus, at a given temperature  $T'$ , subtracting for instance curve 0 from curve I, leads to  $C_p^E > 0$  while the subtraction of curve 0 from III leads to  $C_p^E < 0$ .

From fig. 1b, the following qualitative deduction can be made: at extremely low alcohol concentration, curve III, structure is broken up, the molecules are randomly isolated in the solvent and  $C_p^E$  shows a negative value (curve III lower than curve 0 at this temperature) corresponding to a decrease of structure compared to the pure alcohol molecules. As the concentration is increased, curve II, the alcohol molecules are brought together from over large distances to form higher species, mostly tetramers ( $\phi_c$  of the alcohol in the solution higher than in the pure liquid). Structure is then enhanced in the solution to a higher degree than in the pure alcohol where structure taking place over small distances. As the concentration is further increased (curve I), the molecules are closer and more tetramers are formed. However, at this stage the molecules come together from a smaller distance, therefore structure in the solution is less ( $\phi_c$  for curve I lower than  $\phi_c$  of curve II, for instance).

If now the inert solvent is replaced by a proton acceptor solvent, such as an alkylnitrile or a chlorinated solvent, structure in solution should be created to a lesser extent since the alcohol molecules can now be associated through hydrogen bonds with their immediate neighbours constituted by the proton acceptor solvent. They may, however, also form H-bonds through self-association. Therefore, two types of H-bonds are possible. But, depending on the strength of the proton acceptor (PA), structure will be dominated by the complex formation between the OH-group of the alcohol and the polar group of the PA rather than by the self-association process.

The behaviour of alcohol molecules can be interpreted through association theory. Among several of these theories, Treszczanowicz and Kehiaian (TK) theory<sup>5</sup> is successfully used in alcohol + inert solvent mixtures. The TK theory is based on a consecutive self-association reaction model, where an alcohol molecule attaches itself onto a multimer containing  $i$  molecules which becomes  $i + 1$  mer. The equilibrium

constant for this reaction is expressed in terms of volume fractions of the components in the chemical equation, i.e.

$$K_{i,i+1}^{\phi} = \frac{\phi_{A_{i+1}}}{\phi_A \phi_{A_i}} \quad (1)$$

for  $A + A_i = A_{i+1}$ . It, in fact, corresponds to the free energy of localizing the monomer in the neighbourhood of the growing multimer chain. Similarly for the formation of an  $i$ -mer from  $i$  monomers.

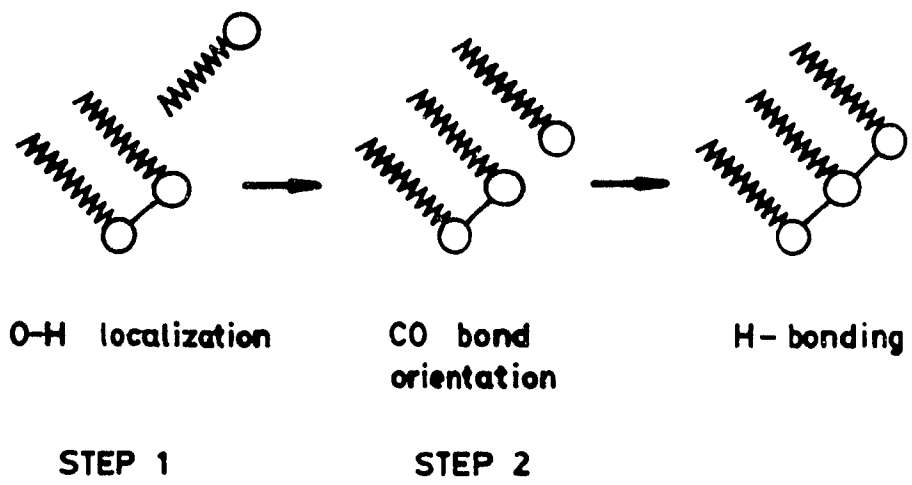
$$K_i^{\phi} = \phi_{A_i} / \phi_A^i \quad (2)$$

The  $K_{i,i+1}^{\phi}$  and  $K_i^{\phi}$  have been interpreted using the Flory lattice theory. It has been suggested in ref. (6) that the formation of an H-bond proceeds in two steps according to fig. 2: The first one corresponds to the localization of the new hydroxyl group at the growing chain of hydroxyls; the second step corresponds to the orientation of the CO group in the proper direction to be incorporated into the chain. The overall process can be represented through the expression of the equilibrium constant

$$K_{i,i+1}^{\phi} = \left[ \frac{1}{r_A} \right] \left[ \frac{i+1}{i} \right] \frac{1}{z(1-f)^2} K_i^{\phi} \frac{\sigma_{A_i} \sigma_A}{\sigma_{A_{i+1}}} \quad (3)$$

The localization of the new hydroxyl is represented by  $1/r_A$ , with  $r_A$  corresponding to the number of segments in the alcohol chain. Thus, the longer the alcohol molecule, the smaller is the equilibrium constant because the greater is the loss of entropy in order to localize the new hydroxyl group into the growing chain. The orientation of the

Fig. 2 Schematic representation of the formation of an H-bond.



CO group is represented by  $1/z$  where  $z$  is the coordination number. Again, the larger is  $z$ , the bigger is the entropic driving force, thus the smaller is  $K^\phi$ .  $\sigma$ 's are the symmetry numbers.  $f$  is an expression for the flexibility of the chain.

Equation (3) leads to a corresponding expression for the equilibrium constant,  $K_i^\phi$ , which is independent of the solvent and depends only upon the number of alcohol segments:

$$K_i^\phi \approx \left[ \frac{K_i}{r_A} \right]^{i-1} \quad (4)$$

Here the factors  $z$ ,  $(1-f)$ , etc. are not written. It is found<sup>4</sup> that tetramers are the dominant species, i.e.  $K_4$  is large corresponding to especially strong H-bonding. Eq. 4 becomes

$$K_4^\phi \approx \left[ \frac{K_4}{r_A} \right]^3$$

The excess heat ( $H^E$ ) and the associational apparent heat capacity ( $\phi_{C(\text{assoc})}$ ) are given by eqns. 5 and 6

$$H^E = \Delta H^0 \left[ \sum_{i=2} \frac{i+1}{i} K_i^\phi \frac{\phi_A^i}{\phi_1} - \sum_{i=2} \frac{i-1}{i} K_i^\phi \phi_A^{oi} \right] x_1 \quad (5)$$

where  $\phi_A^{oi}$  refers to the pure alcohol.

$$\phi_{C(\text{assoc})} = \left[ \frac{\Delta H^0}{T} \right]^2 \frac{1}{R} \frac{\left[ \sum_{i=2} \frac{i-1}{i} K_i \varphi \frac{\varphi_A^i}{\varphi_1} \left[ i-1 + \sum_{j \neq 1} (i-j) K_j^\varphi \varphi_A^{j-1} \right] \right]}{1 + \sum_{j=2} j K_j^\varphi \varphi_A^{j-1}} \quad (6)$$

The fitting of eqns. 5 and 6 to experimental data leads to the energy diagram and the Schottky peaks as seen in fig. 1.

If now the alcohol molecules are mixed with a proton acceptor solvent rather than an inert solvent, the complex formation obeys an equilibrium constant for dimer formation  $K_{AB}$ . Since there exist two types of H-bonds for these mixtures, two different types of eq. constants should be introduced in the TK model: (1) ( $K_2, K_3, K_4$ ) which refer to the eq. constants for the self-association of alcohol molecules into dimers, trimers, although almost exclusively tetramers ( $K_2$  and  $K_3$  are significantly small compared to  $K_4$ ) and (2)  $K_{AB}$  which is the eq. constant for the complex formation. In the model will be also introduced a value for the enthalpy change  $\Delta H_{AB}$  occurring during the formation of the complex. The TK model has been extended in ref. (7) to fulfill these requirements and now the associational part of  $\phi_c$  is given by eqn. 7 taken from ref. (7)

$$\phi_{C(\text{assoc})} = \left\{ \left[ \frac{\Delta H^0}{T} \right]^2 \frac{1}{R} \left[ \sum_{i=2} \frac{i-1}{i} K_i \varphi \frac{\varphi_A^i}{\varphi_1} \left[ (i-1) \left[ \frac{\varphi_2^x}{r} + 1 \right] + \sum_{j \neq i} (i-j) K_j^\varphi \varphi_A^{j-1} \right] \right] - \frac{\Delta H^0 \Delta H_{AB}^0}{RT^2} \left[ \frac{2\varphi_2^x}{r\varphi_1} \sum_{i=2} (i-1) K_i \varphi \frac{\varphi_A^i}{\varphi_1} \right] \right\}$$

$$+ \left[ \frac{\Delta H_{AB}^{\circ}}{T} \right]^2 \frac{1}{R} \left[ \frac{\phi_2^x}{r\phi_1} \left[ \phi_A + \sum_{i=2}^{\infty} K_i^{\phi} \phi_A^i \right] \right] \Bigg/ \left[ 1 + \sum_{j=2}^{\infty} K_j^{\phi} \phi_A^{j-1} + \frac{\phi_2^x}{r} \right] \quad (7)$$

where

$$x = \frac{(r/r+1) K_{AB}^{\phi}}{[(r/r+1) K_{AB}^{\phi} \phi_A + 1]^2} \quad \text{and} \quad \phi_1 = \frac{x_1}{x_1 + r x_2 + r_1 x_3} \quad (8)$$

$\Delta H^{\circ}$  represents the change of enthalpy associated with the self-association leading to the formation of one mole of hydrogen-bond.  $\Delta H^{\circ}$  is negative.  $K_i^{\phi}$  are the eq. constants for every species  $A_i$  in solution,  $\phi_1$  is the volume fraction of component 1 in solution and  $\phi_A$  is the volume fraction of the monomer 1 in solution.  $K_{AB}^{\phi}$  and  $\Delta K_{AB}^{\circ}$  are the equilibrium constant and enthalpy change for the formation of the complex.

In eqn. 7, the first term represents the associational part of the apparent heat capacity of the alcohol due to the self-association process, the third corresponds to the formation of the species AB in solution, while the second is a cross-term.

The eq. constant  $K_{AB}^{\phi}$  is given by eqn. 9:

$$K_{AB}^{\phi} = \frac{\phi_{AB}}{\phi_A \phi_B} = \left[ \frac{1}{r_A} + \frac{1}{r_B} \right] \frac{K_{AB}}{z(1-f)^2} \frac{\sigma_A \sigma_B}{\sigma_{AB}} \quad (9)$$

$r_A$  and  $r_B$  are related to the chain lengths of alcohol and PA. If the length of either the alcohol or PA increases, the entropic driving force for dissociation of H-bond between the OH and CO groups will be increased and  $K_{AB}^{\phi}$  decreases. However, at low alcohol concentration and large  $K_{AB}$ , eqs. 7-9 can be simplified to eqn. 10.

$$\frac{\phi_C}{R} \approx \left[ \frac{\Delta H_{AB}}{RT} \right]^2 \frac{r_B}{K_{AB}} \quad (10)$$

From eqn. (10), it is shown that the heat capacity is independent of alcohol and depends only upon the PA strength. At low concentration, alcohol molecules are surrounded by PA molecules. It is then obvious that the longer the PA chain, the weaker the PA and the larger will be the heat capacity. This seemingly paradoxical result reflects  $K_{AB}$  being large. The highest  $\phi_C$  is found for intermediate PA strength.

The aim of this work is to study through  $C_p^E$  measurements, structural effects due to interactions between alcohol and proton acceptor solvents. Spectroscopists have used, for decades,  $CCl_4$  as an inert solvent for alcohols for various studies such as IR, NMR, etc. This study will show that alcohol +  $CCl_4$  behaviour deviates from the results obtained in inert solvents. Indeed  $CCl_4$  should be taken as a very mild proton acceptor solvent, but it is definitely not an inert environment for alcohols.

## EXPERIMENTAL

Volumetric heat capacities were measured using the Picker flow microcalorimeter from Sodev Inc., for mixtures of methanol + acetonitrile; butanol +  $\text{CCl}_4$ , + acetonitrile, + octanenitrile and decanol +  $\text{CCl}_4$ .

The method and principles are described in ref. 8. A vibrating-cell densimeter (Sodev, Sherbrooke, P.Q.) was used for the measurements of density data necessary to transform volumetric heat capacity into molar heat capacity and also to obtain excess volume data.

The Chemicals from Aldrich were used as obtained without any further purification. They were at least of 99% of purity.

## RESULTS AND DISCUSSION

### 1. Butanol + Acetonitrile

Energy diagrams and Schottky peaks are calculated using the TK model. The fitting of the experimental  $\phi_{C(\text{assoc})}$  and limit ( $\phi_{C(\text{assoc})}^{\text{limit}}$ ) was made using the association parameters listed in Table 1.

Figs. 3a and 3b show respectively the energy diagram and Schottky peaks for butanol + acetonitrile and + n-C<sub>7</sub>. In fig. 3a, three energy levels should be considered. The lowest level corresponds to the associated state (self-association of alcohol molecules into tetramers). The second level corresponds to the A-B complex and the third is for the complete dissociation of the molecules into monomers. Curve 0 corresponds to the pure alcohol, while the other curves correspond to solutions at different concentrations. There is a remarkable difference with the inert case. In the inert solvent, the tetramer dissociates into monomers directly, while here the break up of H-bonds is followed by the formation of a complex between alcohol molecule and the PA solvent. A further increase of T will be followed by the complete dissociation of H-bonds into monomers. This must be more evident at low concentration of alcohol, where it is easier to break up the H-bonds since few alcohol molecules are present in the solution. Yet at extremely low T, for  $x \leq 0.01$ , at  $\Delta H^0 = -15800$  J/mol (the energy necessary to form one mole of complex), the tetramer species (due to self-association) are dissociated and replaced by dimers resulting from the complex formed between butanol and acetonitrile. A plateau is observed in a given range of T. As T is further increased, the complex starts to dissociate up to a temperature where complete dissociation leads to monomer species and another plateau is reached. Fig 3a shows also the comparison between the inert n-C<sub>7</sub> and acetonitrile cases at the different concentrations, the curves shifting to lower T in the case of the PA. The

Fig. 3a Energy diagram for butanol + acetonitrile for the pure butanol and for the solutions at different concentrations and butanol + n-C<sub>7</sub> at different concentrations.

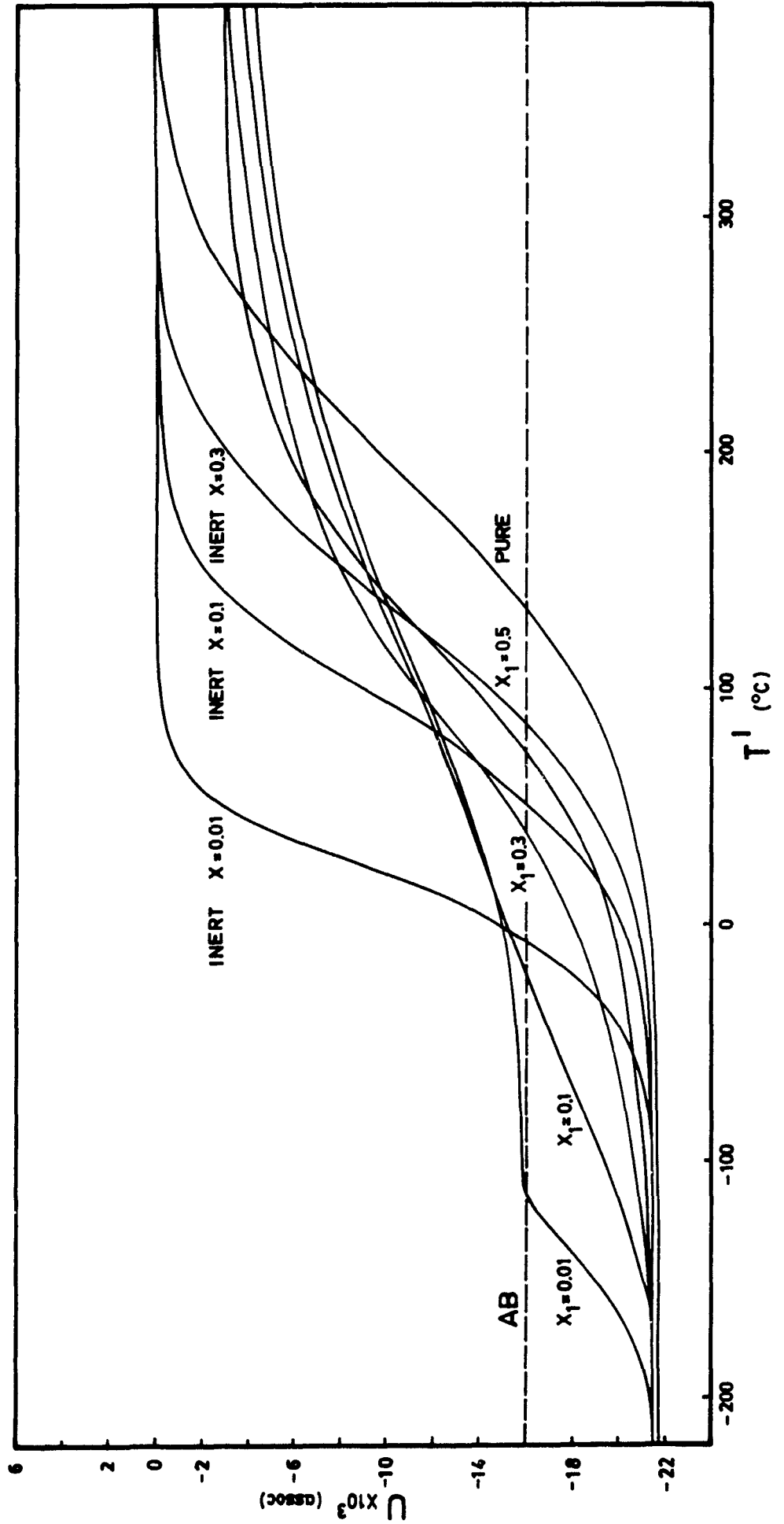


Fig. 3b Schottky peaks for butanol + acetonitrile at different concentrations.

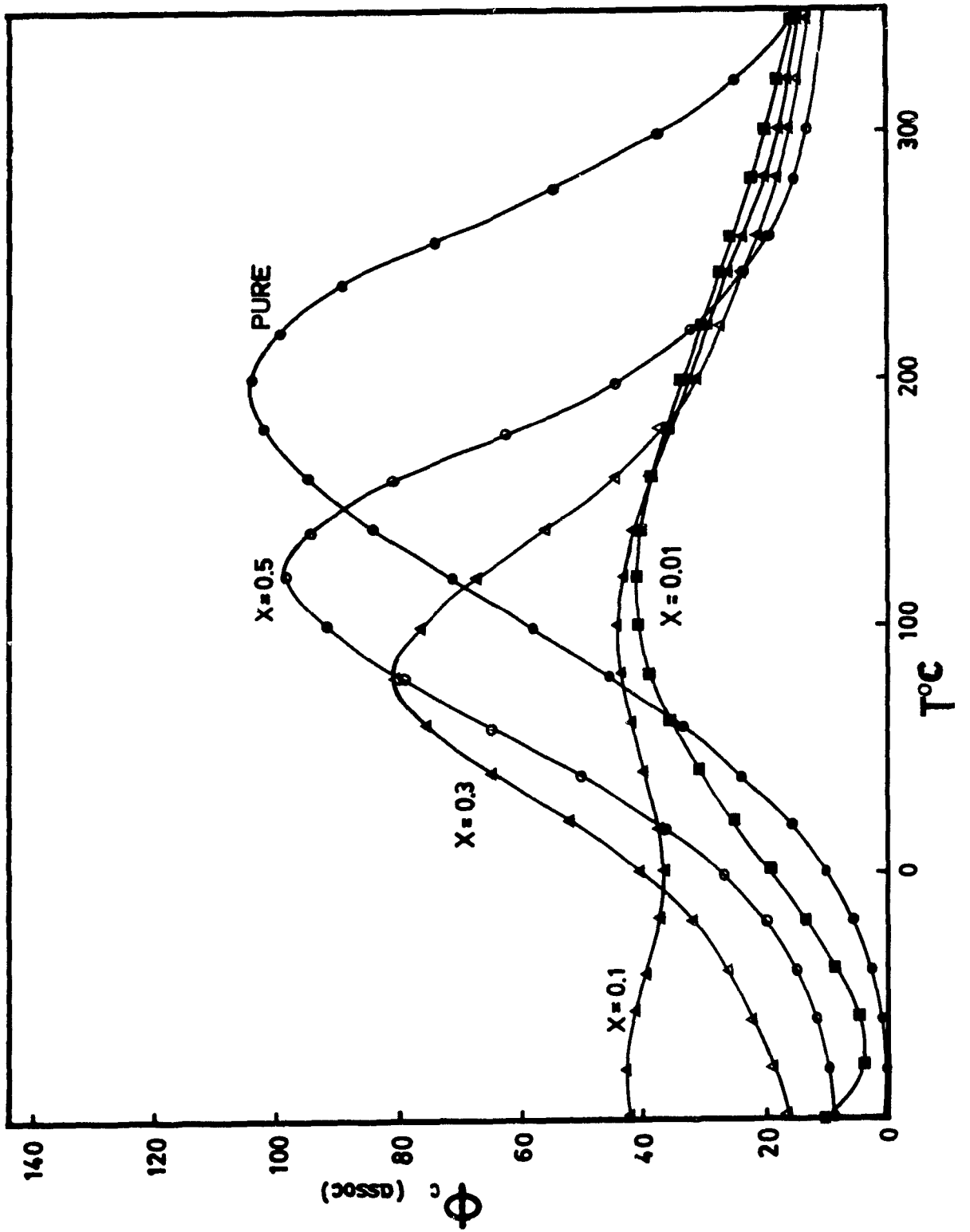


TABLE 1  
 Association parameters for Butanol in  $\text{CCl}_4$ , acetonitrile, octanenitrile at  $25^\circ\text{C}$

	$\text{CCl}_4$	Acetonitrile	Octanenitrile
$\Delta H^\circ$	- 287000	- 28700	-28700
$K_2$	0.115	0.115	0.115
$K_3$ self-association	871	871	871
$K_4$	1666500	1666500	1666500
$\Delta H_{AB}$	- 8800	- 15800	- 15800
$K_{AB}$ complex formation	1.9	29	25
$r$	1.74	0.95	0.59

shifting is remarkable at high dilution ( $x = 0.01$ ). The rise of energy slows down because of the formation of the complex.

Fig. 3b represents the Schottky peaks for butanol + acetonitrile. Here the  $\phi_{C(\text{assoc})}$  maximum is much lower compared with the inert. The sharp maximum, observed with  $n\text{-C}_7$  and even with  $\text{CCl}_4$ , at low concentration ( $x \leq 0.01$ ), has now completely disappeared. Two maxima can be observed corresponding respectively to self-association and the complex. Even at extremely low concentration, monomer species can not be found. The isolated alcohol molecule resulting from the breaking up of H-bonds finds a molecule of acetonitrile to fulfill its H-bond requirements. Therefore the extent of structure is higher than if it was an inert solvent, at this extremely low concentration. Furthermore, conversely to the previous cases at any concentration considered here, the Schottky peaks are always lower than for the pure alcohol. However, the maximum occurs at lower T. Nevertheless at  $25^\circ\text{C}$ ,  $\phi_{C(\text{assoc})}$  of the solutions at any concentration is larger than the value observed for the pure alcohol, as seen in fig. 4.

Fig. 4 shows a comparison between experimental and theoretical curves of  $\phi_{C(\text{assoc})}$  for butanol + acetonitrile. The fitting of the theory to the experimental results gives  $\Delta H_{AB} = -15800$  J/mole which is much bigger (in absolute value) than  $\Delta H_{AB}$  for  $\text{CCl}_4$  mixture. The equilibrium constant  $K_{AB}$  is 29 while it was 1.9 for  $\text{CCl}_4$  (Table 1). These parameters indicate that a stronger complex is formed with acetonitrile.

## 2. Butanol + $\text{CCl}_4$

Figs. 5a and 5b show respectively the energy diagram and the Schottky peaks for butanol +  $\text{CCl}_4$ . Here again, three energy levels should be considered: the self-association energy, the second energy level corresponds to the AB complex

Fig. 4 Comparison between experimental and theoretical  $\phi_{C(\text{assoc})}$  for butanol + acetonitrile at 25°C. × experimental; • theoretical.

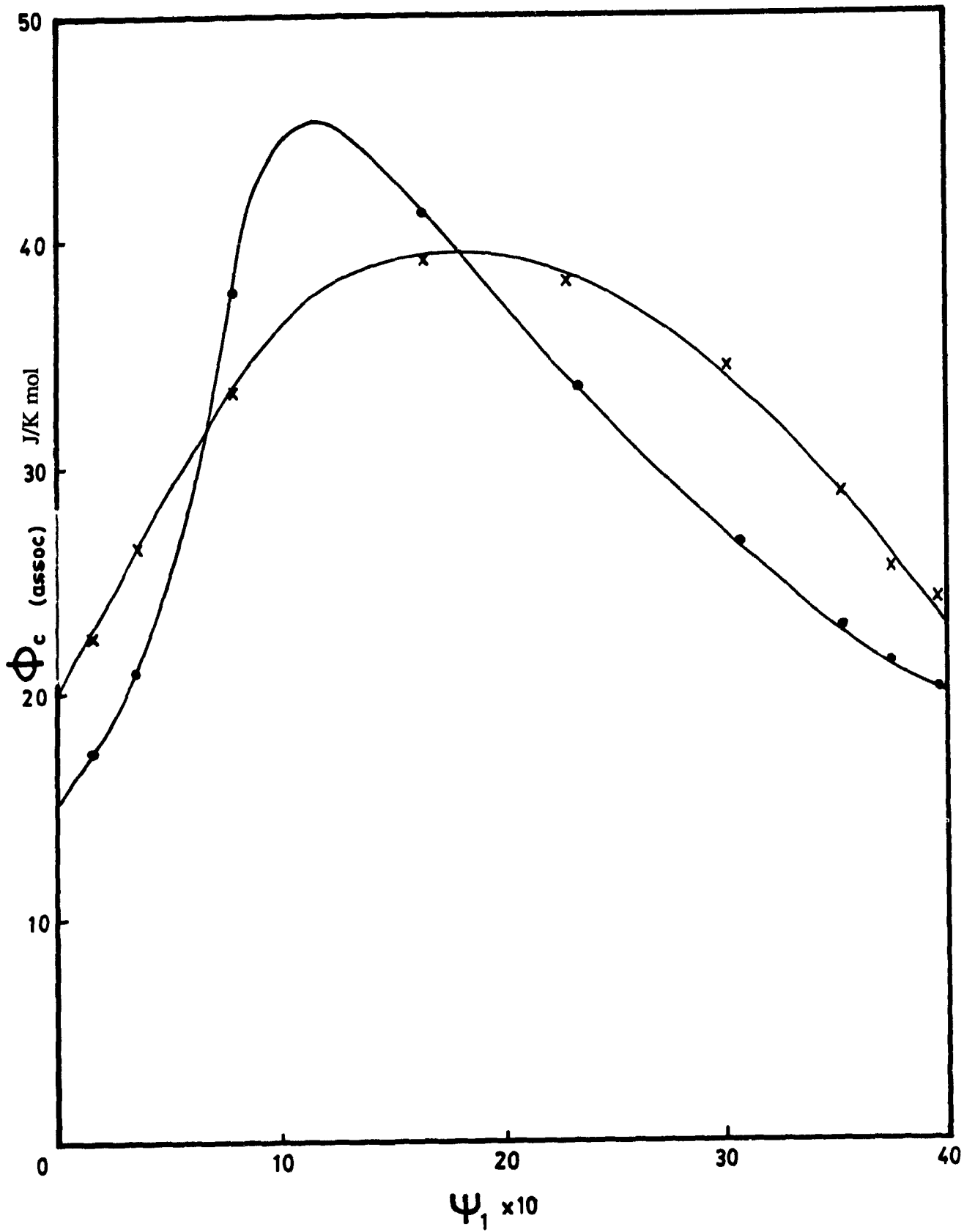


Fig. 5a Energy diagram for butanol +  $\text{CCl}_4$  for  $X = 0.00001, 0.00005, 0.01, 0.1, 0.3$  (●) for the pure butanol and for butanol +  $n\text{-C}_7$  (×) at  $25^\circ\text{C}$ .

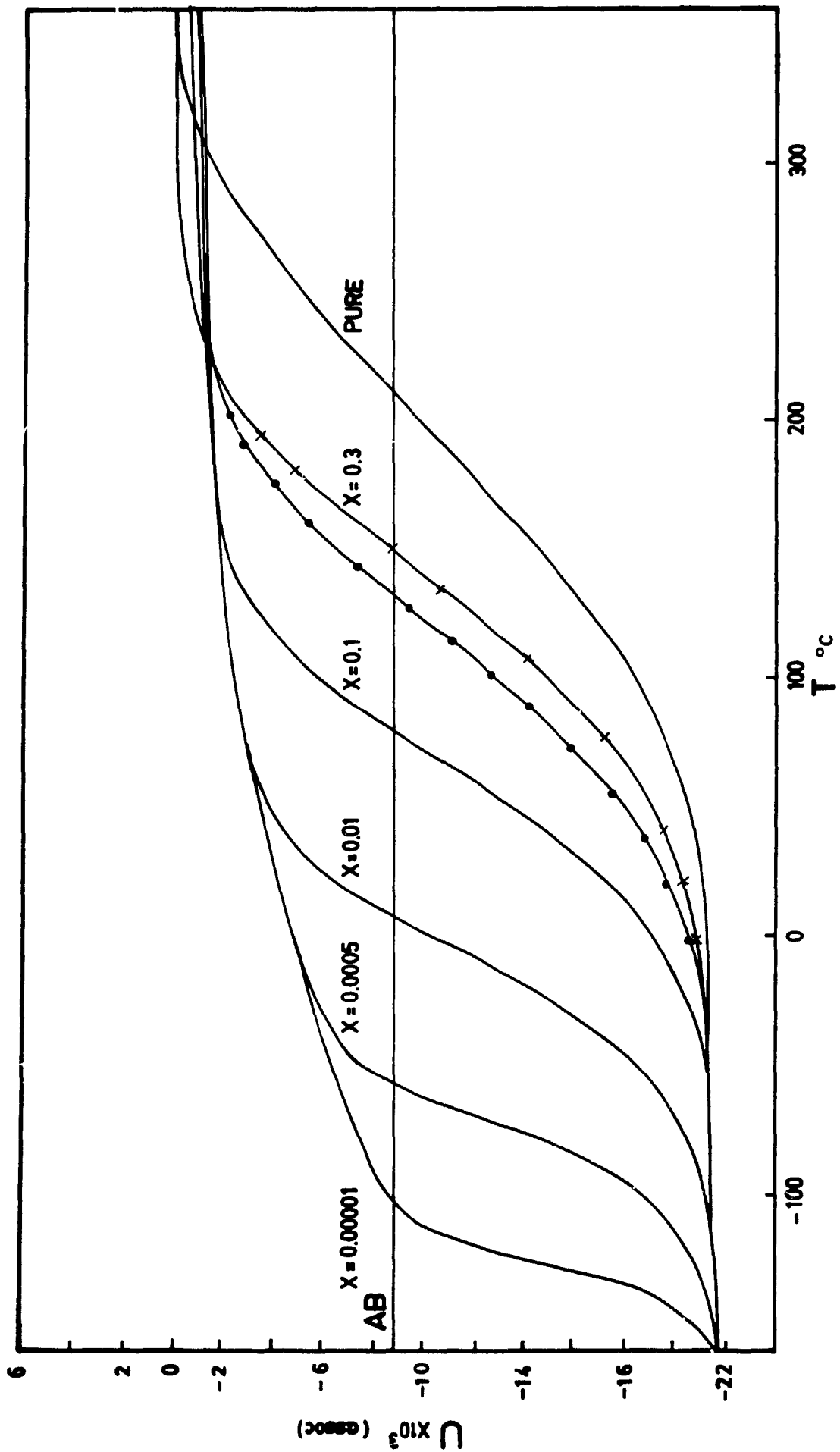
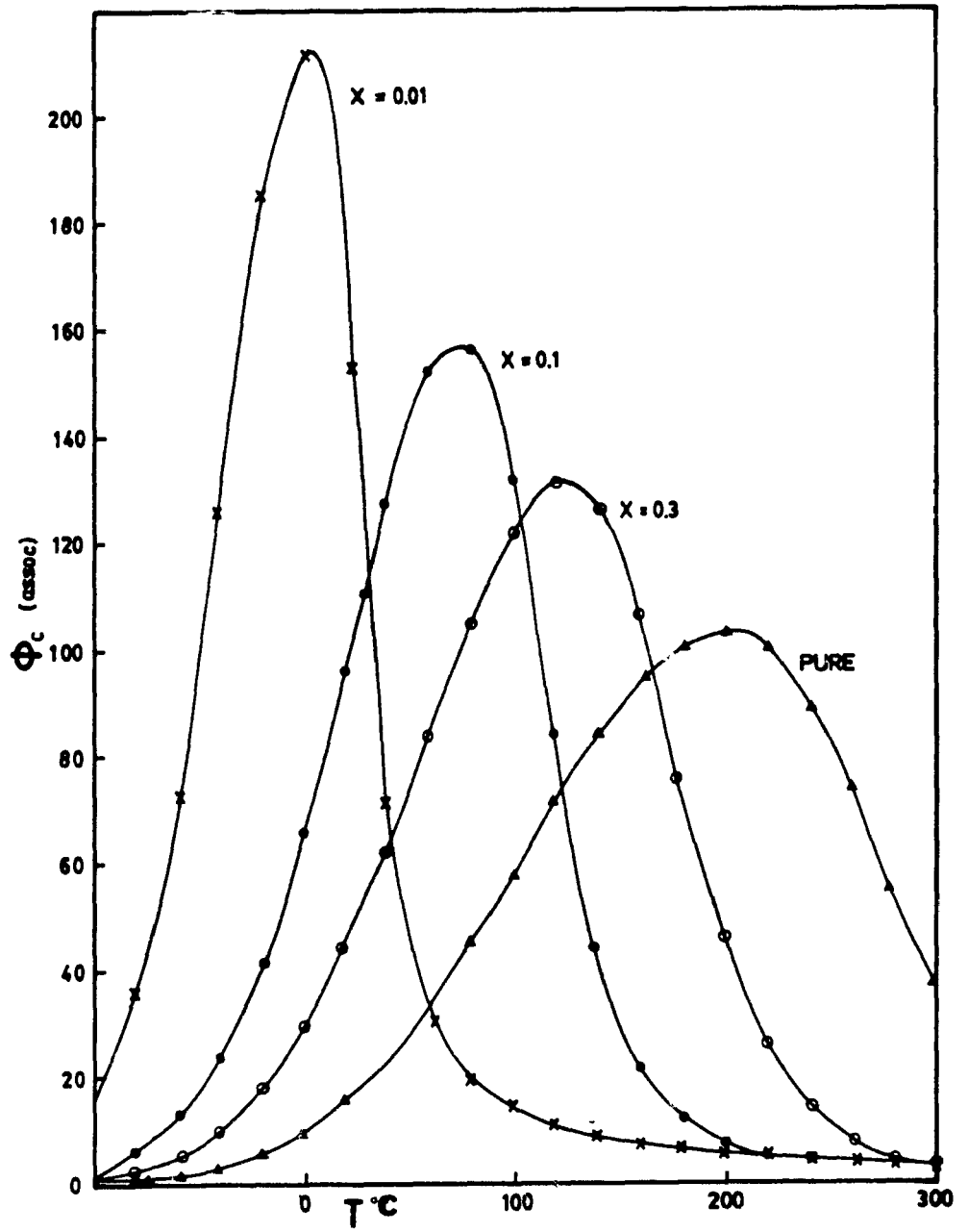


Fig. 5b Schottky peaks for butanol +  $\text{CCl}_4$  at different concentrations.



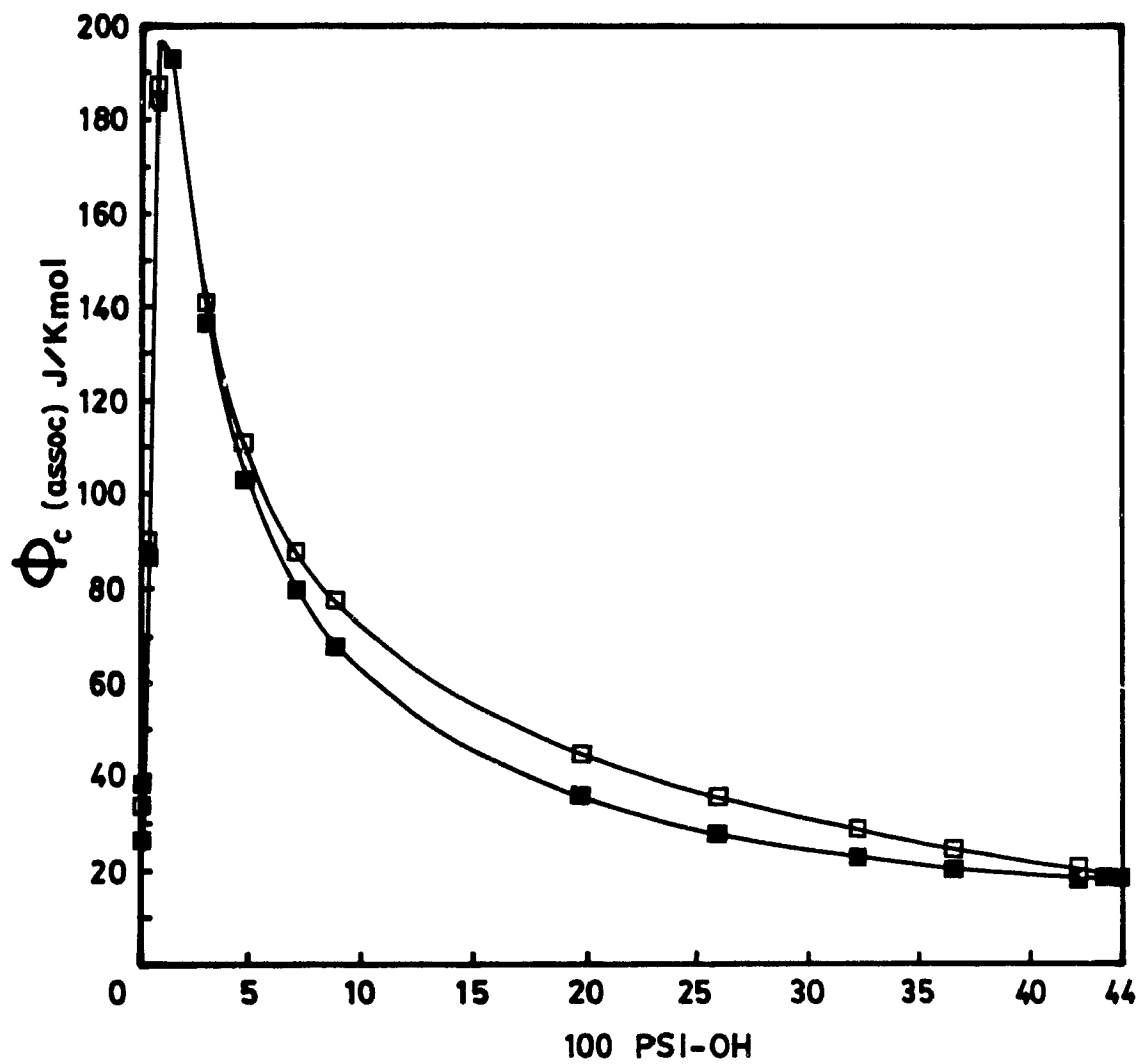
between butanol and  $\text{CCl}_4$  and the third level is the energy of complete dissociation into monomers.

As for acetonitrile, the curves are shifted to the left and the temperature at which dissociation occur is lower than for the inert case. But, since  $\text{CCl}_4$  is an extremely mild PA compare to acetonitrile, the observation of the complex is more difficult and it occurs at extremely low concentration and temperature. It is more difficult to isolate the dissociation of the tetramers from that of the complex, although at  $x = 10^{-5}$ , a plateau seems to indicate the formation of the complex. This concentration is perhaps beyond the limit of any experiment.

Fig. 5b shows the Schottky diagram for butanol +  $\text{CCl}_4$ . Despite a certain similarity with the inert case, dissociation of the alcohol tetramers occurs at a lower temperature for any concentration, i.e. it is easier to break up the H-bond in  $\text{CCl}_4$  than in  $n\text{-C}_7$ , for instance. The maxima of the Schottky peaks move toward lower T and are smaller. However, at a given temperature,  $25^\circ\text{C}$  for instance, it can be observed that  $\phi_{\text{C(assoc)}}$  for  $\text{CCl}_4$  mixtures is higher than the inert, but becomes smaller at low concentration; specially at about 0.01 where the maximum of  $\phi_{\text{C(assoc)}}$  occurs.

The comparison between experimental and theoretical  $\phi_{\text{C(assoc)}}$  is shown in fig. 6. The TK model predicts successfully the experimental trend for this system. The change of enthalpy and the equilibrium constant for the complex formation were fitted as respectively  $-8800 \text{ J/mol}$  and 1.9. Those values indicate the weakness of the AB complex formed. Despite a perfect agreement between the experimental data and the TK prediction at low concentration, the experimental curve is higher than the predicted values at higher concentration. Physical contributions which are not taken into account by the theory might be responsible for this difference.

Fig. 6 Comparison between experimental and theoretical  $\phi_{C(\text{assoc})}$  for butanol +  $\text{CCl}_4$  as a function of concentration of concentration of hydroxyl group in solution at  $25^\circ\text{C}$ .



### 3. Butanol + different PA

#### a. Apparent molar heat capacity

Fig. 7a shows the comparison between Schottky peaks at  $x = 0.1$  for butanol in the pure state and different proton acceptor solvents. Going from the inert to the PA, the maximum of the curve moves towards lower  $T$  and it is smaller as the strength of the PA increases.

Fig. 7b shows a comparison between experimental results, at  $25^{\circ}\text{C}$ , of  $\phi_{\text{C(assoc)}}$  for butanol mixed with normal alkanes and proton acceptor solvents.  $\phi_{\text{C(assoc)}}$  is given as a function of the concentration of hydroxyl groups ( $\psi$ ) in solution. Normal alkanols ( $C = 6$  to  $16$ ) show a single curve for  $\phi_{\text{C(assoc)}}$  when the effective concentration of hydroxyl groups is considered instead of the global concentration of the alcohol molecules.  $\phi_{\text{C(assoc)}}$  is then independent of the length of the alcohol molecules. In an inert solvent,  $\phi_{\text{C(assoc)}}$  increases slowly at extremely low concentration, then a rapid increase is observed as the concentration is about  $0.1 * 10^{-2}$ , where a maximum is observed ( $\phi_{\text{C(assoc)}} \simeq 270 \text{ J/mol K}$ ) and decreases slowly as the concentration is further increased.

If, however, the inert solvent is replaced by a mild PA such as  $\text{CCl}_4$ , at extremely low concentration,  $\phi_{\text{C(assoc)}}$  is higher than in the inert. As the concentration is increased, there is a rapid increase of  $\phi_{\text{C(assoc)}}$  but slower than for the inert and the maximum is moved towards higher concentration of butanol. It is also observed that the maximum of  $\phi_{\text{C(assoc)}}$  takes the value of  $\simeq 200 \text{ J/K mol}$  which is smaller than the value observed with the inert solvent. As the concentration is further increased,  $\phi_{\text{C(assoc)}}$  decreases, but more slowly than for the inert. Therefore another cross-over is observed for the two curves at high concentration. The value of  $\phi_{\text{C(assoc)}}$  is higher for  $\text{CCl}_4$  than for the inert at high concentration.

Fig. 7a Schottky peaks for butanol in  $n\text{-C}_7$ ,  $\text{CCl}_4$ , acetonitrile and octanenitrile for  $x = 0.1$ .  $\times$   $n\text{-C}_7$ ;  $\blacktriangle$   $\text{CCl}_4$ ;  $\bullet$  pure;  $\circ$  acetonitrile;  $\square$  octanenitrile.

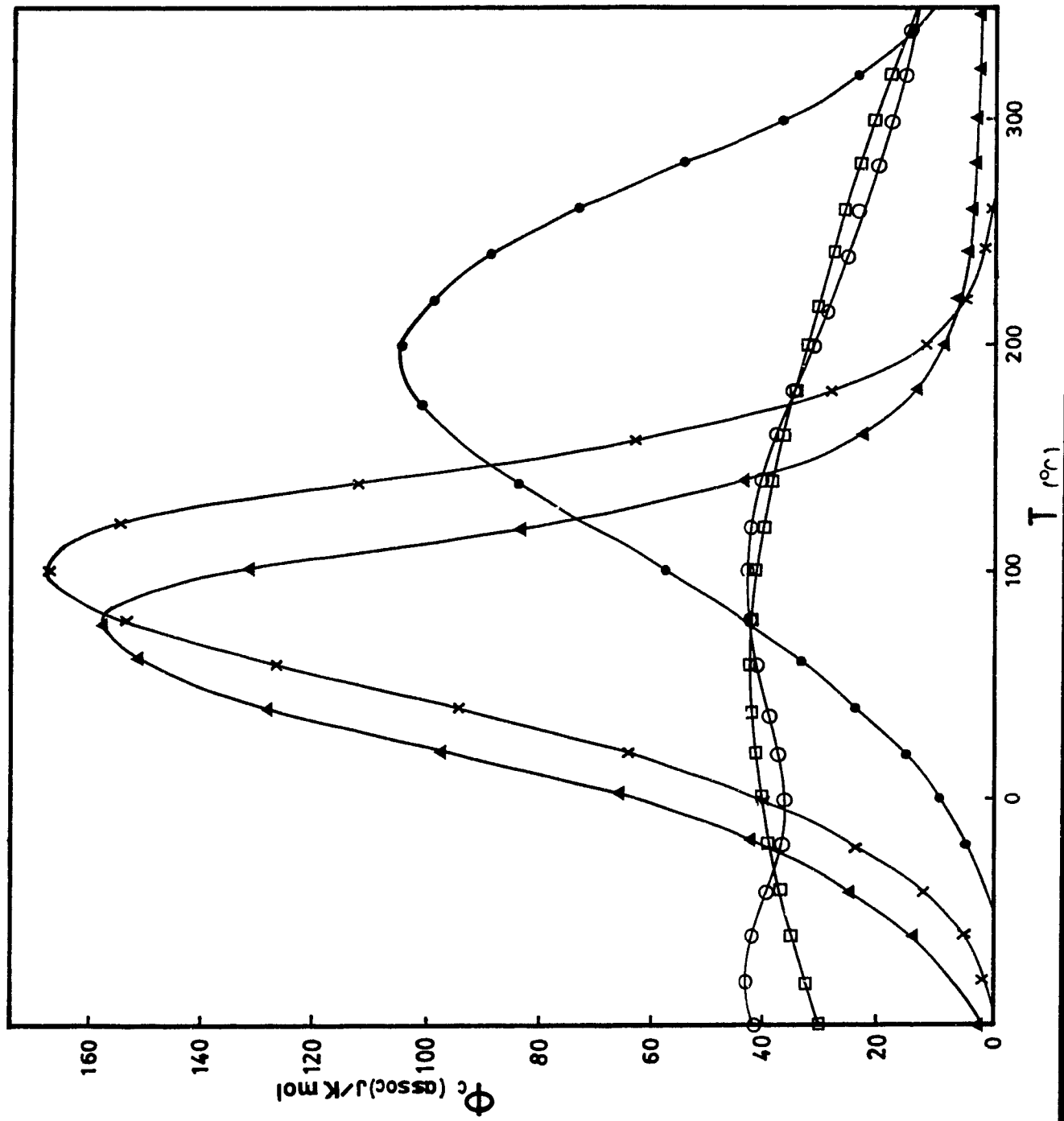
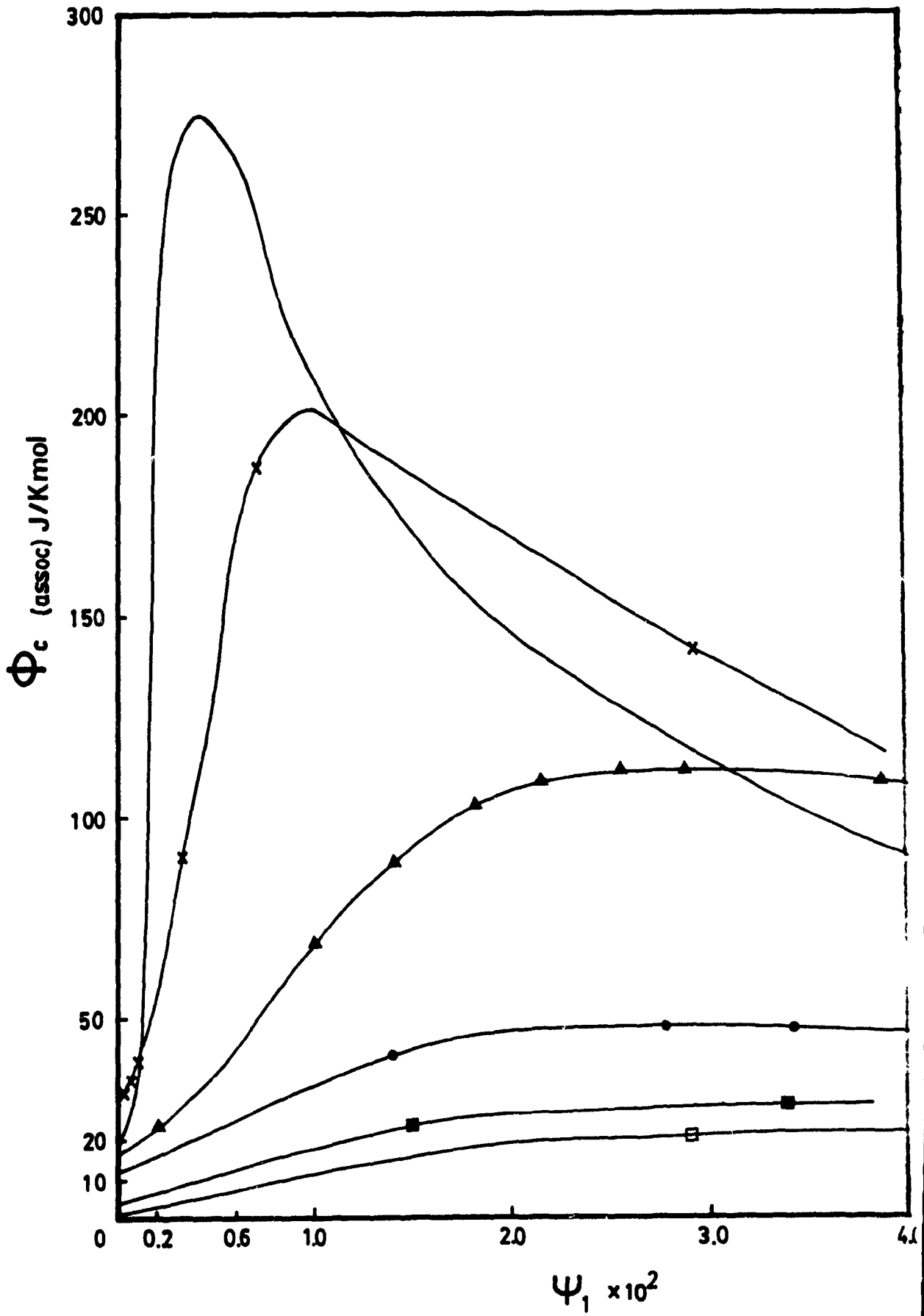


Fig. 7b Experimental  $\phi_{C(\text{assoc})}$  as a function of hydroxyl concentration for butanol in inert and proton acceptor solvents at 25°C.  
inert: full line;  $\times$   $\text{CCl}_4$ ,  $\Delta$  benzene;  $\bullet$  octanenitrile;  $\square$  acetonitrile;  $\square$  methyl acetate.



While self-association leads to tetramer species, complex formation gives dimers. It is known that the higher the species, the bigger is its contribution to the heat capacity. Therefore, the structure created in solution by the formation of tetramers is larger. Hence  $\phi_{C(\text{assoc})}$  should be higher for a solution of alcohol + inert than for alcohol + PA, since in the latter case, two kinds of H-bonds are observed: self-association which gives tetramers and AB complex which leads to dimers. The competition between tetramers and dimers depends upon the strength of the PA.

Now, if a stronger PA is used, more dimers should be produced meaning that the contribution to  $C_p$  will be smaller than previously and therefore  $\phi_{C(\text{assoc})}$  should be much smaller. This can be observed for acetonitrile or octanenitrile mixtures. At low concentration and in the entire concentration range  $\phi_{C(\text{assoc})}$  is always lower than the value observed for the inert. No evident maximum has been observed. The decrease in  $\phi_{C(\text{assoc})}$  is related to the strength of the PA. As can be seen in fig. 7b,  $\phi_{C(\text{assoc})}$  is lower for acetonitrile than for  $\text{CCl}_4$  or octanenitrile where the alkane chain of the nitrile might dilute the OH groups present in the solution.

b. Excess heat capacity ( $C_p^E$ )

Excess heat capacity ( $C_p^E$ ) can be obtained from eqn. 11:

$$C_p^E = (\phi_{C_1} - \phi_{C_1}^0) x_1 \quad (11)$$

It is given as the difference between the molar apparent heat capacity ( $\phi_C$ ) of the solution and the molar heat capacity of the pure component (1), at a given concentration of component (1). Fig. 8a shows experimental results for  $C_p^E$  against concentration (mole fraction) of butanol in various solvents: n-C<sub>7</sub>,  $\text{CCl}_4$ , octanenitrile,

Fig. 8a Experimental results of excess heat capacity  $C_p^E$  as a function of mole fraction of butanol for butanol + acetonitrile  $\times$ ;  $\text{CCl}_4$   $\bullet$ ; and octanenitrile  $\square$  at  $25^\circ\text{C}$ .

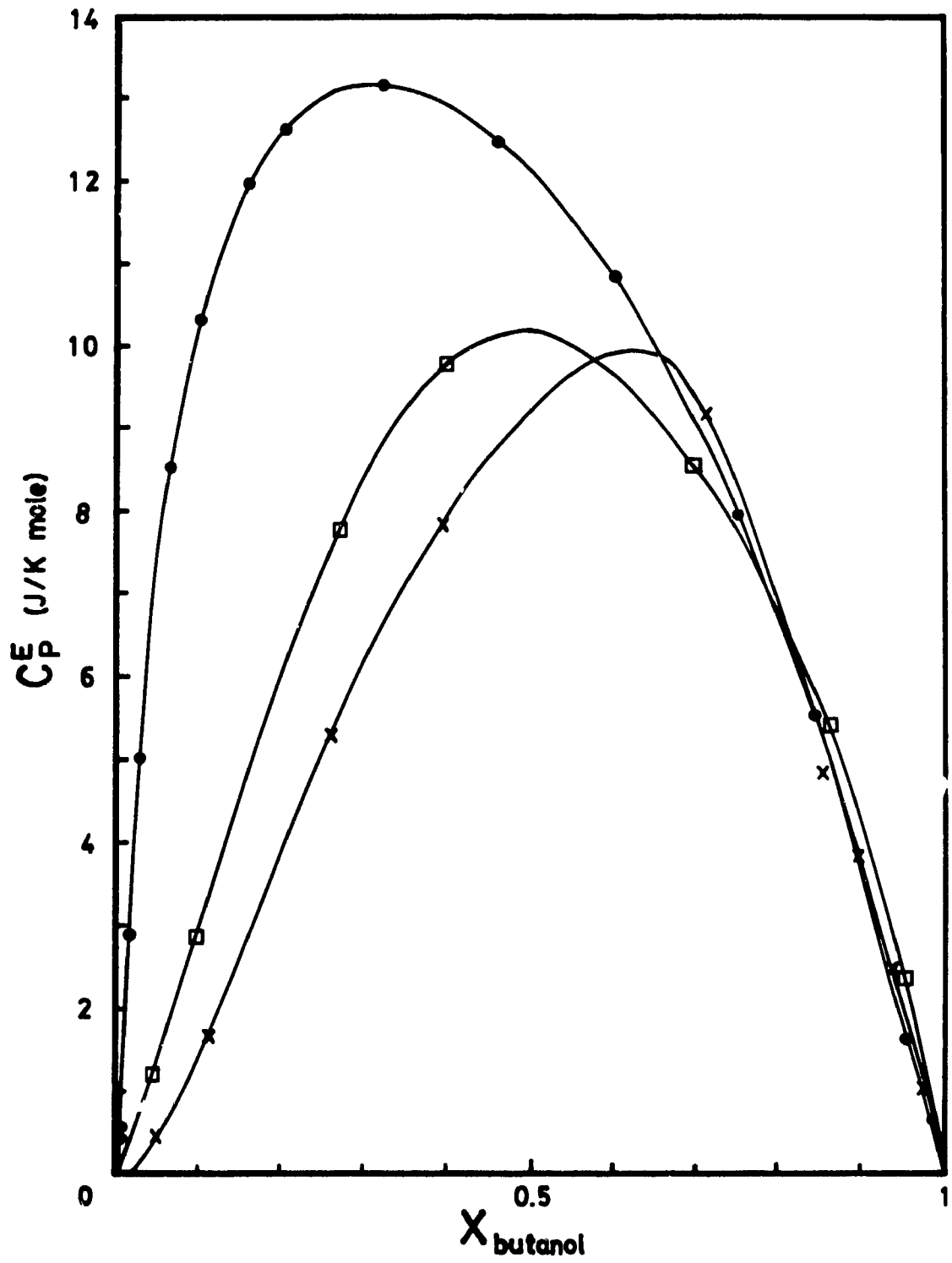
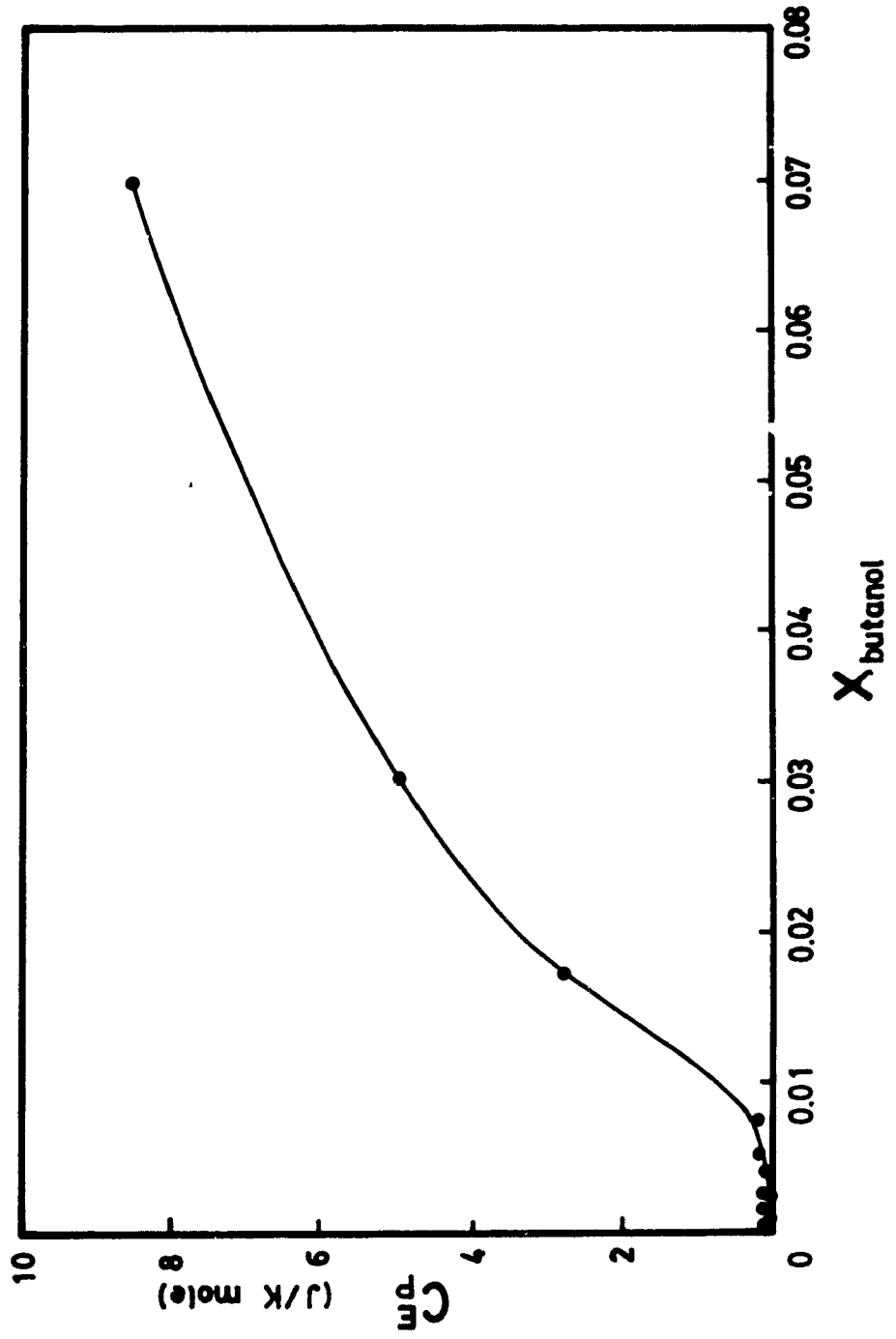


Fig. 8b Experimental  $C_p^E$  as a function of mole fraction of butanol at high dilution of butanol +  $\text{CCl}_4$  at  $25^\circ\text{C}$ .



acetonitrile at 25°C. n-C<sub>7</sub> exhibits the largest value of C<sub>p</sub><sup>E</sup>. C<sub>p</sub><sup>E</sup> shows a slightly negative minimum at high dilution, indicating a decrease of structure in solution compared to the structure existing in the pure components. Then, as the concentration is increased, C<sub>p</sub><sup>E</sup> increases and reaches a maximum of ≈ 13.6 at 0.3 mole fraction of butanol and decreases as the concentration is further increased.

However, C<sub>p</sub><sup>E</sup> for CCl<sub>4</sub> mixture does not show any dependence upon concentration for x > 0.01, as shown in fig. 8b. C<sub>p</sub><sup>E</sup> increases slowly and shows a maximum value of 13.4 J/K mol slightly lower than the inert. As the PA is stronger, C<sub>p</sub><sup>E</sup> is smaller. Acetonitrile shows a maximum of 8.9 J/K mol. However, as the inert tail of the PA increases, C<sub>p</sub><sup>E</sup> increases and exhibits a maximum of 10.5 J/K mol for octanenitrile, for instance.

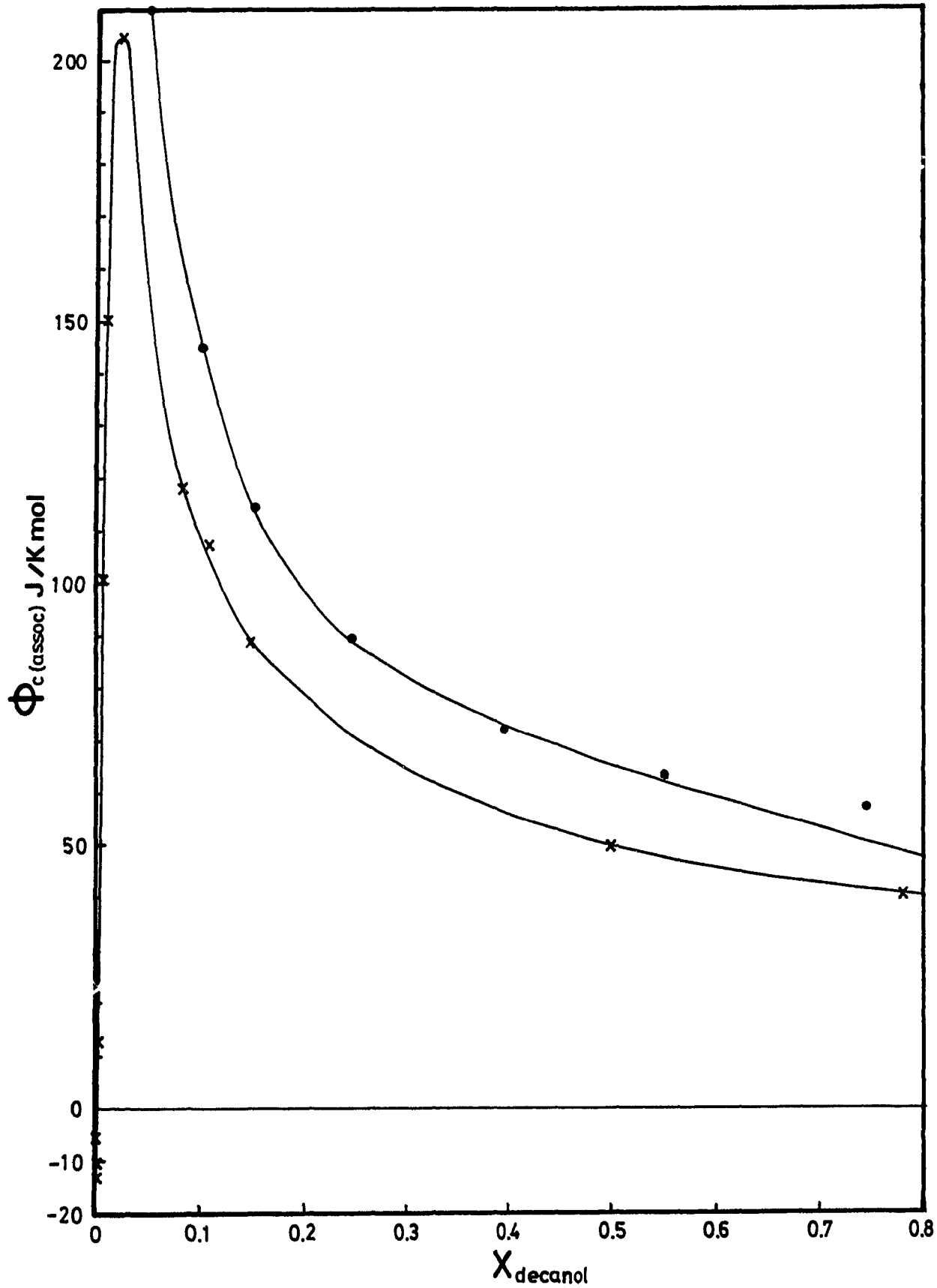
It is also known that the length of the inert tail of the alcohol molecule affects the structure in solution. In the next section, we will study the effect created by a longer and a shorter alcohol than butanol such as decanol in CCl<sub>4</sub> and methanol in acetonitrile.

#### 4. Decanol + CCl<sub>4</sub>

Fig. 9 shows experimental results for φ<sub>C(assoc)</sub> of decanol in CCl<sub>4</sub> and in n-C<sub>7</sub> at 25°C as a function of mole fraction of decanol. φ<sub>C(assoc)</sub> shows a large and sharp maximum of 205 J/K mol at around x = 0.05 for the CCl<sub>4</sub> solution while the n-C<sub>7</sub> solution exhibits a maximum of 211 J/K mol.

The particularity of the CCl<sub>4</sub> system is that φ<sub>C(assoc)</sub> is negative at high dilution (x < 0.01). The limit of φ<sub>C(assoc)</sub> takes the value of -13 J/K mol. The limiting value represents the contribution to the heat capacity of the alcohol in the absence of any association. This negative value is peculiar and it is not observed for lower alcohols. For instance, butanol + CCl<sub>4</sub> shows a limit of 28 J/K mol. The

Fig. 9 Experimental  $\phi_{c(\text{assoc})}$  for decanol +  $\text{CCl}_4$  and +  $n\text{-C}_7$  at  $25^\circ\text{C}$ .  
 $\times \text{CCl}_4$ ;  $\bullet n\text{-C}_7$ .

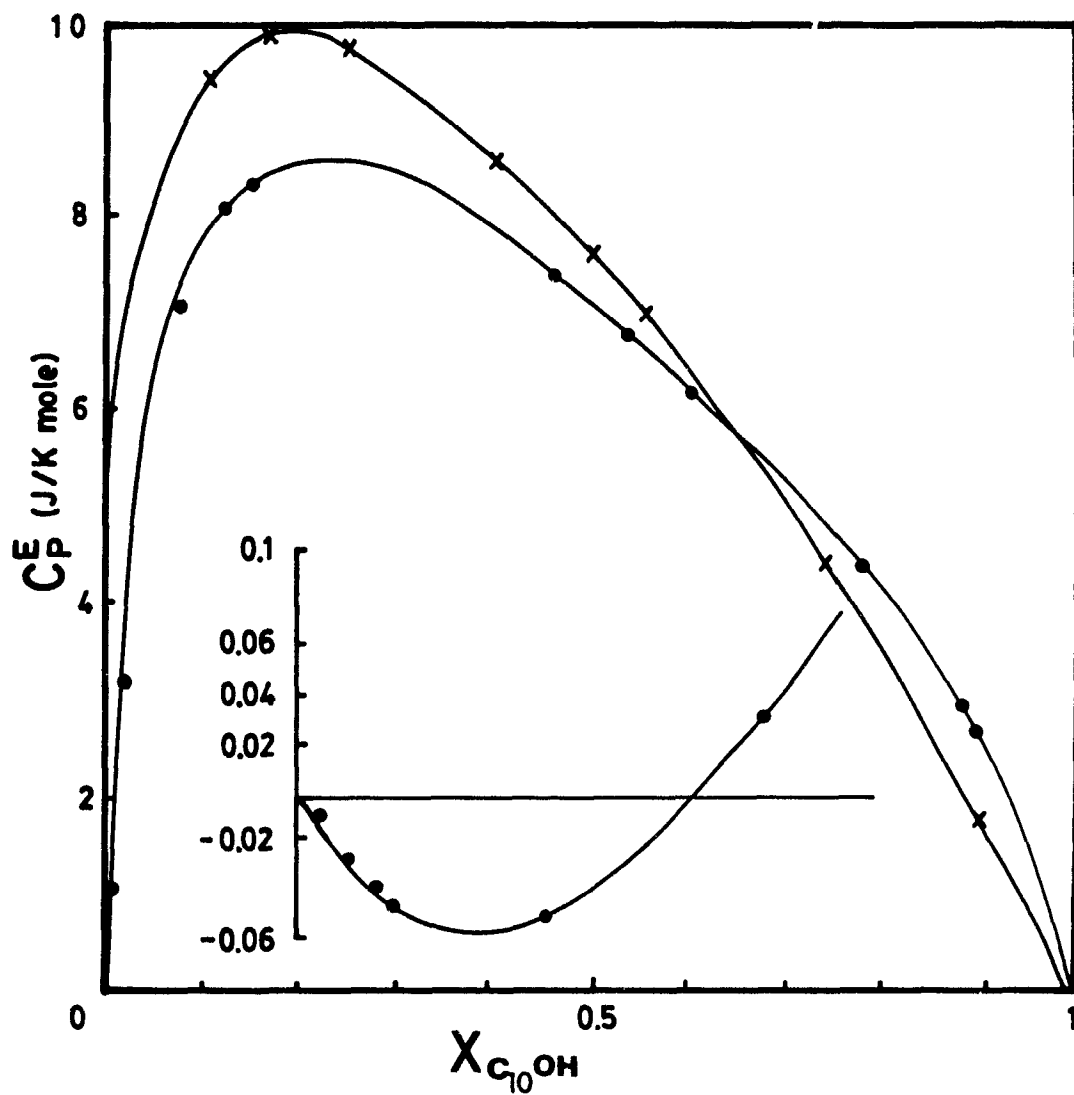


intercept for decanol or butanol in decane was used to obtain  $\phi_{C(\text{assoc})}$ . Conversely to butanol, decanol is a long chain alkanol where it is reasonable that a correlation of molecular order (CMO) takes place<sup>9</sup>. The thermodynamic properties of the solutions are affected by the presence of orientational order in the pure state of a long chain alkane. This order is equivalent to a molecular cohesion which lowers H, S and V and since it is found to fall off rapidly with T, the order makes a positive contribution to  $C_p$ . While these changes are difficult to isolate in the pure state, they manifest themselves in the mixing process. In the same way, mixing a long chain alkanol molecule ( $n \geq 10$ ) with a short or order-breaker molecule such as  $\text{CCl}_4$ , results in a destruction of this CMO which, as a consequence, gives a negative contribution to  $C_p^E$ .

The intercept of  $\phi_C$  for decanol in a long chain alkane such as decane was used to obtain  $\phi_{C(\text{assoc})}$ . Therefore, the value of the intercept (which is the contribution to  $C_p$  in absence of any association) is increased by CMO. However, if decane is replaced by  $\text{CCl}_4$  a pseudo-spherical or order breaker molecule, the value of  $\phi_{C(\text{assoc})}$  obtained by comparing the value in  $\text{CCl}_4$  to the limiting value in decane shows a negative limit of  $\phi_{C(\text{assoc})}$ . The intercept is not raised by CMO in this case. Furthermore,  $\phi_{C(\text{assoc})}$  of  $\text{CCl}_4$  mixture is lower than the value observed for mixture in a short alkane, like n-C<sub>7</sub>. Conversely for butanol, decanol shows at high concentration a smaller  $\phi_{C(\text{assoc})}$  for  $\text{CCl}_4$  than for the inert solvent.

Fig. 10 shows experimental results of  $C_p^E$  for decanol in  $\text{CCl}_4$  at 25°C. At low concentration ( $x \leq 0.01$ ),  $C_p^E$  is negative and shows a minimum value of  $-0.06$  J/K mol, while no concentration dependence has been observed for the butanol mixture at this range of concentration. It can therefore be suggested that two contributions arise in  $C_p^E$  of decanol +  $\text{CCl}_4$  solutions: Firstly, at low concentration, one is due to the breaking up of H-bonds and the second comes from the destruction of CMO by the mixing process. Both contributions are negative in  $C_p^E$ , indicating that decanol should show a more negative value than butanol at very low concentration, since no CMO is

Fig. 10 Experimental  $C_p^E$  results for decanol +  $\text{CCl}_4$  at  $25^\circ\text{C}$ .  
 $\times$  n-C<sub>7</sub>;  $\bullet$   $\text{CCl}_4$ .



possible in butanol. Secondly, at high concentration ( $x > 0.01$ ), while the contribution from destruction of CMO still arises and is negative, another contribution takes place coming from the self-association of decanol molecules and this contribution is positive. Therefore,  $C_p^E$  at high concentration should be a resultant of these 2 contributions which are of opposite signs. Therefore,  $C_p^E$  for decanol at high concentration ( $x > 0.01$ ) should be smaller than  $C_p^E$  for butanol. In fact, decanol shows a maximum of  $C_p^E$  of 8.5 J/K mol compared to 13.5 J/K mol for butanol.

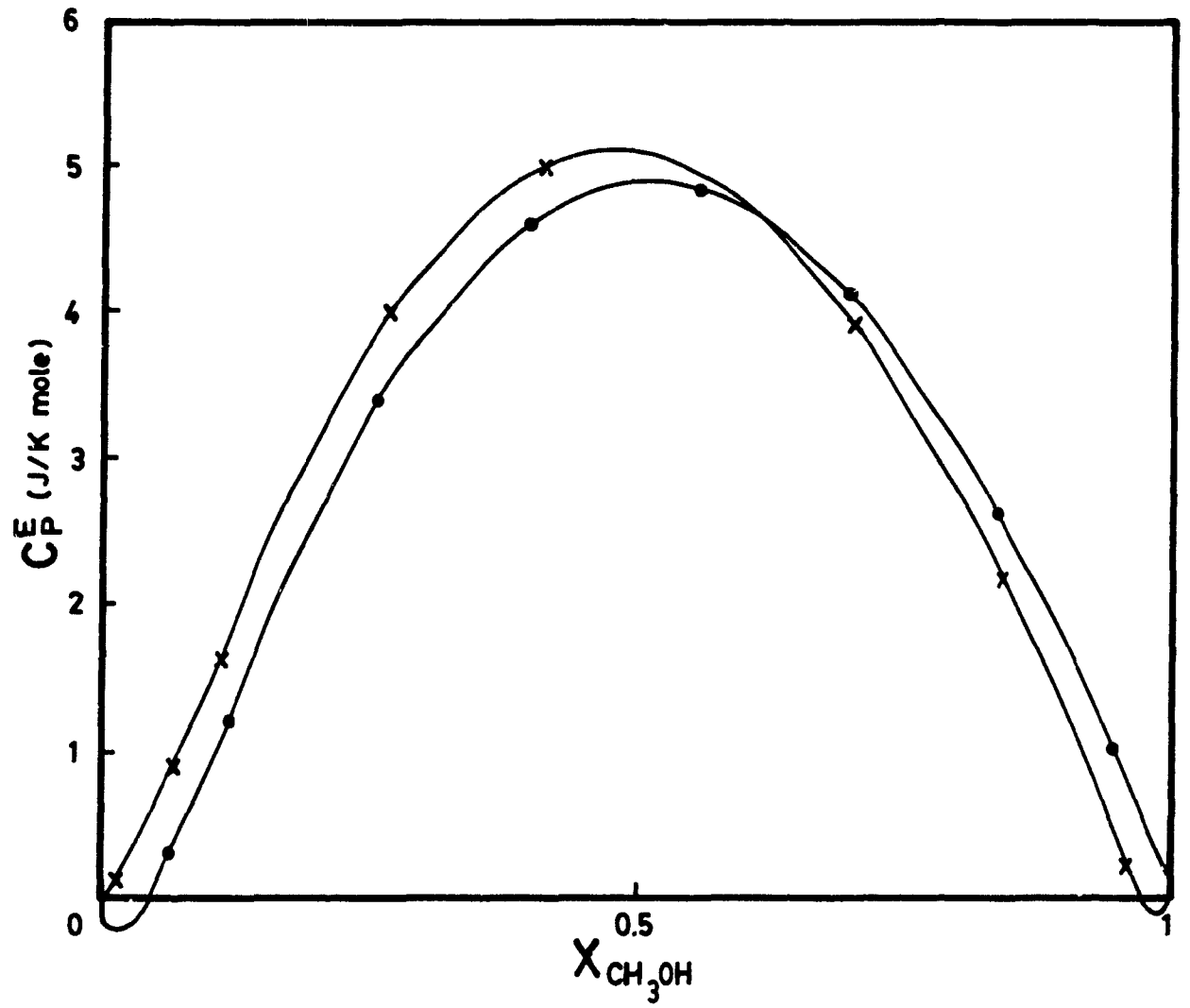
#### 5. Methanol + acetonitrile

Fig. 11 shows experimental  $C_p^E$  results for methanol in acetonitrile at 25°C. As for butanol + acetonitrile,  $C_p^E$  is positive but with a slight negative minimum at high dilution. However  $C_p^E$ 's maximum is considerably smaller, 5 J/K mol compared to 8.9 J/K mol for butanol. This lower value of  $C_p^E$  can be explained by the formation of a stronger complex between methanol-acetonitrile than between butanol-acetonitrile.

This argument is well supported by excess volume results for those systems. Figs. 12 and 13 show experimental  $V^E$  results for respectively butanol + acetonitrile and methanol + acetonitrile. While the former shows a positive  $V^E$  with a slight negative minimum at high concentration of alcohol, the latter exhibits rather negative  $V^E$  with a very small positive maximum at low concentration of alcohol. These results reveal the existence of a competition between two different processes: self-association and complex formation. In the case of butanol, at low concentration, the self-association process overlaps the complex formation.

However, methanol + acetonitrile reveals a different behaviour. At extremely low concentration, there is an expansion due to the breaking up of the H-bonds. But as the concentration increases ( $x > 0.02$ ),  $V^E$  decreases and becomes more and more

Fig. 11 Experimental  $C_p^E$  for methanol + acetonitrile at 25°C (●) and 40°C (x).



negative until a minimum value of  $-0.16 \text{ cm}^3/\text{mol}$ , indicating the presence of a stronger complex between methanol and acetonitrile than butanol and acetonitrile.

Flory's theory has been used to interpret the  $V^E$  results. The predictions shown in Figs. 12 and 13 are much too large. Because of a large endothermic heat,  $X_{12}$  is large and positive. However, when fitted to the equimolar experimental value,  $X_{12}$  turns out to be negative.

It has been found that the theory fails to predict  $V^E$  for most of systems containing associated molecules. As suggested in ref. 10, the discrepancy between experimental and predicted values is an indicator of association which is not taken into account by the theory. In ref. 10, it is also suggested that  $V^E$  can be split into two contributions:  $V_{\text{phys}}^E$  and  $V_{\text{chem}}^E$ .  $V_{\text{phys}}^E$  is given by Flory theory while  $V_{\text{chem}}^E$  is the associational contribution.  $V^E$  can be estimated using a modified version of the theory, i.e. introducing association parameters ( $\Delta H^O$ ,  $\Delta H_{AB}$ ,  $K$  and  $K_{AB}$ ) into the theory. Once again negative value of  $X_{12}$  is required to fit the data. The trend of  $V^E$  is well predicted.

Fig. 12 Theoretical and experimental  $V^E$  results for butanol + acetonitrile at 25°C.  
Broken Line: theoretical.  $X_{12} = -13.75$ .

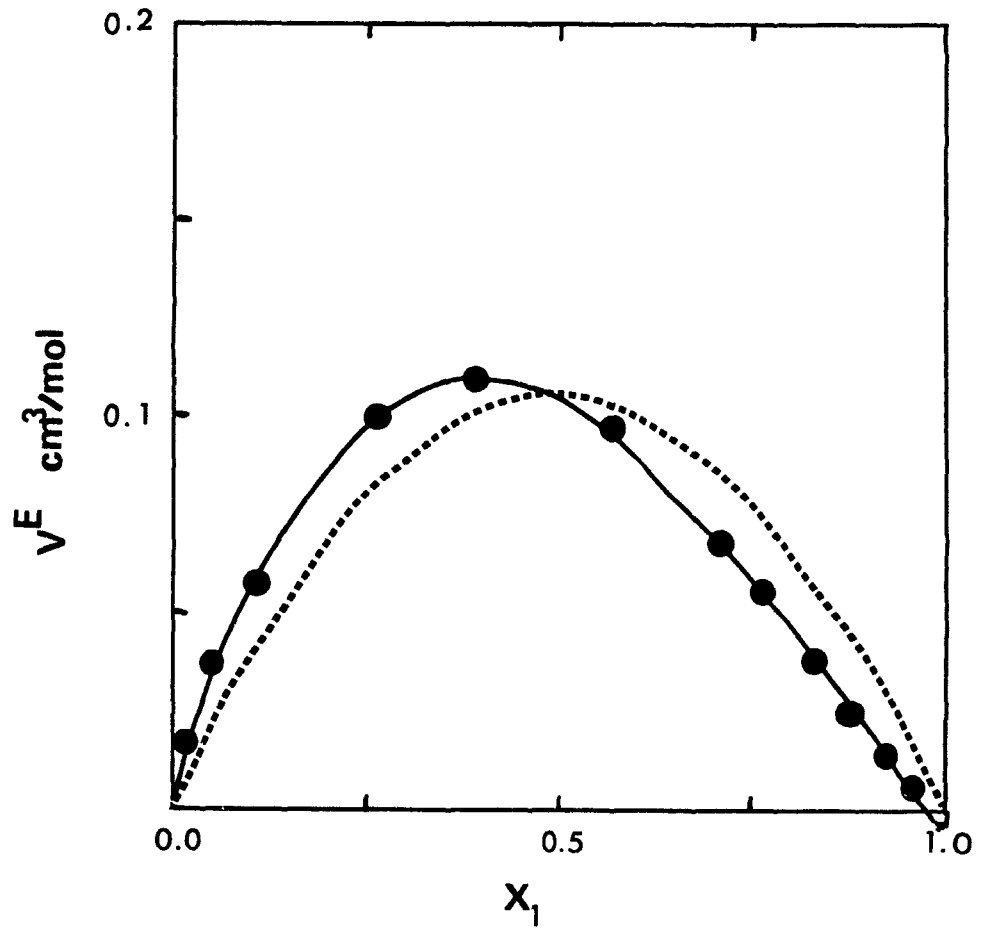
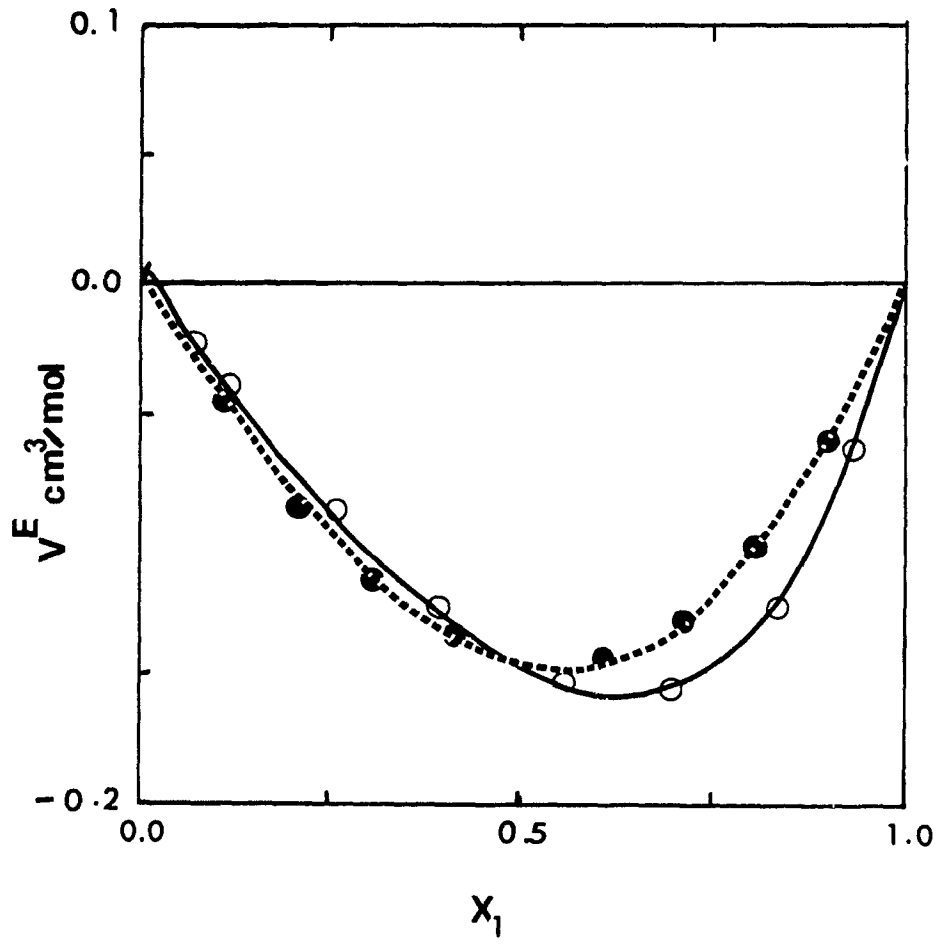


Fig. 13 Theoretical and experimental  $V^E$  results for methanol + acetonitrile at 25°C. Broken line: theoretical.  $X_{12} = -27.9$ .



REFERENCES

1. H. Wolf and H.E. Hoppel, *Ber. Bunsenges Phys. Chem.*, 72, 710, 1968.
2. A.N. Fletcher and C.A. Heller, *J. Phys. Chem.*, 71, 12, 3742, 1967.
3. a) R.H. Stokes and H. Adamson, *J. Chem. Thermodyn.*, 8, 683, 1976.  
b) B.D. Anderson, H.H. Rylting, S. Lindenbaum, and T. Higuchi, *J. Phys. Chem.*, 79, 2340, 1975.  
c) M.K. Kumaran and G.C. Benson, *J. Chem. Thermodyn.*, 16, 175, 1984.  
d) G.C. Benson, P.J. D'Arcy, and M.E. Sugamori, *Thermochim. Acta*, 71, 161, 1983.
4. M. Costas and D. Patterson, *J. Chem. Soc. Faraday Trans.*, 81, 635, 1985.
5. H. Kehiaian and A.J. Treszczanowicz, *Bull. Acad. Chim. Fr.*, 5, 1561, 1969.
6. L. Andreoli-Ball, D. Patterson, M. Costas, and M. Ceres-Alonso, *J.C.S. Faraday 1*, in press.
7. M. Costas and D. Patterson, *J. Chem. Soc. Faraday Trans.*, 81, 655, 1985.
8. a) P. Picker, P.A. Leduc, P.R. Philippe, and J.E. Desnoyers, *J. Chem. Thermodyn.*, 3, 631, 1971.  
b) L. Fortier and G.C. Benson, *J. Chem. Thermodyn.*, 8, 411, 1976.
9. S.N. Bhattacharyya and D. Patterson, *J. Phys. Chem.*, 83, 2979, 1974.
10. M.E. Saint Victor, A.J. Treszczanowicz, and D. Patterson, Submitted to *Fluid Phase Equilibria*, 1988.

APPENDIX 4

Tables of Results

TABLE 2

Excess heat capacities and excess volumes as a function of mole fraction of butanol in acetonitrile at 25°C

$x_1$	$C_p^E$ J/K mol	$V^E$ cm <sup>3</sup> mol <sup>-1</sup>
0.01992	0.08	0.0171
0.0490	0.41	0.0370
0.1087	1.63	0.0576
0.2582	5.35	0.0996
0.3895	7.78	0.1108
0.5663	9.05	0.0969
0.7093	9.21	0.0668
0.7642	5.26	0.0550
0.8312	4.84	0.0383
0.8763	3.59	0.0254
0.9214	2.46	0.0141
0.9502	0.91	0.0177
0.9905	0.35	0.0151

TABLE 3

Excess heat capacities and excess volumes as a function of mole fraction of butanol in  $\text{CCl}_4$  at  $25^\circ\text{C}$

$x_1$	$C_p^E$ J/K mol	$V^E$ $\text{cm}^3\text{mol}^{-1}$
0.00130	0.02	0.0111
0.00244	0.05	0.0166
0.0078	0.56	0.0187
0.0170	2.85	0.0487
0.0291	5.00	0.0535
0.0695	8.52	0.0794
0.1116	10.37	0.0758
0.1683	11.91	0.0765
0.2097	12.64	0.0676
0.4595	12.39	-0.0158
0.5998	10.82	-0.0768
0.7375	7.90	-0.1100
0.8334	5.47	-0.0985
0.9486	1.59	-0.0337
0.9780	0.58	-0.0082

TABLE 4

Excess heat capacities and excess volumes as a function of mole fraction of decanol in  $\text{CCl}_4$  at  $25^\circ\text{C}$

$x_1$	$C_p^E$ J/K mol	$V^E$ $\text{cm}^3\text{mol}^{-1}$
0.0005	–0.03	$-4 \times 10^{-3}$
0.0006	–0.03	–0.003
0.0009	–0.05	–0.0070
0.0026	–0.06	0.0012
0.0048	0.32	0.0111
0.0054	0.07	0.0119
0.0102	1.18	0.0250
0.0197	3.35	0.1076
0.0845	7.06	
0.1100	8.03	0.1336
0.1504	8.21	0.1431
0.3011	7.17	0.1868
0.4469	6.89	0.1707
0.7242	6.24	
0.7778	4.43	0.1595
0.8969	2.99	
0.8974	2.69	

TABLE 5

Excess heat capacities and excess volumes as a function of mole fraction of methanol in acetonitrile at 25°C

$x_1$	$C_p^E$ J/K mol	$V^E$ cm <sup>3</sup> mol <sup>-1</sup>
0.0687	0.58	-0.0228
0.1151	1.27	-0.0382
0.2616	3.44	-0.0867
0.3949	4.61	-0.1236
0.5530	4.90	-0.1518
0.6951	4.22	-0.1553
0.8365	2.70	-0.1234
0.9402	1.05	-0.0614

TABLE 6

Excess heat capacities and excess volumes as a function of mole fraction of methanol in acetonitrile at 15°C

$x_1$	$C_p^E$ J/K mol	$V^E$ cm <sup>3</sup> mol <sup>-1</sup>
0.0126	0.22	-0.0064
0.0676	0.98	-0.0271
0.1112	1.71	-0.0432
0.2743	4.01	-0.0985
0.4188	5.00	-0.1349
0.5679	4.90	-0.1571
0.7012	4.00	-0.1563
0.8413	2.22	-0.1156
0.9528	0.29	-0.0453
0.9718	0.09	-0.0332

TABLE 7

Excess heat capacities and excess volumes as a function of mole fraction of butanol in octanenitrile at 25°C

$x_1$	$C_p^E$ J/K mol	$V^E$ cm <sup>3</sup> mol <sup>-1</sup>
0.0529	1.22	0.0176
0.1006	2.86	0.0524
0.2748	7.81	0.1003
0.4110	9.73	0.1342
0.5539	9.93	0.1503
0.6944	8.57	0.1434
0.8415	5.39	0.830
0.9414	2.33	0.0504

CHAPTER 5

THERMODYNAMIC STUDIES OF THE SELF-ASSOCIATION OF  
ALKYLNITRILES IN INERT AND PROTON ACCEPTOR SOLVENTS

## INTRODUCTION

A number of recent studies attest to the growing interest in thermodynamics of molecular association. The most obvious examples of associated systems are those which contain a hydrogen bond. However, molecules containing nitrile, nitro or ester groups also show association effects.

A few studies have been reported on the self-association of nitrile components. Spectroscopic studies of Saito et al<sup>2</sup> and Fujiwara et al<sup>3</sup> on nuclear magnetic resonance of nitriles suggested the formation of dipole-dipole association. Excess volume measurements by Trejo et al<sup>4</sup> and Prausnitz et al<sup>5</sup> etc. give evidence of association taking place in both the pure state and in solution.  $V^E$  shows an S-shape i.e. positive at low concentration suggesting an expansion of the solution due to the breaking of nitrile self-association. Blander et al<sup>6,7</sup> study the self-association of various components using pressure and temperature dependence of thermal conductivity. It was suggested that nitriles in general exist as dimers, all these studies agree on the existence and the nature of the association taking place in the nitrile compounds. Thus structure as a manifestation of this self-association should be observed in both the pure state and solution. Heat capacity, as a good structure indicator, has revealed interesting features in the determination of various association processes, for instance self-association of alcohols. The change occurring in the heat capacity during the mixing process, the excess heat capacity,  $C_p^E$ , is positive over almost all of the concentration range, but negative in extremely dilute solution which is characteristic of self-association. Furthermore, the apparent heat capacity,  $\phi_C$ , provides a valuable guide to the nature of the self-association process involved.

Several theories and theoretical models have been applied to explain the behaviour of associated components. Among them, the Treszczanowicz and Kehiaian (TK) theory<sup>8</sup> successfully treated the self-association of alcohols where the

predominant species are tetramers<sup>9</sup>, dimers being almost absent. It is believed, however, that dimers should be the predominant species in moderately associated components. The aim of this work is to study the self-association of dodecanenitrile in decane,  $\text{CCl}_4$  and xylene and the self-association of acetonitrile in  $\text{CCl}_4$  using excess heat capacity and excess volume measurements. The TK model is used to predict the nature of the self-association process involved. The experimental results are interpreted through the TK model.

## EXPERIMENTAL

The chemicals are from Aldrich and are of at least 99% of purity. They were used as received, no further purification was made.

Excess heat capacities were measured using a Picker flow microcalorimeter (Sodev, Sherbrooke, Quebec, Canada). Methods and procedures have been described in the literature<sup>10</sup>. Apparent heat capacity and its associational part were obtained using  $C_p$  values.

A flow densitometer from Sodev was used to measure densities of both pure components and solutions. Density data were used to transform volumetric heat capacity into molar and also to calculate excess volumes of the solutions. Densities of the pure components are shown in Table 1.

Excess heat capacity ( $C_p^E$ ), apparent heat capacity ( $\phi_c$ ) and excess volumes ( $V^E$ ) have been measured or calculated for mixtures of: dodecanenitrile ( $C_{11}CN$ ) + decane ( $n-C_{10}$ ) at 25°C; + carbon tetrachloride ( $CCl_4$ ) at 25°C; + xylene at 25°C; octanenitrile ( $C_7CN$ ) +  $n-C_{10}$  at 25°C; acetonitrile +  $CCl_4$  at 25°C and 40°C.

The apparent heat capacity ( $\phi_c$ ) and associational apparent heat capacity ( $\phi_{c(assoc)}$ ) of component 1 have been calculated using the following equations:

$$\phi_c = \left[ C_p - x_2 C_{p,2}^0 \right] / x_1 \quad (1)$$

where  $C_p$ ,  $C_{p,2}^0$  are the molar heat capacities of the solution and the pure component 2, and  $x_1$  and  $x_2$  are mole fractions. The associational part of  $\phi_c$  is obtained through

$$\phi_{c(assoc)} = \phi_c - \lim_{x \rightarrow 0} \phi_c \quad (2)$$

TABLE 1  
Density and heat capacity of the pure components at 25 and 40°C

	Density (g/cm <sup>3</sup> )		Cp (J/K mol)	
	25°C	40°C	25°C	40°C
CH <sub>3</sub> CN	0.7766	0.7546	90.69	91.96
C <sub>7</sub> CN	0.8094	—	264.45	396.99
C <sub>11</sub> H <sub>23</sub> CN	0.8204	0.8098	386.72	323.53
C <sub>10</sub> H <sub>22</sub>	0.7262	0.7150	312.95	323.53
CCl <sub>4</sub>	1.5844	1.5558	132.99	133.08
Xylene	0.8570	—	183.65	—

Measurements at high dilution of nitriles were used to calculate the limit of  $\phi_C$ . Since dimer formation starts in an early stage of the dilution process, it requires extremely dilute solutions in order to evaluate the limit of  $\phi_C$  in the eventual existence of dimers. Therefore, an extrapolation of  $\phi_C$  to infinite dilution can be inaccurate. To counter these difficulties, we have estimated the limit of  $\phi_C$  in the following way. It is assumed that the pure nitrile is partially dimerized and that the heat capacity of the pure state follows the TK model. This gives a value of  $C_{p(\text{assoc})}^0$  for the pure nitrile, which then allows a determination of  $\lim_{x \rightarrow 0} \phi_C = C_p^0 - C_{p(\text{assoc})}^0$ .

Furthermore, we know from reference 1 that the maximum value of  $\phi_{C(\text{assoc})}$  is given by:

$$\frac{\phi_{C(\text{assoc})}}{R} = 0.0858 \left[ \frac{\Delta H^0}{RT} \right]^2 \quad (3)$$

Knowing the  $\phi_{C(\text{assoc})}$  and using the following equation, we obtain the limit:

$$\frac{\phi_C - \lim \phi_C}{\phi_{C(\text{max})} - \lim \phi_C} = \frac{\phi_{(\text{assoc})}}{\phi_{(\text{assoc})\text{max}}} = \tilde{\phi} \quad (4)$$

The maximum of  $\phi_C(x)$  was fitted to the reduced CSC obtained from reference 9.  $\tilde{\phi}$  is extrapolated from the reduced curve at  $\Psi$

$$\Psi \text{ being equal to } \frac{x_{1\text{max}} * 40.7}{x_{1\text{max}} * V_1 + x_{2\text{max}} * V_2} \quad (5)$$

## RESULTS AND DISCUSSION

### 1. Alkane nitrile + inert solvent

#### A. Heat Capacity

Fig. 1 shows experimental results of the apparent molar heat capacity  $\phi_C$  and the TK predictions for  $C_{11}CN + n-C_{10}$  at  $25^\circ C$ . The association parameters used for the fitting of the experimental values are given in Table 2.  $\phi_C$  shows a maximum at about  $x_1 = 0.2$  and decreases as  $x_1$  increases. Both experimental and theoretical  $\phi_C$  exhibit a maximum displaced towards high concentration of  $C_{11}CN$ , as compared with alcohol molecules. The larger concentration of nitrile molecules needed to promote structure in solution indicates that a low degree of association is involved in these solutions compared with alcohol systems.

Fig. 2 shows experimental and theoretical values of  $\phi_{C(\text{assoc})}$  for  $C_{11}CN + n-C_{10}$  at  $25^\circ C$ . There is a good agreement between experimental and predicted curves. The calculations were made assuming that the species formed are exclusively dimers, with an equilibrium constant  $K_2$  of 5.56,  $K_3$  and  $K_4$  being kept zero. The enthalpy of formation of the dimers is  $\Delta H^\circ = -12953.7 \text{ J/mole}$ .

As it can be seen, experimental data agree perfectly with the prediction for dimers. The results not only bring evidence of the dimerization of dodecanenitrile in inert solvent, but also show the usefulness of this reduced CSC curve<sup>9</sup> which was originally made for alcohol mixtures and now revealed to be capable of predicting the type of association involving in any system.

Fig. 3 shows experimental  $C_p^E$  results of dodecanenitrile ( $C_{11}CN$ ) +  $n$ -decane as a function of concentration of nitrile at  $25$  and  $40^\circ C$ .  $C_p^E$  exhibits a negative minimum at low concentration of  $C_{11}CN$ :  $x_1 < 0.02$ . As  $x_1$  increases,  $C_p^E$  becomes positive and

Fig. 1 Theoretical and experimental  $\phi_c$  for  $C_{11}CN + n-C_{10}$  at  $25^\circ C$ :  $\bullet$ ; and  $40^\circ C$ :  
 $\times$ ; broken lines: theoretical.

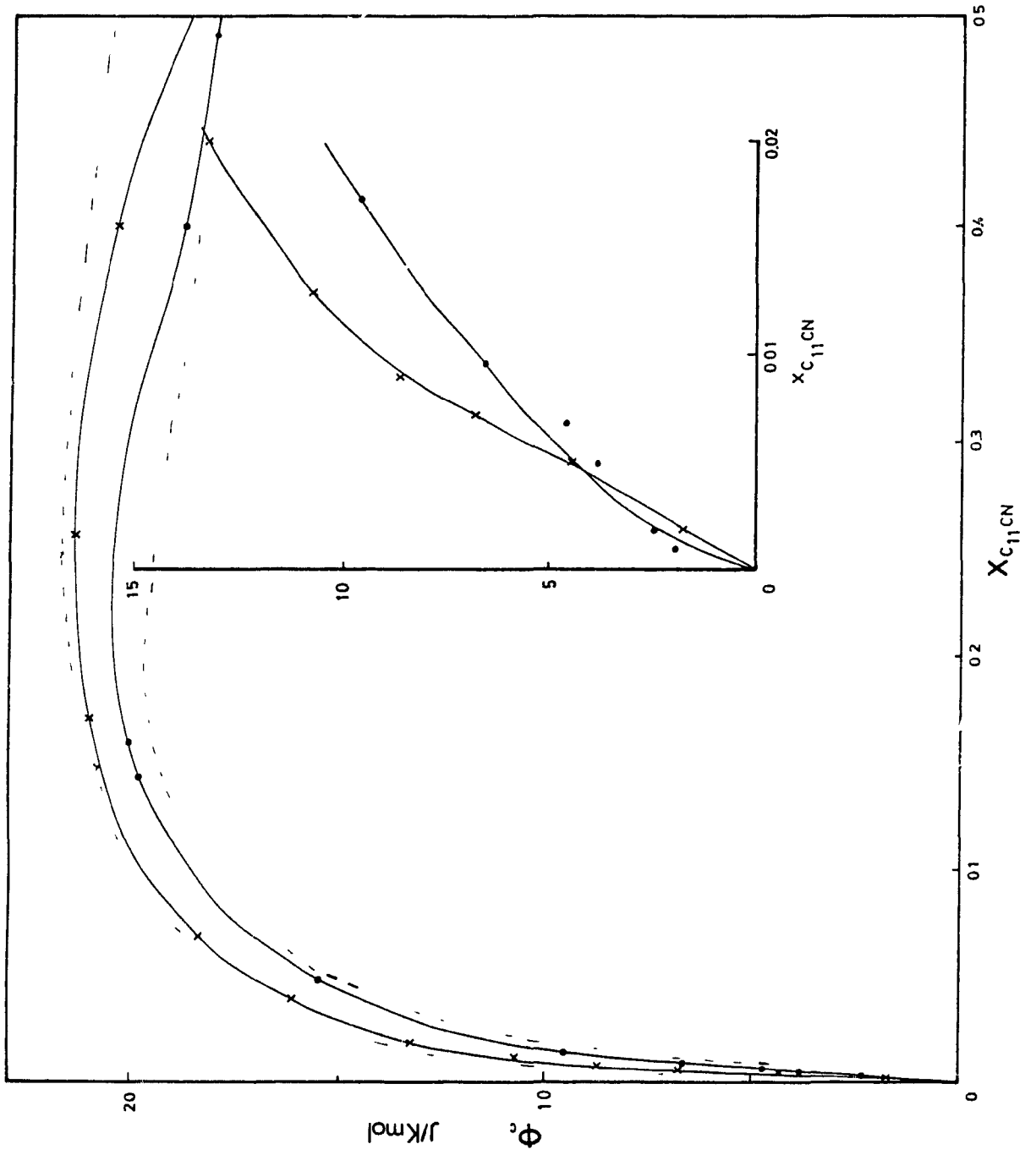


Fig. 2 Theoretical and experimental  $\phi_{C(\text{assoc})}$  for  $C_{11}CN + n-C_{10}$  at 25:  $\circ$  and 40°C:  $\times$ ; broken lines: theoretical.

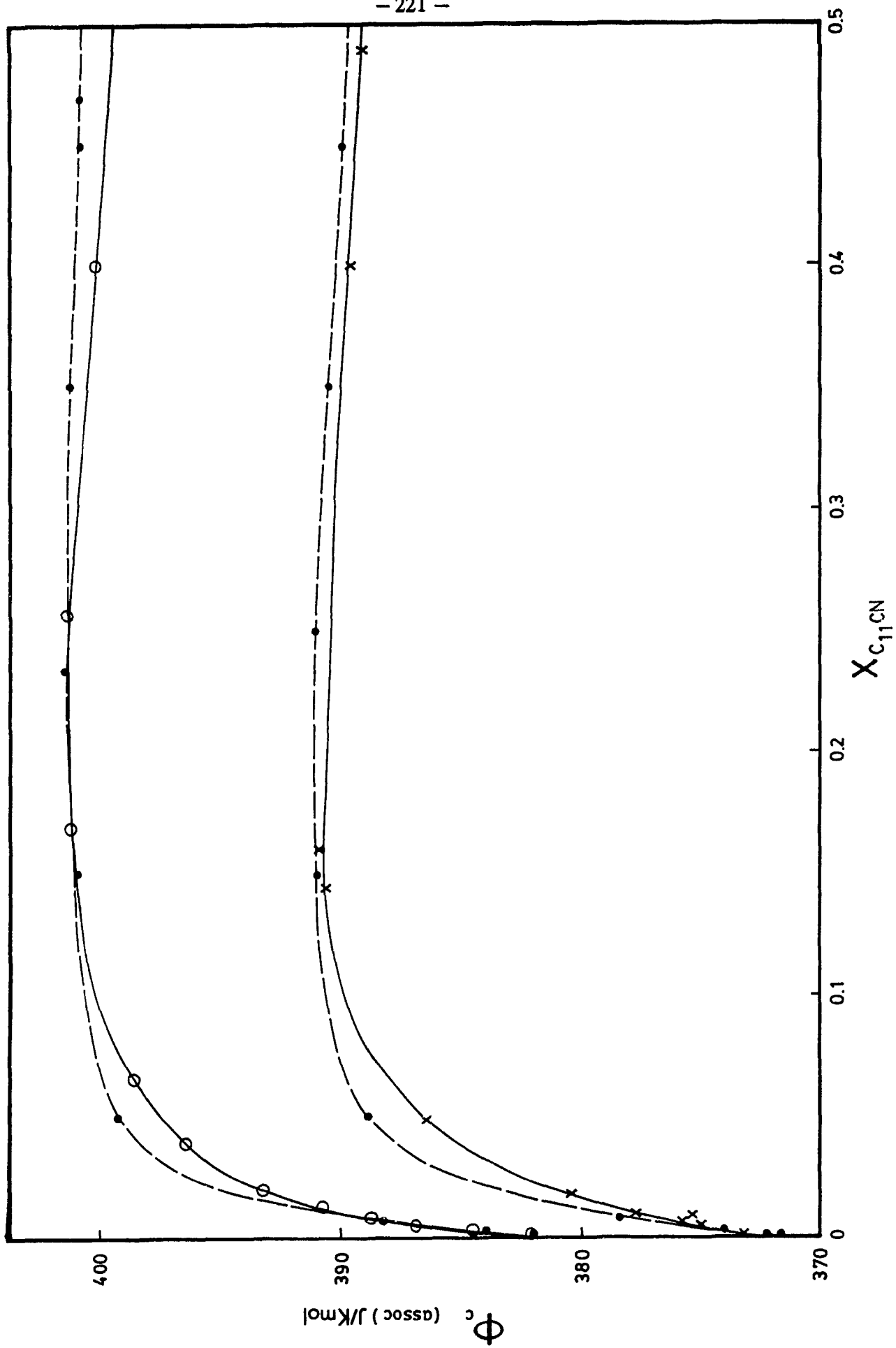


Fig. 3 Experimental  $C_p^E$  for  $C_{11}CN + n-C_{10}$  at  $25^\circ C$ :  $\bullet$ ; and  $40^\circ C$ :  $+$ .

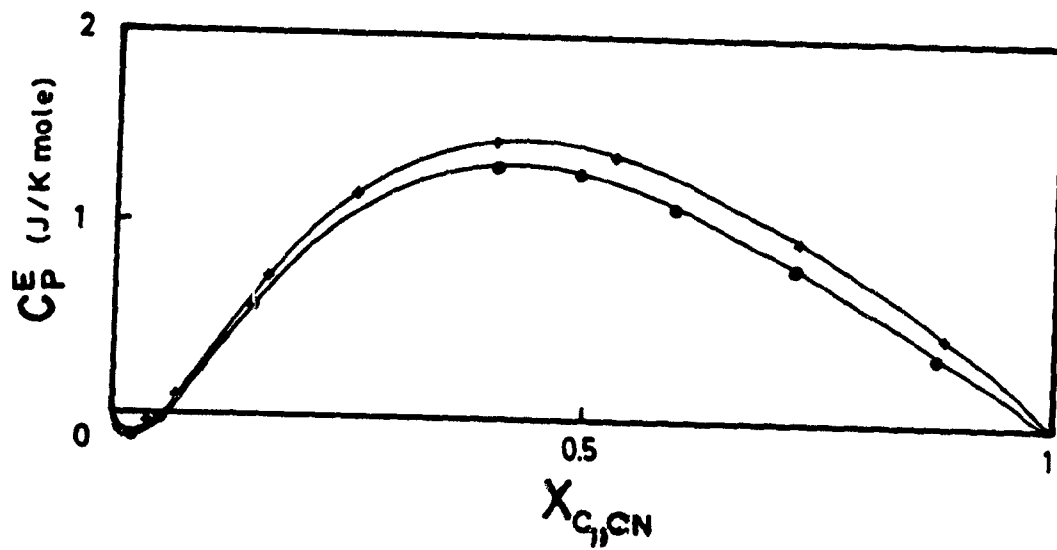


TABLE 2  
TK Model Parameters for Solutions of  $C_{11}CN$  at  $25^{\circ}C$

	$\Delta H^0$	$\Delta H_{11}$	$H^E$	$K_2$	$K_{11}$
Decane	- 13100	0.00	869.5	5.56	0.00
$CCl_4$	- 13100	- 1000		5.56	0.50
Xylene	- 13100	- 12000		5.56	0.18

goes through a maximum at  $x_1 = 0.4$ . The shape of  $C_p^E$  is typical of associated components i.e. S-shape. But it is extremely small compared to  $C_p^E$  observed for alcohol mixtures. Further, the maximum occurs at higher concentration indicating that more  $C_{11}CN$  molecules are needed to "structure" the solutions. At high dilution,  $C_p^E$  is negative, corresponding to a breaking of structure existing in the pure molecules. At high dilution, the solution is less structured than the pure, the isolated molecules being too far apart to form new species.

### B. Excess Volumes

Fig 4 shows experimental  $V^E$  for dodecanitrile mixed with decane at 25°C and 40°C.  $V^E$  exhibits an S-shape curve. At low concentration of dodecanitrile  $V^E$  is positive and it is negative at higher concentration.  $V^E$  results are in harmony with those of  $C_p^E$ , in showing self-association: The positive value of  $V^E$  at low concentration arises from an expansion of the solution caused by a breaking of structure (self-association) during the mixing process.

The TK model in its original form can not be used to predict  $V^E$ , since the theory assumes  $V^E = 0$ . Hence we use Flory's theory to explain  $V^E$  curves. Equation of state parameters are given in Table 3. According to this latter theory<sup>11</sup>,  $V^E$  is a resultant of two contributions – interactional and free volume. The interactional term is given by the interaction parameter ( $X_{12}$ ) coming from  $H^E$ . It almost always contributes positively to  $V^E$ . However the free volume term is a summation of two terms: the first one being related to the difference between the degrees of expansion of the two components and the second is a function of the difference of internal pressures of the two components. The free volume term has a negative effect on  $V^E$ . It has been shown that  $V^E$  resulting from those three terms may be positive, negative or S-shaped.

Fig. 4 Experimental  $V^E$  for  $C_{11}CN + n-C_{10}$  at 25: •; 40°C: +; and octanenitrile at 25°C: o.

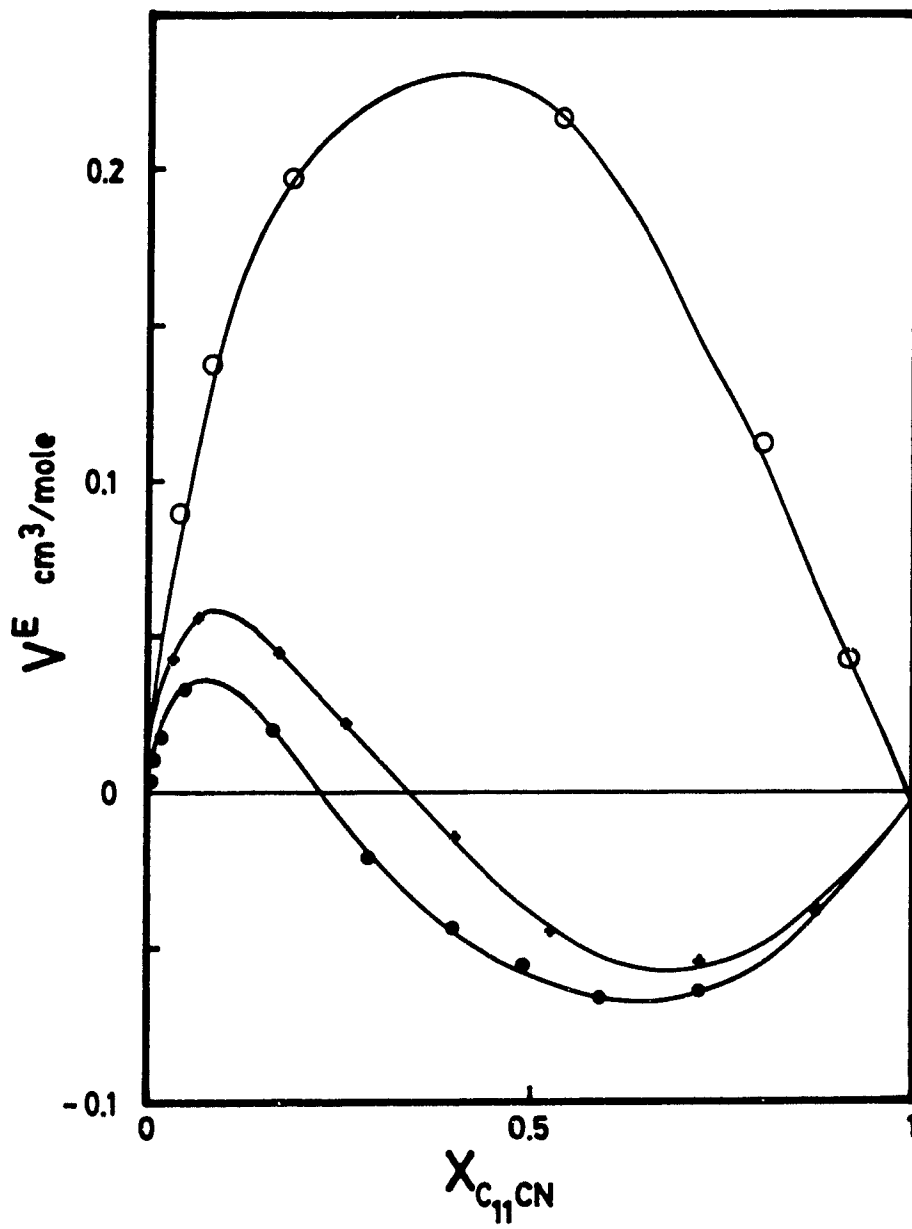


TABLE 3  
Equation of State Parameters for the Pure Components at 25°C\*

	$X_{12}$	$*10^3$ K <sup>-1</sup>	P* J/cm <sup>3</sup>	s A <sup>-1</sup>
CH <sub>3</sub> CN		0.875	477	0.93
C <sub>7</sub> CN	11.4	1.055	441	0.95
C <sub>11</sub> H <sub>23</sub> CN	4.6	1.219	561	1.00

\* data from ref. (4).

And these predictions are well fitted by experimental data<sup>11</sup> for mixtures of alkane molecules. However, structural effects due to association and order in general, are not taken into account in Flory's theory. It is then not surprising that the theory is not in good agreement with the experimental data.  $V^E(\text{theoretical})$  is predicted to be small and negative towards the concentration range, and  $dV^E/dT$  theoretical is negative. However,  $V^E(\text{experimental})$  shows an S-shape (Fig. 4), i.e., positive at low concentration of  $C_{11}CN$ , undoubtedly due to an expansion of the solution resulting from a breaking down of self-association and negative at higher concentration, due to an increase of molecular cohesion as the concentration of  $C_{11}CN$  is increased. Obviously, a third term has to be added to the Flory theory in order to predict the structural effect in  $V^E$

However, if the alkane chain of the nitrile is decreased, thus lowering the associational term compared to the interactional,  $V^E$  becomes entirely positive and leading to a good agreement with the Flory predictions.  $V^E$  for octanenitrile ( $C_7CN$ ) is shown also on Fig. (4). Furthermore, the difference in internal pressures (the  $P^*$  term) is lower leading to a lower free volume contribution. The overall  $V^E$  is then more positive than  $V^E$  for  $C_{11}CN$  mixtures. The Flory theory shows the qualitative trend even though a quantitative agreement is not observed.

## 2. Alkanenitrile + active solvent

### A. Dodecanenitrile + $CCl_4$ and + Xylene

Figs. 5 and 5a show respectively  $\phi_{C(\text{assoc})}$  for dodecanenitrile mixed with xylene and  $CCl_4$  at  $25^\circ C$  and  $C_p^E$  for  $C_{11}CN + CCl_4$ . The respective maxima have moved up and down compared to the inert. The maximum in the case of  $CCl_4$  as solvent is just slightly lower than with the inert, while a remarkable increase

Fig. 5 Comparison between  $\phi_{C(\text{assoc})}$  for  $C_{11}CN + \text{xylene}$ :  $\circ$ ; and  $+ CCl_4$  at  $25^\circ C$ :  $\times$ ;  $+ n-C_{10}$ :  $\bullet$ .

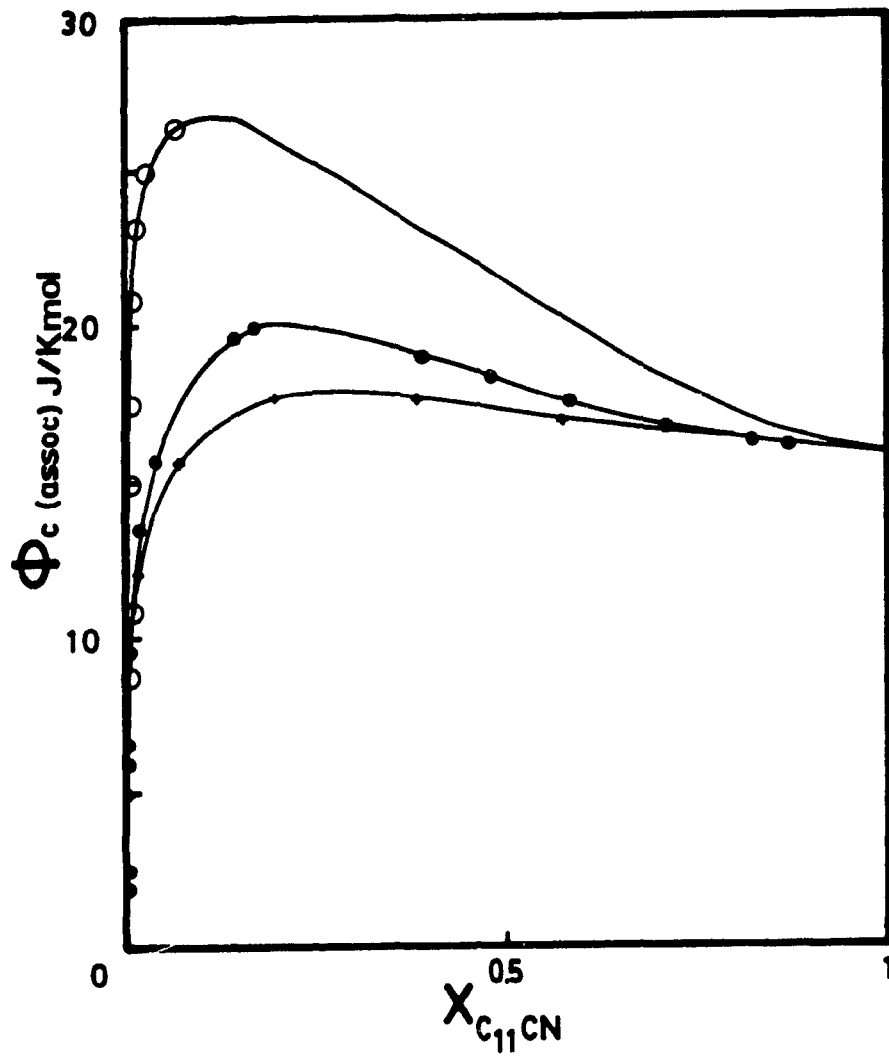
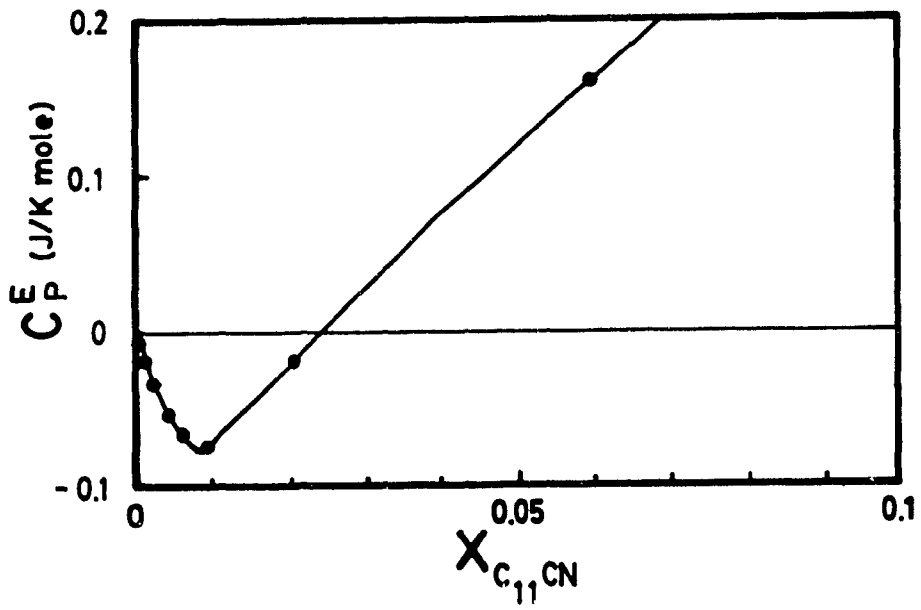
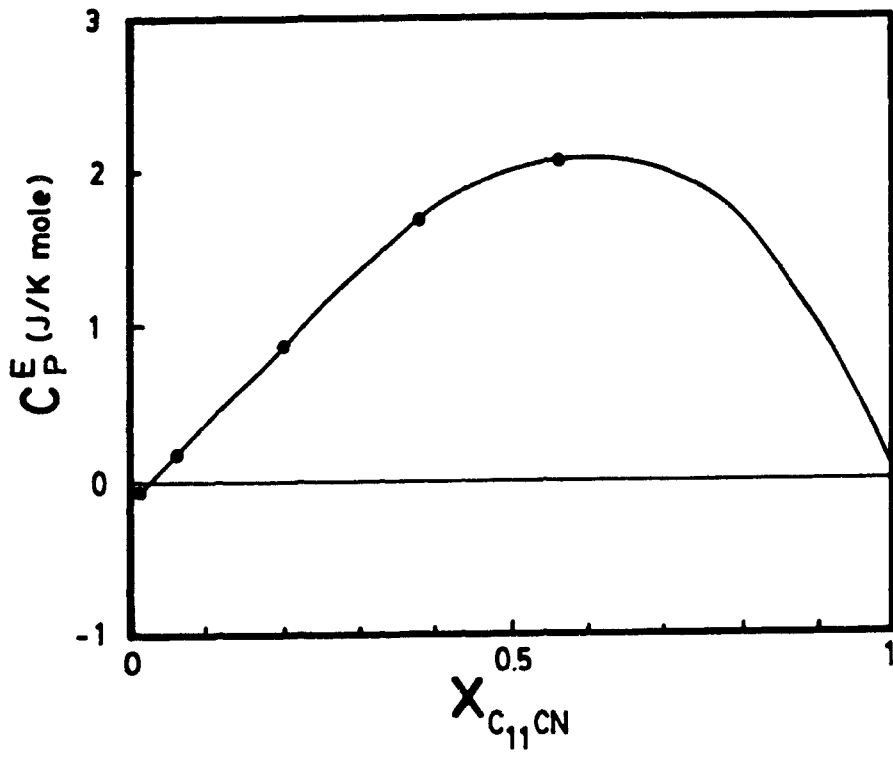


Fig. 5a Experimental  $C_p^E$  for  $C_{11}CN + CCl_4$  at  $25^\circ C$ . Lower curve: dilute concentration.



characterizes the maximum for xylene solutions. The theory gives fairly good predictions in both cases. The values of the parameters are representative of the strength of the interactions. A unique value of  $K_2$  (equilibrium constant for the self-association) is used for all of the systems while respective values of  $K_{AB}$  (complex formation equilibrium constant) are 0.5 and 0.18 for  $\text{CCl}_4$  and xylene. The heat of complex formation  $\Delta H_{AB}$  is  $-1000$  and  $-12000$  J/mole for respectively  $\text{CCl}_4$  and xylene. It is then obvious from these values that xylene is a much stronger proton acceptor than  $\text{CCl}_4$ , therefore the CN-xylene complex should be stronger than the CN-Cl one. A tentative explanation of the nature of the process involved can be made in the following way: It is believed to proceed in two steps. (1) Association of CN-CN bonds at extremely low concentration. The isolated CN molecules are associated ipso facto with the medium. (2) As the concentration of CN molecules is increased, CN-CN dimers are formed as well as the CN-xylene or CN-Cl dimers. The fitting of the theory reveals very similar values of  $\Delta H_{AB}$  for both CN-CN and CN-xylene, therefore, the competition should lead to the formation of both species. Hence, structure should be enhanced and  $\phi_{C(\text{assoc})}$  should be much higher than for the inert solvent. On the other hand, CN-Cl mixtures show a much weaker  $\Delta H_{AB}$  than for self-association ( $-1000$  compare to  $-12900$  J/mole). The competition should then favor the CN-CN species. Therefore,  $\text{CCl}_4$  will behave mostly as a "structure breaker". Structure should then break up slightly and this agrees with the values observed for both experimental and theoretical  $\phi_{C(\text{assoc})}$  which lie slightly below the curve of the inert.

Marsh et al <sup>(12)</sup> have compared heat of mixing results for nitrocompounds mixed with alkanes,  $\text{CCl}_4$  and aromatic solvents. The equimolar  $H^E$  for 2-nitropropane mixed with hexane,  $\text{CCl}_4$  and benzene are respectively 1459, 415 and 65 J/mole.  $H^E$  decreases considerably as we go from hexane to  $\text{CCl}_4$  and the decrease is smaller going from  $\text{CCl}_4$  to benzene. The authors suggested the formation of a

complex between nitropropane and  $\text{CCl}_4$  and benzene. However, the species formed with benzene are stronger than with  $\text{CCl}_4$ . Indeed, their conclusion is in agreement with ours.

### B. Acetonitrile + $\text{CCl}_4$

Figs. 6 and 7 show  $C_p^E$  and  $V^E$  at  $25^\circ\text{C}$  and  $40^\circ\text{C}$  for acetonitrile +  $\text{CCl}_4$ , with  $C_p^E$  maxima at respectively 4.05 and 4.80  $\text{J/K mol}^{-1}$ ,  $dC_p^E/dT$  is therefore very small. Furthermore,  $C_p^E$  values are rather larger than values observed for  $\text{C}_{11}\text{CN} + \text{CCl}_4$  whose maximum  $C_p^E$  is of 2.1  $\text{J/K mol}$ .  $C_p^E$  is positive over all of the concentration range, even at high dilution. This seems to suggest that the destruction of  $\text{CN-CN}$  bonds at very low concentration is compensated by the formation of a  $\text{CN-Cl}$  bond and indeed, structure is enhanced. As the concentration increases both  $\text{CN-CN}$  and  $\text{CN-Cl}$  dimers are formed leading to  $C_p^E$  values higher than in the inert solvent. Structure in this case is a resultant of both self-association and complex formation. Acetonitrile<sup>6</sup> has been suggested to form dimers in the pure state.  $\phi_C$  exhibits almost a flat curve with a small maximum at low concentration. The sharp peak currently observed for  $\phi_C$  at low concentration for associated systems has disappeared. This flatness of  $\phi_C$  should be due to interactions taking place between the  $\text{CN}$  and  $\text{Cl}$  groups and this suggests that  $\text{CCl}_4$  interacts better with a shorter nitrile than a longer one where the long alkyl chain attached to the polar group might lower the donating capability of the nitrile or simply by diluting the  $\text{A-B}$  interaction.

$V^E$  exhibits a positive maximum at very low concentration, due to self-association but as the concentration increases  $V^E$  becomes more and more negative which could be attributed to the complex formed between acetonitrile and  $\text{CCl}_4$ . The Flory theory predicts this negative  $V^E$  at high concentration, if a negative  $X_{12}$  is fitted, reflecting in fact the formation of a complex. Nevertheless, the theory

does not reproduce the positive  $V^E$  observed at low concentration. This is not surprising, since as pointed earlier, the theory does not take account of self-association effect.

Fig. 6 Experimental  $C_p^E$  for acetonitrile +  $CCl_4$  at 25: •; and 40°C: +.

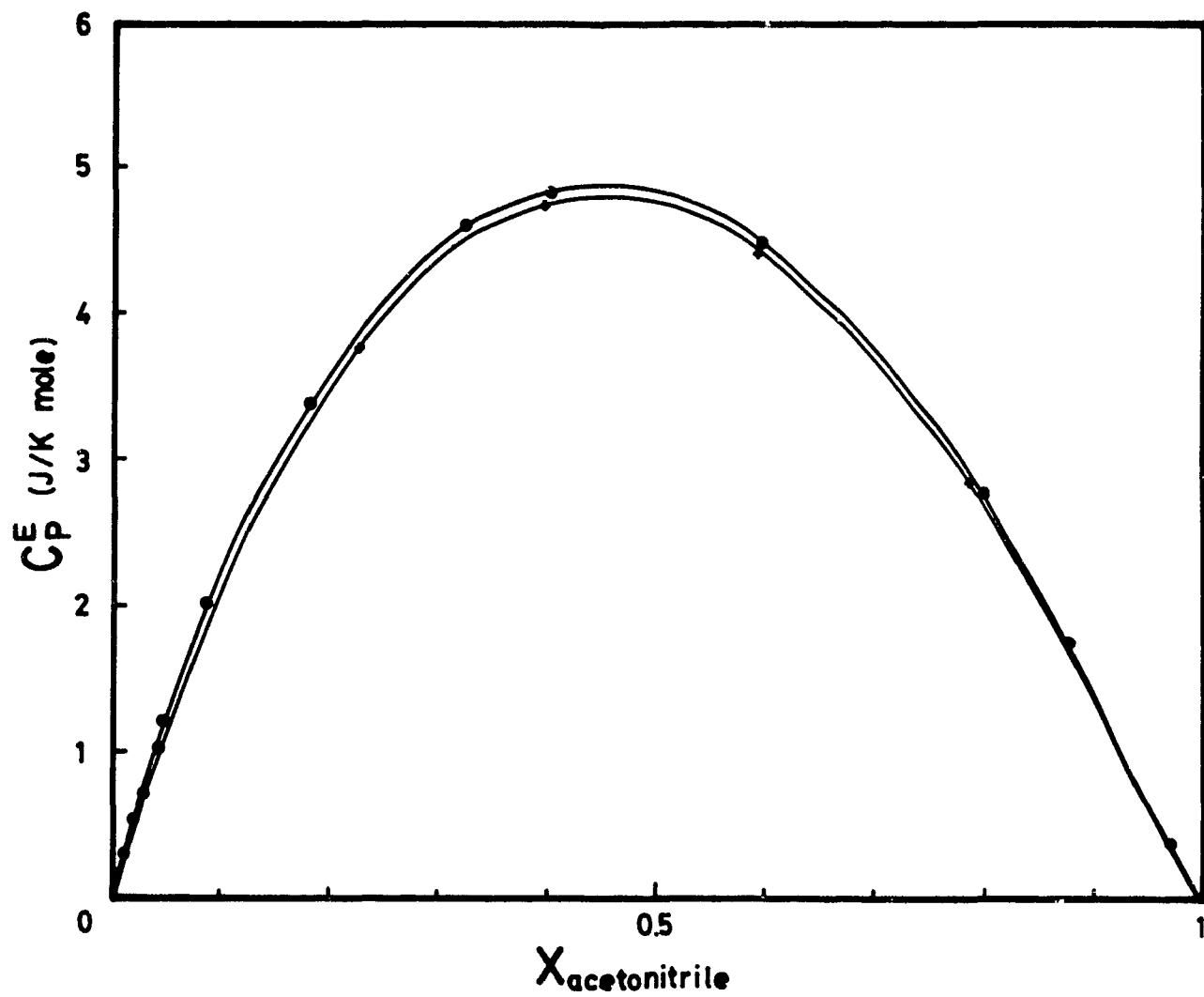
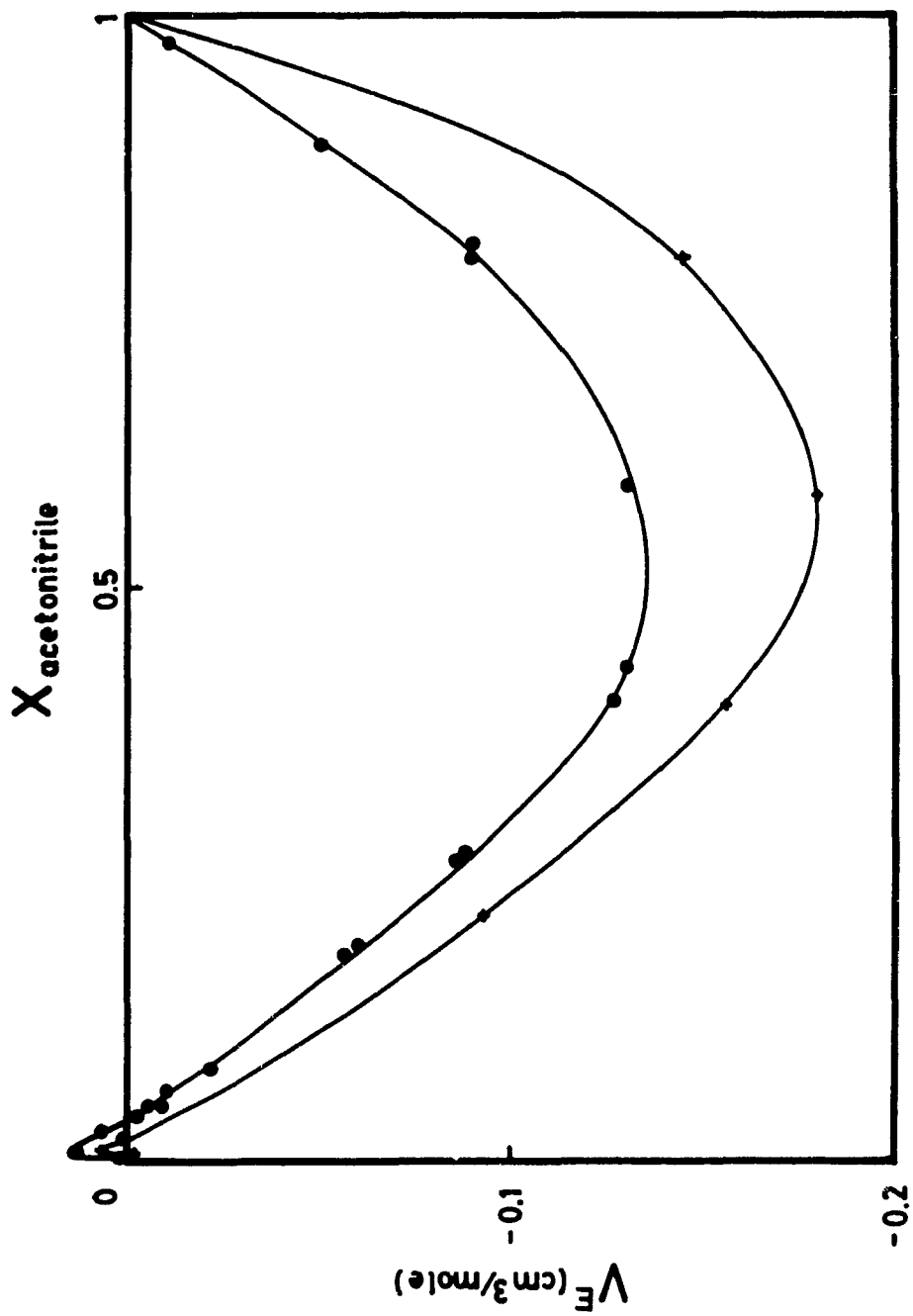


Fig. 7 Experimental  $V^E$  for acetonitrile +  $\text{CCl}_4$  at 25: •; and 40°C: +.



**REFERENCES**

1. S.N. Bhattachayya and D. Patterson, *J. Phys. Chem.*, 83, 2979, 1979.
2. H. Sarto, Y. Tanaka, S. Nogata, and K. Nukada, *Can. J. Chem.*, 51, 2118, 1973.
3. H. Fujiwara, T. Kahaba, Y. Yamazaki and Y. Sasaki. *Chem. Soc. J. Faraday Trans. I*, 75, 79, 1979.
4. a) Q. Valero, M. Gracia and C.G. Losa, *J. Chem. Thermodyn.*, 15, 985, 1983.  
b) R. Gonzalez, F. Murrietta-Guevara and A. Trejo, *J. Sol. Chem.*, 15, No. 10, 791, 1986.
5. R. Anderson, R. Cambio and J.M. Prausnitz, *A.I.Ch. J.*, 66, 1962.
6. T.A. Reimer and M. Blander, *J. Phys. Chem.*, 81, No. 9, 857, 1977.
7. L.A. Curtiss, D.J. Frurip and M. Blander, *J. Phys. Chem.*, 86, 1120, 1982.
8. H. Kehiaian and A. Treszczanowicz, *Bull. Soc. Chem. France*, 5, 1561, 1969.
9. L. Andreoli-Ball, D. Patterson, M. Costas and M. Caceres-Alonso, *J.C.S. Faraday I*, in press.
10. a) P. Picker, J.P. Leduc, P.R. Philip and J.-E. Desnoyers, *J. Chem. Thermodyn.*, 3, 63, 1971.  
b) J.L. Fortier, G.C. Benson, and P. Picker, *J. Chem. Thermodyn.*, 8, 21, 1976.  
c) J.L. Fortier and G.C. Benson, *J. Chem. Thermodyn.*, 8, 411, 1976.
11. a) H. Tra Van and D. Patterson, *J. Sol. Chem.*, 11, No. 11, 1982.  
b) M. Costas and D. Patterson, *J. Sol. Chem.*, 11, 807, 1982.
12. K. Marsh, *J. Chem. Thermodyn.*, 17, 600, 1985.

APPENDIX 5

Tables of Results

TABLE 4  
 Excess heat capacities and excess volumes of dodecanenitrile +  
<sub>1</sub>  
 n-decane at T = 25°C  
<sub>2</sub>

$x_1$	$C_p^E$ (J/K mol)	$V^E$ (cm <sup>3</sup> /mol)
0.0010	–0.01	0.0031
0.0020	–0.03	0.0009
0.0051	–0.06	0.0005
0.0069	–0.08	
0.0093	–0.11	0.0186
0.0097	–0.09	0.0020
0.0173	–0.11	0.0158
0.0437	–0.01	0.0337
0.1590	0.70	0.0206
0.1440	0.58	0.018
0.4023	1.33	–0.0434
0.4891	1.26	–0.0531
0.5873	1.10	–0.0655
0.7240	0.83	–0.632
0.8750	0.38	–0.0369

TABLE 5  
 Excess heat capacities and excess volumes of  
 dodecanenitrile + n-decane at  $T = 40^{\circ}\text{C}$   
<sub>1</sub>                      <sub>2</sub>

$x_1$	$C_p^E$ (J/K mol)	$v^E$ ( $\text{cm}^3/\text{mol}$ )
0.002	-0.03	0.0216
0.0051	-0.06	0.0223
0.0070	-0.07	0.0220
0.009	-0.07	0.0218
0.0129	-0.08	0.0208
0.0205	-0.08	0.0240
0.0398	-0.03	0.0429
0.0673	0.10	0.0580
0.1700	0.72	0.0472
0.2565	1.17	0.0214
0.3991	1.42	-0.0141
0.5304	1.35	-0.0439
0.7223	0.94	-0.552
0.8833	0.53	-0.0376

TABLE 6  
 Excess heat capacities and excess volumes of dodecanenitrile +  $\text{CCl}_4$  at  $25^\circ\text{C}$

$x_1$	$C_p^E$ (J/K mol)	$V^E$ ( $\text{cm}^3/\text{mol}$ )
0.001	-1.59	-0.0034
0.0024	-0.03	-0.0032
0.0046	-0.05	
0.0064	-0.07	-0.002
0.0093	-0.07	0.0127
0.0209	-0.02	0.0184
0.0603	0.17	0.0797
0.1994	0.92	0.1849
0.3811	1.72	0.3221
0.5723	2.13	0.5021

TABLE 7  
Heat capacities and excess volumes of dodecanenitrile + xylene at 25°C

$x_1$	$C_p^E$ (J/K mol)	$V^E$ (cm <sup>3</sup> /mol)
0.0007	—	–0.0019
0.0010	—	–0.0024
0.0026	–0.001	–0.0071
0.0046	0.01	–0.0109
0.0067	0.03	–0.0153
0.0104	0.08	–0.0236
0.0105	—	–0.0235
0.0246	0.23	–0.0471
0.0710	0.76	–0.1289

TABLE 8  
Excess heat capacities and excess volumes of octanenitrile + n-decane at 25°C

$x_1$	$C_p^E$ (J/K mol)	$V^E$ (cm <sup>3</sup> /mol)
0.0436	0.06	0.0811
0.0770	0.47	0.1203
0.1698	1.40	0.1906
0.2601	1.81	
0.3958	3.53	0.7991
0.5338	2.28	0.2115
0.7957	1.24	0.1098
0.9150	0.51	0.0426

TABLE 9  
 Excess heat capacities and excess volumes of acetonitrile +  $\text{CCl}_4$  at  $25^\circ\text{C}$

$x_1$	$C_p^E$ (J/K mol)	$v^E$ ( $\text{cm}^3/\text{mol}$ )
0.0042	0.08	0.0045
0.0134	0.31	0.0106
0.0240	0.53	0.0009
0.0327	0.73	0.0060
0.0467	1.83	0.2528
0.4288	1.03	-0.0038
0.0498	1.21	-0.0067
0.0892	2.03	-0.0237
0.1822	3.43	-0.0583
0.3264	4.54	-0.1275
0.4070	4.80	-0.1278
0.5936	4.49	-0.1329
0.8045	2.76	-0.0913
0.8841	1.82	-0.0543
0.9706	0.47	-0.0180

TABLE 10  
Excess heat capacities and excess volumes for acetonitrile + CCl<sub>4</sub> at 40°C

$x_1$	$C_p^E$ (J/K mol)	$v^E$ (cm <sup>3</sup> /mol)
0.0042	—	0.0066
0.0078	0.15	-0.0008
0.2261	3.79	-0.0921
0.4009	4.77	-0.1566
0.5946	4.43	-0.1796
0.7871	2.87	-0.1425

PART III

CHAPTER 6

LCST AND SPECIFIC INTERACTIONS IN POLYMER-SOLVENT AND  
POLYMER-POLYMER MIXTURES

## INTRODUCTION

As commercial synthetic polymers continue to grow both in numbers and in variety, new applications are constantly appearing. Synthetic polymers find their main uses in various fields such as fibers, films, surface coatings, model objects, construction materials, adhesives etc. Growth in these fields is associated with a need of better understanding of the physical properties of mixtures containing such materials.

The last decades have seen a remarkable development in the study of the physical properties of polymers in both the pure state and solution<sup>1</sup>. Increased interest has been promoted not solely by the wide range of applications but also by the availability of new theories such as Flory–Huggins<sup>2</sup> or Prigogine–Flory theory<sup>3</sup> which interpret either the nature of the interactions involved when a polymer molecule is mixed with a solvent or with another polymer. At least three effects are known to determine the stability of a polymer solution: (1) an energetic term arising from any differences in contact energy or intermolecular forces between the two species; (2) a combinatorial entropy of mixing; (3) a third effect due to the solvent liquids; (4) a fourth effect probably exists arising from the correlation of orientational order (CMO) between the polymer segments in the pure state.

According to the second law of thermodynamics any process that proceeds spontaneously must lower the Gibbs free energy of the system. Thus, a negative  $\Delta G_M$  favours a homogeneous solution (stable), while a positive value or negative curvature of  $\Delta G_M$  against composition indicates an unstable solution which tends to phase separate.

Many binary liquid mixtures which form a single homogeneous phase at high temperature possess an upper critical solution temperature (UCST) below which phase separation occurs.

In simple binary mixture, the UCST results from a competition between the

interparticle interactions acting against mixing and the entropy of mixing which favours mixing. As  $T$  is lowered the effect of entropy decreases and the UCST occurs. However, mixtures containing highly directionally specific, attractive interparticle forces (such as hydrogen-bonds or dipolar forces) can exhibit miscibility at low temperature. This leads to a closed-loop temperature-composition ( $T$ - $x$ ) phase diagram (Fig. 1) and an associated lower critical solution temperature (LCST) below which a single homogeneous phase exists. Fig. 1 shows a typical phase diagram observed when water is the solvent. Aqueous systems often exhibit an LCST at low temperature and as the temperature is raised a UCST is observed and the solution is homogeneous again. The LCST in aqueous systems may be due to specific interactions or associated with water structure in solution<sup>4</sup>, i.e. to "iceberg" formation. The UCST and LCST are not confined to mixtures of small molecules. They are even more widely observed for polymer mixtures, although the typical LCST in polymer solutions is usually observed at extremely high temperature. It has been observed<sup>4</sup> that all polymer solutions can phase separate either by lowering the temperature until a UCST is reached or by raising  $T$  up to an LCST which occurs usually above the boiling point of the solvent. Fig. 2 shows schematically the typical phase diagram of a polymer-solvent mixture, where a region of miscibility is comprised between two regions of immiscibility. It has been shown<sup>5</sup> that the LCST, in this case, is due to free volume dissimilarity between the polymer and the solvent. Moreover, the LCST is also often observed in a polymer-polymer mixture. Fig. 3 shows the typical phase diagram of a polymer-polymer mixture. A one-phase region is observed at low  $T$  and at the LCST, the solution phase separates into two different phases. The LCST value varies with the strength of the interactions involved.

Several systems have been reported in the literature showing an LCST, which occurs at a low temperature but where the polymer (H-bonded or polar) is in solution in non-aqueous media. A few systems are reported in Table 1. They all exhibit a low

Fig. 1 Closed-loop temperature-composition (T-x) phase diagram.

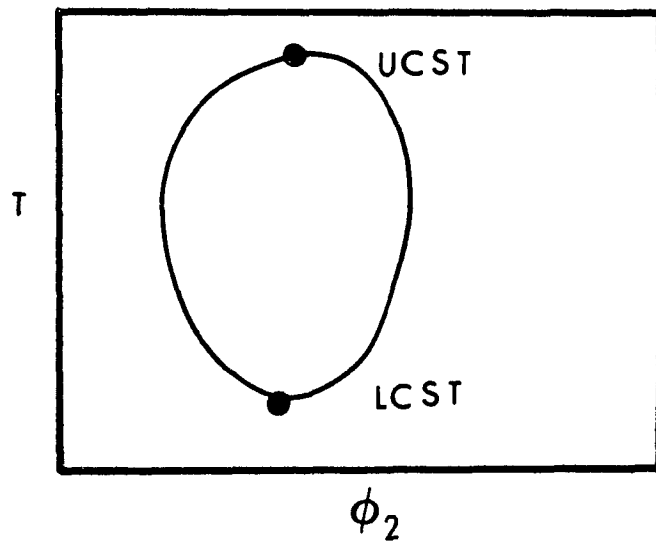


Fig. 2 Schematic phase diagram for a polymer-solvent system.

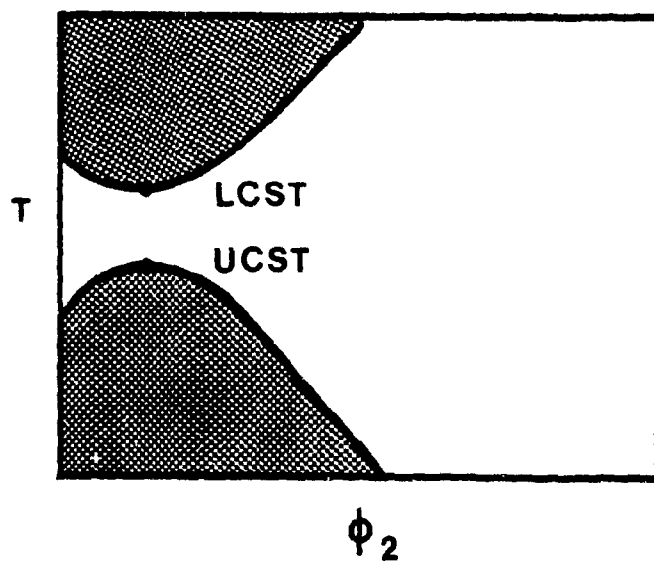
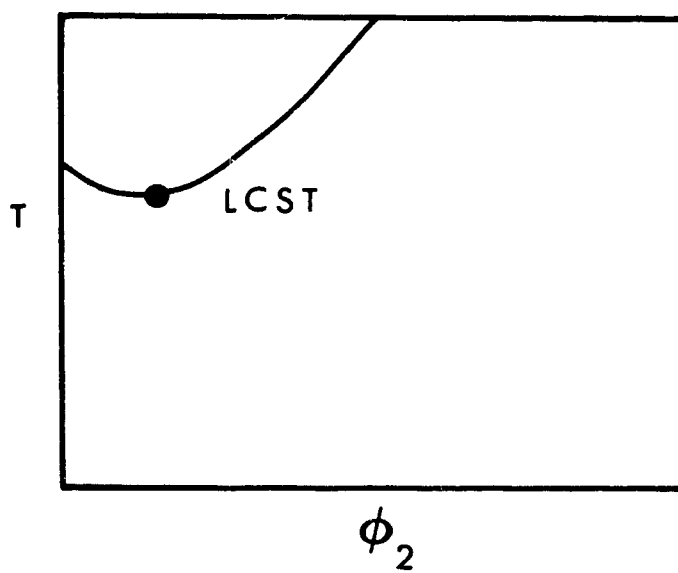


Fig. 3 Schematic representation of a typical phase diagram of a polymer-polymer system.



temperature LCST. The polymer is usually a polar or H-bonded component.

The purpose of this work is to study the kind of structure created by specific interactions in polymer systems, either polymer-solvent or polymer-polymer, when the solvent is either a small molecule or another polymer. Structure will be associated to the occurrence of an LCST in the solution. Through this work, the origin of the low temperature LCST will be discussed in both polymer-solvent and polymer-polymer mixtures. A mathematical model will be suggested for the interpretation of the role of the LCST in polymer-polymer compatibility and polymer-solvent interactions.

TABLE 1

Several systems exhibiting low temperature LCST

Components	LCST
Poly(ether sulfone) + $\text{CHCl}_3$	$-10^\circ\text{C}^{\text{a}}$
Poly(ether sulfone) + $\text{CH}_2\text{Cl}_2$	$20^\circ\text{C}^{\text{a}}$
Poly(methacrylonitrile) + butanone	$7^\circ\text{C}^{\text{b}}$
Poly(acrylic acid) + dioxane	$29^\circ\text{C}^{\text{b}}$
Poly(acrylonitrile) + toluene	$< 0^\circ\text{C}^{\text{c}}$

<sup>a</sup> From D.A. Blackadder and H. Ghavamikia, *Polymer* 19, 255, 1978.

<sup>b</sup> From A.R. Schultz and P.J. Flory, *J. Polym. Sci.* 15, 231, 1955.

<sup>c</sup> From Banderet, private communication

## THEORETICAL MODEL FOR THE PREDICTION OF THE LCST

Several theories or mathematical models<sup>6</sup> have been proposed for the interpretation of polymer solution stability and the LCST occurring at both low and high temperatures. While some theories are very sophisticated and mathematically complex, most of them, however, are based on the Flory-Huggins or Flory-Prigogine theories of polymer solution. Although quite simple, the Flory or extended Flory theory provide yet a good interpretation of simple systems such as those governed by dispersion forces only. Improvement of the theories is required, however, for more complicated mixtures i.e. strongly interacting components. The theories fail to predict the low LCST typical of specific interactions. The interactional term, in this case, favors mixing and the  $\chi$  parameter should be modified in order to take into account this new contribution.

Recently Goldstein<sup>7</sup> has proposed a simple approach which includes the possibility of hydrogen-bonding interactions. The model is based on the Flory-Huggins theory i.e. it is only interactional. The model suffers of the same restrictions as the Flory-Huggins theory and therefore the predictions are only qualitative.

### 1. Goldstein model

Two different energy levels of interactions are considered: The bonded and non-bonded states. The free energy  $\chi$  parameter is the summation of the free energy associated with both states. Based on the Flory-Huggins theory, the model expresses  $\chi_{12}$  as  $W/k_B T$  where  $W$  is the exchange interaction energy and is  $T$ -dependent. The free energy of interaction is given as:

$$\Delta G_M = -k_B T \ln Z_{12} \quad (1)$$

where

$$Z_{12} = e^{-BF_{12}^*} + e^{-BF_{12}^0} \quad (2)$$

$F^*$  and  $F^0$  represent the free energies associated with the bonded and non-bonded configurations;  $B$  being equal to  $\frac{1}{k_B T}$ . Taking into account eqn. 2, the exchange interaction energy,  $W$  is rewritten as follows:

$$W = (E_{11}^0 - TS_{11}^0) + (E_{22}^0 - TS_{22}^0) + 2k_B T \ln Z_{12} \quad (3)$$

Where  $E_{11}^0$  and  $E_{22}^0$  represent the standard state of energy associated with these respective 1-1 and 2-2 pair contacts;  $S_{11}^0$  and  $S_{22}^0$  are standard state entropy associated with 1-1 and 2-2 pairs;  $Z_{12}$  being the partition function.

The entropy term ( $S_{11}^0 + S_{22}^0 - 2S_{12}^0$ ) is negligible. The critical  $\chi_{12}$  as given by Goldstein can be expressed by eqn. 4

$$\frac{1}{C} \chi_{crit} = x - \ln(1 + \exp(y + Z)) \quad (4)$$

where  $C$  is the coordination number,

$$x = -\frac{B}{2} (E_{11}^0 + E_{22}^0 - 2E_{12}^0) \quad (5)$$

$$y = B (E_{12}^0 - E_{12}^*) \quad (6)$$

$$Z = (S_{12}^* - S_{12}^0) / k_B \quad (7)$$

and 
$$\chi_{\text{crit}} = (1 + N^{1/2})^2 / 2N \quad (8)$$

This model presents interesting features by allowing specific interactions in the  $\chi$  parameter. But, it does not take into account the free volume dissimilarity contribution which is an important contribution in a polymer–solvent mixture.

However, more realistic results may be expected, if the Goldstein approach of a T dependent and different–configuration–energy W is used with the possibility of a free volume change i.e. using the Prigogine–Flory theory.

## 2. New model for LCST in hydrogen–bonding polymer solutions

The  $\chi$  parameter is considered as a free energy interaction parameter i.e.

$$\begin{aligned} \chi_{\text{total}} = \chi_G &= (\chi_{\text{H(interac)}} + \chi_{\text{H(FV)}}) + (\chi_{\text{S(interac)}} + \chi_{\text{S(FV)}}) \\ &= \chi_{\text{G(interac)}} + \chi_{\text{G(FV)}} \end{aligned} \quad (9)$$

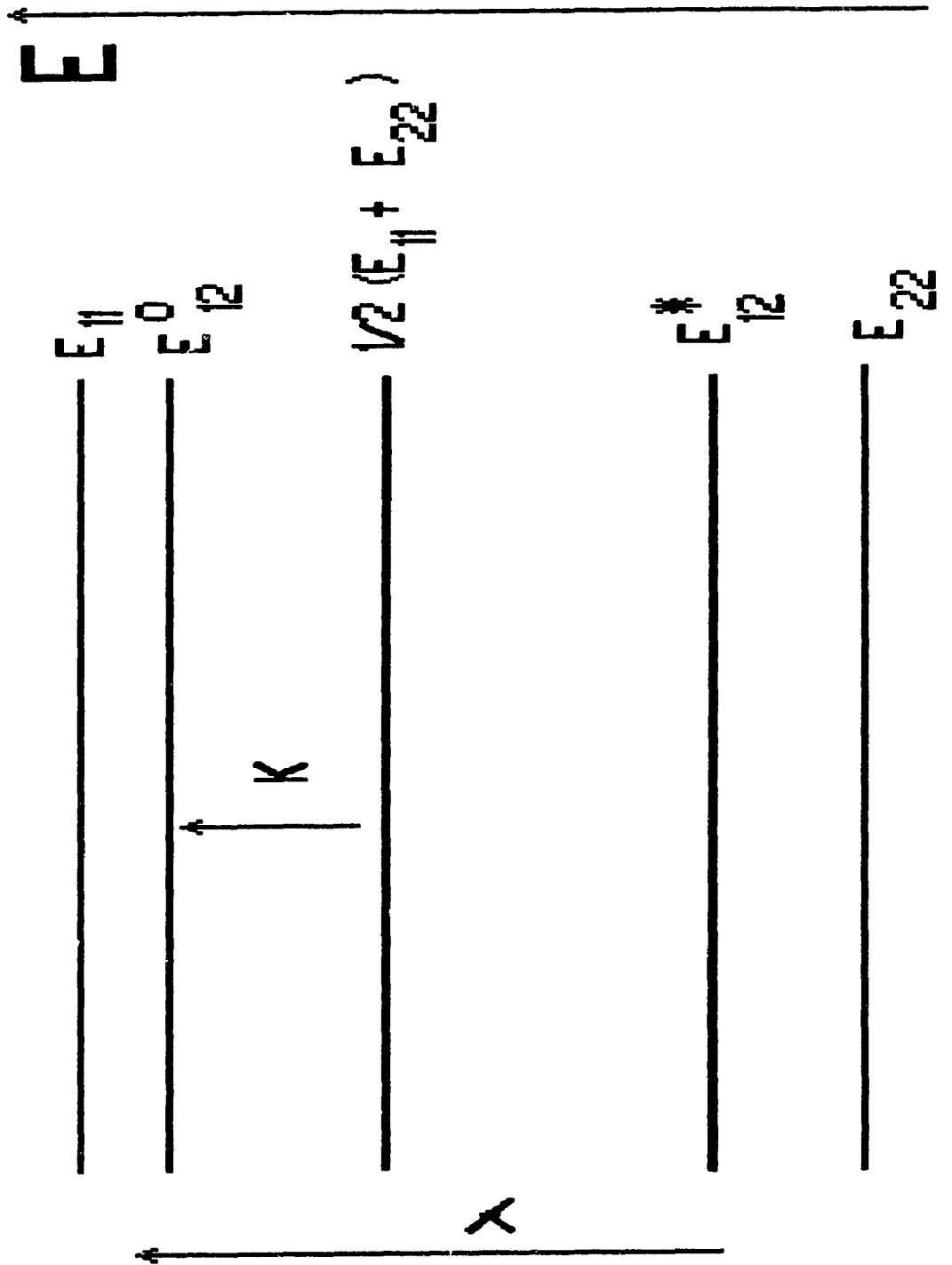
### A. The interactional term

The free energy of mixing is given as the difference between the free energy of the bonded and the non–bonded configurations:

$$\frac{\Delta G_M}{RT} = \frac{G^0 - G^*}{RT} = \frac{(E^0 - E^*)}{RT} - \frac{(S^0 - S^*)}{R} \quad (10)$$

Different states of energy can be considered depending upon the configuration of the components. On fig. 4, the lowest energy level corresponds to the energy of pure

Fig. 4 Schematic representation of the energy diagram of the pure components and their mixtures.



component 2 while the highest level refers to the energy of pure component 1.  $E_{12}^*$  represents the bonded energy ("good interaction") while  $E_{12}^0$  refers to the non-bonded energy ("bad interaction"). The interchange energy  $\Delta W$  is the energy change necessary to break 1-1 and 2-2 contacts and form 1-2 contacts

$$\Delta W = E_{12}^0 - \frac{1}{2}(E_{11}^0 + E_{22}^0) \quad (11)$$

Four adjustable parameters are considered:

1. The first one,  $K$ , which has the dimension of  $T$ , is mainly the interchange parameter. It is given as:

$$K = \Delta W/R \quad (12)$$

Where  $R$  is the gas constant.

2. The second parameter,  $\lambda$ , is characteristic of the specific interaction.  $\lambda$  is given as the ratio of the difference between the bonded and non-bonded energy over the interchange energy

$$\lambda = \frac{E_{12}^0 - E_{12}^*}{\Delta W} \quad (13)$$

$\lambda$  can be simplified to eqn. 14, taking into account eq. 13

$$\lambda = \frac{E_{12}^0 - E_{12}^*}{R K} \quad (14)$$

Where  $R$  is the gas constant. The bigger  $\lambda$ , the higher the specific interaction.

Both  $\lambda$  and  $K$  are energetic terms.

3. The third parameter,  $z$ , is an entropic term. It is given as the non-dimensional difference between the entropy of the bonded and non-bonded component configurations

$$-z = \frac{S_{12}^0 - S_{12}^*}{R} \quad (15)$$

4. The fourth parameter,  $T^0$ , is the ratio between energetic and entropic terms

$$T^0 = \frac{E^0 - E^*}{S^0 - S^*} \quad (16)$$

$T^0$  is a fixed parameter for a given system.  $z$  can also be calculated from eqn. (16). In this case, it is given as:

$$-z = \frac{K \lambda}{T^0} \quad (17)$$

and therefore  $z$  is considered as a characteristic temperature.

At the critical conditions,  $\chi_c$  interactional can be given by equation 4. However, the number of possible sites of interactions on each molecule is taken into account and equation 4 becomes equation 18, where  $C$  is the coordination number and  $x$  being  $\frac{\Delta W}{RT}$  or simply  $x = \frac{K}{T}$ . The global interactional part of the free energy is given as

$$\frac{\chi_c}{C} = x - \ln(1 + e^{\lambda x + z}) + \ln 2 \quad (18)$$

Where  $C \ln 2$  is the entropy contribution to the  $\chi_G$  (free energy (interaction)).  $C \ln 2$  takes into account the number of possible sites of interaction on each molecule, where  $C$  is the coordination number.

From eqn. 18,  $\chi_H$  and  $\chi_S$  can be derived since ( $\chi_G = \chi_H + \chi_S$ ).  $\chi_H$  is also given by

$$\chi_H = -T \frac{\partial \chi_G}{\partial T} \quad (19)$$

therefore,

$$\frac{\chi_{H(int)}}{C} = \frac{\Delta W}{R} \left[ 1 - \frac{1}{1 + e^{-(K \lambda / T + z)}} \right] \quad (20)$$

$$\chi_{S(int)} = \chi_{G(int)} - \chi_{H(int)} \quad (21)$$

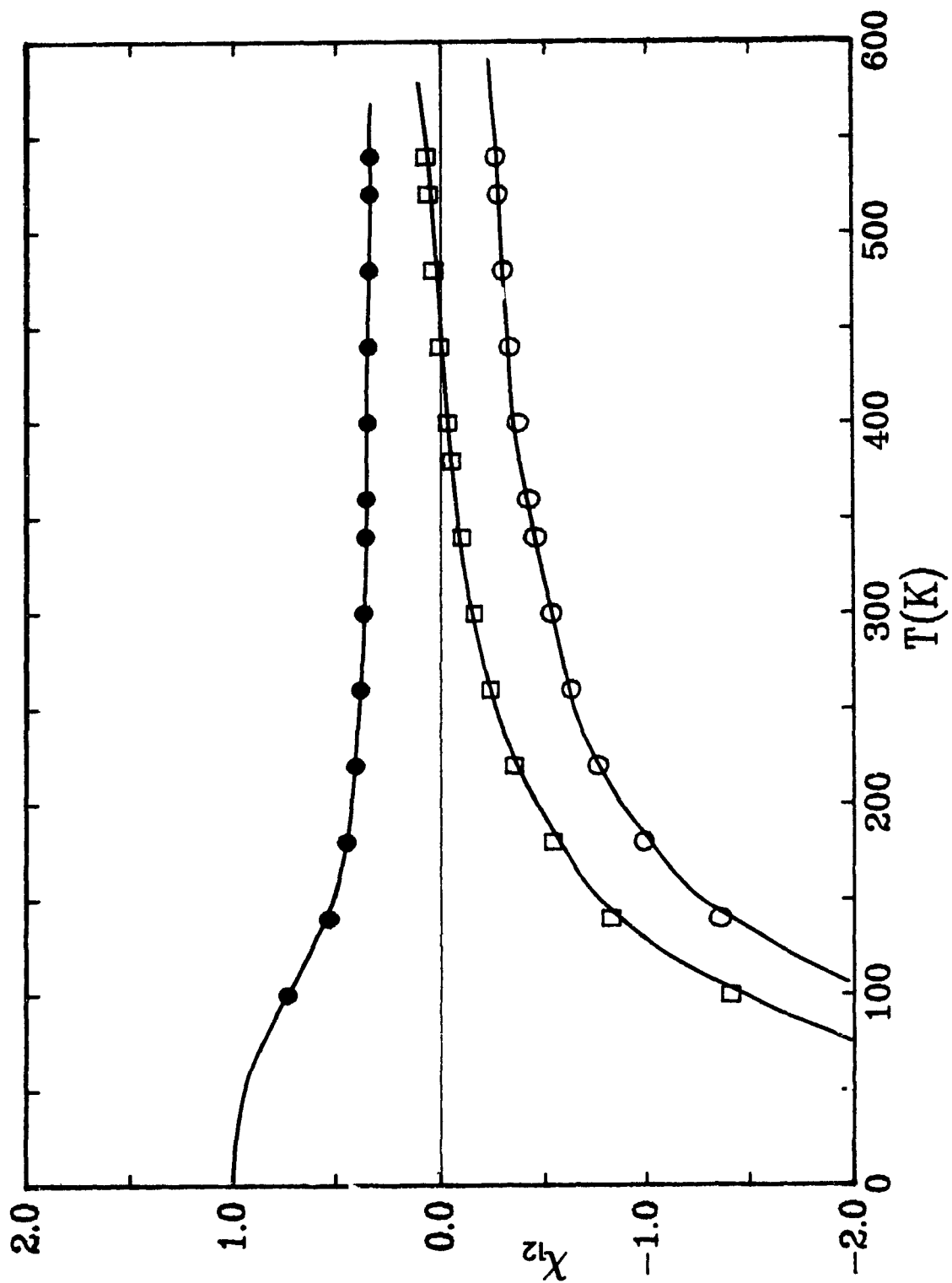
$$\begin{aligned} \frac{\chi_{S(int)}}{C} = & -\ln \left[ 1 + e^{\frac{K \lambda}{T} + z} \right] \\ & + \frac{K \lambda T}{1 + e^{-(K \lambda / T + z)}} + \ln 2 \end{aligned} \quad (22)$$

Fig. 5 shows  $\chi_{G(int)}$ ,  $\chi_{H(int)}$  and  $\chi_{S(int)}$  as a function of  $T$ , with the adjustable parameters  $K, \lambda, z, T^0$  having the respective values of: 400, 1.45, -1, 600.

#### B. The free volume term

Given by Bardin et al<sup>8</sup>, the free volume term is defined by eqn. 23, according to

Fig. 5 Theoretical interactional parameter:  $\square$  total  $\chi_{G(int)}$ ;  $\circ$   $\chi_{H(int)}$ ;  $\bullet$   $\chi_{S(int)}$  as a function of T.



the Prigogine-Flory theory

$$\chi_{(FV)} = \frac{1}{2} \bar{C}_p (\bar{P}, \bar{T}) \tau^2 C_1 \quad (23)$$

Where  $\bar{C}_p$  is the reduced heat capacity or configurational  $C_p$  of the solvent;  $\tau^2$ , a temperature independent parameter, characteristic of the free volume difference which is determined from the temperature reduction parameter  $T_1^*$  of component 1 and 2

$$\tau^2 = \left[ 1 - \frac{T_1^*}{T_2^*} \right]^2 \quad (24)$$

The  $C_1$  parameter of the solvent is defined according to eqn. 25, based on the equation of state parameters of the solvent

$$C_1 = \frac{1}{R} \frac{P_1^* V_1^*}{T_1^*} \quad (25)$$

The equations of state parameters,  $P^*$ ,  $V^*$ ,  $T^*$  are calculated as following

$$V^* = \frac{M}{\rho} \left[ 1 + \frac{\alpha T}{3(1 + \alpha T)} \right]^{-3} \quad (26)$$

Where  $M$  is the molecular weight of the solvent,  $\rho$  the density of the solvent, and  $\alpha$  the thermal expansion coefficient of the solvent.  $P^*$  is usually obtained from the isothermal compressibility  $\beta_T$  which is, in turn, calculated from  $\beta_s$  obtained from velocity of sound measurement

$$P^* = \frac{\alpha T \bar{V}^2}{\beta_T} \quad (27)$$

where

$$\beta_T = \beta_s + \frac{\alpha^2 VT}{C_p} \quad (28)$$

where  $\alpha$  is the expansion coefficient,  $V$  the molar volume of the pure component,  $C_p$  its molar heat capacity,  $\beta_s$  the isentropic compressibility and given as  $\frac{1}{u^2\rho}$ ,  $u$  being the velocity of sound, and  $\rho$  the density of the solvent.

$$T^* = T / \frac{\bar{V}^{4/3}}{\bar{V}^{1/3} - 1} \quad (29)$$

Where  $\bar{V}$  is the reduced volume given by eqn. 30

$$\bar{V} = \left[ \frac{1 + \alpha T}{3(1 + \alpha T)} \right]^3 \quad (30)$$

Combining eqns. 23 to 30,  $C_{p1}$  may be expressed as follows:

$$C_p^{-1}(\bar{P}, \bar{T}) = (\bar{V}^{-1} \bar{T})(1 - \bar{V}^{-1/3}) \quad (31)$$

The expression of the free volume contribution to the  $\chi$  parameter then becomes:

$$\chi_{FV} = \frac{1}{2R} \frac{P_1^* V_1^*}{T_1^*} \left[ \frac{T_2^* - T_1^*}{T_2^*} \right]^2 \left[ \frac{1}{4/3 \bar{V}^{-1/3} - 1} \right] \quad (32)$$

$\bar{V}^{1/3}$  may be obtained from

$$\bar{T} = \frac{T}{T^*} = \frac{\bar{V}^{1/3} - 1}{\bar{V}^{4/3}} \quad (33)$$

The free volume contribution is split into two contributions: energetic and entropic. Knowing that  $\chi_H = -T \frac{\partial \chi}{\partial T}$  and  $\chi_S = \chi_G - \chi_H$  or  $\chi_S = \frac{\partial(\chi T)}{\partial T}$ , expressions for  $\chi_{H(FV)}$ , and  $\chi_{S(FV)}$  can be derived:

$$\chi_{H(FV)} = \frac{-\frac{C_1 \tau^2}{2} (4/9 \bar{V}^{1/3} - 1)}{\bar{V}^{2/3} (4/3 \bar{V}^{-1/3} - 1)^3} \quad (34)$$

$$\chi_{S(FV)} = \frac{C_1 \tau^2}{2} \frac{\bar{V}^{2/3} - (20/9) \bar{V}^{1/3} + 4/3}{\bar{V}^{2/3} (4/3 \bar{V}^{-1/3} - 1)^3} \quad (35)$$

Fig. 6 shows the variation of  $\chi_{G(FV)}$ ,  $\chi_{H(FV)}$  and  $\chi_{S(FV)}$  as a function of T.

Combining eqns. 22 and 35, the expression for the total free energy  $\chi$  parameter then becomes:

$$\frac{\chi_C}{C} = x - \ln(1 + e^{(\lambda x + z)}) + \ln 2$$

$\longleftarrow$  interactional  $\longrightarrow$

$$+ \frac{1}{2R} \left[ \frac{P_1^* V_1^*}{T_1^*} \right] \left[ \frac{T_2^* T_1^*}{T_2^*} \right]^2 \left[ \frac{1}{4/3 \bar{V}_1^{-1/3} - 1} \right]$$

$\longleftarrow$  Free volume  $\longrightarrow$

(36)

Fig. 7 shows the variation of the  $\chi_{total}$ ,  $\chi_{(int)total}$  and  $\chi_{(FV)total}$  with T.

The intersection of  $\chi$  with the critical line gives the low T LCST, then the UCST as T increases. As T increases further the free volume LCST is reached.

Fig. 6 Theoretical free volume  $\chi$  parameter: ■  $\chi_{G(FV)}$ ; ○  $\chi_{H(FV)}$ ; •  $\chi_{S(FV)}$  as a function of T.

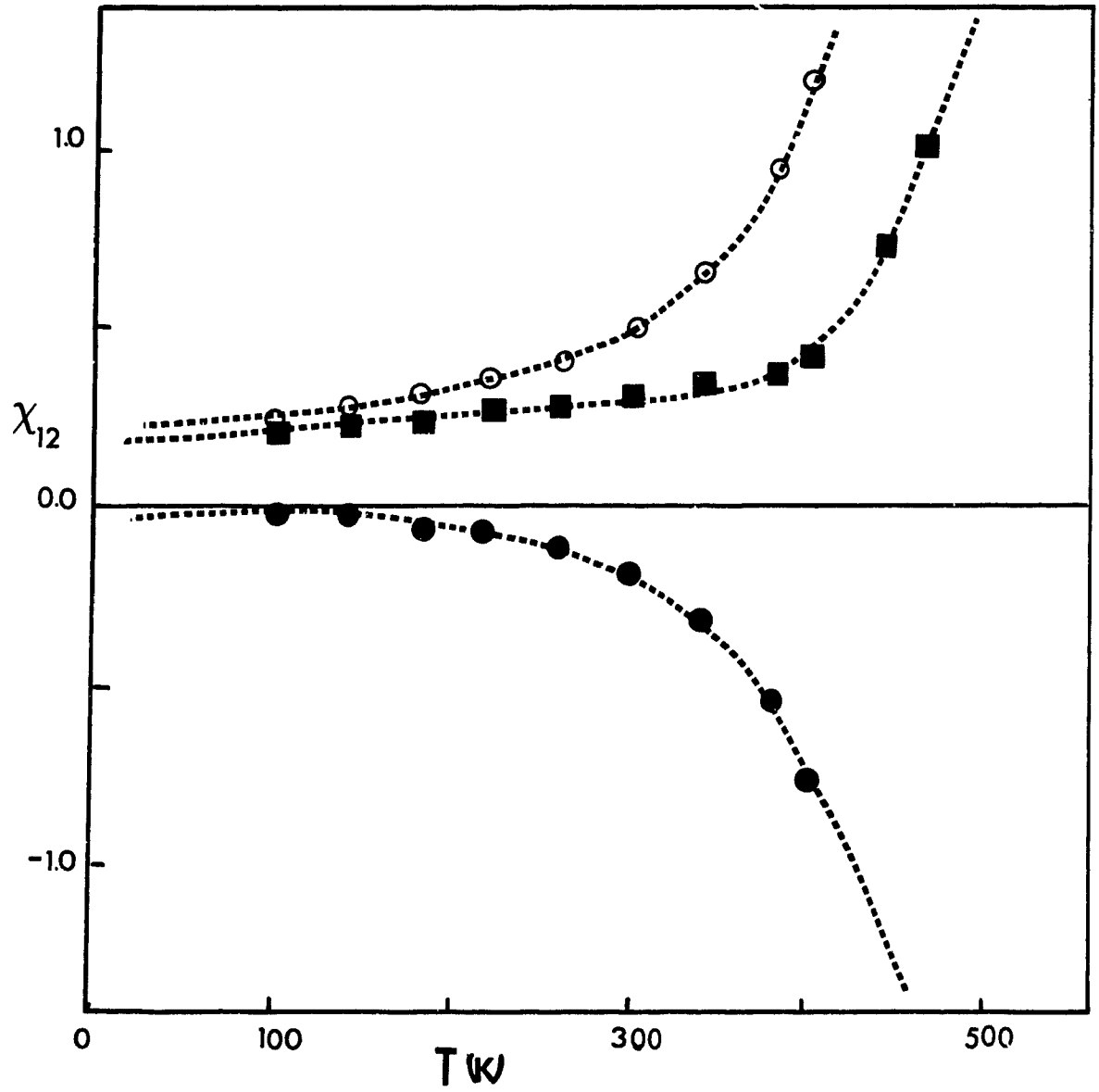
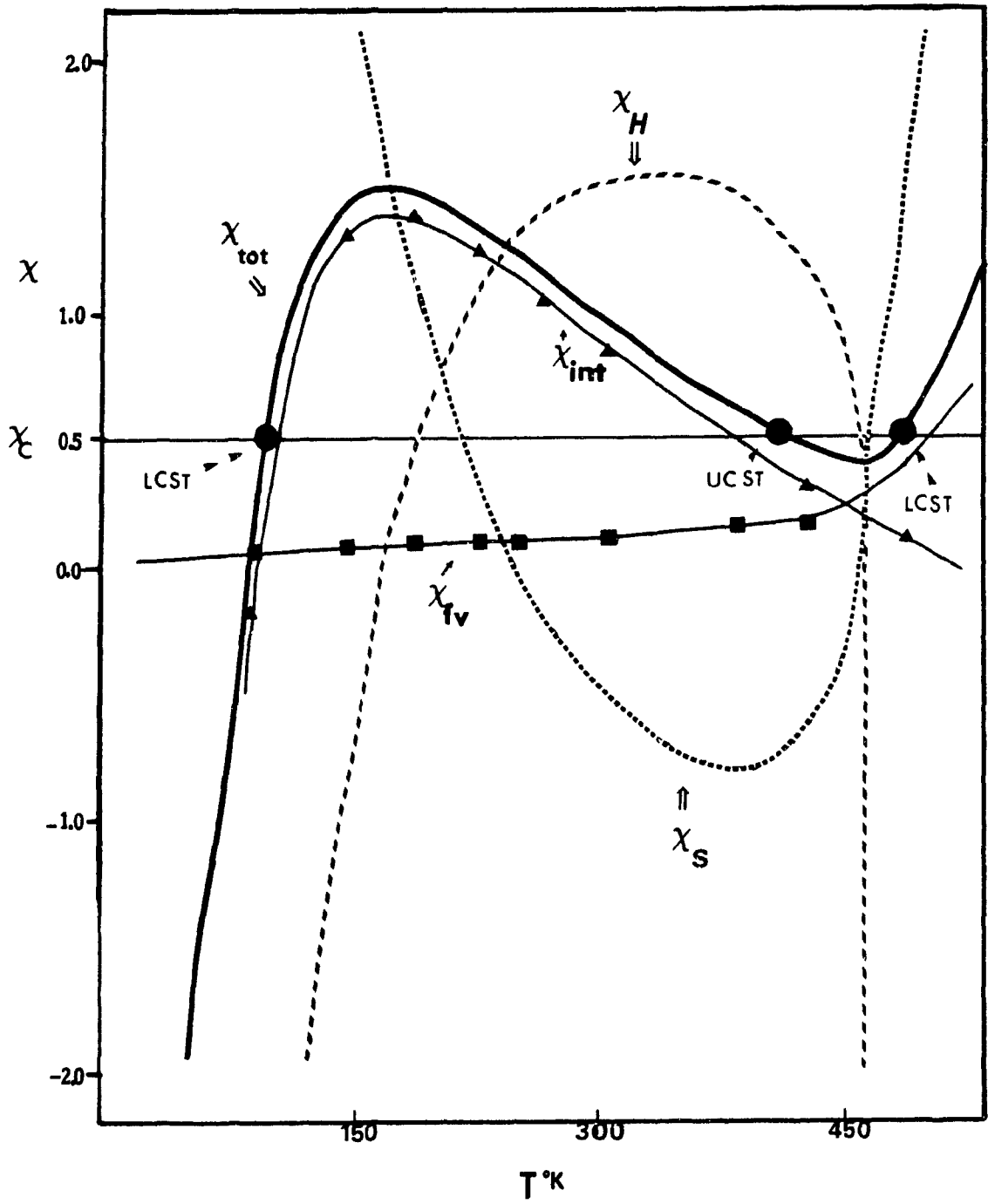


Fig. 7 Theoretical curve for polymer-solvent system: ●  $\chi_{(\text{total})}$ ; ▲  $\chi_{\text{int}(\text{total})}$ ;  
■  $\chi_{\text{FV}(\text{total})}$  as a function of T.



## EXPERIMENTAL

### 1. Methods

Several systems have been investigated in the search of a low temperature LCST and a closed-immiscibility loop. Among them, only a few showed, in fact, the expected results. For instance, polyethylene oxide (PEO) shows an immiscibility loop in aqueous systems i.e. a LCST followed by an UCST at higher T. However, in non-aqueous systems, the concentrated phase precipitates above the LCST. Crystallization on heating is rather peculiar. This phenomenon justifies the choice of visual observations of the T of the phase separation instead of light scattering or optical methods. Although visual observation is the simplest and oldest method, in spite of the primitiveness of the method, the accuracy of the cloud point temperature determined is not lower than 0.2°C.

### 2. Apparatus

A silicone oil bath (polydimethylsiloxane, from Dow Corning) was used. The heating elements were two immersion heaters of 300 and 200 watts. A Quartz thermometer (Hewlett Packard) indicated the temperature of the bath while the temperature was set up by a T control. The homogeneity of the bath temperature was maintained through the movement of a 360° rotator.

The solutions were made and kept in sealed glass tubes which were constantly stirred by a 360° rotating side-arm connected to a mechanical pump.

With this device, accumulation of the concentrated phase at the bottom of the tube and temperature gradient in the tubes were avoided. Many runs of observations were done to verify the reproducibility of the cloud point temperature.

3. Materials

The Chemicals are from Aldrich Chemical Company and were used without any further treatment. The solvents were at least of 98% of purity.

Observations were made for polyethylene oxide, (M.W.: 4000, 14000, 100000, 300000, 600000) in water and in chlorinated solvents such as dichloromethane, trichloroethylene, chloroform and  $\text{CCl}_4$ ; polyacrylic acid (M.W.: 32000, 180000, 250000) in p-dioxane and poly(p-phenylene ether sulfone) in dichloromethane.

## RESULTS AND DISCUSSION

### LCST and specific interactions in polymer-solvent mixtures

#### 1. Polyethylene oxide + water

Table 2 gives the critical temperature values as a function of molecular weight and concentration of solutions of polyethylene oxide in water. The immiscibility loop has been reported for this system in the literature<sup>9</sup>, and Table 2 shows an immiscibility loop for the 4000 M.W. sample with a LCST at  $\sim 145^{\circ}\text{C}$  and an UCST at  $\sim 162^{\circ}\text{C}$ . The higher molecular weight samples show a LCST at respectively 110,  $100^{\circ}\text{C}$  for 14000 and 100000 M.W., while the 600000 M.W. is insoluble at room temperature indicating that the LCST is  $< 25^{\circ}\text{C}$ .

One notes the strong dependence of the critical temperature on the molecular weight of the samples. The highest M.W. shows the lowest LCST, but also the highest UCST. As the M.W. increases the UCST increases and it is higher than  $180^{\circ}\text{C}$  for any M.W. higher than 14000.

#### 2. Polyethylene oxide + chlorinated solvents

Polyethylene oxide behaviour was also studied in non-aqueous solvents such as chlorinated solvents.

Table 3 shows the critical temperature as a function of M.W. of PEO in different solvents at a given concentration. Here one observes that the critical T increases as we go from trichloroethylene ( $56^{\circ}\text{C}$ ) to  $\text{CCl}_4$  ( $120^{\circ}\text{C}$ ), while dichloromethane and chloroform system lie in the middle and show respective critical temperatures of  $70^{\circ}\text{C}$  and  $100^{\circ}\text{C}$ . The value of the LCST depends on the strength of

TABLE 2

Critical temperatures of Polyethylene oxide + water as a function of M.W.

Heating rate: 10°C/5.7 min

M.W. of PEO	conc W%	LCST		UCST T°C
		starting T of turbidity	T°C T of complete turbidity	
4000	13.6	145	150	162
14000	11.6	110	118	
100000	13.6	100		
600000	1.9 (limit of solubility)	< 25		

TABLE 3

Critical temperatures for polyethylene oxide + chlorinated solvents  
as a function of M.W. Heating rate: 10°C/min

M.W. of PEO	Solvent	conc W%	critical T °C
600000	Dichloromethane	1.2	70
300000	Trichloroethylene	2.0	114
600000		2.03	56
600000	Chloroform	1.0	100
600000	CCl <sub>4</sub>	0.6	120

the interactions. The better the interaction, the higher the LCST.

a. Heat precipitation of PEO solutions

Solutions of PEO in all the chlorinated solvents listed in Table 3 show a peculiar behaviour. Above the critical temperature, the polymer precipitates from the concentrated phase. Morawetz<sup>10</sup> has pointed out that whenever the dissolution of a polymer is exothermic, the driving force toward the dissolution will decrease with rising temperature and the polymer may precipitate.

Solutions of PEO in  $\text{CCl}_4$  for instance, exhibit a large and exothermic  $\Delta H_M$  at high concentration of PEO ( $\Delta H_M = -1343 \text{ K/J mol}$  for M.W. = 654 at  $300^\circ\text{C}$ ) and the heat is more negative as the M.W. increases. In the same vein, multifunctional polymers lead after phase separation to a highly viscous and concentrated phase which turns to a gel.

3. Poly(p-phenylene-ether sulfone) + dichloromethane

Highly diluted solutions of low M.W. poly(p-phenylene ether sulfone) (PPES) + dichloromethane show an LCST at about  $32^\circ\text{C}$ . As the concentration of PPES increases, fig. 8 shown, in a relatively low T range, two regions of immiscibility separated by a narrow region of miscibility, i.e. the solutions phase separate until a UCST is reached. They are homogeneous over an extremely small T range and phase separate again (LCST) a few degrees from the UCST. An extremely low heating rate had to be used in order to observe this miscibility region. Otherwise, the solutions remain turbid at any temperature.

However, fig. 9 shows for a very high M.W. sample, a LCST at about  $22^\circ\text{C}$  in the dilute region. But at higher concentration, the solutions show instead the typical

Fig. 8 (T-x) phase diagram for mixture of low M.W. poly(p-phenylene ether sulfone) + dichloromethane.

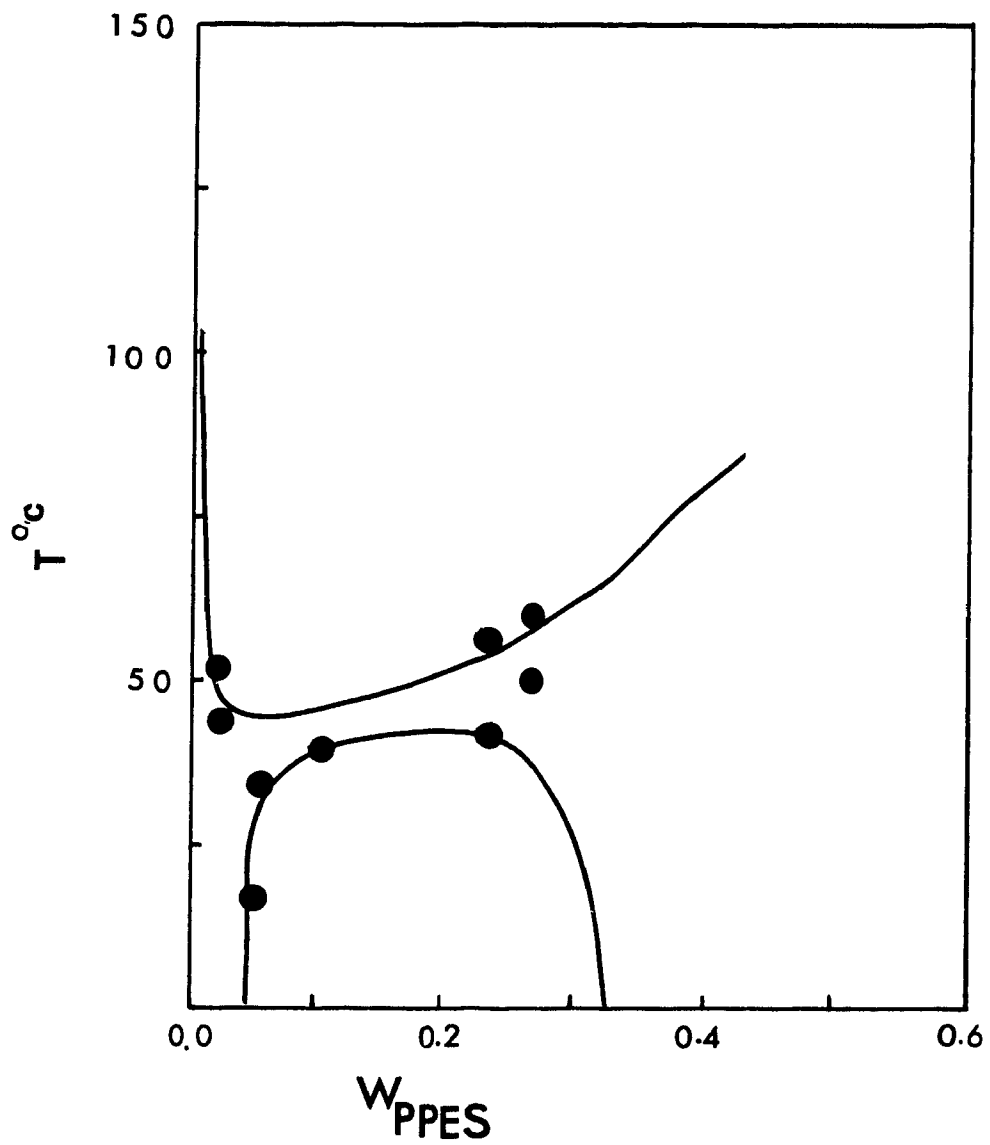
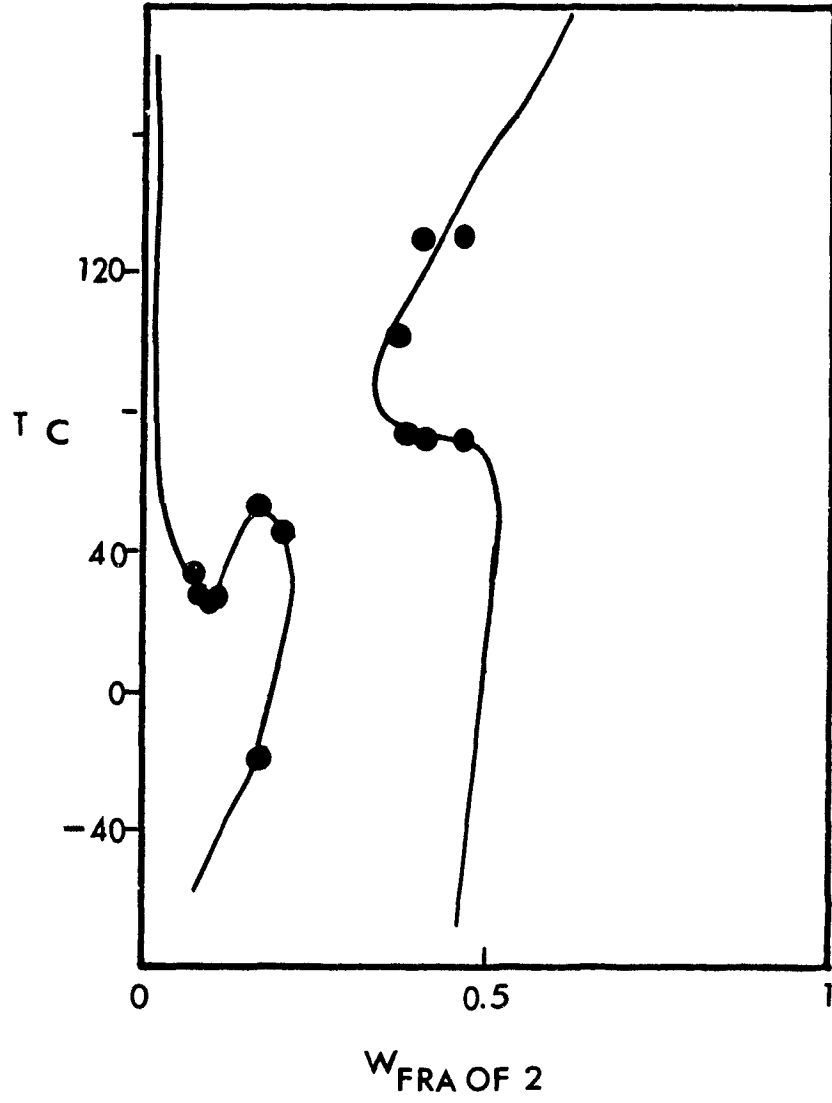


Fig. 9 (T-x) phase diagram for mixture of high M.W. poly(p-phenylene ether sulfone) + dichloromethane).



"hour-glass" boundary phase reported for several polymer-solvent mixtures. Ghavamikia et al<sup>11</sup> have reported LCST values of  $-10$  and  $20^{\circ}\text{C}$  for infinite M.W. PPES in respectively  $\text{CHCl}_3$  and  $\text{CH}_2\text{Cl}_2$  at infinite dilution.

The phase diagrams for this system look rather peculiar. Nevertheless, they are the results of many observations. Furthermore, there is a certain correlation between the diagrams for the two M.W. samples. The region of miscibility diminishes with increase of M.W., and finally for a very high M.W. sample, the UCST and LCST collapse and lead to the "hour-glass" shape observed.

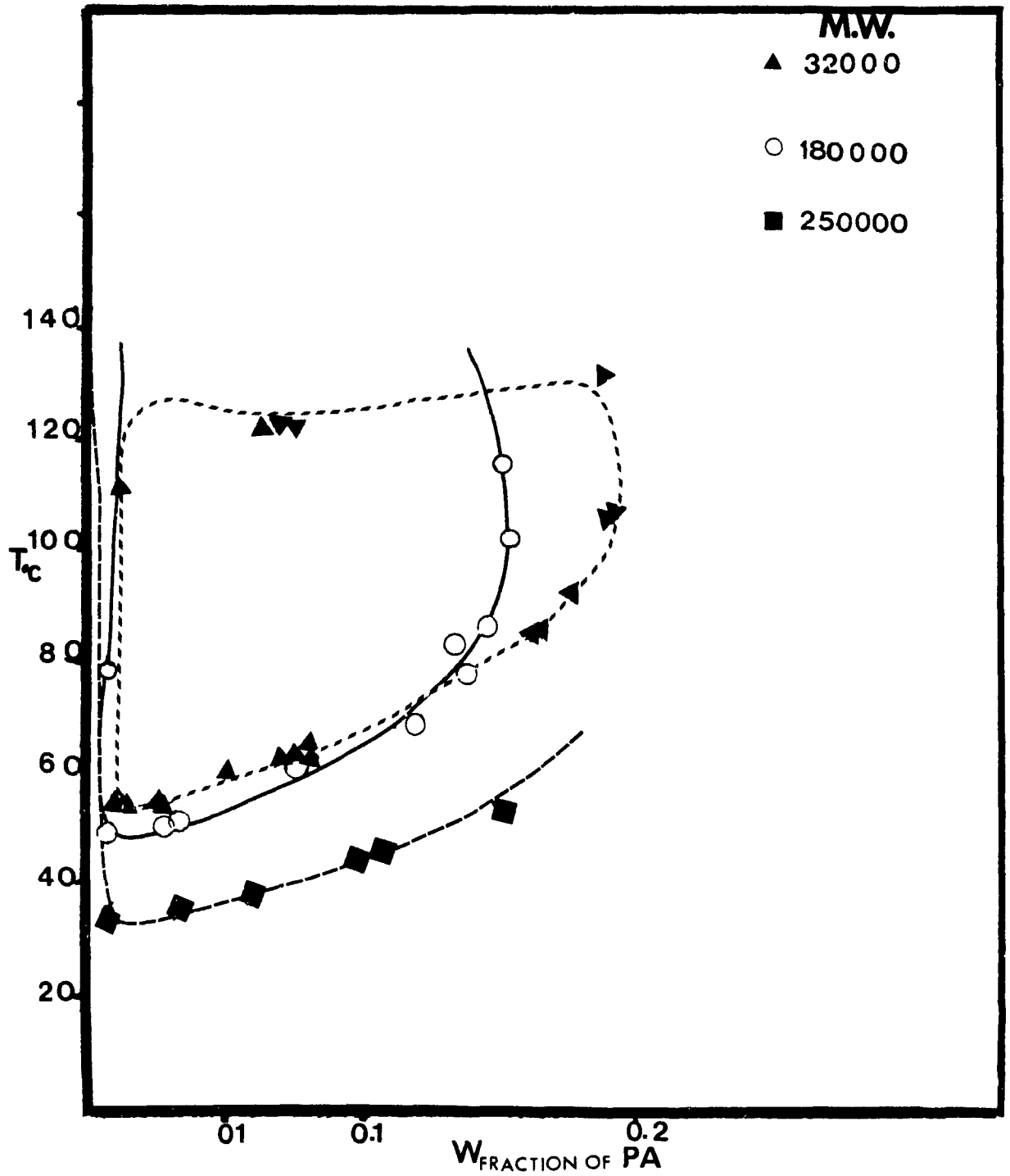
#### 4. Polyacrylic acid + p-dioxane

Fig. 10 shows the T vs composition (W%) phase diagram for solutions of polyacrylic acid (PA) and dioxane. Diagrams I, II, and III refer to different molecular weight samples respectively 32000, 180000, 250000. As expected  $T_c$  is strongly dependent on the molecular weight of the polymer. The LCST decreases as the M.W. increases, while the UCST increases with any increase of the M.W. The value of the LCST for the 250000 sample ( $32^{\circ}\text{C}$ ) agrees with the value extrapolated at infinite M.W. proposed by Flory et al<sup>12</sup> (LCST:  $29^{\circ}\text{C}$ ).

One should note that the shape of the T-x diagram is affected by the molecular heterogeneity of the polymer. The effect of the polydispersity of PA is responsible for the cross-over observed between the diagram of different M.W. samples. This polydispersity has also a critical effect on the critical point and specifically the UCST.

The highest M.W. shows the lowest LCST, but also the highest UCST. In fact, it does not show any further homogeneity in the range of temperature studied. No free volume LCST could be observed for either sample, since the polymer decomposes before this T could be reached.

Fig. 10 (T-x) phase diagram for mixture of poly(acrylic acid) + p-dioxane for different M.W. samples: ▲ 32000, ○ 180000, ■ 250000.



5. Stabilization of a partially miscible solution by the presence of a small amount of electrolytes

It is often found that a small amount of an electrolyte or a hydrogen bond acceptor solvent stabilizes partially miscible solutions which become completely miscible. Through this cosolvency phenomenon the hydrogen bonding requirements of the polar or H-bond groups caused by the polymer are satisfied. Such a behaviour has been tested for partially miscible pairs studied above, PA + dioxane and PPES + dichloromethane.

When PA is dissolved in a solution containing 80% dioxane + 20% water, the solutions of any M.W. of PA studied above, remain homogeneous in the entire temperature range studied earlier. However, if PA is dissolved in a solution composed of 50:50 dioxane–water, the polymer is totally insoluble at any T.

A similar observation was made for PPES + dichloromethane solutions. PPES was added to a mixture of 90:10 of dichloromethane + dimethyl formamide (DMF) and the solution is homogeneous until a LCST is observed at 185°C. This LCST may be due to free volume dissimilarity caused by the expansion of the solvent. Again the low T LCST disappears.

LCST in polymer–polymer mixture: PS + PVME

Application of the new model described in this work

The model was applied to PS + PVME mixture which shows an LCST at 400°K<sup>13</sup>. From reference 14, the enthalpic and entropic contributions can be evaluated.  $\chi_H$  is about – 0.4 while  $\chi_S = 0.4$ . The value of  $\chi_H$  was fitted to the model and then the LCST can be predicted perfectly well as shown in Table 4 and Fig. 11.

TABLE 4

Temperature-Composition-Phase Diagram including Free Volume for  
PS + PVME mixture

T (K)	$\chi_{H \text{ int}}$	$\chi_{S \text{ int}}$	$\chi_{\text{int}}$	$\chi_{H \text{ FV}}$	$\chi_{S \text{ FV}}$	$\chi_{\text{FV(total)}}$	$\chi_{H(\text{total})}$	$\chi_{S(\text{total})}$	$\chi_{C/C}$
100	-2.137	.727	-1.411	-.011	.023	0.22	-2.139	.75	-1.389
120	-1.673	.607	-1.065	-.002	.024	.022	-1.674	.631	-1.043
140	-1.365	.533	-.832	-.002	.024	.022	-1.367	.558	-.81
160	-1.365	.485	-.665	-.002	.025	.023	-1.151	.059	-.642
180	-.99	.451	-.539	-.003	.026	.023	-.992	.476	-.516
200	-.868	.426	-.441	-.003	.026	.023	-.871	.453	-.516
220	-.771	.408	-.363	-.003	.027	.024	-.775	.435	-.34
240	-.694	.394	-.3	-.004	.028	.024	-.698	.422	-.276
260	-.63	.384	-.247	-.004	.029	.024	-.635	.412	-.222
280	-.577	.375	-.202	-.005	-.03	.025	-.582	.405	-.177
300	-.532	.368	-.164	-.006	.031	.025	-.537	.399	-.139
320	-.493	.362	-.131	-.006	.032	.025	-.499	.394	-.105
340	-.459	.358	-.102	-.007	.033	.026	-.467	.391	-.076
360	-.43	.354	-.076	-.008	.034	.026	-.438	.388	-.05
380	-.404	.35	-.054	-.009	.036	.027	-.413	.386	-.027
400	-.381	.347	-.034	-.01	.037	.027	-.391	.385	-.007
420	-.361	.345	-.016	-.011	.039	.028	-.372	.384	.012
440	-.342	.343	.001	-.013	.041	.028	-.355	.384	.029
460	-.325	.341	.016	-.014	.043	.029	-.34	.384	.044
480	-.31	.339	.029	-.016	.046	.03	-.326	.385	.059
500	-.296	.338	.041	-.018	.048	.03	-.315	.386	.072
520	-.284	.337	.053	-.021	.052	.031	-.304	.388	.084
540	-.272	.335	.063	-.024	.055	.032	-.296	.391	.095

Fig. 11 Variation of  $\chi_{\text{total}}$  with T for mixture of polystyrene + poly(vinyl methyl ether).

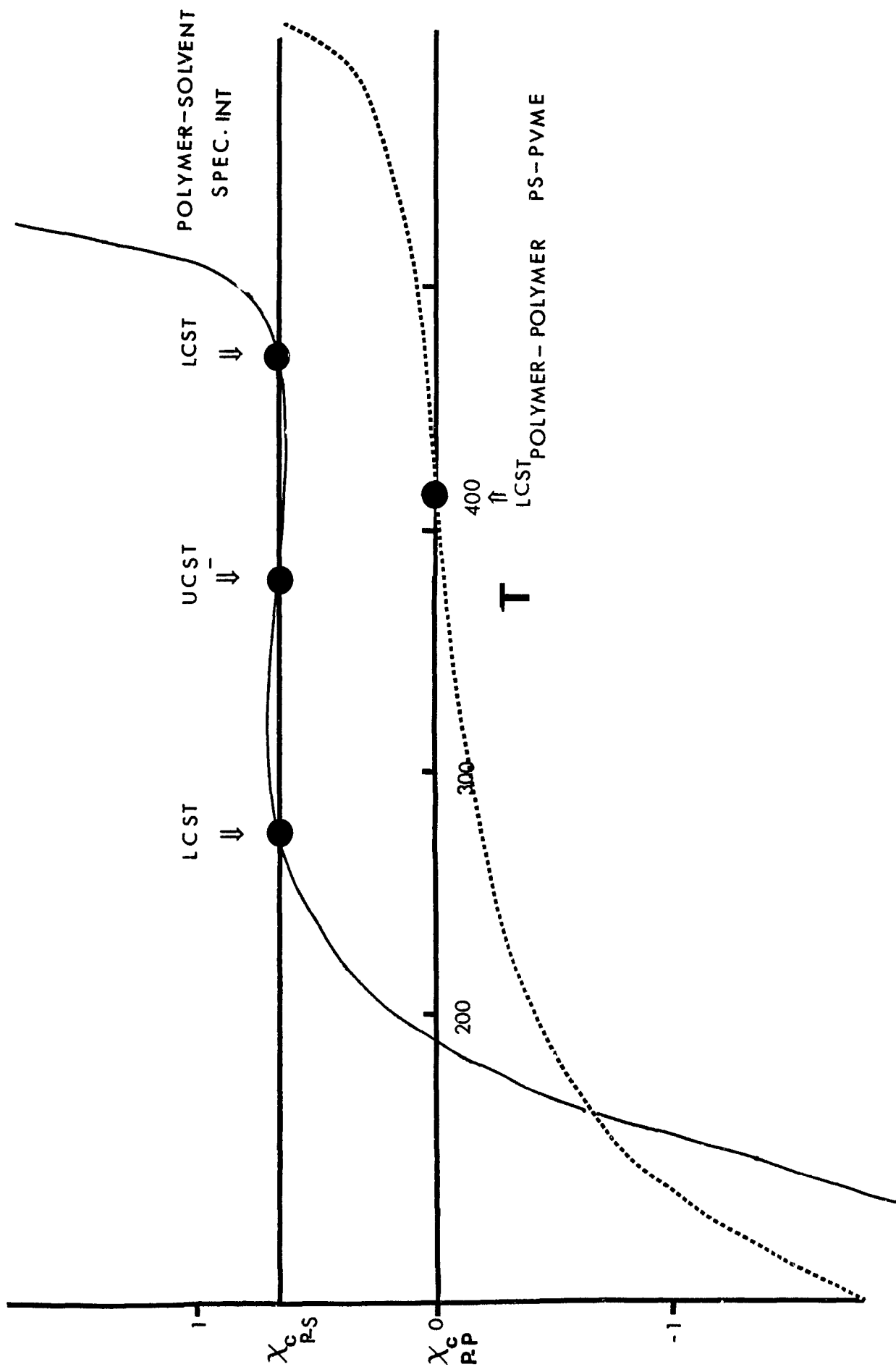


Table 4 shows the parameters used to fit the experimental data. Table 4 shows as well, the different contributions into  $\chi$  and the total  $\chi$  which is negative at low T and crosses the critical line at 400°K and turns positive at higher T as shown in Fig. 11.

From Table 4, it can also be seen that as expected the free volume contribution is quite small compared to the interactional term. It is even negligible at low T and below  $T_c$  compared to the interactional contribution, indicating that the LCST is mainly caused by specific interactions.

The model successfully predicts the  $\chi$  parameter and the LCST for PS–PVME mixture as well as for several polymer–polymer or polymer–solvent systems tested. It is a good tool in the study of specific interactions for those systems and can undoubtedly be used in the prediction of polymer compatibility.

REFERENCES

1. O. Olabisi, L.H. Robeson, and M.T. Shaw, *Polymer–Polymer Miscibility*, Ed. Academic Press, 1979.
2. P.J. Flory, *Principles of Polymer Chemistry*, Cornell University Press, 1953, Chapters 12 and 13.
3. a) I. Prigogine, A. Bellemans, and V. Mathot, *The Molecular Theory of Solutions*, Ed. North Holland Publishing Co., Amsterdam, 1957.  
b) P.J. Flory, *Disc. Faraday Soc.* 49, 7, 1970.
4. D. Patterson, *Polym. Eng. Soc.* 22, 2, 1982.
5. K. Shinoda, *J. Phys. Chem.* 81, 1300, 1977.
6. a) R.H. Lacombe and I.C. Sanchez, *J. Phys. Chem.* 80, #23, 2568, 1976.  
b) J.S. Walker and C.A. Vause, *Phys. Lett. A* 79, 421, 1980.  
c) J.C. Wheeler, *J. Chem. Phys.* 62, 433, 1975.
7. R.E. Goldstein, *J. Chem. Phys.* 80, #110, 5340, 1984.
8. J.M. Bardin and D. Patterson, *Polymer* 10, 247, 1969.
9. G.N. Malcom and J.S. Rowlinson *Trans Faraday Soc.* 53, 921, 1957.
10. H. Morawetz, *Macromolecules in Solution*, Ed. Interscience Publishers, 1965.
11. a) D.A. Blackadder and H. Ghavamikia, *Polymer* 19, 255, 1978.  
b) *ibid*, 20, 781, 1979.  
c) D.A. Blackadder, H. Ghavamikia, and A. Windle, *Polymer* 20, 781, 1979.
12. A.R. Schultz and P.J. Flory, *J. Polym. Sci.* 15, 231, 1955.
13. T.K. Kwei, T. Nishi, and R.F. Roberts, *Macromolecules* 7, #5, 667, 1974.
14. C. Herkt–Maetzky and J. Schelten, *Phys. Rev. Lett.* 51, #10, 896, 1983.

APPENDIX 6

Phase diagram ( $\chi$ -T) program

LCST PROGRAM

```
DECLARE SUB KHIFRVOL (XHF!)
DECLARE SUB KSFRVL (XSF!)
DECLARE SUB KIFV (KfV!, Cone!, ToSQ!)
DECLARE SUB VRedu (VR!)
DECLARE SUB KIS (KS!)
DECLARE SUB KIH (KH!)
DIM SHARED P1star AS SINGLE, V1star AS SINGLE, T1star AS
SINGLE
DIM SHARED T2star AS SINGLE
DIM SHARED TK AS SINGLE, Tred AS SINGLE, VR AS SINGLE, KfV
AS SINGLE
DIM SHARED C AS SINGLE, X AS SINGLE, Z AS SINGLE, K AS
SINGLE
DIM SHARED KH AS SINGLE, KS AS SINGLE, LAMBDA AS SINGLE
DIM SHARED Cone AS SINGLE, ToSQ AS SINGLE
DIM SHARED KHtotal AS SINGLE, KStotal AS SINGLE
DIM SHARED XHF AS SINGLE, XSF AS SINGLE
5
'=====
6 '****This program calculates the X parameter for polymer-
solvent system
7 'where an immiscibility loop is expected, including
contributions from
8 'enthalpy entropy and free volume.****
9
'=====
10 REM **** LCST printing the total contributions ****
11 WHILE RESP$ <> "N"
15 INPUT "PRINT?"; ANSWER$
20 INPUT "Coordination number"; C
35 INPUT "T2star"; T2star
40 INPUT "T1star"; T1star
50 INPUT "V1star"; V1star
55 INPUT "P1star"; P1star
61 INPUT "DE/R : K"; K
62 INPUT "ENTROPY FACTOR (Z)"; Z
63 INPUT "IS LAMBDA CONSTANT ?"; REPON$
69 IF REPON$ = "Y" THEN INPUT "LAMBDA"; LAMBDA
70 IF ANSWER$ = "Y" THEN
71 LPRINT "TEMPERATURE-COMPOSITION-PHASE DIAGRAM
including Free Volume"
72 LPRINT
74 LPRINT
75 LPRINT "K"; K
80 LPRINT "Coordination number(C)"; C
85 LPRINT "Entropy Factor(Z)"; Z
90 LPRINT "P1*"; P1star
100 LPRINT "V1*"; V1star
110 LPRINT "T1*"; T1star
111 LPRINT "T2*"; T2star
112 END IF
130 FOR I = 1.1 TO 1.5 STEP .2
```

```
140 IF REPON$ <> "Y" THEN LAMBDA = I
142 PRINT "LAMBDA ="; LAMBDA
143 IF ANSWER$ = "Y" THEN
144     LPRINT
145     LPRINT " LAMBDA ="; TAB(10); LAMBDA
146     LPRINT
147 END IF
150 TK = 100!
151 BIP = 40 * K
152 IF ANSWER$ = "Y" THEN
156     LPRINT
157     LPRINT TAB(2); "TK"; TAB(9); "KH"; TAB(15); "KS";
158     LPRINT TAB(22); "KT";
159     LPRINT TAB(32); "KHF"; TAB(40); "KSF"; TAB(48);
160     LPRINT "KFV"; TAB(55);
161     LPRINT "KHttl"; TAB(64); "KSttl"; TAB(72); "Xttl"
162     LPRINT
163     LPRINT
164     LPRINT
165 ELSE
166     PRINT TAB(2); "TK"; TAB(9); "KH"; TAB(15); "KS";
167     PRINT TAB(22); "KT";
168     PRINT TAB(32); "KHF"; TAB(40); "KSF"; TAB(48);
169     PRINT "KFV"; TAB(55);
170     PRINT "KHttl"; TAB(64); "KSttl"; TAB(72); "Xttl"
171 END IF
172 FLAG = 0!
173 WHILE TK <= BIP AND FLAG < 1!
174     X! = K! / TK
175     xInv! = 1 / X
176     xInv = INT((xInv * 1000) + .5) / 1000
177     TRed! = TK / Tistar
178     CALL KIH(KH!)
179     CALL KIS(KS!)
180     CALL VRedu(VR!)
181     VR = INT((VR * 1000) + .5) / 1000
182     CALL KIFV(KFV!, Cone, ToSQ)
183     CALL KHIFRVOL(XHF!)
184     CALL KSFRVL(XSF!)
185     KHtotal! = KH + XHF
186     KStotal! = KS + XSF
187     KT! = KH + KS
188     KT = INT((KT * 1000) + .5) / 1000
189     KHItotal! = KHtotal + KStotal
190     'PRINT "TRed="; TRed, "KFV="; KFV, "VR="; VR
191     'PRINT "KH="; KH; "KS="; KS; "KHItotal=";
192     KHItotal
193     Xtotal! = KH + KS + KFV
194     XHF = INT((XHF * 1000) + .5) / 1000
195     XSF = INT((XSF * 1000) + .5) / 1000
196     KFV = INT((KFV * 1000) + .5) / 1000
197     KH = INT((KH * 1000) + .5) / 1000
```

```
225     KS = INT((KS * 1000) + .5) / 1000
226     KHtotal = INT((KHtotal * 1000) + .5) / 1000
227     KStotal = INT((KStotal * 1000) + .5) / 1000
228     KFV = INT((KFV * 1000) + .5) / 1000
229     Xtotal = INT((Xtotal * 1000) + .5) / 1000
230     'PRINT "Xtotal="; Xtotal
240     IF ANSWER$ = "Y" THEN
241         LPRINT TK; TAB(6); KH; TAB(14); KS; TAB(21);
                KT; TAB(30);
242         LPRINT XHF; TAB(38); XSF; TAB(46); KFV;
                TAB(54); KHtotal;
                LPRINT TAB(62); KStotal; TAB(70); Xtotal
243     ELSE
244         PRINT TK; TAB(6); KH; TAB(14); KS; TAB(21); KT;
                TAB(30);
245         PRINT XHF; TAB(38); XSF; TAB(46); KFV; TAB(54);
                KHtotal;
                PRINT TAB(62); KStotal; TAB(70); Xtotal
246     END IF
247     TK! = TK + 20!
        'IF TK = 400 THEN TK = TK + 6
248     RATIO! = 256 / 27
249     FLAG! = RATIO * TK / Tistar
250     WEND
255     IF FLAG > 1! AND ANSWER$ = "Y" THEN
256         LPRINT
257         LPRINT
260         LPRINT "PROGRAM STOPS AT T ="; TK, "TEMPERATURE TOO
                HIGH:"
262         LPRINT "9.5 x TRed > 1 SUBROUTINE VRedu CAN NOT BE
                PERFORMED"
263     ELSEIF FLAG > 1! THEN
264         PRINT "TEMPERATURE TOO HIGH:IN SUB VRedu: 1- COT <
                O"
265     END IF
270     IF ANSWER$ = "Y" THEN
275         LPRINT
276         LPRINT
277     END IF
278     'LAMBDA = 0!
279     IF REPON$ = "Y" THEN EXIT FOR
280     NEXT
281     INPUT "DO YOU WANT TO CONTINUE ?"; RESP$
282     IF RESP$ = "Y" THEN
283         INPUT "PRINT ?"; ANSWER$
284         INPUT "DO YOU WANT TO CHANGE ONLY K Z AND
                LAMBDA?"; RP$
285         IF RP$ = "Y" THEN GOTO 61
286         INPUT "DO YOU WANT TO CHANGE THEM "; REN$
287         INPUT " DO YOU WANT TO CHANGE ONLY LAMBDA ?";
                RAPO$
288         IF RAPO$ = "Y" THEN GOTO 63
289         INPUT " DO YOU WANT TO CHANGE IT "; RRV$
290         INPUT "DO YOU WANT TO CHANGE ALL ?"; RC$
```

```
300     IF RC$ = "Y" THEN GOTO 15
310     INPUT "DO YOU WANT TO CHANGE COMPONENT2* ?"; R$
320     IF R$ = "Y" THEN INPUT "T2*"; T2star
325     INPUT "DO YOU WANT TO CHANGE COMPONENT1* ?"; RA$
329     IF RA$ = "Y" THEN GOTO 40
335     IF R$ = "Y" AND REN$ = "Y" THEN GOTO 61
336     IF R$ = "Y" AND RRV$ = "Y" THEN GOTO 63
337     IF R$ = "Y" GOTO 70
339     END IF
340     INPUT "ARE YOU SURE YOU WANT TO CONTINUE ?"; RR$
350     IF RR$ = "Y" THEN GOTO 284 ELSE RESP$ = "N"
370     WEND
390     END
```

```
SUB KHIFRVOL (XHF!)
DEFSNG A-Z
2020    STATIC CONS1
2040    CONS1! = 4 / 3
2060    CONS2! = 4 / 9
2080    B! = VR ^ (2 / 3)
2100    CCP! = VR ^ (1 / 3)
2120    D! = 1 / CCP
2140    DD! = CONS1 * D
2160    E! = DD - 1
2180    EE! = E ^ 3
2200    NUM! = CONS2 * (CCP - 1)
2220    DENO! = B * EE
2240    RATIO! = NUM / DENO
2245    'PRINT "CONE="; Cone, "ToSQ="; ToSQ
2260    KHI! = Cone * ToSQ * RATIO
2261    'PRINT "B="; B, "CCP="; CCP, "D="; D
2262    'PRINT "DD="; DD, "E="; E, "EE="; EE
2263    'PRINT "NUM="; NUM, "DENO="; DENO
2265    'PRINT "KHI="; KHI, "RATIO="; RATIO
2280    XHF! = -(KHI)
END SUB
```

```
900    SUB KIFV (KFV, Cone, ToSQ)
901    STATIC CONS, R
909    CONS = 1.333333
910    R! = 8.3143
911    NUM! = P1star * V1star
912    NUM1! = T1star * R
913    NUM2! = NUM1 * 2!
914    NUM3! = NUM / NUM2
940    DEN! = (T2star - T1star) / T2star
945    'PRINT "VR="; VR
950    DAS! = VR ^ (1 / 3)
960    DAS1! = 1 / DAS
965    PRO! = CONS * DAS1
966    PRO1! = PRO - 1!
967    PRO0! = 1 / PRO1
990    DENN! = DEN ^ 2
994    'PRINT "NUM3 ="; NUM3
```

```
996 PROD! = DENN * PROO
1000 KFV = NUM3 * PROD
1001 Cone! = NUM3
1005 ToSQ! = DENN
1020 'PRINT "ConeM="; Cone, "TOSQM="; ToSQ
END SUB
```

```
400 SUB KIH (KH)
420 M! = LAMBDA * X + Z
440 MM! = 1 + EXP(-M)
460 MMM! = LAMBDA / MM
480 KHH! = X * (1 - MMM)
490 KH! = KHH * C
END SUB
```

```
500 SUB KIS (KS)
520 AA! = X * LAMBDA
540 FF! = AA + Z
550 BA! = EXP(-FF)
560 BB! = 1 + BA
580 EE! = AA / BB
585 DA! = EXP(FF)
590 DD! = LOG(1 + DA)
600 KSS! = EE - DD
620 KS! = (KSS + LOG(2)) * C
END SUB
```

```
SUB KSFRVL (XSF)
DEFSNG A-Z
STATIC CONS1, CONS2
3000 CONS1! = 4 / 3
3020 CONS2! = 20 / 9
3040 A! = VR ^ (1 / 3)
3060 B! = VR ^ (2 / 3)
3080 CCO! = 1 / A
3200 D! = CONS1 * CCO
3220 DD! = D - 1
3240 DDD! = DD ^ 3
3260 DENO! = B * DDD
3280 NUM! = B - CONS2 * A + CONS1
3390 'PRINT "CCOS="; CCO; "BS="; B; "DDS="; DDS; "DDDS=";
      DDD
3300 RATIO! = NUM / DENO
3301 'PRINT "NUMS="; NUM, "DENOS="; DENO
3305 'PRINT "CONES="; Cone, "ToSQS="; ToSQ
3320 Kh1S! = Cone * ToSQ * RATIO
3330 'PRINT "KHIS="; Kh1S; "RATIOS="; RATIO
3340 XSF! = Kh1S
END SUB
```

```
700 SUB VRedu (VR)
701 STATIC CO, CP, CPP
710 CO = 256 / 27
711 CP = 16!
```

```
712 CPP = 4!
730 COT! = CO * TRed
735 I! = 1! - COT!
740 A1! = SQR(I)
760 B1! = (1! + A1) ^ (1 / 3)
780 B2! = (1! - A1) ^ (1 / 3)
781 BB! = B1 + B2
782 U! = 2! * TRed ^ 2
783 UA! = U ^ (1 / 3)
785 UI! = 1! / UA
800 UU! = UI * BB
802 CU! = UU ^ 2
805 CX! = TRed * CU
809 CTV! = CP / CX
810 CXX! = CPP - CTV
820 CC! = SQR(CXX)
830 UX! = SQR(UU)
835 U1X! = UX / 2!
836 U2X! = CC! - 1!
838 U3X! = SQR(U2X)
839 U4X! = 1! - U3X
840 XXX! = U1X! * U4X!
860 VR! = XXX! ^ 3
865 'PRINT "TRed="; TRed
END SUB
```

CHAPTER 7

POLYMER-POLYMER COMPATIBILITY IN TERNARY SYSTEMS:  
A CALORIMETRIC APPROACH

## INTRODUCTION

Polymer blends have attracted remarkable attention during the past years. Polymer–polymer interactions are important to understand the phase behaviour and mechanical properties of both miscible and immiscible polymer blends.

In most compatible pairs, specific interactions, such as hydrogen bonding or a charge transfer complex, are involved and lower the free energy of mixing. A negative free energy of mixing is the necessary criterion for miscibility:

$$\Delta G_M = \Delta H_M - T\Delta S_M \leq 0$$

For high molecular weight components  $\Delta S_M \rightarrow 0$  (at least expressed per unit–solution volume) as M.W.  $\rightarrow \infty$ , therefore  $\Delta G_M \leq \Delta H_M \leq 0$ . Miscibility is then linked to an exothermic heat due to these specific interactions.

Poly(vinyl chloride) (PVC) is one of the most investigated polymers<sup>1</sup>. It has been found to be miscible with several polymers. It is capable of forming H–bonds with a large number of components. PVC molecules contain two sites of interactions: (1) the  $\alpha$ –hydrogen which may be involved in a hydrogen bond with a proton acceptor component, for instance, those having a carbonyl group or showing basic properties; (2) the pendant chloride group which may be involved in charge–transfer or an acid–base (Lewis type) complex with the ester or ether oxygen.

The family of polyesters exhibits a unique situation in that they constitute plasticizers for PVC i.e. they decrease the glass transition temperature (T<sub>g</sub>) of PVC and their mixtures with PVC show a single T<sub>g</sub> i.e. compatibility. Many diverse miscible systems containing polyesters have been observed. The most significant polyesters are poly( $\epsilon$ –caprolactone) (PCL), poly(methylmethacrylate) (PMMA), polyvinyl acetate and also oligomers of polyesters.

Polyethers also show miscibility not only with PVC, but with polyhydrocarbons. Miscibility results either from hydrogen bonding interactions with a proton donor

component such as PVC or from charge transfer or dipole–dipole interactions. The blend of poly(styrene)–poly(vinylmethylether) has been rigorously investigated<sup>1</sup> either in fundamental polymer–polymer studies or applied research. The Flory–Huggins interaction parameter  $\chi$  is widely used<sup>2</sup> in the study of polymer compatibility, and plays a dominant role in explaining the critical phase behaviour of a compatible pair. However, direct measurement of  $\chi$  is not always possible. It has mainly been experimentally evaluated using gas–liquid chromatography, vapor sorption, film castings, spectroscopy etc. Nevertheless, calorimetry is amongst the most direct methods for determining miscibility, or evaluating the  $\chi$  parameter.

The  $\chi$  parameter of a miscible pair depends primarily on an exothermic enthalpic contribution in  $\Delta G_M$ , as shown in ref. 2b. The  $\chi$  parameter has to be negative or zero perhaps. Hence, heat of mixing should be a good indicator of compatibility. It is given by equations 1.

$$\frac{\Delta H_M}{RTV} = \left[ \frac{z \Delta W_{12}}{kTV_s} \right] \phi_1 \phi_2 = \frac{\chi_{12}}{V_1} \phi_1 \phi_2 \quad (1)$$

Here  $z$  is the lattice coordination number,  $k$  the Boltzman constant,  $\Delta W_{12}$  the energy change associated with the formation of (1–2) segment contacts from the breaking of (1–1) and (2–2) segment pairs,  $V_s$  is the molar volume of a segment and  $\chi_{12}$  is the Flory–Huggins interaction parameter; it is expressed as:

$$\chi_{12} = \frac{z \Delta W_{12} r_1}{kT} \quad (2)$$

$r_1$  being the number of segments of component 1. Heat of mixing measurement for mixing of two polymers requires, however, a third component i.e. a mutual solvent. Yet, the solvent itself is not always an inert medium and may interact with the

polymers. Maximum miscibility between two polymers is achieved only with solvents having comparable affinities for the polymers. Any difference in strength of the polymer-solvent interactions ( $\chi_{13}$ ,  $\chi_{23}$ ) which manifests itself through  $\Delta\chi$  i.e. ( $\chi_{13} - \chi_{23}$ ) may weaken the polymer-polymer  $\chi$  parameter. In other words,  $\Delta\chi$  has to be zero or negligible in order to observe a stable solution. The mixing of the two polymers proceeds in the following way: Two solutions composed respectively of polymer 1 + the mutual solvent are mixed in the calorimeter and the change of enthalpy ( $\Delta H_M$ ) associated with the mixing may be expressed as follows:

$$\Delta H_M = H_{123} - H_{13} - H_{23} \quad (3)$$

Where 1 and 2 refer to polymers 1 and 2, while 3 refers to the solvent.  $H_{123}$  is the heat resulting from mixing the ternary solution.  $H_{13}$  is the heat of mixing of polymer 1 with the solvent;  $H_{23}$  is the heat of mixing of polymer 2 with the solvent.

From eqns. 1 and 3,  $\Delta H_M$  can be rewritten:

$$\begin{aligned} \frac{\Delta H_M}{V^*} = & \frac{\phi_1 \phi_2 z \Delta W_{12}}{V^*} \\ & + \frac{\phi_1(\phi_1' - \phi_2') (N_2 r_2 + N_{32} r_3) z \Delta W_{13}}{(\sum N_i r_i) V^*} \\ & + \frac{\phi_2(\phi_2' - \phi_1') (N_1 r_1 + N_{31} r_3) z \Delta W_{23}}{(\sum N_i r_i) V^*} \end{aligned} \quad (4)$$

Where  $\phi_1$ ,  $\phi_2$  are volume fractions of polymers 1 and 2 in the ternary solution, while  $\phi_1'$  and  $\phi_2'$  are volume fractions of the polymers in the respective binary solutions (i.e. polymer + solvent),  $\Delta W_{13}$  and  $\Delta W_{23}$  are the energy changes associated respectively with polymer 1 - solvent and polymer 2 - solvent segment contacts;  $V^*$  (i.e.  $\sum W_i V_i^*$ )

being the "hard-core" volume of the solution, expressed on a molar basis.  $V_i^*$  being  $N_i r_i c_i^*$  sp,  $N_i$  and  $r_i$  are respectively numbers of molecules and segments of components  $i$ .  $N_{32}$  and  $N_{31}$  are the number of molecules of solvent in solution containing respectively polymer 2 and polymer 1. The quantities  $\frac{N_2 r_2 + N_{32} r_3}{\sum n_i r_i}$  and  $\frac{N_1 r_1 + N_{31} r_3}{\sum n_i r_i}$  may be approximated to the mole fraction of the solvent in solution with polymer 2 and polymer 1 respectively. The second and third terms have been found to be very small and would be zero if  $\phi_1' = \phi_2'$  i.e. if the concentrations of the two binary solutions are equal. Full details of the derivation of  $\Delta H_M$  are given in Appendix 7.

In the course of this work, the heat of mixing has been measured for well established compatible pairs of polymers dissolved in a common solvent. The results are interpreted according to the Flory-Huggins theory applied to ternary systems. The effect of the solvent upon miscibility of two polymers is also studied.

## EXPERIMENTAL

Table 1 summarizes the various polymers and solvents used. The systems studied may be classified into two broad groups:

1. Mixtures composed of components from group 1 with those from either group 2, group 3 or group 4, + a common solvent.
2. Mixtures of components coming from groups 2 and 3 and their analogs plus a common solvent.

### 1. Materials

Table 2 lists the sources and nature of the various polymers and solvents used. They were taken without further treatment, save PVC which was washed with a solution of 50:50 methanol–water and dried in an oven for 24 hours. A small amount (1%) of a stabilizer (thermolite–35), from M&T Chemicals was incorporated into the PVC samples in order to prevent oxidation and degradation.

THF was purified by distillation and was kept under nitrogen. Special devices of glass vessels were built to allow the preparation of the samples under constant nitrogen circulation from the freshly distilled solvent. The solutions were then hermetically kept until complete dissolution of the polymer. Solutions of about 20% weight percent of each polymer in the mutual solvent were prepared.

### 2. Methods

#### A. Heat of mixing

The heat of mixing ( $\Delta H_M$ ) was measured for several systems listed in Table 3–6

TABLE 1

Chemical structure of the polymers and their analogs

1. Polyhydrocarbons

aliphatic: poly(isobutylene) (PIB)  
or poly(1,1-dimethylethylene)

chlorinated: poly(vinyl chloride) (PVC)  
or poly(1-chloroethylene)

aromatic: poly(styrene) (PS)  
or poly(1-phenylethylene)

2. Polyesters:

poly( $\epsilon$ -caprolactone) (PCL)  
or poly(1-oxohexamethylene)

poly(methyl methacrylate) (PMMA)  
or poly[1-(methoxycarbonyl)1-methyl ethylene]

poly(dimethyl siloxane) (PDMS)

poly(ethylene-vinylacetate carbon monoxide  
(Elvaloy)

poly(ethylene-vinyl acetate)  
(Elvax)

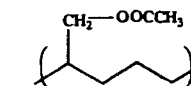
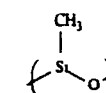
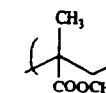
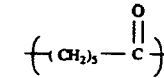
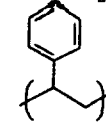
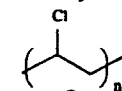
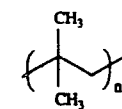


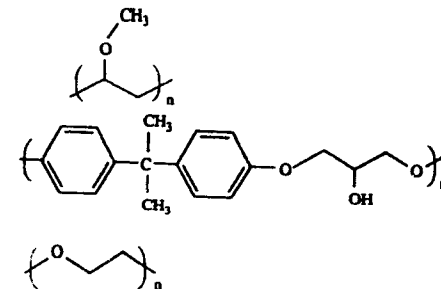
TABLE 1 (continued)

3. Polyethers:

poly(vinyl methyl ether (PVME)

poly(hydroxyether of bisphenol A)  
(Phenoxy)

poly(ethylene oxide)  
or poly(oxyethylene)



4. Plasticizers

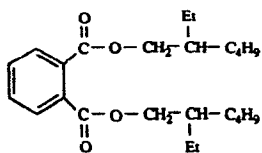
Di-(2-ethyl)hexyl phthalate (DOP)

Di-(2-ethyl)hexyl adipate (DOA)

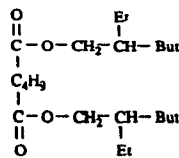
Di-(2-ethyl)hexyl sebacate (DOS)

Tri butyl phosphate (TBP)

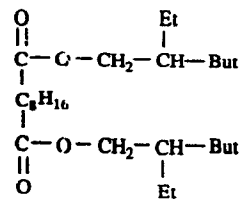
a  
b  
c  
d



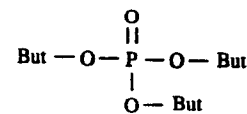
a



b



c



d

TABLE 2

List of polymers and solvents used and their sources

Chemicals	Sources
Phenoxy	Union Carbide
Poly( $\epsilon$ -caprolactone)	Aldrich Chemical Co.
Poly(ethylene glycol)	J.T. Baker Chemical Co.
Poly ethylene, vinyl acetate (Elvax)	Dupont
Poly ethylene, vinyl acetate carbon monoxide (Elvaloy)	Dupont
Poly dimethyl siloxane	Dow Corning Silicones Interamerica Ltd
Poly(isobutylene)	Polysciences
Poly(methyl methacrylate)	SP <sup>2</sup> Scientific Polymer Products Inc.
Poly(styrene)	Polysciences
Poly(vinyl methylether)	Polysciences
Poly(vinylchloride)	Sp <sup>2</sup> Scientific Polymer Products Inc.
<u>Plasticizers</u>	
Di-(2-ethyl)hexyl phtalate	Carlew Chemicals, St. Remi, PQ
Di-(2-ethyl)hexyl adipate	Monsanto Chemicals
Di-(2-ethyl)hexyl sebacate	CIBA-GEIGY
Tri-butyl phosphate	Monsanto Chemicals

TABLE 2 (continued)

---

Solvents

Cyclohexane	Aldrich Chemical Co.
Ethyl acetate	Aldrich Chemical Co.
Phenol	Aldrich Chemical Co.
Tetra-hydrofuran	Aldrich Chemical Co.
Tetra ethylene glycol	Aldrich Chemical Co.
Tri ethylene glycol	Aldrich Chemical Co.
Toluene	Aldrich Chemical Co.

---

using a Tian–Calvet microcalorimeter (Setaram, France). Measurements were made at given concentrations i.e. relative amounts of polymer for all of the systems. However, PS + PVME in toluene and PIB + PDMS in  $\text{CyC}_6$  were measured over the entire concentration range. Method and procedures are described in ref.3. The accuracy on  $\Delta H_M$  results is of 0.5 to 1%. Reproducibility was verified through measurement over the entire concentration range of a reference system:  $\text{CyC}_6 + n\text{-C}_6$ . The results agree within 2 J/mol with those of Benson et al<sup>4</sup>.

#### B. Heat of dilution

The Picker flow microcalorimeter, as well as the Tian–Calvet microcalorimeter was used to measure the heat of dilution ( $\Delta H_d$ ) for binary and ternary systems composed respectively of polymer 1 + solvent, polymer 2 + solvent and polymer 1 + polymer 2 + solvent. The systems studied were PS, PVME in toluene and  $\text{CyC}_6$  over the entire concentration range. The accuracy of the results is about 1% in the middle of the concentration range.

Details of instrumentation and procedures of the Picker flow microcalorimeter are provided in ref. 5.

## RESULTS AND DISCUSSION

### 1. Mixtures of poly(vinylchloride) + component 2 + THF

Table 3 summarizes the heats of mixing and interaction parameter  $\chi_{12}$  results obtained for mixtures composed of PVC + a second polymer or oligomer + THF.

#### A. PVC + PCL + THF mixtures

Table 3 shows exothermic heat of mixing for the ternary system of PVC-PCL. Hence  $\chi_{12}$  is negative throughout the entire composition range. The two polymers are then compatible over the whole concentration range. Fig. 1 shows the concentration dependence of the interaction parameter  $\chi_{12}$ .

$\chi_{12}$  tends to increase with increasing PVC concentration i.e.  $\chi_{12}$  is more negative, indicating better miscibility as PVC concentration increases. The specific interactions between PVC and PCL are probably due to hydrogen bonding between the  $\alpha$ -hydrogen of PVC and the carbonyl group of PCL. It has also been suggested<sup>1,6,7</sup> that the interaction might be due to a charge transfer complex between the pendant Cl of PVC and the oxygen of the carbonyl. Although a large number of data have been reported for the binary mixtures of PVC-PCL, no one has ever brought conclusive arguments in favor of one or the other possible explanations.

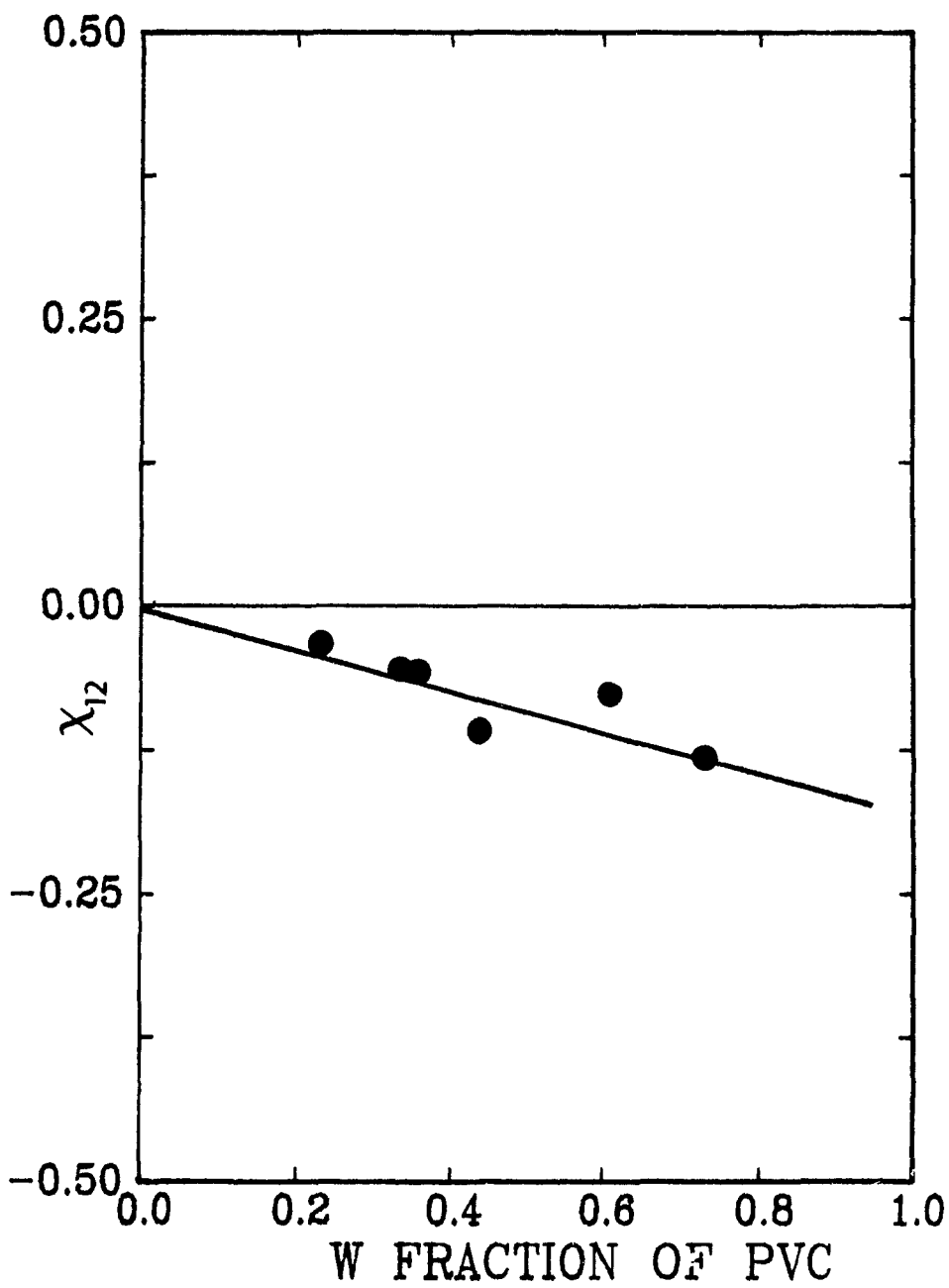
Ternary studies for this pair are rather rare, save the work of Olabisi<sup>7</sup>. Using inverse gas chromatography, he determined  $\chi_{12}$  for PVC-PCL in the presence of various probes. The study shows a net effect of the solvent on miscibility in the ternary system.  $\chi_{12}$  ranges from 0.10 to 1.16. However, polar probes such as MEK, for instance, lead to negative values. In MEK:  $\chi_{12} = -0.10$  which is not too far from our value.

TABLE 3

Heat of mixing and interaction parameter  $\chi_{12}$  for mixtures of PVC + polymer 2  
in THF at 25°C as a function of weight fraction of PVC

Polymer 2	conc (w <sub>fraction</sub> PVC)	$\Delta H_M$ J/g $\times 10^{-2}$	$\chi_{12}$
Poly( $\epsilon$ -caprolactone) (PCL)	0.23	-1.77	-0.032
	0.34	-3.95	-0.056
	0.36	-4.13	-0.057
	0.44	-8.10	-0.11
	0.61	-5.66	-0.076
	0.73	-6.61	-0.132
Poly(ethylene vinyl acetate carbon monoxide) (Elvaloy)	over all concentration range	< 0	< 0
Poly(ethylene vinyl acetate) (Elvax)	over all concentration range	> 0	> 0
Poly(methyl methacrylate) PMMA		< 0	< 0
Plasticizers			
TBP	0.36	< 0(large)	< 0
DOP	0.38	< 0(small)	< 0
DOA	0.34	> 0	> 0
DOS	0.39	> 0	> 0

Fig. 1 Concentration dependence of the  $\chi_{12}$  parameter as a function of weight fraction of PVC + PCL at 25°C.



B. PVC – terpolymer and copolymer of ethylene vinyl acetate (Elvaloy, Elvax) + THF

As shown in Table 3, a terpolymer of ethylene, vinylacetate and carbon monoxide (Elvaloy) shows miscibility with PVC in THF. Table 3 gives an exothermic heat for this mixture. Once again, specific interactions between the oxygen of the carbonyl group and the Cl of PVC are responsible for this negative  $\Delta H_M$ . However, mixtures with the co-polymer of ethylene-vinyl acetate (Elvax) where the carbon monoxide is removed show instead a positive  $\Delta H_M$  when mixed in THF. It has been reported<sup>8</sup> that binary mixtures of Elvax and PVC show limited miscibility. Miscibility is contingent on the vinyl acetate content of the copolymer. In fact, resins containing less than 60% of VA have been found immiscible. However, binary mixtures of Elvaloy and PVC show instead miscibility over the entire composition range.

C. PVC + PMMA + THF

Mixtures of PMMA and PVC show miscibility as well in THF. Exothermic heat has been recorded as shown in Table 3. Binary studies, however, reveal a definite influence of tacticity upon miscibility of the blend<sup>9</sup>. With isotactic PMMA, a miscible blend is observed, while syndiotactic PMMA indicated miscibility for a monomer ratio of 1:1 PMMA – PVC. Phase separation may be observed for higher content of PMMA. With the samples used in our study no such behaviour has been observed, indicating rather syndiotacticity of the samples.

D. PVC + Plasticizers + THF

The use of small molecules as plasticizers for PVC, is well-known. These

plasticizers are oligomers of polyester, although higher molecular weight polyesters might as well plasticize PVC.

Here again complex formation has been proposed based on a hydrogen-bonding interaction of the type C-O...Cl-C. However, because of the steric hindrance of the plasticizer molecules it seems more probable that H-bond interactions are involved between the  $\alpha$ -hydrogen and the carbonyl of the esters.  $\Delta H_M$  is exothermic for mixtures containing TBP and very small or zero for those of DOP. However,  $\Delta H_M$  is endothermic for DOA and DOS mixtures. An explanation of this behaviour could be advanced from the chemical structure of the various proton acceptors as shown in Table 1. The steric hindrance of DOS and DOA lead to a less basic carbonyl group than in the case of TBP which shows more negative  $\Delta H_M$ . The results agree with values reported by Roy<sup>10</sup> or Anagnostopoulos et al<sup>11</sup>. In the latter work, negative  $\chi_{12}$  has been found for PVC + TBP ( $\chi_{12} = -0.53$ ) and almost zero for DOP + PVC ( $\chi_{12} = -0.03$ ), while positive  $\chi_{12}$  have been determined for DOS (0.53) and DOA (0.28).

2. Mixtures containing components both having carbonyl group.

A. Phenoxy + PCL + THF

As shown in Table 4, mixtures of phenoxy + PCL in THF exhibit large and exothermic heats over the entire concentration range, due to hydrogen-bonding interactions involving the hydrogen from the hydroxyl group of phenoxy and the carbonyl group of PCL. Both calorimetry and dynamic mechanical measurements of  $T_g$ <sup>12</sup>, indicate miscibility for the binary pair. No ternary data have been reported so far in the literature, except inverse gas chromatography data showing negative  $\chi_{12}$  in the presence of various probes<sup>1</sup>.

TABLE 4

Heat of mixing for mixtures composed of phenoxy + polymer 2 or analogs  
in THF as a function of weight fraction of phenoxy at 25°C

Polymer 2	conc w <sub>fraction</sub>	$\Delta H_M$ J/g $\times 10^{-2}$	$\chi_{12}$
Poly( $\epsilon$ -caprolactone)	over entire concentration range	< 0	< 0
Poly(ethylene glycol)	"	> 0	> 0
Triethylene glycol	0.81	-0.660	-1.60
Tetraethylene glycol	0.42	1.53	1.08

B. Phenoxy + Polyethylene glycol + THF

Mixtures of Phenoxy + PEG exhibit, instead, an endothermic heat in THF. The oxygen of PEG is less basic than that of the carbonyl leading probably to a complex too weak to achieve miscibility in the ternary system.

Furthermore,  $\Delta H_M$ , measured for the two polymers with the solvent reveals an exothermic and large  $\Delta H_M$ , hence negative  $\chi_{13}$  for phenoxy + THF, and positive  $\Delta H_M$ , then positive  $\chi_{23}$  for PEG + THF. Therefore  $\Delta\chi$  will be large and unfavorable to mixing, and acts against the complex formation. This results in a positive  $\Delta H_M$  and positive  $\chi_{12}$ . The  $\chi_{12}$  for the ternary system is determined from  $\Delta H_M$ , therefore endothermic  $\Delta H_M$  leads inevitably to  $\chi_{12} > 0$ . However, it has been shown by Robard and Patterson<sup>13</sup> that incompatibility is not necessarily associated with positive  $\chi_{12}$ . Phase separation is observed for systems exhibiting large value of  $\Delta\chi$  even if  $\chi_{12}$  is negative. That tells that compatibility in a ternary system is more governed by  $\Delta\chi$  than by the sign of  $\chi_{12}$ . Moreover, this difference in the behaviour of the two polymers with the solvent creates non-randomness in the solution. This non-randomness is mainly due to preferential interaction between phenoxy and THF.

Heat of mixing was measured for analogs of both phenoxy and PEG in THF. Phenol was taken as an analog for phenoxy, while oligomers of PEG were used. Table 5 shows the results of this investigation. Both phenol and phenoxy show exothermic and large  $\Delta H_M$ , when mixed with triethylene glycol; hence negative  $\chi_{12}$  are also obtained,  $-2.15$  and  $-1.60$  respectively at mole fractions of  $0.60$  and  $0.81$  for phenol and phenoxy solution respectively. However as the chain-length of ethylene glycol increases, the miscibility seems to decrease. Hence,  $\Delta H_M$  for phenol + tetraethylene-glycol in THF is almost zero, while endothermic heat is observed for phenoxy + tetraethylene glycol + THF ( $1.53$  J/g) and positive  $\chi_{12}$  is also obtained ( $+1.08$ ).

TABLE 5

Heat of mixing as a function of phenol for mixtures of phenol + component 2  
in THF at 25°C

Component 2	conc w <sub>fraction</sub> of phenol	$\Delta H_M$ J/g	$\chi_{12}$
Triethylene glycol	0.60	-2.47	-2.15
Tetraethylene glycol		~ 0	~ 0

However  $\chi_{13}$  for phenol + tetraethylene glycol (without THF) is largely negative (- 1.74) comparable with  $\chi_{13}$  for phenol + tetraethylene glycol (- 2.15). The ternary system of phenol + tetraethylene glycol in THF exhibits an extremely small  $\chi_{12}$  which is essentially zero. This supports the argument of  $\Delta\chi$  being responsible for the incompatibility of phenoxy and PEG in THF. This behaviour is observed for any ternary system showing any disparity in the behaviour of the polymers with the solvent.

### 3. Polystyrene + PVME

#### A. Heat of mixing

#### in toluene

Table 6 shows  $\Delta H_M$  results for PS + PVME in toluene and the values are plotted in fig 2.  $\Delta H_M$  is small and endothermic. Fig.3 and table 6 exhibit  $\chi_{12}$  values as a function of volume fraction of PS.  $\chi_{12}$  is very small and positive. It is almost concentration independent at low concentration and increases slowly as the concentration increases. However, normalized values of  $\chi_{12}$  ( $\chi'_{12}$ ) show instead concentration dependence over the entire concentration range. The results are in agreement with values reported by Shiomi et al<sup>14</sup> for PS + PVME in toluene and obtained from osmotic pressure measurements. Some agreement can also be found with the results of Su and Patterson<sup>15</sup> obtained from GLC using toluene as a probe. This positive value of  $\chi_{12}$  and endothermic  $\Delta H_M$  result probably from a non-random distribution of the molecules in solution. Binary mixtures exhibit small but negative  $\chi_{12}$  which is the result of a weak complex between the oxygen of the ether and the aromatic ring. But in a ternary system, the solvent may preferentially interact with PVME and may decrease the polymer-polymer interaction.

Fig. 2 Experimental  $\Delta H_M$  as a function of volume fraction for PS + PVME at 25°C.

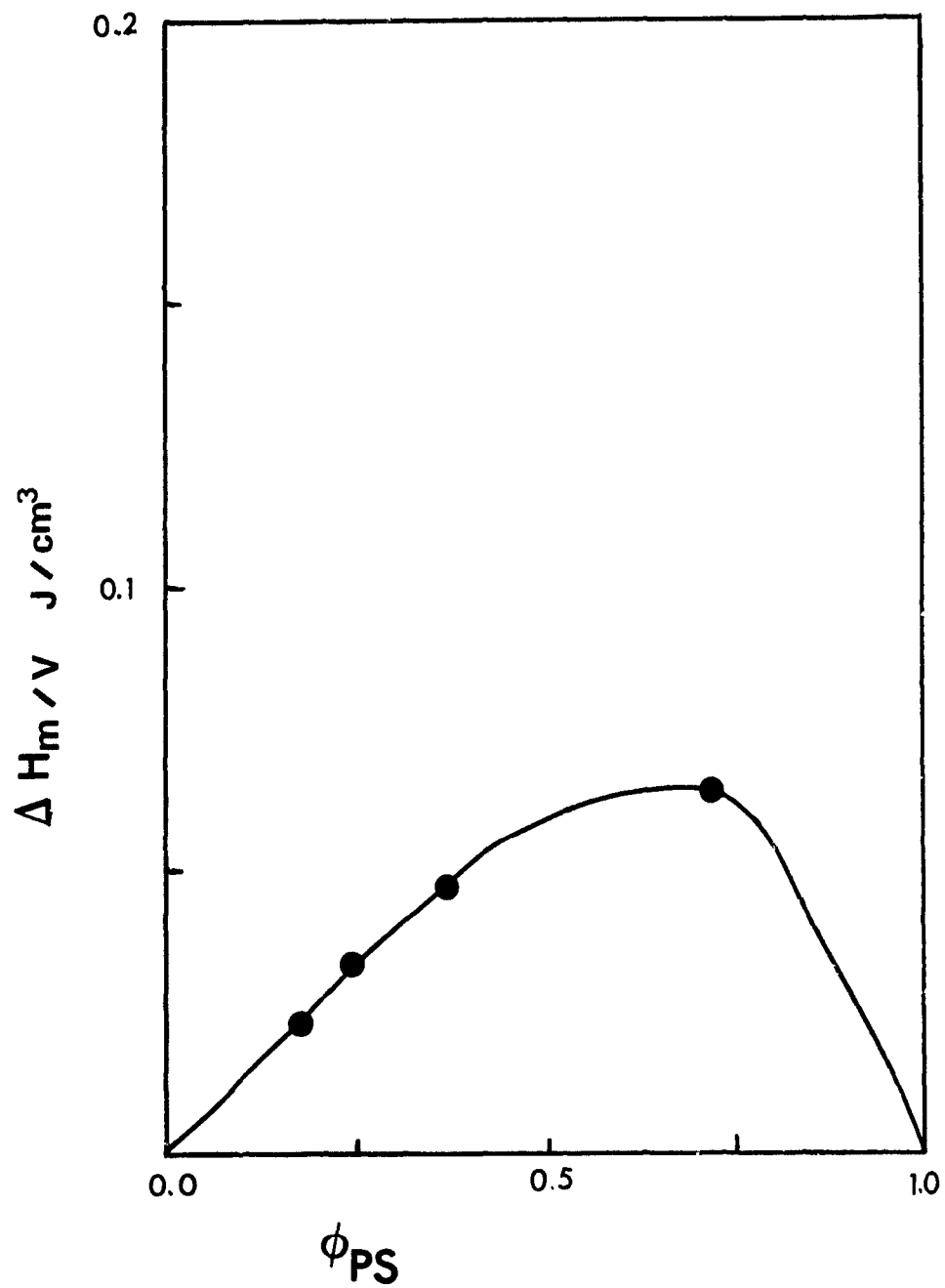
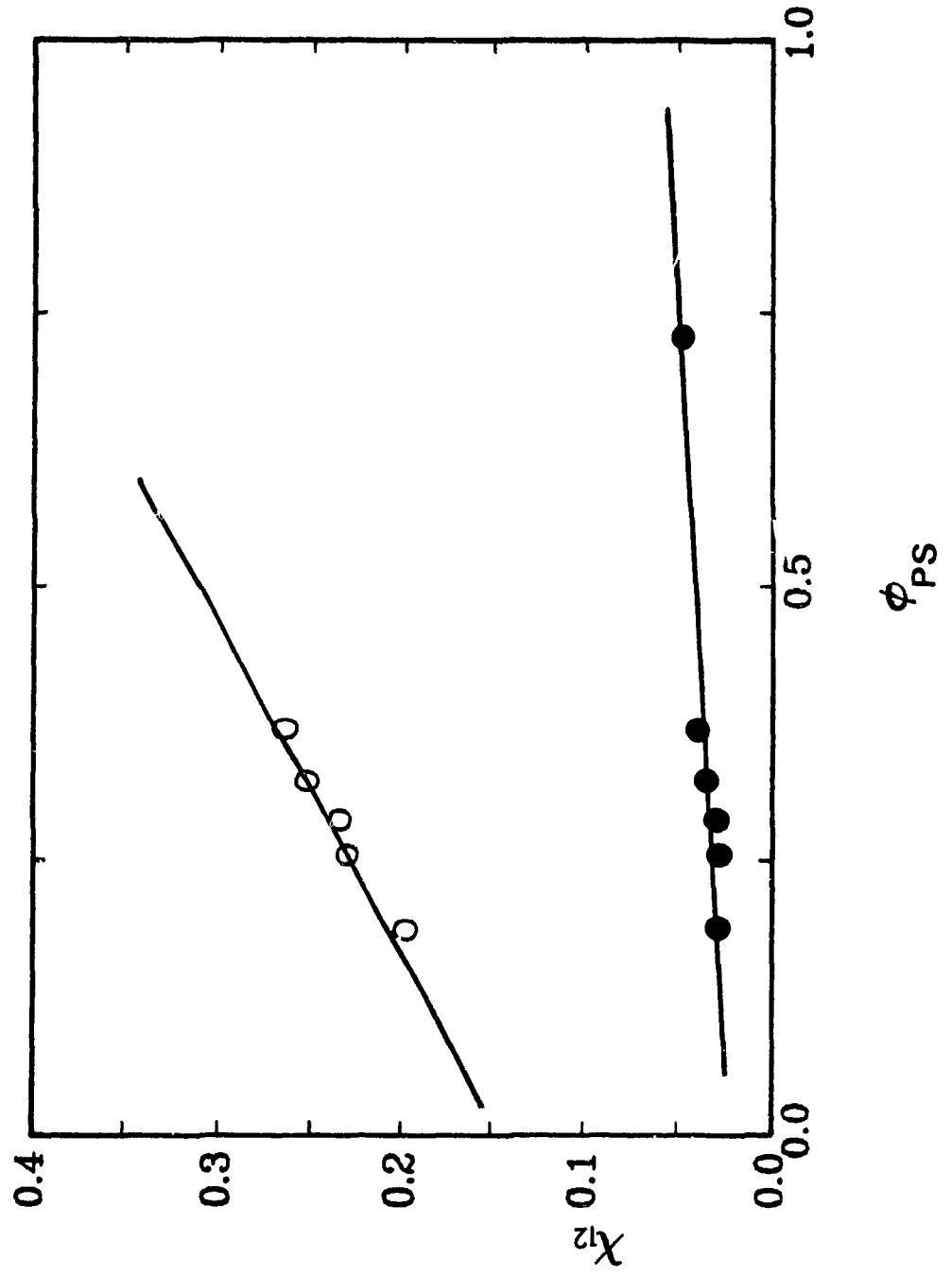


Fig. 3 Variation of  $\chi_{12}$  as a function of volume fraction of PS for PS + PVME at 25°C. ○:  $\chi_{12}/V^*$ ; ●:  $\chi_{12}$ .



### in Ethylacetate

Ternary solutions with ethylacetate as the solvent shows sign of compatibility:  $\Delta H_M < 0$  and  $\chi_{12} < 0$  over the entire concentration range. For instance, at  $W_{\text{fraction}}$  of PS = 0.64,  $\Delta H_M = -0.15$  J/g and  $\chi_{12} = -0.07$ . Su and Patterson<sup>15</sup> have reported  $\chi_{12} = -0.04$  from GLC measurement using propyl acetate as a probe solvent. Ethyl acetate should therefore show a slightly more negative value, which would be in perfect agreement with our calorimetric value.

### B. Heat of dilution

The heat of dilution was measured for both PS and PVME in toluene and for the ternary system. Both PS and PVME exhibit negative  $\Delta H_d$  and  $\chi_{\text{PS}(d)}$  as was already reported by Amaya et al<sup>16</sup>, Lewis and Johnson<sup>17</sup> and also by Gaeckle and Patterson<sup>18</sup>. It was suggested that this exothermic heat of dilution was the result of a volume contraction on dilution. Heat of dilution for the ternary system is also exothermic, leading to negative  $\chi_{12(d)}$ . If one agrees with this volume contraction occurring upon dilution in binary solution, diluting the ternary system would also mean that there is a volume contraction, meaning that as we add more solvent, each polymer interacts more with the solvent.

### 4. Polyisobutylene + PDMS

Endothermic heat of mixing can be seen as a function of concentration ( $W_{\text{fraction}}$ ) of PDMS for PIB + PDMS mixture in  $\text{CyC}_6$ .  $\chi_{12}$  is then positive. No specific interactions exist between those two polymers. And yet, the weak dispersion forces can not bring miscibility in ternary system. Therefore, miscibility is not

expected, at least in the ternary solution.

It is of interest to point out some conclusive remarks about the miscibility of two polymers in ternary systems:

1. Strong to moderate specific interactions is the necessary criterion for achievement of miscibility in a ternary system as observed using  $\Delta H_M$  measurement.
2. For weak interactions, non-randomness plays a dominant role in the miscibility or immiscibility of the polymers.
3. The nature of the solvent and the geometry of both components (since H-bonds are angle dependent) may be key factors for or against miscibility.

**REFERENCES**

1. O. Olabisi, L.M. Robeson, and M.T., Shaw, *Polymer-Polymer miscibility*, Academic Press, 1979, chapter 5.
2. a) references 2 to 16 of ref. 2b.  
b) M.E. Saint Victor, doctoral thesis Chapter 6.
3. P. Tancrede, doctoral thesis.
4. G.C. Benson and S. Murakami, *J. Chem. Thermo.* 1, 559, 1969.
5. P. de St.Romain, doctoral thesis.
6. B. Riedl and R.E. Prud'Homme, Miscibility phenomena in polyester chlorinated polymer blends, Paper presented at NRCC, IMRI mini-symposium series "Polymer Blends - 1981", Montreal, Quebec, April 1981.
7. O. Olabisi, *Macromolecules* 8, 316, 1975.
8. L.M. Robeson and J.E. McGrath, *Polymer Eng. Gc.*, 17, #5, 300, 1977.
9. J.W. Schruer, A de Boer and G. Challa, *Polymer*, 16, 201, 1975.
10. S. Roy, Master thesis.
11. C.E. Anagnostopoulos, A.Y. Coran and H.R. Gamrath, *Modern Plastics*, 141, 1965.
12. J.M. Jouza and R.S. Porter, *Macromolecules*, 19, 1946, 1986.
13. A. Robard and D. Patterson, *Macromolecules*, 10, 1021, 1977.
14. T. Shiomi, K. Kolmo, K. Yoneda, T. Tomita, M. Miya and K. Imai, *Macromolecules*, 18, 414, 1985.
15. C.S. Su and D. Patterson, *Macromolecules*, 10, 708, 1977.
16. K. Amaya and R. Fujishiro, *Bull. Chem. Soc. Japan*, 29, 270, 1956.
17. G. Lewis and A.F. Johnson, *J. Chem. Soc. (A)*, 1816, 1969.
18. D. Gaeckle, W.P. Klao and D. Patterson, *J. Chem. Soc. Faraday Trans. I*, 69, 1849, 1973.

APPENDIX 7

Derivation of  $\Delta H_M$  for ternary system

The following equations derive the heat of interaction of two polymers 1 and 2 in a mutual solvent 3.  $N_1$  molecules of polymer 1 are in solution in  $N_{31}$  molecules of solvent, while  $N_2$  molecules of polymer 2 are in solution in  $N_{32}$  molecules of solvent. The total amount of solvent is then given of  $N_3$  molecules or  $N_{31} + N_{32}$ .

The heat of mixing respectively polymer 1 and 2 with the solvent are given by equations (1) and (2)

$$\Delta H_{13} = H(1 + 3) - H(1) - H(31) \quad (1)$$

$$\Delta H_{23} = H(2 + 3) - H(2) - H(32) \quad (2)$$

where  $H(1 + 3)$  and  $H(2 + 3)$  are the enthalpies of the solutions resulting from mixing the polymers with the solvent;  $H(1)$  and  $H(2)$  are enthalpies of the pure polymers and  $H(31)$  and  $H(32)$  are the enthalpies of the two amounts of solvent.

The heat of mixing the polymers with the total solvent to form a ternary (1 + 2 + 3) is

$$\Delta H_{123} = H(1 + 2 + 3) - H(1) - H(2) - H(31) - H(32) \quad (3)$$

while the heat change from mixing the two binary polymer–solvent solutions is

$$\Delta H_M = H(1 + 2 + 3) - H(1 + 3) - H(2 + 3) \quad (4)$$

and this may be shown to be given by

$$\Delta H_M = \Delta H_{123} - \Delta H_{13} - \Delta H_{23} \quad (5)$$

Application of the Flory–Huggins expression of  $\Delta H_M$  leads to equations 6 to 8 for the binary and ternary solutions.

$$\Delta H_{13} = \frac{N_1 r_1 (N_{31} r_3)}{N_1 r_1 + N_{31} r_3} z \Delta W_{13} \quad (6)$$

$$\Delta H_{23} = \frac{N_2 r_2 (N_{32} r_3)}{N_2 r_2 + N_{32} r_3} z \Delta W_{23} \quad (7)$$

$$\Delta H_{123} = [\sum z W_{ij} \phi_i \phi_j] [\sum N_i r_i] \quad (8)$$

Where  $z$  is the coordination number;  $\Delta W_{13}$ ,  $\Delta W_{23}$  are energy changes associated with the formation of polymer–solvent segment contacts and  $\Delta W_{ij}$  is the energy change associated with the formation of polymer–polymer segment contacts;  $\phi_i$ ,  $\phi_j$  are volume fractions of species  $i$  and  $j$  in the ternary solution;  $r_i$  are segment numbers of  $i$  species. The volume fractions  $\phi_i$  of each species in the ternary are given by equations 9 to 11

$$\phi_1 = \frac{N_1 r_1}{\sum N_i r_i} \quad (9)$$

$$\phi_2 = \frac{N_2 r_2}{\sum N_i r_i} \quad (10)$$

$$\phi_3 = \frac{(N_{31} + N_{32}) r_3}{\sum N_i r_i} \quad (11)$$

Substituting equations (6) to (11) into (5) leads to equation (12)

$$\frac{\Delta H}{\sum N_i r_i} = z W_{12} \varphi_1 \varphi_2 + z W_{13} \varphi_1 \varphi_3 + z W_{23} \varphi_2 \varphi_3$$

$$- z W_{13} \frac{N_1 r_1 N_{31} r_3}{N_1 r_1 + N_{31} r_3} \frac{1}{\sum N_i r_i} - \frac{z W_{23} N_2 r_2 N_{32} r_3}{N_2 r_2 + N_{32} r_3} \frac{1}{\sum N_i r_i}$$

(12)

Consecutive rearrangements give the following expression for  $\Delta H_M$

$$\frac{\Delta H_M}{(\sum N_i r_i) V^*} = \frac{z W_{12} \varphi_1 \varphi_2}{V^*} + \frac{\varphi_1 (\varphi_1' - \varphi_2') (N_2 r_2 + N_{32} r_3)}{\sum N_i r_i V^*} z W_{13}$$

$$+ \frac{\varphi_2 (\varphi_2' - \varphi_1') (N_1 r_1 + N_{31} r_3)}{\sum N_i r_i V^*} z W_{23}$$

(13)

where  $V^*$  is the hard-core volume of the solution;  $\varphi_i'$  are volume fractions of polymer 1 in the binary (polymer-solvent) solutions;  $\varphi_i$  are volume fractions in the ternary solution.

## CONTRIBUTIONS TO ORIGINAL KNOWLEDGE

In this thesis several types of structure have been studied through their thermodynamic effects.

1. In part one of the thesis,  $C_p^E$  was measured for mixtures, where structure is caused by a molecular antipathy between the two components of the mixtures.  $C_p^E$  data exhibit a W-shape which has been shown to increase drastically as T moves towards the UCST. A correlation has been made between the W-shape  $C_p^E$  and a local composition non-randomness in solution. It has been found that the W-shape  $C_p^E$  is the resultant of two contributions to the thermodynamics: random and non-random. The concept of non-randomness in solution was also investigated through the concentration-concentration correlation function  $S_{CC}$ . Excellent correlations are made between non-randomness as given by  $S_{CC}$  and the effect of non-randomness on W-shape  $C_p^E$  for systems approaching their UCST.
2. Other second-order quantities such as  $\frac{dV^E}{dT}$  and  $\frac{dV^E}{dP}$  were also investigated, since both  $\alpha_p$  and  $\kappa_T$  tend to infinity with the same critical exponent as  $C_p$ . The W-shape should be observed at special conditions of T within a fraction of a degree of  $T_c$ .
3. The non-random contribution to  $\frac{dV^E}{dT}$  was determined experimentally using the Flory theory to estimate the random contribution to this quantity. The theory successfully reproduced the trend of the experimental results for the systems studied.

4. In part two, structure associated with stronger interactions (self-association or complex formation) are studied through  $C_p$  measurements of alcohol molecules in proton acceptor solvents. The complex formed between the two species lowers the level of structure created in the solution, compared to that produced in an inert solvent. The Treszczanowicz–Kehiaian model reproduces very well the experimental data.
5. The Treszczanowicz–Kehiaian model was used for a weaker self-associated component such as dodecanenitrile in inert and proton acceptor solvent.  $\phi_c$  and  $C_p^E$  show much lower values for alcohol molecules. But, still, the model reproduces successfully the experimental trend. It has been suggested that the nitriles dimerize in both the pure nitrile and solution.
6. In part three of the thesis, thermodynamic effects of structure due to specific interactions (H-bonds or complex formation) were studied in polymer solution where the second component may be a solvent or another polymer. The LCST due to specific interactions was observed at low temperature for mixtures of PA + p-dioxane, PEO + H<sub>2</sub>O and + chlorinated solvents and PPES + dichloro methane. As T increases, the solutions become miscible again above the UCST, leading to the so-called "immiscibility loop". It has been shown that this loop is strongly M.W. dependent, i.e. the higher the M.W., the lower the LCST and the higher the UCST, making often difficult the observation of the UCST which may occur at very high T.
7. A new model, based on the Flory–Huggins and Prigogine–Flory theories, has been proposed in the course of this work for a mathematical interpretation of the phase diagram of specifically interacting polymer–solvent or polymer–polymer

systems.

8. A calorimetric approach has been considered for the study of polymer–polymer compatibility. Since specific interactions are responsible for the miscibility between two polymer molecules, compatibility is therefore linked to the presence of an exothermic heat of mixing.  $\Delta H_M$  were presented for ternary systems composed of two polymers and a mutual solvent.  $\Delta H_M < 0$  for strongly interacting pairs and  $\Delta H = 0$  or  $> 0$  for weakly interacting pairs of polymers.  $\Delta H_M$  may also be positive if the two polymers do not interact in a similar way with the mutual solvent. In this case, incompatibility is due to the presence of non–randomness in solution.

### SUGGESTIONS FOR FURTHER WORK

1. It has been suggested that local composition non-randomness is a manifestation of critical state over  $\sim 100^\circ\text{C}$  from  $T_c$ . From calculated values of  $S_{CC}$ , it has been shown how non-randomness decreases as  $T$  increases over  $100^\circ\text{C}$  from  $T_c$ . Therefore it would have been very interesting to see the disappearance of the non-randomness effect on  $C_p^E$  as  $T$  is removed far from the UCST ( $\sim 100^\circ\text{C}$ ).  $C_p^E$  should go from a sharp positive W-shape to a normal negative parabola.
2. The Flory theory has successfully predicted the trend of  $V^E$  for non-electrolyte mixtures. But, the predictions are much too large for associated mixtures. Recently two theoretical approaches have been developed by Treszczanowicz and Benson and Heintz, in which a hydrogen-bond formation reaction volume  $\Delta v$  has been introduced. These extended Flory theories give good predictions for self-association process. Association involving two molecules of different nature is also important. In this case, both self-association and complex formation processes are observed. It would, therefore, be of great interests to extant these theories to association process involving two molecules of different nature, i.e. complex formation.
3. According to the Schultz-Flory treatment for partially miscible polymer mixtures,  $\Delta C_p$  or  $C_p^E$  changes sign depending on the nature of the critical point, i.e.  $\Delta C_p > 0$  if specific interaction LCST,  $\Delta C_p > 0$  near a UCST and  $\Delta C_p < 0$  near a free volume LCST. It would be very interesting to measure  $C_p$  as a function of  $T$  near the different critical points. DSC measurement should be an asset. The sign of  $\Delta C_p$  will differentiate between the two LCST.

4. Specific interactions in polymer solutions are made through H-bonding or complex formation. Therefore, application of association theory to these systems should give good predictions of experimental data, provided that the theory takes account of the free volume effect, essential in polymer solutions.